(NASA-TT-F-14336) MECHANICS OF MACHINES, NO. 27/28 (Translation Consultants, Ltd.) 235 p HC $13.75 CSCL 05H

N73-26073 THRU N73-26092 Unclas G3/05 05891

NASA TECHNICAL TRANSLATION

NASA TT F-14,336

MECHANICS OF MACHINES
No. 27/28

I. I. Artobolevskiy

Translation of "Mekhanika Mashin," Vypusk 27-28, Moscow, "Nauka" Press, 1971, pp. 1-171.

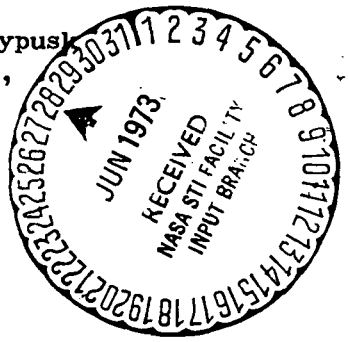

NATIONAL AERONAUTICS AND SPACE ADMINISTRATION
WASHINGTON, D.C. 20546 JUNE 1973

235 pg

ANNOTATION

Published in this collection are the materials from the Second Symposium on the Theory and Principles of Manipulator Design, held under the auspices of the Institute of the Science of Machines, and sponsored by the Scientific Council on the Theory of Machines and Working Processes of the Division of Mechanics and Control Processes of the Academy of Science of the USSR. The symposium was under the leadership of Academician I. I. Artobolevskiy and Doctor of Technical Sciences Professor A. Ye. Kobrinskiy.

The articles reflect the results of research in the field of theory and methods for analyzing and designing mechanisms for manipulators, and of their systems of manual, bioelectric, and automatic control.

A number of the articles raise questions concerned with the development of manipulators for a variety of functional purposes using electromechanical, electrohydraulic, magneto-mechanical, and other design principles.

PRECEDING PAGE BLANK NOT FILMED

TABLE OF CONTENTS

Page

Second Symposium on the Theory and Principles of Manipulator Design (February 8-9, 1968), I. I. Artobolevskiy, A. Ye. Kobrinskiy 1

Features of the Kinematics of Manipulators and Volumes Methods, I. B. Vinogradov, A. Ye. Kobrinskiy, Yu. A. Stepanenko, L. I. Tyves. 4

Some Remotely Controlled Master-Slave Manipulator Design Problems, N. A. Lakota, V. I. Lobachev. 20

Kinematic Analysis of Spatial Slave Mechanisms for Manipulators by the Matrix Method, Ye. I. Vorob'yev 37

Some Questions of the Discrete Control of Deep-Water Manipulators, E. L. Onishchenko 48

Prospects for the Building and Use of Computer Controlled Manipulators, M. B. Ignat'yev, F. M. Kulakov, A. M. Pokrovskiy. 58

Some Principles Involved in the Construction of Unamplified Control Systems for Electromechanical Manipulators, Ya. I. Aronov 73

Principal Parameters and Operating Indices for Reversible Follow-Up Systems, V. S. Kuleshov, I. N. Yegorov. 83

Some Questions From the Use of Reversible Follow-Up Systems With Independent Follow-Up and Force Reproduction Channels, B. A. Petrov, V. Ye. Paramonov. 98

An Analytical Method For the Synthesis of Reversible Follow-Up Systems, M. S. Voroshilov 113

The Question of Manipulator Activation by Reversible Follow-Up Systems, Yu. A. Stepanenko. 131

An Investigation of Engineering Methods of Designing Electro-Hydraulic Follow-Up Drives for Underwater Manipulators, V. S. Yastrebov 138

The First Experiment in Building an Airtight Magnetomechanical Master-Slave Manipulator, V. A. Ovsyannikov 154

The Influence of Manipulator Kinematics on the Selection of the Geometric Parameters of Boxes and Chambers, G. I. Lukishov, Yu. V. Miloserdin 162

Page

Principles of the Curtailment of Sources of Command Signals in Multifunctional Bioelectric Control Systems, Ye. P. Polyan, A. Yu. Shneyder, E. I. Plamm. 174

Synchronism and Heterochronism of Synkinesis in Man, I. P. Blokhin, A. B. Gandel'sman, G. S. Kan, A. M. Pokrovskiy. 187

The Possiblities of Making Quantitative Evaluations of the Functioning of Closed People-Operator Control Systems, V. A. Taran, A. D. Korotkov, Yu. N. Kofanov, A. A. Belov, I. G. Shramkov. 200

The Question of Modeling Certain Motor Functions of the Human Arm, A. V. Smirnov, B. S. Yastrebov 220

Determining of the Spatial Positions of the Links in a Manipulator Mechanism, A. V. Sinev, Yu. A. Stepanenko 226

N73-26074

SECOND SYMPOSIUM ON THE THEORY AND PRINCIPLES OF MANIPULATOR DESIGN (FEBRUARY 8-9, 1968)

I. I. Artobolevskiy, A. Ye. Kobrinskiy

ABSTRACT. The Second Symposium on the Theory and Principles of Manipulator Design is discussed. Different uses of manipulators are presented, including their use as space equipment. The main questions covered by the articles in the collection are presented, and designations are suggested for the basic elements of a manipulator.

Analysis and design methods, as well as the development of concrete manipulator schemes and designs have developed substantially in the Soviet Union, and abroad, since the first symposium, which took place at the Institute of the Science of Machines on July 4-5, 1965. /3*

The history of the creation of manipulators is barely 20-25 years old. Its beginning is connected with the demands of the atomic industry. The tempo of work in the field of creating facilities such as these is growing very rapidly, and in proportion to the expansion of these demands.

At the present time, the field of their functional purpose is expanding, with space research, utilization of the underwater world, problems of automation of production processes, medicine and prosthetics, and the number of organizations concerned with the creation of designs, devices, and systems intended for the accomplishment of a particular class of motor functions, approximately reproducing the movements of human limbs, has systematically increased.

Thus, according to information in the foreign press, scores of submarines intended for operation at shallow, medium, and great depths have already been built and are in use at the present time. No doubt most of them are equipped with manipulators. As regards space equipment, it now is possible to list at least three groups of such systems (sometimes called anthropomorphic - "human like"), the development of which is of great scientific interst and practical importance.

1. Manipulators intended for use in space and on the surface of planets. The reference here is to the simplest mechanisms and devices, as well as the

---

* Numbers in the margin indicate pagination in the foreign text.

most workmanlike systems, including long-range television communication between the operator and the manipulator, and providing great possibilities for copying arm movements.

2. Devices of the "Ekzoskeleton" (exterior skeleton) type, worn by the operator, and having degrees of mobility sufficient to avoid hindering the operator's movements. They are fitted with servomotors so the operator can work under complex conditions.

3. Pedipulators, devices intended for the reproduction of the motor functions of the legs, in connection with the creation of transport vehicles capable of moving over surfaces not readily traversable.

The scope of the scientific problems arising in connection with the development of the theory and principles of the building of anthropomorphic systems is unusually broad. There is no question that specialists working in the most diverse fields of the theory of machines can make a serious contribution to the resolution of these problems. /4

The task of the second symposium was to make certain summaries of the theoretical and experimental research that had been done in the field of manipulators. In the future it will be necessary to expand significantly the subject matter of symposiums to include other types of anthropomorphic machines and systems for controlling them.

This collection includes 18 articles setting for the basic content of the reports discussed at the symposium. These reports embrace questions of the theory and the principles of building manipulators connected with: (1) the building of manipulators and with the kinematic and dynamic properties of manipulator slave organs; (2) the transmission of control information from the master to the slave organ and the "activation" of manipulators; (3) the control of manipulators. Several questions of biomechanics and bioelectric control were discussed at the symposium. These materials also are reflected in the collection. Finally, the necessity of adhering to standard terminology was stressed by many participants in the symposium. The necessity for this will become all the more imperative in the future as investigations in the field of the theory and principles of the building of manipulators expand. Now, it seems to us, it is the right time to suggest certain designations for the basic elements of manipulator "arms"

(see drawing).

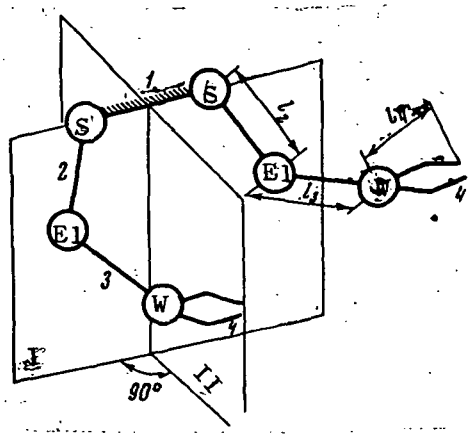

Basic elements of manipulator arms.

1 - rack, or body; 2 - shoulder; 3 - forearm; 4 - hand, or tongs; S - shoulder mechanism; E1 - elbow mechanism; W - wrist, or hand mechanism; I - frontal plane; II - sagittal plane.

N73-26075

FEATURES OF THE KINEMATICS OF MANIPULATORS AND VOLUMES METHODS

I. B. Vinogradov, A. Ye. Kobrinskiy, Yu. A. Stepanenko, L. I. Tyves

ABSTRACT. A volumetric method of kinematic analysis of a manipulator which can be used in addition to the conventional trajectory method is presented. An ideal manipulator, the influence of limitations on the angles of rotation of the manipulator, and a manipulator with limitations in all joints are discussed.

1. Introduction. Conventional methods of kinematic analysis of mechanisms permit investigating the kinematics of a manipulator for given laws of motion of all its drive links. The difficulties caused by the great many degrees of system mobility are purely technical in nature. However, this approach, based on the study of particular trajectories of motion, tells nothing of the general kinematic properties of the manipulator. This makes it desirable to use another method, the volumetric method, along with the trajectory method of kinematic analysis for it permits obtaining general, integral evaluations of the kinematic properties of the manipulator characterizing some of its qualities when developing a set of trajectories.

A manipulator can function in a working space determined by the length of its links and the movements in its joints. The manipulator tongs can reach any point in this space, but the functional potentials of the mechanisms differ at different points. That is, inherent in the particular manipulator are definite properties characterizing the potential for performing different working operations at each point in the working space. Investigation of these working space properties, imparted by the manipulator, provides the means for evaluating important kinematic characteristics of the manipulator as a unit.

When the manipulator is at work it must be able to orient and move the tongs in different ways relative to the object of manipulation. However, structural and design limitations prevent moving the tongs to any point in the working space at any angle. Some solid angle, ψ, within which the tongs can be brought to this point, can be determined for each point in the space. Let us call angle ψ the spatial servicing angle, or the service angle. Let us call the relationship

$$\psi/4\pi = \Theta \qquad (1)$$

the service factor at a particular point. Some scalar field thus can be

established above the working space, or, putting it another way, each point in the space is set up in accordance with its service factor. The factor can change from 0 for points on the boundary of the working space to 1 for points in the so-caleed 100%, or full service, zone. It is technically justified to characterize the quality of the manipulator as a whole by the mean magnitude of the service factor, $\overline{\Theta}$, in the working space, dV

/6

$$\overline{\Theta} = \frac{1}{V}\int_{(V)} \Theta dV,$$

which can be called the full servicing factor, or the manipulator service.

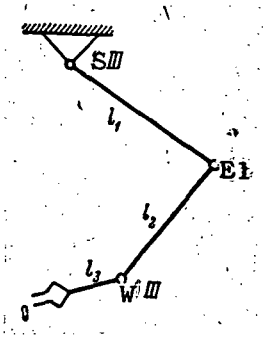

Figure 1.

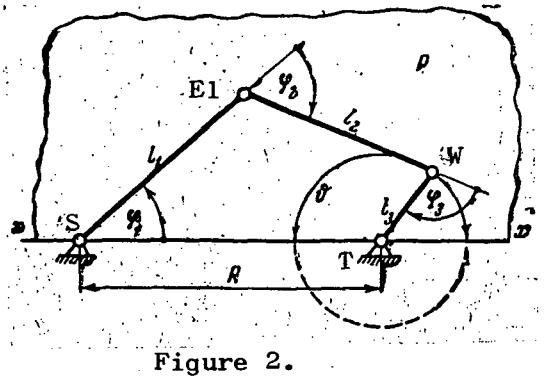

Figure 2.

In determining the magnitude of the service factor at the particular point, let us submit that the manipulator has gripped some object of negligibly small size located at this point with the jaws of the tongs. Let us now assume that the tongs can be moved, changing their orientation in the space, but that the object does not leave the particular point. At the same time, the coupling superposed on the manipulator by the object is similar to the coupling superposed by the ball joint located at the point of interest to us and coupling the tongs and the support. The manipulator is, in this case, converted into a three-dimensional mechanism, and Θ now can be determined by the spatial angle through which the axis of the tongs can be turned. Thus, the task of determining Θ is reduced to investigating a family of three-dimensional mechanisms with several degrees of mobility. The relative mobility of the links is limited by mechanism dimensions and by the drive systems for the kinematic couples. Therefore, it is desirable first to examine the properties of the "ideal" manipulator without regard for design and structural factors. This is done in what follows by using the example of a manipulator with eight degrees of freedom and one degree

of maneuverability [1]. A general algorithm for determining the volumetric kinematic properties in the case of arbitrary limitations on movements in the kinematic couplings then is presented.

2. The ideal manipulator. We will understand the ideal manipulator to be one with no limitations on movements in all kinematic couples, and in which the thicknesses of the links and the dimensions of the joints can be ignored.

Let us investigate the configuration of the service zones for an ideal manipulator with one degree of maneuverability (Figure 1). Its "arm" has Class III spherical turning couples in the "shoulder," and in the "wrist," and a Class V turning couple in the "elbow." We shall designate the kinematic couples by the first letter of the name of the corresponding joint in the human arm, and the degrees of freedom in the particular couple by Roman numerals. Let us designate the lengths of the links as l_1, l_2, l_3. The manipulator under consideration has one degree of maneuverability. The process of arbitrary reorientations of the tongs can be represented as the rotation of link WT with respect to fixed point T such that the trajectories of point W will lie in a sphere of radius l_3. The result is a three-dimensional 4-link mechanism with support ST (Figure 2). All links in this mechanism can be located in a single plane, P, the base plane, and can be rotated in turn around an axis passing through points S and T. Let us designate this axis x. In this case, point W will describe a circle in plane P and, together with plane P, a spherical surface around point T. Thus, investigation of the service provided by a 3-link manipulator with eight degrees of freedom can be reduced to the investigation of a series of flat 4-link closed mechanisms that differ by the length of the ST link. At the same time, the service factor for any point on the x-axis and, by changing the position of the x-axis in the space, for any point in the working space, can be determined. The Θ values for points on the x-axis will not depend on the position of the x-axis in space for the ideal manipulator being investigated so, it is sufficient to investigate one arbitrary position of this axis. Angles φ_1, φ_2, and φ_3 characterize the relative positions of the links.

/7

The movement of point T along x in the direction of the shoulder, S, as well as away from it, it limited by two maxima corresponding to the two limit positions of the mechanism. In one, the tongs are at the maximum distance from the shoulder

and point T will be at a distance from point S equal to $R_{max} = l_1 + l_2 + l_3$. In the other, angle φ_2 is maximum and the tongs are at the greatest distance from the first limit position.

Let us determine the configuration of the manipulator service zones. Known crankability conditions [2] provide the first zone, the full service zone. This zone is in the limits $l_1 + l_2 - l_3 \geq R \geq l_1 - l_2 + l_3$. when $l_1 > l_2 > l_3$ Figure 2). The magnitude of the service, Θ, changes from 0 to 1 beyond the limits of this zone.

The second zone is the limits $l_1 + l_2 + l_3 \geq R \geq l_1 + l_2 - l_3$, and

$$\frac{l_3^2 + R^2 - (l_1 + l_2)^2}{2Rl_3} = \cos\vartheta. \tag{2}$$

is valid.

Here ϑ is the maximum angle, read from the x-axis (see Figure 2), within which link l_3 can turn for a given R value. We shall call angle ϑ the service angle in the base plane. The manipulator can occupy positions symmetrical relative to the x-axis, so we shall take it that angle ϑ can change from 0 to π. The boundaries of the second zone correspond precisely to these limit values of ϑ.

The equality

$$\frac{l_3^2 + R^2 - (l_1 - l_2)^2}{2Rl_3} = \cos\vartheta, \tag{3}$$

is valid for the third zone, and

$$l_1 - l_2 + l_3 \geqslant R \geqslant l_1 - l_2 - l_3. \tag{4}$$

If the manipulator links are matched with the inequality $l_2 > l_1 > l_3$, the limits, using Eq. (3) when ϑ is equal to 0 and π, will be

$$l_2 - l_1 + l_3 \geqslant R \geqslant l_2 - l_1 - l_3. \tag{5}$$

Combining Eqs. (4) and (5), we obtain

$$|l_1 - l_2| + l_3 \geqslant R \geqslant |l_1 - l_2| - l_3.$$

Eqs. (2) and (3) provide angle ϑ for points along the x-axis. On the other hand, angle ϑ uniquely determines the spatial servicing angle, ψ, and the service factor Θ. There is a spherical sector in space corresponding to angle ϑ in the /8

base plane. The area of its spherical surface is determined by

$$F = 2\pi l_3^2 (1 - \cos\vartheta).$$

In accordance with the service factor definition, Eq. (1), we obtain

$$\Theta = \frac{2\pi l_3^2 (1 - \cos\vartheta)}{4\pi} = \frac{1 - \cos\vartheta}{2}. \tag{6}$$

Excluding ϑ from Eqs. (2) and (3), and solving for Θ, we obtain:

for the first zone

$$\Theta = 1; \tag{7}$$

for the second zone

$$\Theta = \frac{(l_1 + l_2)^2 - (R - l_3)^2}{4Rl_3}; \tag{8}$$

for the third zone

$$\Theta = \frac{(R + l_3)^2 - (l_1 - l_2)^2}{4Rl_3}. \tag{9}$$

Eqs. (7), (8), and (9) can be used to plot a graph of change in Θ with movement of the tongs (point T) from R_{max} to R_{min} (Figure 3). It corresponds to the $|l_1 - l_2| > l_3$ case, and has shown on it the limits of the zones differing by the nature of the change in Θ and considered above.

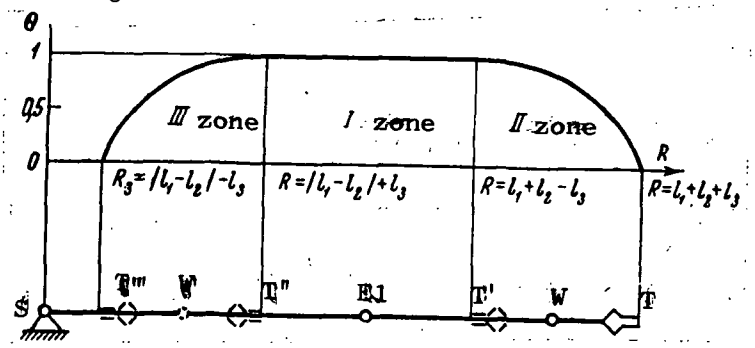

Figure 3.

Now let us consider the case when the manipulator length relationships yield $|l_1 - l_2| = l_3$. The distribution of the service zones now is completely subordinate to the previously obtained behavior patterns over the entire range of radius changes, except for the case when the tongs coincide with point S ($R = 0$). In this position, because of the rotation of the entire manipulator in the shoulder joint, the tongs can be oriented relative to point S in any manner, so $\Theta = 1$, and when $|l_1 - l_2| = l_3$, point S can be called a special point. There also are certain

special features present in the distribution of Θ in the third zone when $|l_1 - l_2| < l_3$. In particular, there is a sector in this zone with Θ = 1 (Figure 4). In accordance with Eq. (9), Θ = 1 when $R = R_1 = l_3 + |l_1 - l_2|$ and $R = R_2 = l_3 - |l_1 - l_2|$. Θ is a minimum when $R = R_3 = \sqrt{l_3^2 - (l_1 - l_2)^2}$. Thus when $R < R_2$ the tongs acquire a crankability (Figure 5) that is retained to R = 0. We obtain $R_1 = R_2 = R_3$ when $l_1 = l_2$ and we will have Θ = 1 on the Θ = f (R) graph (Figure 4) in the limits $l_1 + l_2 - l_3 \geq R \geq 0$. Obviously, $l_1 = l_2$ and $l_3 \to 0$ are, from the point of view of increase in service, the most advantageous link length relationships because Θ will be maximum. /9

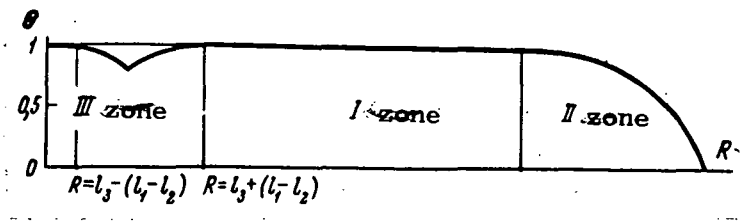

Figure 4.

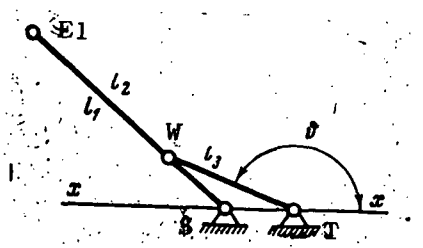

Figure 5.

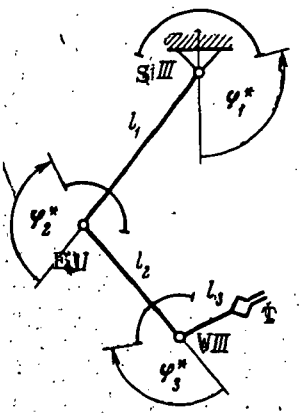

Figure 6.

3. <u>The influence of limitations.</u> Structural limitations on the angles of rotation of the manipulator links in all kinematic couples have a significant influence on manipulator volumetric properties. We shall designate the limiting values of the angles of rotation in the i^{th} joint φ_i^* (Figure 6). Here we shall consider the limitations on the angles of rotation of the links to the symmetrical with respect to the axes of the preceding links.

A. Let us examine the influence of limitation of angle φ_3, assuming that the limitations imposed on the remaining angles are $\varphi_2^* = \pi$, $\varphi_1^* = \pi$.

Let point T move from R_{max} to R_{min} (Figure 7). Here $\Theta = f(R)$ will be determined by a function of Eq. (8) until angle φ_3 reaches the boundary value $\varphi_3 = \varphi_3^*$. Radius R_1 will correspond to this value

$$R_1 = \sqrt{(l_1 + l_2)^2 + l_3^2 + 2l_3(l_1 + l_2)\cos\varphi_3^*}. \quad (10)$$

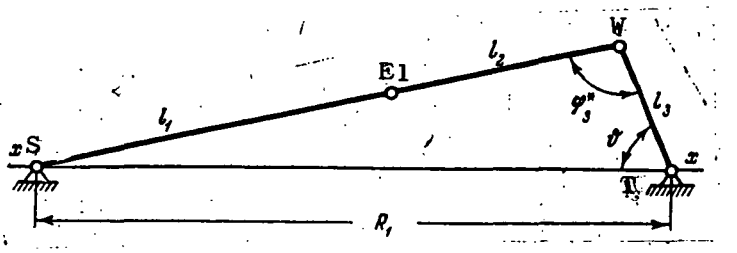

Figure 7.

Limitation φ_3^* influences the magnitude of the service angle, ϑ, when there is a further reduction in R, but this influence differs with different R values. Now ϑ can be depicted as the difference between two angles characterizing the limits in the position of link l_3 as it turns clockwise (α) and counterclockwise (β) (Figure 8). The manipulator under consideration has one degree of maneuverability so the values of α and β on only one side of the x-axis, that is, in the limits

$$0 \le \alpha \le \pi, \quad (11)$$

$$0 \le \beta \le \pi, \quad (12)$$

are of interest to us.

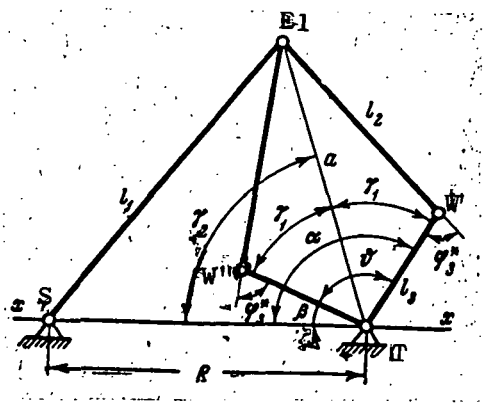

Figure 8.

Here the set of permissible wrist positions forms a ring on the surface of a sphere of radius l_3 and area $F = 2\pi l_3^2(\cos\beta - \cos\alpha)$, from whence

$$\Theta = \frac{\cos\beta}{2} - \frac{\cos\alpha}{2}. \quad /10$$

Let us examine change in $\cos\alpha$ and $\cos\beta$ as a function of R.

The limiting position for links l_2 and l_3 is angle α on the section $R_1 \ge R \ge R_{min}$. The links are positioned at angle φ_3^*. Angle α can be represented in the form of the sum of two angles, γ_1 and γ_2, determined by the equalities

3

$$\sin\gamma_1 = \frac{l_2}{a}\sin\varphi_3^*;$$

$$\cos\gamma_2 = \frac{a^2 + R^2 - l_1^2}{2aR};$$

$$a = \sqrt{l_2^2 + l_3^2 + 2l_2 l_3 \cos\varphi_3^*}.$$

After the transformations, we obtain

$$\cos\alpha = \cos(\gamma_1 + \gamma_2) = \pm\frac{a^2 + R^2 - l_1^2}{2a^2R}\sqrt{a^2 - l_2^2\sin^2\varphi_3^*} - \frac{l_2\sin\varphi_3^*}{2a^2R}\sqrt{4a^2R^2 - (a^2 + R^2 - l_1^2)^2}. \quad (13)$$

Let us put a "+" sign in front of the first term when $l_3 + l_2\cos\varphi_3^* \geq 0$ ($\gamma_1 \leq \pi/2$ corresponds to this), and a "-" sign when $l_3 + l_2\cos\varphi_3^* < 0$ (here, $\gamma_1 > \pi/2$).

Angle α increases with a decrease in R, reaching the value $\alpha = \pi$ when

$$R_2 = \sqrt{l_1^2 - l_2^2\sin^2\varphi_3^*} - l_2\cos\varphi_3^* - l_3.$$

Taking it that $R_2 \geq R \geq R_{min}$ in the zone, we have $\alpha > \pi$. In accordance with Eq. (11), we will conditionally consider $\alpha = \pi$.

Moving on to consideration of change in β as a function of R, we note that for small R values angle β depends only on the link length relationship, but also depends on φ_3^* when R values are large (Figure 9). Let us designate the boundary value of R separating these two regions R_3.

$$R_3 = \sqrt{l_3^2 + (l_1 - l_2)^2 - 2l_3(l_1 - l_2)\cos\varphi_3^*}.$$

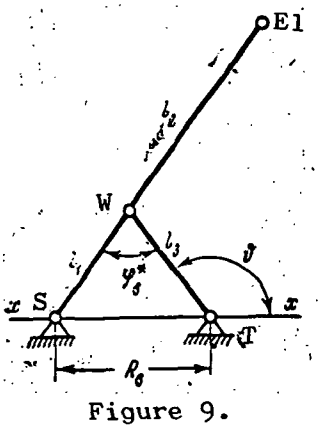

Figure 9.

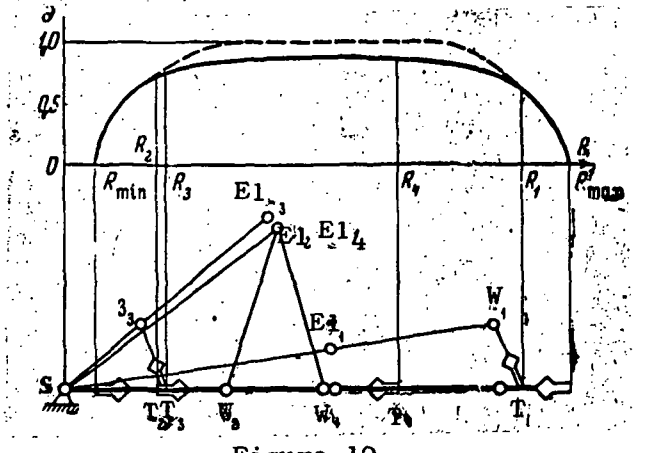

Figure 10.

The limiting position for links l_2 and l_3 is angle β on the section $R_1 \geq R \geq R_3$. The links are positioned at angle φ_3^*. Angle β can be represented in the form of the difference between angles $\gamma_2 - \gamma_1$ (Figure 8), so

$$\cos\beta = \cos(\gamma_2 - \gamma_1) = \pm\frac{a^2+R^2-l_1^2}{2a^2R}\sqrt{a^2 - l_2^2\sin^2\varphi_3^*} + \\ + \frac{l_2\sin\varphi_3^*}{2a^2R}\sqrt{4a^2R^2-(a^2+R^2-l_1^2)^2}.$$

Selection of the sign in front of the first term is determined in the same way as in Eq. (13).

Angle β decreases with increase in R, and equals zero when

$$R_4 = \sqrt{l_1^2 - l_2^2\sin^2\varphi_3^*} + l_2\cos\varphi_3^* + l_3.$$

We have $\beta < 0$ in the zone $R_{max} \geq R \geq R_4$ so, in accordance with Eq. (12), we will conditionally take $\beta = 0$ for this zone.

Limitation φ_3^* has no influence on manipulator movement near R_{min}, when $R_2 \geq R \geq R_{min}$ and $R_3 \geq R \geq R_{min}$ (given the condition that $|l_1 - l_2| \geq l_3$) and $\Theta = f(R)$ is determined from Eq. (9).

Figure 10 shows change in the service factor for the different zones. Shown are Θ values for the ideal manipulator (dashed curve) and the characteristic positions of the manipulator in each of the zones.

B. Let us now investigate the influence of the limitation on angle φ_2. Let us put $\varphi_2^* \leq \varphi_2 \leq \varphi_2^*$; $\varphi_3^* = \pi$; $\varphi_1^* = \pi$. As in the preceding case there are several characteristic zones in the range of changes in radius R from R_{min} to R_{max}. Let us first consider the zone near R_{min}. Figure 11 shows the position of the manipulator in this zone when $\varphi_2 = \varphi_2^*$. From triangle SWT we have

$$R = \sqrt{l_1^2 + l_2^2 + 2l_1l_2\cos\varphi_2^* - l_3^2\sin^2\theta} - l_3\cos\theta.$$

Using Eq. (6), we find

$$\theta = \frac{(R+l_3)^2 - (l_1^2 + l_2^2 + 2l_1l_2\cos\varphi_2^*)}{4Rl_3}.$$

This expression is valid when $R_1 \geq R \geq R_{min}$, where boundary R_1 can be determined from (see Figure 12) /12

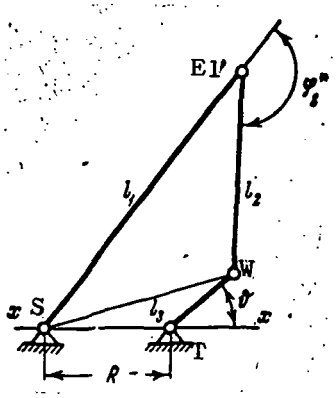

Figure 11.

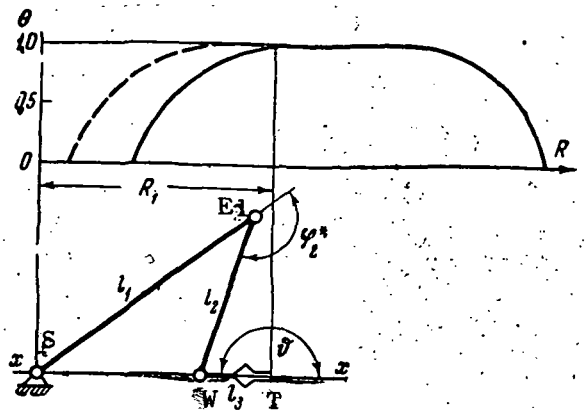

Figure 12.

Angle φ_2 always will be less than φ_2^* for the larger values of radius R, so the Θ distribution will be what it is for the ideal manipulator. Figure 12 shows $\Theta = f(R)$ for the φ_2 limitation. The solid line shows the function $\Theta = f(R)$ for a manipulator with the φ_2^* limitation, and the dashed line that for the ideal manipulator. Thus, if the φ_3 limitation influenced the Θ distribution at all points in the working space, reducing the service magnitude as compared to the ideal manipulator, the φ_2 limitation reduces the service factor only near the shoulder.

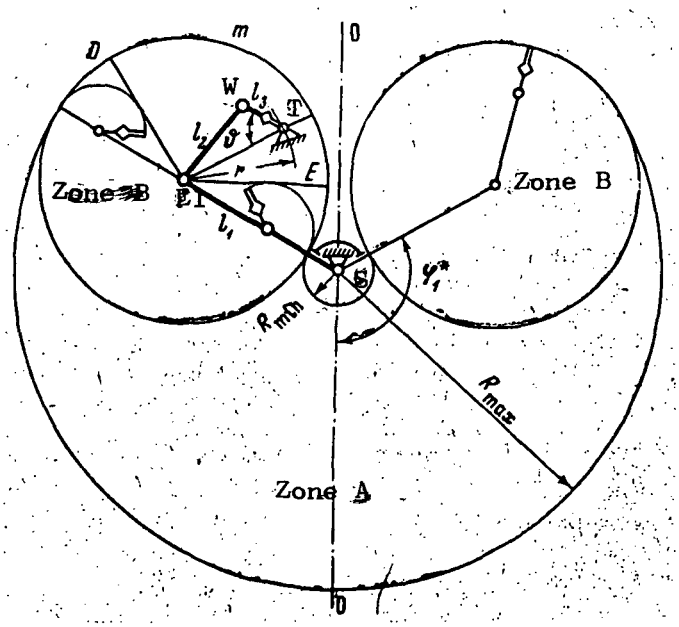

Figure 13.

C. Let us examine the case when $\varphi_1^* \leq \varphi_1 \leq \varphi_1^*$; $\varphi_2^* = \pi$; $\varphi_3^* = \pi$. The introduction of a limitation on angle φ_1 means that movement of link SE1 (Figure 13) over the sphere is limited by the solid angle formed by the rotation of the straight line SE1 around axis OO, which it interesects at angle φ_1^*. Now the space around point S does not possess identical properties along any radius-vector R, so let us investigate the individual regions of the space serviced by the manipulator. The working space can be presented as consisting of two zones, in the first of which, zone A, the Θ distribution will be the same as for the ideal manipulator, but in the second, zone B, will change from 0 to 1. The function $\Theta = f(R)$ is extremely complex.

/13

The total manipulator working space is limited by two concentric spheres with radii R_{max} and R_{min}, and part of the surface of the torus joining them. Figure 13 shows the cross section of the working space in the form of a plane passing through the OO axis.

Let us examine the distribution of service zones in the area delimited by lines DmEE1. We will select the coordinates of the points here in a polar coordinate system, (r), with center in point E1. We note that angle ϑ increases in this zone with movement of the tongs (point T) from the periphery to point E1. Because they are maneuverable, the tongs can rotate around axis E1T as well, so angle ϑ can characterize the service factor. Thus,

$$\Theta = \frac{l_2^2 - (r - l_3)^2}{4 r l_3}. \qquad (14)$$

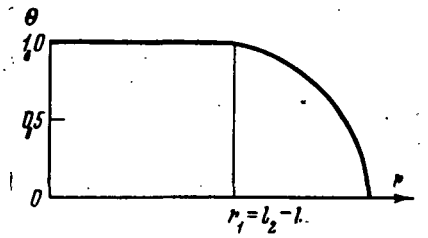

Figure 14.

We obtain the limiting value $r_1 = l_2 - l_3$ when $\Theta = 1$. Eq. (14) is valid when $r_1 \leq r \leq l_2 + l_3$, but when $r_1 \geq r \geq 0$ the service factor is constant and equals 1 (see Figure 14).

Considering the nature of the changes introduced in the distribution of the service zones by limitations on angles φ_1, φ_2, φ_3, it can be taken as an approximation that angle φ_3^* determines the maximum value of the service magnitude Θ, and that angles φ_1^* and φ_2^* influence the volume of space serviced by the manipulator, the service near the shoulder, and the boundaries of the space serviced.

4. Manipulator with limitations in all joints. Up to this point we have been considering manipulators with Class III spherical couples as joints. But manipulators use Class V couples for the most part and Class III spherical couples usually are replaced by a combination of three Class V couples, each of which has its own limitation in angle of rotation. These design features are reflected in the distribution of service zones.

Figure 15 shows a manipulator whose kinematic chain contains only Class V rotary kinematic couples. I is the frontal plane, II is the sagittal plane, and III is the base plane. The Mascot manipulator [3], for example, has this type of kinematic diagram. Its position in space can be determined by the generalized coordinates φ_i (i = 0, 1, ..., 5), determining movements in the

corresponding drives. Movements in each drive are limited, and the corresponding limiting values of the angles, as before, are designated by φ_i^*.

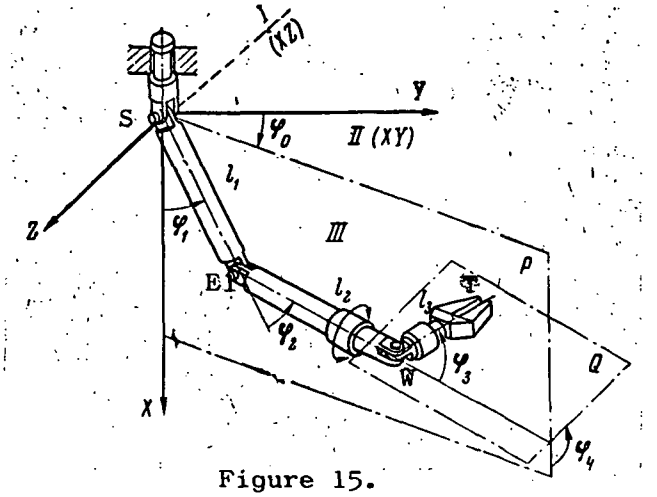

Figure 15.

/14

We will act in a manner similar to that preceding, wherein we replace the tongs with a ball joint located at some point T in the working space with coordinates (X_T, Y_T, Z_T). We obtain a three-dimensional arrangement with two degrees of freedom (rotation of link l_3 relative to its longitudinal axis is not considered). Movement will cause point W to move over the surface of a sphere with radius l_3 and center in point T. The task of determining Θ involves finding the spatial angle formed by the set of positions l_3, permitted by limitations φ_i^*.

Bear in mind that when the position of the tongs, T (X_T, Y_T, Z_T) is fixed, the wrist, W (X_W, Y_W, Z_W), and elbow, E1 (X_{E1}, Y_{E1}, Z_{E1}) can occupy two different positions. Both positions therefore must be checked from the point of view of satisfying limitations φ_i^*.

The coordinates of points T and W are set by the assigned position of the tongs, and angle φ_0, formed by the base plane, P (in which the shoulder, elbow, and wrist lie), and the Y-axis, is determined (Figure 15)

$$\varphi_0 = \operatorname{arctg} \frac{Z_3}{Y_3}.$$

Let us find angles φ_1 and φ_2.

$$\varphi_2 = \pm \arccos \frac{1}{2l_1l_2}\left(\frac{Y_3^2}{\cos^2\varphi_0} + x_3^2 - l_1^2 - l_2^2\right).$$

We can use

to find φ_1, from whence

$$\frac{Y_3}{\cos\varphi_0} = l_1 \sin\varphi_1 + l_2 \sin(\varphi_1 + \varphi_2),$$

$$\sin\varphi_1 = \frac{AB \pm \sqrt{C^2(C^2+B^2-A^2)}}{B^2+C^2}.$$

$$A = \frac{Y_3}{\cos\varphi_0}; \quad B = l_1 + l_2\cos\varphi_2; \quad C = l_2\sin\varphi_2. \tag{15}$$

We will take it that angle φ_1 can change in the limits $-\pi/2 \le \varphi_1 \le \pi/2$. Eq. (15) then will yield two values for φ_1, with the negative value of φ_2 corresponding to the larger φ_1 value.

Let us measure the relative rotation of the axes of joints E1 and W by the angle, φ_4, between planes P and Q (the latter is determined by points E1, W, T), read in the direction from plane P counterclockwise toward plane Q looking from point W to point E1. Let us find the coordinates of the point E1 /15

$$X_{E1} = l_1\cos\varphi_1; \; Y_{E1} = l_1\sin\varphi_1\cos\varphi_0; \; Z_{E1} = l_1\sin\varphi_1\sin\varphi_0.$$

The plane P equation will be

$$A_1X + B_1Y + C_1Z + D_1 = 0.$$

Here

$$A_1 = 0; \; B_1 = -\sin\varphi_0; \; C_1 = \cos\varphi_0; \; D_1 = 0.$$

The equation of the plane passing through the coordinate origin and of parallel plane Q, is found by solving

$$\begin{cases} A_2X_{E1} + B_2Y_{E1} + C_2Z_{E1} = 0, \\ A_2X_W + B_2Y_W + C_2Z_W = 0, \\ A_2X_T + B_2Y_T + C_2Z_T = 0. \end{cases}$$

Now

$$\varphi_4 = \pm\arccos\frac{C_2\cos\varphi_0 - B_2\sin\varphi_0}{\sqrt{A_2^2+B_2^2+C_2^2}}.$$

The φ_4 limitations in manipulators usually are symmetrical, so the sign of φ_4 is not significant.

We determine angle φ_3, the flexure in the wrist, to be the angle between vectors $\overline{E1W}$ and $\overline{WT}$

$$\varphi_3 = \pm\arccos\frac{(X_T - X_W)(X_W - X_{E1}) + (Y_T - Y_W)(Y_W - Y_{E1}) + (Z_T - Z_W)(Z_W - Z_{E1})}{l_2l_3}.$$

Let us use the relationship

(16)

$$X_T = l_1\cos\varphi_1 + l_2\cos(\varphi_1+\varphi_2) + l_3\cos\varphi_3\cos(\varphi_1+\varphi_2) - l_3\sin$$
$$\times\cos\varphi_4\sin(\varphi_1+\varphi_2)$$

obtained from the vector equation $\bar{l}_1 + \bar{l}_2 + \bar{l}_3 = \overline{ST}$ to establish the sign of φ_3. The φ_3 value in identity (16) that reverses will be that sought.

The result will be the finding of the angle φ_i values. Comparing them with the φ_i^* limitations, we can reach a conclusion as to the reality ($\varphi_i \leq \varphi_i^*$), or unreality ($\varphi_i > \varphi_i^*$), of the manipulator configuration for a given position of link l_3.

We now change the position of point W, leaving point T in its former place, and we repeat all the operations. We thust can establish the outlines of the spatial angle at given point T formed by real positions of the manipulator. If the manipulator has maneuverability, the whole set of positions of the mechanism satisfying the limitations imposed must be verified.

A given algorithm was used to write a program and a "Minsk-22M" electronic digital computer was used to calculate the full service factor for a manipulator with seven degrees of freedom (Figure 15). A number of variants were checked in which the lengths of the links (Table 1), and the magnitudes of the limitations on the angle of relative rotation of the links (Table 2), were changed.

The following relationships, in addition to the full service factor (Θ), were calculated: (a) the number of points in the working space at which the tongs can be oriented in the positive direction along the X-axis to the total number of points in the working space ($\bar{\delta}_1$); (b) the number of points at which the tongs can be oriented in the positive direction along the Z-axis to the total number of points in the working space, ($\bar{\delta}_2$); (c) the number of points at which the tongs can be oriented in the positive direction along the X-axis as well as in the positive direction along the Z-axis to the total number of points in the working space ($\bar{\delta}_{12}$).

Calculations were made for 245 points lying in the plane of symmetry of the working space for all variants. 256 positions of link l_3 were checked at each point. Table 3 lists the results of the calculations corresponding to each of the combinations of variants in Tables 1 and 2. /16

As may be seen from Table 3, variant 2T is the most advantageous. The example cited shows that an evaluation of the kinematic properties of a manipulator based on the service factor, $\bar{\Theta}$, permits ready selection of the most advantageous design variant.

TABLE 1

Length of links	A	B	C
l_1	98	88	108
l_2	83	93	73
l_3	25,5	25,5	25,5

TABLE 2

Limitation	1	2	3
φ_1	+45 −90	+45 −90	±90 ±90
φ_2	+135 0	+135 0	±90
φ_3	±90	+150 −30	±90
φ_4	±90	±90	±90

TABLE 3

Link length variants	1	2	3
A	$\bar{\theta} = 0,569$	$\bar{\theta} = 0,701$	$\bar{\theta} = 0,403$
	$\bar{\delta}_1 = 0,885$	$\bar{\delta}_1 = 0,889$	$\bar{\delta}_1 = 0,567$
	$\bar{\delta}_2 = 0,624$	$\bar{\delta}_2 = 0,710$	$\bar{\delta}_2 = 0,412$
	$\bar{\delta}_{12} = 0,546$	$\bar{\delta}_{12} = 0,608$	$\bar{\delta}_{12} = 0,241$
B	$\bar{\theta} = 0,498$	$\bar{\theta} = 0,675$	$\bar{\theta} = 0,374$
	$\bar{\delta}_1 = 0,844$	$\bar{\delta}_1 = 0,820$	$\bar{\delta}_1 = 0,567$
	$\bar{\delta}_2 = 0,575$	$\bar{\delta}_2 = 0,685$	$\bar{\delta}_2 = 0,396$
	$\bar{\delta}_{12} = 0,489$	$\bar{\delta}_{12} = 0,534$	$\bar{\delta}_{12} = 0,245$
C	$\bar{\theta} = 0,628$	$\bar{\theta} = 0,726$	$\bar{\theta} = 0,414$
	$\bar{\delta}_1 = 0,930$	$\bar{\delta}_1 = 0,922$	$\bar{\delta}_1 = 0,371$
	$\bar{\delta}_2 = 0,673$	$\bar{\delta}_2 = 0,722$	$\bar{\delta}_2 = 0,371$
	$\bar{\delta}_{12} = 0,618$	$\bar{\delta}_{12} = 0,649$	$\bar{\delta}_{12} = 0,371$

REFERENCES

1. Kobrinskiy, A. Ye., Stepanenko, Yu. A., "Some Problems of Manipulator Theory," V sb. Mekhanika mashin [In collection: Mechanics of Machines], No. 7-8, "Nauka" Press, 1967.

2. Artobolevskiy, I. I., Teoriya mekhanizmov [Theory of Mechanisms], "Nauka" Press, 1967.

3. Mancini, C., Roncaglia, F., "The C.N.E.N. Electric Servomanipulator Mascot," Alta frequenza, No. 6, 1963, p. 32.

N73-26076

SOME REMOTELY CONTROLLED MASTER-SLAVE MANIPULATOR DESIGN PROBLEMS

N. A. Lakota, V. I. Lobachev

ABSTRACT. A number of specific requirements for designing remotely controlled master-slave manipulators, including the kinematics and the dimensions of the master and slave members, are presented. General requirements for master-slave manipulator control systems are discussed.

A number of specific requirements, determined by the following factors, must be considered when designing remotely controlled master-slave manipulators: (a) the types of operations the manipulator must perform; (b) the peculiarities of the human operator, the working movements of whose hands are copied by the manipulator slave elements; (c) the kinematics and dimensions of the manipulator master and slave elements. It is the second and third factors that permit the formulation of certain general requirements for master-slave manipulator control systems. /17

Peculiarities of the Human Operator Considered in Designing Master-Slave Manipulators

Master-slave manipulators, as distinguished from other types, should, to a considerable degree, correspond to the anthropometric and physiological peculiarities of the human operator performing the control function. We shall consider only certain of these peculiarities with significant effect on the properties of master-slave manipulators.

Kinematics of the Human Arm

A number of authors have written of their studies of the kinematics of the human arm. However, reference [1] is the most meaningful from the point of view of manipulator design, pointing out that the human arm can be depicted as an open kinematic chain with 12 degrees of freedom. However, the total number of degrees of freedom in the kinematic chain of the human arm can be reduced to nine, I-IX (Figure 1), if we consider the shoulder joint immobile. We will consider this scheme of the kinematic chain as the original one in determining the kinematics of manipulator master and slave elements.

The Operator's Work Zone

Knowing the kinematic peculiarities, and the typical dimensions of the human arm as cited in reference [2], we obtain the limits of the zone in which the

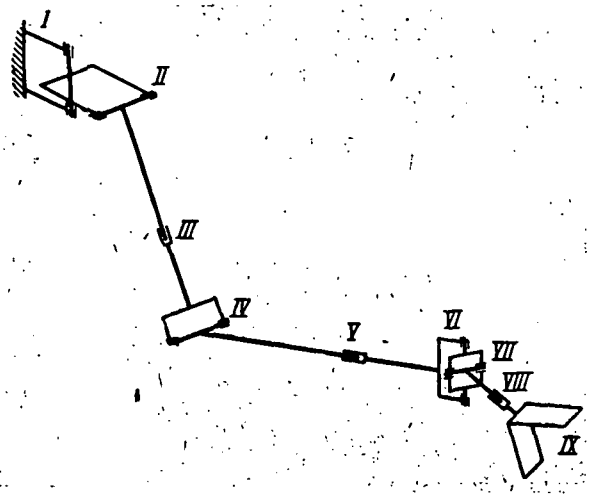

Figure 1.

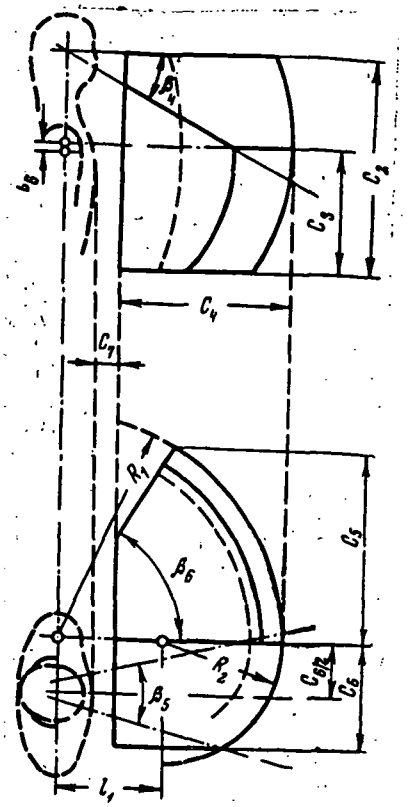

Figure 2. The arm's normal work zone.

$\beta_4 = 30°$; $\beta_5 = 30°$; $\beta_6 = 60°$; $c_2 = 679$; $c_3 = 360$; $c_4 = 520$; $c_5 = 590$; $c_6 = 315$; $l_1 = 326$; $l_8 = 25$; $R_1 = 643$; $R_2 = 367$; $c_7 = 10 \div 50$

operator can work, in which objects can be gripped. Reference [3] notes that from the physiological point of view it is undesirable to use all of the zone when working. The least fatiguing movements prove to be those in which only the forearm, hand, and fingers participate. The whole arm, up the shoulder, moves when the work cycle is short (1-2 minutes) and short rests are permitted. The shoulder joint should not move during work movements. As a result, we can distinguish the arm's so-called normal work zone (Figure 2). /18

The space occupied by the operator's body and head should be made inaccessible to the master element for safety reasons by providing a space of to 5 to 10 cm between the zone in which the master elements work and the body when control systems are used under conditions when there is active force reflection. The height of the work zone depends on the working operations to be performed and can be selected equal to the height of the forearm, or of the eyes, above the lower limit of the zone. The complex form of the upper limit of the work zone is explained by the fact that the spatial area within the operator's field of view is not in the work zone.

The determination of the normal work zone, in addition to purely physiological factors must include operator working conditions when, because of cramped quarters, or because his attitude makes it inconvenient for him to move his arms, the zone can be quite restricted. This is typical, for example, of deep submergence vehicles.

Knowing the operator's normal work zone, let us determine the scaled work zone for the manipulator slave elements. We will understand this to mean the reduced (increased) copy of the given work zone for the slave elements completely inscribed in the volume of the operator's normal work zone. The master element tongs (the operator's hand) will move within the limits of the scaled work zone for the slave element. The scale factor, K_s, equal to the ratio of the linear dimensions of the scaled work zone and the given work zone for the slave elements determines the ratio between the linear dimensions of master and slave elements of the master-slave manipulator. /19

The Nature of Movements of the Hand of an Unloaded Arm

According to existing systems for classifying man's work movements [4], any work operation can be made up of a limited number of elementary movements. Of the elementary movements characteristic of working with master-slave manipulators, the precise (careful) movement of the hand without a load to a specific point in space has the greatest velocities and accelerations. The purpose of the movement is determined by the operator. A series of experiments was conducted under the conditions listed to determine the nature of hand movements. Figure 3a shows the results for the range of change in arm trajectories obtained in the different experiments, and the averaged trajectory. Figure 3b portrays the experimentally obtained trajectories for different distances between the initial and end points of hand movement. We see (1) the operator's hand movements are monotonic, (2) that the acceleration processes are the same for the majority of the reactions, (3) that the speed of movement remains constant over the mean section of the trajectory when hand movement is more than 2 to 3 cm, (4) and that the greatest scatter in the nature of the reactions is observed over the braking portion, where the type of trajectory is determined by the purpose of the movement and the operator's state of training.

The results agree well with the results of the investigation of the hand

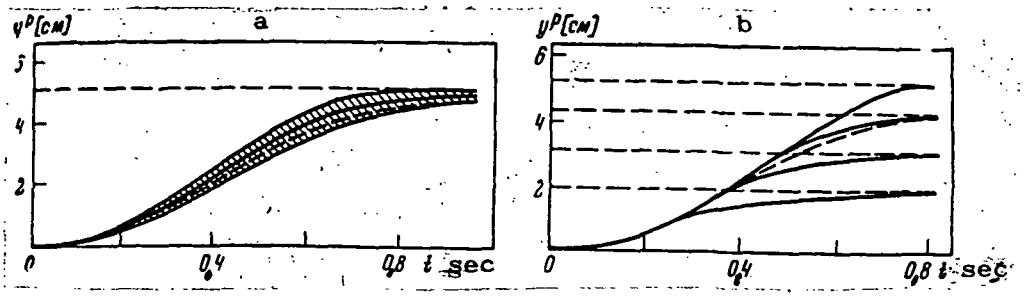

Figure 3. Change in arm trajectory.
a - range of change in trajectories; b - trajectories for different distances between the beginning and end points of hand movements.

movements of an operator's unloaded arm when the purpose of the movement is assigned by the experimenter. As reference [5] points out, the movement process in this case has the form shown in Figures 3a and 3b by the dashed line, and is described by the expression

$$Y^p = L[1 - (1 + 6t + 18t^2)e^{-6t}], \quad (1)$$

where L is the distance the hand moves. The different nature of the braking portions evidently can be explained by the different goals assigned the operators in the experiments. The indicated differences are insignificant, so when L = 5 cm, Eq. (1) can be used to describe the acceleration and deceleration processes in our case, too.

Having ascertained the nature of the hand movements of an unloaded arm, we have determined the type of input action for master-slave manipulator control systems.

Kinematics of Master and Slave Elements of Master-Slave Manipulators /20

The kinematic scheme for master and slave elements of master-slave manipulators should meet the following requirements: (1) ensure the reach of the tongs of the master or slave element to any point in the work zone and the orientation of the tongs as necessary at each of these points; (2) provide the operator with the ability to control all the degrees of freedom of the master slave elements; (3) ensure the absence of intensive moments of the intermdiate kinematic links between the point where the kinematic chain is attached and the tongs of the master or slave element with change in orientation of the tongs at any point in the work zone; (4) when obstacles are present in the work zone of the slave

elements which hinder access to individual points in the zone, ensure mobility of individual kinematic links when the tongs are fixed that will establish the maneuverability of the manipulator [6]. Let us examine possible variants of kinematic diagrams for the master and slave elements of master-slave manipulators.

The Kinematic Scheme When Following the Positions of the Operator's Shoulder, Forearm, and Hand

The master element of the master-slave manipulator, which follows the position of the operator's shoulder, forearm, and hand, is fastened to the operator's shoulder girdle. The kinematic scheme for master and slave elements is similar to that of the human arm and has nine degrees of freedom, including the degree of freedom for the tongs (see Figure 1).

The point at which the master element is attached to the operator's girdle is movable in space, so the one-to-one correspondence between positions of master and slave will be constantly disrupted (the point of attachment of the latter is stationary relative to the body of the manipulator carrier. Therefore, in existing manipulator designs every effort is made to keep the point of attachment of the master element stationary in space, and this often restricts the capacity to follow the positions of the operator's hand, or of his forearm and hand.

The Kinematic Scheme When Following the Position of the Operator's Hand

The master element following the position of the operator's hand has a number of advantages as compared to the variation examined above: the point of attachment of the master element is stationary in space; the number of degrees of freedom of the master element can be less than the number of degrees of freedom of the human arm itself; there is no need to match the master element to the individual features of the arm of a specific operator; the operator's arm can be freed from the master element very simply and quickly.

The movement of the tongs within the limits of a specified work zone is possible with the help of a kinematic scheme that contains a minimum of three degrees of freedom characterizing either translation, or rotative, motion. Figure 4 shows eight possible variations in the position of degrees of freedom I, II, and III in the kinematic chain of the master or slave element. Some are widely used in existing manipulators. The difficulties in obtaining extensive translation motions have led to the use of a kinematic scheme with

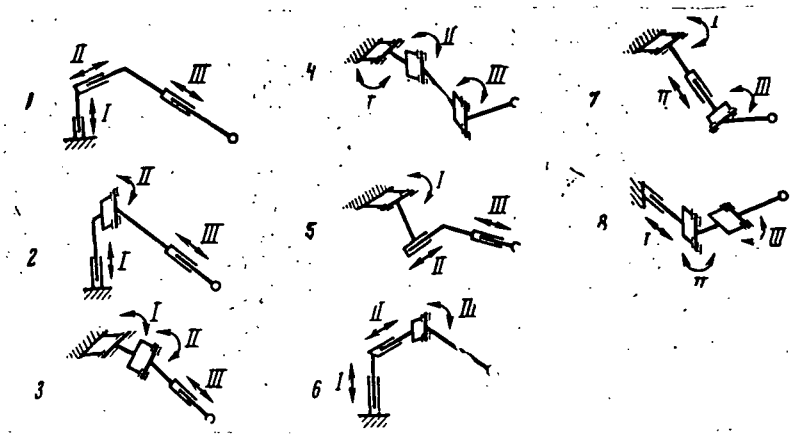

Figure 4.

eight degrees of freedom, obtained from the scheme in Figure 1 by the exclusion of the degree of freedom for the rotation of the shoulder (III) and which, consequently, is variant 4 in Figure 4. /21

Let us consider another possibility for reducing the number of degrees of freedom in the kinematic scheme for master and slave elements, that of excluding, from the scheme in Figure 1 the degrees of freedom of rotation of the tongs (VIII) and rotation of the forearm (V). Figure 5a shows this kinematic scheme (the numbers of the degrees of freedom I, II, III, IV, VI, VII, IX, here and in subsequent variants of simplified kinematic schemes correspond to the numbers in Figure 1). Here rotation of the tongs is possible only when its position is completely determined, that is, when the axis of rotation passes through the point at which the master element is attached, and we now will say the tongs have selective rotation. Intensive movements of the shoulder and forearm of the master and slave elements will be observed upon rotation, and the elbow hinge will describe an arc equal to the angle of rotation. The two shortcomings noted are substantial and limit the use of the simplified variant considered.

Inherent in the kinematic scheme that results upon the elimination from the kinematic scheme in Figure 1 of the degree of freedom of rotation of the tongs (VIII), and of one of the degrees of freedom causing it to adduct-abduct, or flex-extend, (VI) or (VII), are the same shortcomings noted for the preceding simplified scheme, except for the fact that the tongs have two selective rotations.

The addition of the freedom of rotation of the tongs (VIII) returns to both variants the possibility of arbitrary orientation of the tongs to any

point in the work zone. But if the longitudinal axis of stationary tongs passes through the point at which the master (slave) element is attached, the elbow hinge will be able to move in an arbitrary manner along a circle with its center in the longitudinal axis of the tongs, that is, the kinematic scheme has one degree of maneuverability. This indicates that a certain class of kinematic schemes has the property of selective maneuverability because the presence, or absence, of maneuverability is determined by the position of the tongs in space.

If the master element following the position of the operator's hand has one degree of maneuverability for arbitrary orientation of the tongs (Figure 1), or selective maneuverability (Figure 5b), the operator cannot control the position of the shoulder hinge by moving the tongs. Any external influence on the master or slave element (the element's own weight, contact with foreign objects, hydrodynamic forces) will cause the elbow hinge to move. Such movement usually is undesirable, and sometimes even is dangerous for the operator, and for objects in the work zones. Thus, it is possible to control all degrees of freedom of the master element following the position of the operator's hand if its kinematic /22 chain does not have a single degree of maneuverability.

Complete lack of maneuverability while retaining the ability to orient the tongs arbitrarily to any point in the work zone can be obtained from the above-considered simplified variants of the kinematic scheme (see Figure 1) only by eliminating the shoulder rotation degree of freedom (III) and providing for two degrees of freedom (I and II) in the shoulder hinge so the shoulder can swing (Figure 6, modification I). The hand joint can be made with modifications 1, 2, and 3 in Figure 6. Selection of the particular modification depends on providing the necessary orientation of the tongs with the gearing and motors used in the control systems.

Figure 5c is a kinematic scheme that differs little externally from that portrayed in Figure 6, modification 1. The only difference is that the axis of rotation of one of the degrees of freedom of the shoulder hinge passes through the work zone of the master (slave) element; that is, the shoulder hinge imparts rotation and swing to the shoulder. The result is to give the kinematic scheme selective maneuverability; that is the kinematic schemes in Figure 6 are suitable /23

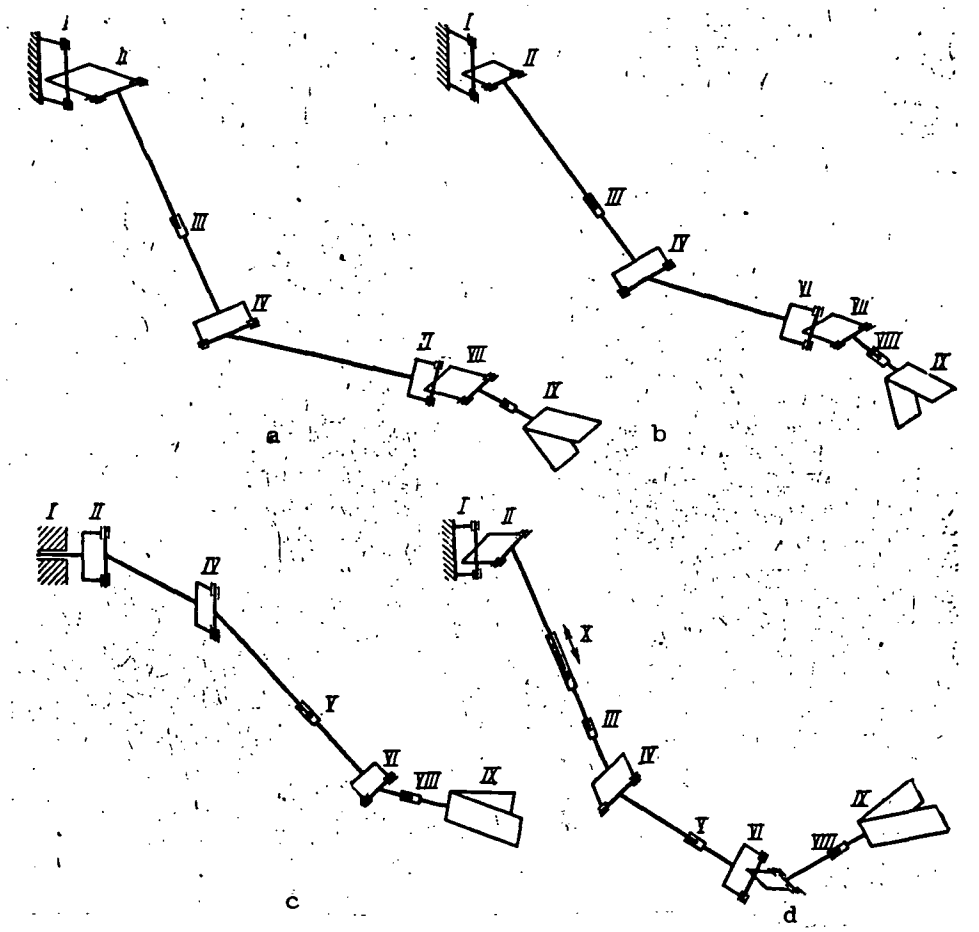

Figure 5. Kinematic schemes in which the number of degrees of freedom change (see Figure 1). a - kinematic scheme obtained by the elimination from the scheme (see Figure 1) of degrees of freedom V and VIII; b - kinematic scheme with selective maneuverability; c - kinematic scheme in which the shoulder hinge communicates rotation and swing to the shoulder; d - kinematic scheme with ten degrees of freedom.

for use in the master and slave elements of master-slave manipulators that follow the position of the operator's hand if the axes of rotation of the degrees of freedom of the shoulder hinge (I and II) do not intersect the work zones.

Kinematic Scheme When Following the Positions of the Operator's Forearm and Hand

The need to preserve the maneuverability of the master and slave elements of a master-slave manipulator when the operator must be able to control all the degrees of freedom in their kinematic schemes requires that the positions of the operator's forearm and hand be followed. If the point of attachment of the

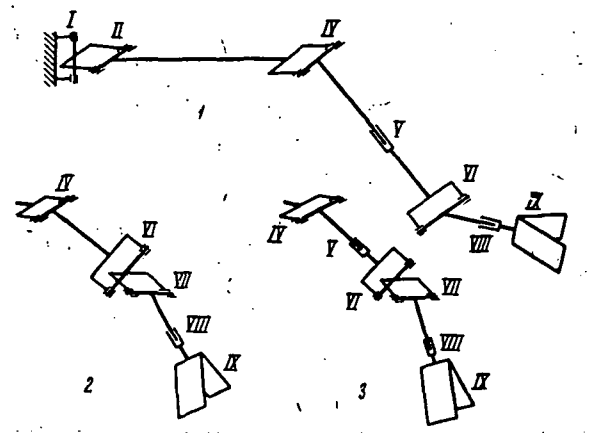

Figure 6.

master element is not at the operator's shoulder girdle, the positioning of the elbow hinge of the master element at any point in space accessible to the elbow joint of the operator's arm can be accomplished by three degrees of freedom with rotational or translational movements, variants in the disposition of which are presented in Figure 4. The kinematic scheme shown in Figure 5d, for example, can be used to follow the positions of the operator's forearm and hand in a mockup of a master element designed to investigate the motion parameters of the human arm [1]. The number of degrees of freedom in the master (slave) element of a master-slave manipulator in this case is 10.

Thus, if there is no need for the slave elements of a master-slave manipulator to have maneuverability, it is desirable to use the master element to follow the position of the operator's hand and to use a kinematic scheme with seven or eight degrees of freedom (Figure 6). If the slave elements must be maneuverable, the master elements must be selected on the basis of the need to follow the positions of the operator's forearm and hand, and the number of degrees of freedom in the kinematic scheme is increased to 10 (see Figure 5d).

Dimensions of the Master and Slave Elements of Master-Slave Manipulators

The original data for determining the dimensions of the mater and slave elements are: the kinematic scheme selected for the master and slave elements; the dimensions of the work zone for the slave elements; the dimensions of the normalized work zone for the slave elements, or the magnitude of the scale factor K_s; the position of the points of attachment of the slave elements relative to the work zone; the possible orientation of the tongs at each of the points on the boundary of the work zone, determined by manipulator working conditions and the list of work operations; the dimensions of the hand kinematic link of the slave element, determined during the draft design study state and based on the condition that here the arrangement of the slave elements and gearing

/24

will provide specified forces for compressing and rotating the jaws of the tongs.

Dimensions of Master and Slave Elements for Following the Position of the Operator's Hand

If the master and slave elements of a master-slave manipulator follow the position of the operator's hand, the dimensions of the slave element are established first.

Knowing the magnitude of the work zone for the slave element, the dimensions of the hand kinematic link, and the necessary orientation of the tongs at each point on the boundary of this work zone, we select the region in space in which the hand hinge is located when performing the operations. Let us determine the dimensions of the shoulder and forearm of the slave element. Because its kinematic scheme has no degree of freedom for rotation of the shoulder, movement of the forearm relative to the shoulder is possible only in the plane in which the longitudinal axes of these kinematic links are located. The cross section of this plane of the three-dimensional figure formed as the end of the forearm (hand hinge) moves is a part of a circular ring (Figure 7). The following designation are used in the figure: OA is the internal radius; OB is the external radius; OC is the length of the shoulder; BC is the length of forearm; δ_{El} is the angle of rotation in the elbow hinge; δ_{Sh} is the angle of rotation in the shoulder hinge (central angle of the circular ring); δ'_{Sh} is the complementary angle of rotation in the shoulder hinge because of movement of the forearm; γ is the auxiliary angle.

Parameters OA, OB, and δ_{Sh} are determined by the location of the point of attachment of the slave element relative to the work zone and the magnitude of the region in space in which the hand hinge is located when performing work operations.

The calculations include the determination of the shoulder and forearm dimensions for given angles of rotation, δ_{El} and δ'_{Sh}. Analysis of all possible variants involves a great many calculations, so a simplfying nomogram shown in Figure 8a, has been developed. The sequence in which the nomogram is used is as follows:

we lay off the value of angle δ'_{Sh} on scale 1, and on scale 2 read the points corresponding to the dimensions (OA + OB) and (OB - OA); we read the magnitude of

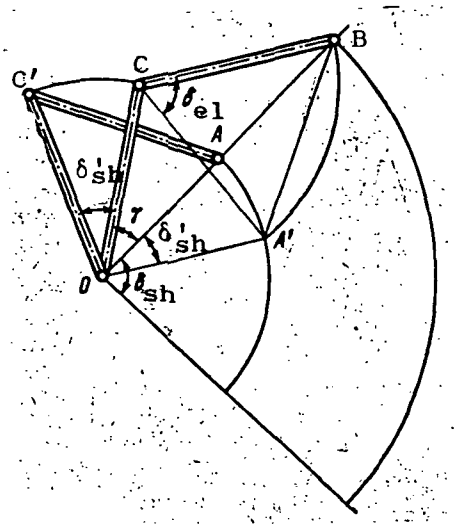

Figure 7.

the difference in angles OA'B and OBA' off irregular scale 3 (Figure 8b);

we read the magnitude of angle OA'B off scale 4 (see Figure 8b);

setting dimension OB, we read dimension A'B from scale 8 (see Figure 8b);

setting the angle of rotation of the elbow hinge, δ_{El}, we read the dimension of the forearm BC from scale 7 (see Figure 8c); /26

going back to scales 1 and 2, we lay off ($\angle OA'B - \angle CA'B$) and (BC $\pm$ OA') (see Figure 8d);

we read angle ($\delta_{Sh} + \gamma$) from scale 4 (see Figure 8d);

we read the shoulder dimension OC from scale 8 (see Figure 8d).

Figures 9a and b show the results of the calculations of slave element shoulder and forearm dimensions for different values of angles of rotations, δ_{El} and δ'_{Sh} for OA/OB = 0.5.

Let us determine the dimensions of the master element of a master-slave manipulator. The dimensions of its kinematic links are equal to those of the kinematic links of the slave element multiplied by the scale factor K_s. The angles of rotation in the hinges of the master and slave elements are the same. The distance between the points of attachment of the master elements is equal to the distance between the points of attachment of the slave elements multiplied by the scale factor K_s.

Dimensions of Master and Slave Elements for Following the Positions of the Operator's Hand and Forearm

The dimensions of the master element are determined first if the master and slave elements of a master-slave manipulator follow the positions of the operator's hand and forearm.

1. Knowing the necessary orientation of the tongs of the slave element at each point of the boundary of its work zone, we determine the region of space in which the hand hinge is located when at work.

2. Using the known scale factor K_s, we determine the region of space in which operator's wrist joint is located when performing specified work operations.

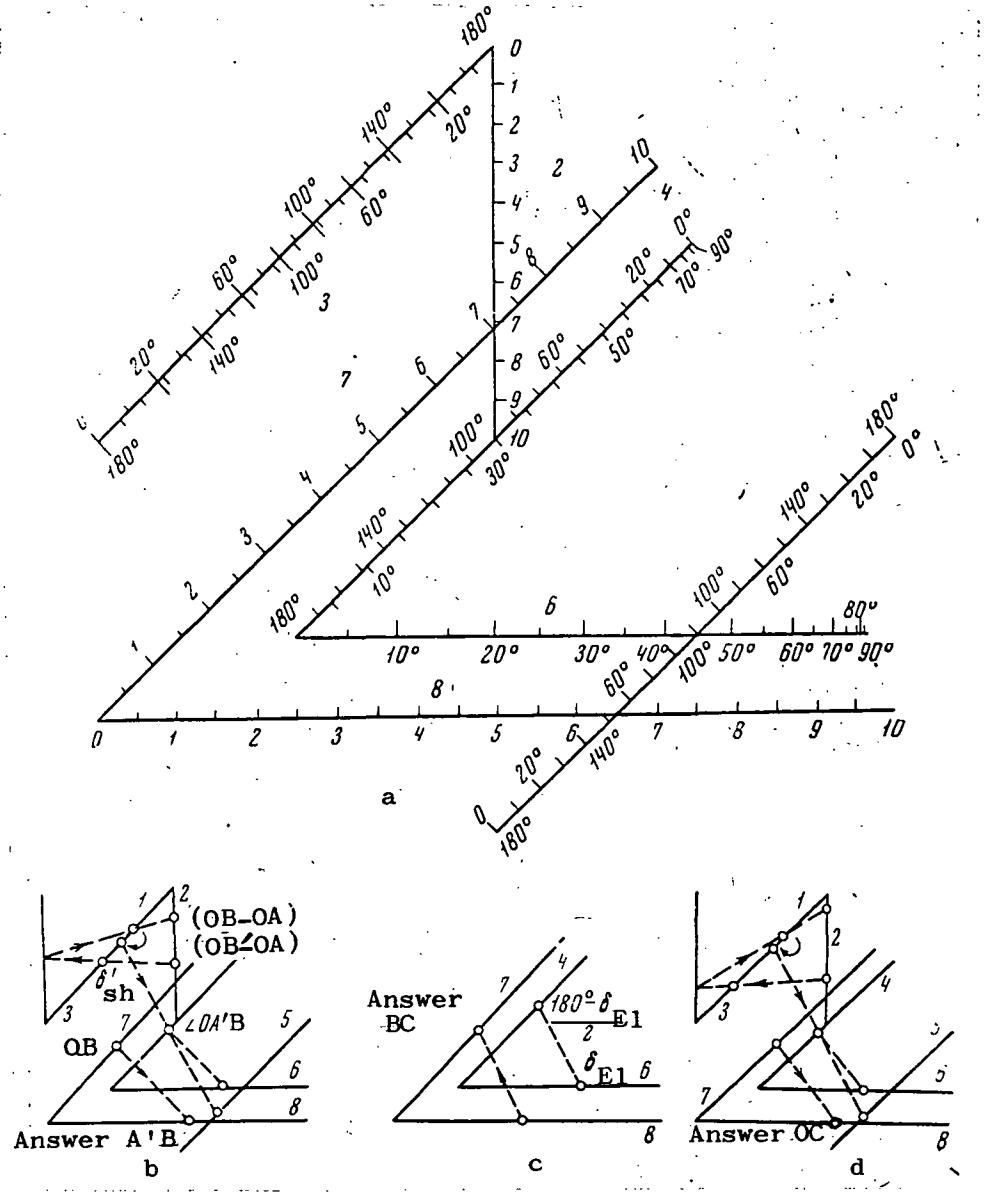

Figure 8. Determination of shoulder and forearm dimensions for given angles of rotation δ_{El} and δ_{Sh}. a - nomogram for determining dimensions; b, c, d - sequence in which nomogram is used.

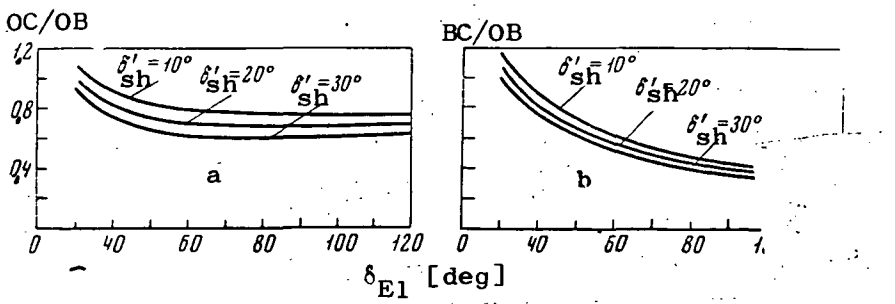

Figure 9. Results of calculations of shoulder and forearm dimensions. a - for ratio OC/OB; b - for ratio BC/OB.

3. Knowing the region of space in which the wrist joint should move, and the dimensions of the operator's forearm, we establish the region of space in which the elbow joint can be located.

4. We determine the distance between the points of attachment of the master elements in terms of the known magnitude of the distance between the points of attachment of the slave elements and the magnitude of K_s.

5. If variant 3 of the kinematic scheme in Figure 4 is used to follow the position of the elbow joint, it is sufficient to find the nearest and farthest positions of the elbow joint (of the elbow hinge of the master element) with respect to the point of attachment of the master element. The difference in these distances is equal to the magnitude of the linear movement in the corresponding degree of freedom. Determined simultaneously are the dimensions of the kinematic shoulder link and the angles of rotation in the degrees of freedom of the shoulder hinge.

6. Using the scale factor K_s, we determine the dimensions of the slave elements. The angles of rotation and the linear movements in the corresponding degrees of freedom of the master and slave elements should be the same.

This calculation procedure provides the dimensions of the master and slave elements of master-slave manipulators built in accordance with the kinematic schemes recommended.

Requirements for Systems for Controlling the Different Degrees of Freedom of the Slave Element of a Master-Slave Manipulator

/27

Once we have analyzed the peculiarities of the human operator, and the kinematics and dimensions of the master and slave elements of a master-slave manipulator, we can formulate some requirements for the systems for controlling the different degrees of freedom of the slave element.

Power Required for Systems for Controlling the Different Degrees of Freedom

Reference [1] determined the power the human arm develops at the different degrees of freedom of the master element. These data can be used to calculate the power required for systems controlling the different degrees of freedom of the slave element of a master-slave manipulator with the same dynamic properties as the arm. Considering that the load is made up of dynamic and

static components, the maximum power values can be calculated from

$$N^{se}_{max} = N^{30}_{max} \frac{1 + K_s K_{st} K'_w D}{K_s^2 K_{st}^2 K_w (1 + D)}, \qquad (2)$$

where

$$D = \frac{g}{r\ddot{\delta}_{max}};$$

g is the free fall acceleration;

δ_{max} is the maximum acceleration for the corresponding degree of freedom;

r is the coordinate of the center of gravity of the kinematic links of the arm set in motion by the degree of freedom considered;

N^{30}_{max} is the maximum power developed in the corresponding degree of freedom of the master element;

K_s is the scale factor;

K_w is the weight factor, equal to the ratio of the weights of the kinematic links of the arm and slave element set in motion by the degree of freedom considered;

K'_w is a coefficient, the magnitude of which is determined by the ratio of the weights of the load which can be borne by the slave element and the kinematic links of the slave element set in motion by the degree of freedom considered.

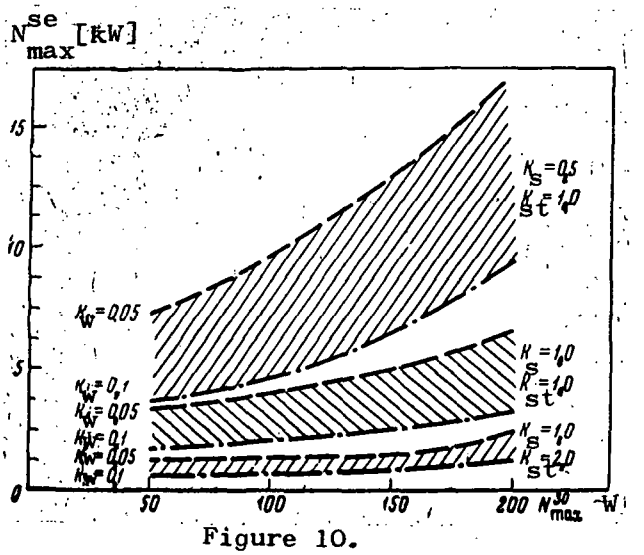

Figure 10.

The weight of the slave element can be taken preliminarily as equal to the maximum load capacity of the manipulator. $K'_w = 3$ for degrees of freedom I and II in the kinematic scheme in Figure 10; $K'_w = 5$ for IV and V; and $K'_w = 15$ for VI, VII, and VIII. Figure 10 gives the powers required for systems for controlling the different degrees of freedom of the slave element of a master-slave manipulator for concrete values of the coefficients. The maximum powers required for systems for controlling a master-slave manipulator are 1.5 - 2.5 kW, given the same magnitude of work zones for master and slave elements ($K_s = 1.0$) and a manipulator load capacity of 40 kg ($K_w = 0.1$). If the magnitude of the work zone for the master elements is half that of the work zone for the slave elements ($K_s = 0.5$), powers increase to 3.5 - 9.5 kW for the same load capacity. /28

These results are valid for a tentative estimate of the powers required for systems for controlling the slave element following the position of the operator's hand.

Input Influences of Systems for Controlling the Different Degrees of Freedom

Considered above were the peculiarities of trajectories over which the tongs of the master element of a master-slave manipulator move. Movement of the tongs can cause movement of any of the degrees of freedom of the kinematic chain of the master element. Eq. (1) therefore describes the input influence of any of the master-slave manipulator control systems. The amplitude of the input influence is different for each of the control systems, and is determined by the distance of the tongs from the axis of the rotation of the corresponding degree of freedom; that is, by the dimensions of the master element.

Maximum Velocities and Accelerations of the Different Degrees of Freedom. Equivalent Working Frequency for Control Systems

Knowing the maximum linear velocities and accelerations of movements of the master element tongs, one readily can determine the maximum angular velocities and accelerations developed in each of the degrees of freedom of the master element's kinematic chain for known kinematics and dimensions

$$\dot{\delta}_{max} = \dot{y}^p_{max}/l;\ \ddot{\delta}_{max} = \ddot{y}^p_{max}/l,$$

where l is the minimum possible distance between the tongs and the axis of rotation of the given degree of freedom.

The equivalent working frequency of the harmonic influence for any of the master-slave manipulator control systems will equal

$$\omega_p = \ddot{\delta}_{max} / \dot{\delta}_{max} = 5\left[\frac{1}{sec}\right].$$

Quality of Transients in Master-Slave Manipulator Control Systems

Characteristic of master-slave manipulator control systems are several operating modes for each of which there are definite requirements with respect to the quality of the transients in the systems.

1. The transport mode, during which the positions in space of the master and slave elements are matched when the master-slave manipulator is energized. The master elements are fixed in space, or are kept immobile by the operator. /29

The quality criterion for the transients in the systems in this mode is the magnitude of the overcontrol, selected on the basis of the characteristics of the work zone for the manipulator's slave elements. If the work zone is free of foreign objects when the manipulator energized the overcontrol can be comparatively great, reaching 20-30%, but if foreign objects or the manipulator carrier housing, are present in the zone when the manipulator is energized, the overcontrol should be 5 to 10%.

2. The following mode, the basic control system operating mode, when following (copying) the movements of the master element. An Eq. (1) type signal is supplied to the control system input, as has been noted above. The control system transients should have a maximum duration of $t_{max} = t_a + t_1$ in order to ensure naturalness in the work of the operator. Here t_a is the duration of the arm movement process. Time $t_1 = 0.2$ second is determined by the delay in the operator's reaction to the incoming external signal (by the latent period). In other words the transients in the control systems should be over when the operator begins the next stage of work.

3. The abrupt change in load mode when the tongs of the slave element come in contact with or, conversely, lose contact with, the object or load being moved during the work process. This same mode is encountered during collisions between the slave element and objects in the work zone.

Given the condition of naturalness of work by the operator, the duration of transients in master-slave manipulator control systems when there is an abrupt change in load should not exceed t_1 = 0.2 second. The magnitude of the relative maximum deviation also is limited because the work is conducted close to objects located within the limits of the work zone.

The requirements for control system for powerful master-slave manipulators formulated in this paper will make it possible to obtain the initial data for their design.

REFERENCES

1. Bor-Ramenskiy, A. Ye., Kuleshov, V. S., Lakota, N. A., Lobachev, V. I., "Some Principles of the Construction of Remotely Controlled Master-Slave Manipulators," V sb: Mekhanika mashin [In collection: Mechanics of Machines], No. 7-8, "Nauka" Press, 1967.

2. Varlamov, R. G., Osnovy khudozhestvennogo konstruirovaniya radioelektronnoy apparatury [Principles of Artistic Design of Radioelectric Equipment], Sov. Radio Press, Moscow, 1967.

3. Lomov, B. F., Chelovek i tekhnika [Man and Technology], Sov. Radio Press, 1966.

4. Baumgarten, Fr., "Classification of Hand Movements in Science and Industry," Industrielle Organisation, No. 2, 1957, p. 26.

5. Gidikov, A. A., Kibernetika i kortikal'naya regulyatsiya dvizheniya [Cybernetics and the Cortical Regulation of Movement], Sofia, 1964.

6. Kobrinskiy, A. Ye., Stepanenko, Yu. A., "Some Problems in Manipulator Theory," V sb. Mekhanika mashin [In collection: Mechanics of Machines], No. 7-8, "Nauka" Press, 1967.

N73-26077

KINEMATIC ANALYSIS OF SPATIAL SLAVE MECHANISMS FOR MANIPULATORS BY THE MATRIX METHOD

Ye. I. Vorob'yev

ABSTRACT. The use of spatial mechanisms with many degrees of freedom as manipulator slave mechanisms is discussed. An analysis of these mechanisms by the matrix of 3rd order method is presented.

The recent development of a number of new branches of engineering requires 230 the employment of manipulators [1]. Spatial mechanisms with many degrees of freedom are used as the slave mechanisms in manipulators. A natural method of kinematic analysis of such mechanisms is the matrix method, which permits a more complete investigation to be made of their kinematics, as well as to order and reduce computations and thus facilitate the use of computer technology. Some of the first papers on the application of the matrix calculation to mechanisms were references [2, 3]. Reference [4] is devoted to the use of matrices with complex elements to analyze spatial mechanisms. Homogeneous coordinates, and matrices of 4th order were used successfully to analyze spatial gearing and spatial mechanisms in references [5, 6].

This paper analyzes the kinematics of spatial mechanisms for manipulators by using the matrix of 3rd order method. This method, as distinguished from known matrix methods for analyzing spatial mechanisms, is based on the simultaneous use of two matrix equations to transform the coordinates of a point and vector, and thus manage with matrices of 3rd order.

Let us establish the connection between the generalized coordinates characterizing the movement of the solid transported, and the generalized coordinates determining the position of the slave.

Let us examine first the slave without spherical pairs in Figure 1 (the mechanism of the "Mascot-1" manipulator [1]).

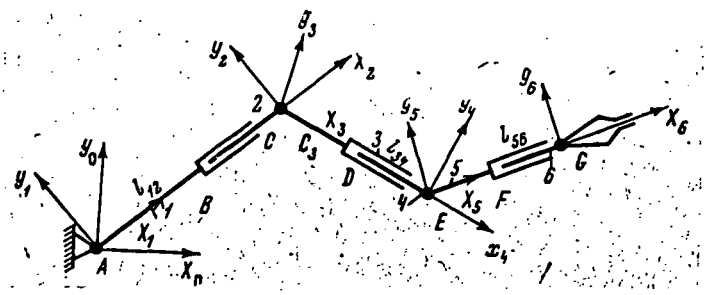

Figure 1.

Let us associate a system of coordinates with each link in the mechanism. 31
Let us associate the $X_0Y_0Z_0$ system with the support, placing the origin at A, and let us direct the Z_0 axis along the axis of pair A. Let us associate the $X_1Y_1Z_1$ system with link 1, placing the origin at A, and let us direct the X_1 axis along the axis of link 1, and the Z_1 axis parallel to the Z_0 axis. Let us associate the $X_2Y_2Z_2$ system with link 2, placing the origin at C, and let us direct the X_2 axis along the axis of link 2, and the Z_2 axis along the axis of turning pair C. Let us associate the $X_3Y_3Z_3$ system with link 3, placing the origin at C, and directing the X_3 axis along the axis of link 3, and the Z_3 axis along the axis of turning pair C. Let us asscoiate the $X_4Y_4Z_4$ system with link 4, placing the origin at E, and directing the X_4 axis along the axis of link 4, and the Z_4 axis along the axis of turning pair E. Let us associate the $X_5Y_5Z_5$ system with link 5, placing the origin at E, and directing the X_5 axis along the axis of link 5, and the Z_5 axis along the axis of turning pair E. And finally, let us associate the $X_6Y_6Z_6$ system with link 6, placing the origin at 6, and let us direct the X_6 axis along the axis of link 6, and the Z_6 axis along the axis of rotation of the tongs of pair G.

Let the coordinates of the pole of an arbitrary point, O, in the $X_6Y_6Z_6$ system rigidly coupled to the tongs link be equal to X_6, Y_6, Z_6. Let us write the coordinates of this same point in the $X_5Y_5Z_5$ system, using the matrix equation

$$X_5 = M_{56}X_6 + L_6, \tag{1}$$

where

X_5, X_6 are, respectively, the columns of the coordinates of point O in the $X_5Y_5X_5$ and $X_6Y_6Z_6$ systems;

M_{56} is the matrix of rotation for the transition from the $X_6Y_6Z_6$ system to the $X_5Y_5Z_5$ system;

L_6 is the parallel transfer matrice for the transition from the $X_6Y_6Z_6$ system to the $X_5Y_5Z_5$ system.

The $X_5Y_5Z_5$ system can be combined with the $X_6Y_6Z_6$ system by rotation about the X_5 axis through angle α_{56}, and by transfer along the X_5 axis by l_{56}, so the matrices have the forms

$$M_{56} = \begin{Vmatrix} 1 & 0 & 0 \\ 0 & \cos\alpha_{56} & -\sin\alpha_{56} \\ 0 & \sin\alpha_{56} & \cos\alpha_{56} \end{Vmatrix}, \tag{2}$$

$$L_{56} = \begin{Vmatrix} l_{56} \\ 0 \\ 0 \end{Vmatrix} \tag{3}$$

The $X_4Y_4Z_4$ system can be combined with the $X_5Y_5Z_5$ system by rotation about the Z_4 axis through angle γ_{45}.

Now the rotation matrix will have the following form for transition from the $X_5Y_5Z_5$ system to the $X_4Y_4Z_4$ system.

$$M_{45} = \begin{Vmatrix} \cos\gamma_{45} & -\sin\gamma_{45} & 0 \\ \sin\gamma_{45} & \cos\gamma_{45} & 0 \\ 0 & 0 & 1 \end{Vmatrix} \tag{4}$$

The matrix equation for the transition to the $X_4Y_4Z_4$ system is

$$X_4 = M_{54}(M_{56}X_6 + L_{56}), \tag{5}$$

where

X_4 is the column of the coordinates of point O in the $X_4Y_4Z_4$ system.

The $X_3Y_3Z_3$ system can be combined with the $X_4Y_4Z_4$ system by transfer along the X_3 axis by the magnitude l_{34} and by rotation about the X_3 axis through angle α_{34}. The rotation matrix for the transition from the $X_4Y_4Z_4$ system to the $X_3Y_3Z_3$ system is /32

$$M_{34} = \begin{Vmatrix} 1 & 0 & 0 \\ 0 & \cos\alpha_{34} & -\sin\alpha_{34} \\ 0 & \sin\alpha_{34} & \cos\alpha_{34} \end{Vmatrix} \tag{6}$$

The transfer matrix is

$$\begin{Vmatrix} l_{34} \\ 0 \\ 0 \end{Vmatrix} \tag{7}$$

The matrix equation for the transition to the $X_3Y_3Z_3$ system is

$$X_3 = M_{34}M_{54}(M_{56}X_6 + L_{56}) + L_{34}, \tag{8}$$

where

X_3 is the column of the coordinates of point O in the $X_3Y_3Z_3$ system.

The $X_2Y_2Z_2$ system can be combined with the $X_3Y_3Z_3$ system by rotation about the Z_2 axis through angle γ_{23}. The rotation matrix for the transition from the $X_3Y_3Z_3$ system to the $X_2Y_2Z_2$ system has the form

$$M_{23} = \begin{Vmatrix} \cos\gamma_{23} & -\sin\gamma_{23} & 0 \\ \sin\gamma_{23} & \cos\gamma_{23} & 0 \\ 0 & 0 & 1 \end{Vmatrix}. \tag{9}$$

The matrix equation for the transition to the $X_2Y_2Z_2$ system has the form

$$X_2 = M_{23}[M_{34}M_{45}(M_{56}X_6 + L_{56}) + L_{34}], \tag{10}$$

where

X_2 is the column of the coordinates of point 0 in the $X_2Y_2Z_2$ system.

The $X_1Y_1Z_1$ system can be combined with the $X_2Y_2Z_2$ system by transfer along the X_1 axis by the quantity l_{12} and by rotation about the OX_1 axis through angle α_{12}. The rotation matrix for the transition from the $X_2Y_2Z_2$ system to the $X_1Y_1Z_1$ system has the form

$$M_{12} = \begin{Vmatrix} 1 \\ 0 \\ 0 \end{Vmatrix} \tag{11}$$

The transfer matrix has the form

$$L_{12} = \begin{Vmatrix} l_{12} \\ 0 \\ 0 \end{Vmatrix}. \tag{12}$$

The matrix equation for the transition to the $X_0Y_0Z_0$ system has the form

$$X_1 = M_{12}M_{23}[M_{34}M_{45}(M_{56} \cdot X_6 + L_{56}) + L_{34}] + L_{12}, \tag{13}$$

where

X_1 is the column of the coordinates of point 0 in the $X_1Y_1Z_1$ system.

The $X_0Y_0Z_0$ system can be combined with the $X_1Y_1Z_1$ system by rotation about the Z_0 axis angle γ_{01}. The rotation matrix for the transition from the $X_1Y_1Z_1$ system to the $X_0Y_0Z_0$ system has the form

(14)

The matrix equation for the transition to the $X_0Y_0Z_0$ system has the form /33

$$X_0 = M_{01}\{M_{12}M_{23}[M_{34}M_{45}(M_{56}\cdot X_6 + L_{56}) + L_{34}] + L_{12}\}. \quad (15)$$

Substituting the matrices into Eq. (15), and operating on them, we derive expressions linking the coordinates of the arbitrary point of the tongs link 6, to the $X_0Y_0Z_0$ and $X_6Y_6Z_6$ systems

$$\left.\begin{aligned} X_0 &= \cos\gamma_{01}(X_3\cos\gamma_{23} - Y_3\sin\gamma_{23} + l_{12}) - \sin\gamma_{01}\cos\alpha_{12}\times \\ &\times (X_3\sin\gamma_{23} + Y_3\cos\gamma_{23}) - Z_3\sin\gamma_{01}\sin\alpha_{12}; \\ Y_0 &= \sin\gamma_{01}(X_3\cos\gamma_{23} - Y_3\sin\gamma_{23} + l_{12}) + \cos\gamma_{01}\cdot\cos\alpha_{12}\times \\ &\times (X_3\sin\gamma_{23} + Y_3\cos\gamma_{23}) - Z_3\cos\gamma_{01}\sin\alpha_{12}; \\ Z_0 &= \sin\alpha_{12}(X_3\sin\gamma_{23} + Y_3\cos\gamma_{23}) + Z_3\cos\alpha_{12}, \end{aligned}\right\} \quad (16)$$

where

$$X_3 = \cos\gamma_{45}(X_6 + l_{56}) - \sin\gamma_{45}(Y$$

$$Y_3 = \cos\alpha_{34}\sin\gamma_{45}(X_6 + l$$
$$- Z_6\sin\alpha_{56}) - \sin\alpha_{34}$$

$$Z_3 = \sin\alpha_{34}\sin\gamma_{45}(X_6 + l_{56}) + \sin$$
$$+ \cos\alpha_{34}(Y_6\sin\alpha_{56} + Z_6\cdot\cos\alpha_{56}$$

The velocities and accelerations of arbitrary point O of the tongs link can be determined by differentiation of the expressions in (16) with respecto to time. The velocities and acclerations of tong link points obviously will depend on the velocities and accelerations of change in the mechanism's generalized coordinates. Let us now find the Euler angles fixing the position of the tongs link with the solid moved. The matrix of the direction cosines fixing the position of the $X_6Y_6Z_6$ system, which is rigidly connected to the tongs link, relative to the stationary coordinate system has the form

$$M_{60} = \begin{Vmatrix} m_{11}m_{12}m_{13} \\ m_{21}m_{22}m_{23} \\ m_{31}m_{32}m_{33} \end{Vmatrix}. \quad (17)$$

$$
\begin{aligned}
m_{11} &= \cos\varphi_{60}\cos\psi_{60} - \sin\varphi_{60}\cos\theta_{60}\sin\varphi_{60};\\
m_{12} &= -\sin\varphi_{60}\cos\psi_{60} - \cos\varphi_{60}\cos\theta_{60}\sin\psi_{60};\quad m_{13} = \sin\varphi_{60}\cdot\sin\theta_{60};\\
m_{21} &= -\sin\varphi_{60}\cdot\cos\psi_{60} - \cos\varphi_{60}\cos\theta_{60}\sin\psi_{60};\\
m_{22} &= -\sin\varphi_{60}\sin\psi_{60} + \cos\varphi_{60}\cdot\cos\theta_{60}\cdot\cos\psi_{60};\\
m_{23} &= \cos\varphi_{60}\cdot\sin\theta_{60};\quad m_{31} = \sin\psi_{60}\cdot\sin\theta_{60};\\
m_{32} &= -\cos\psi_{60}\sin\theta_{60};\quad m_{33} = \cos\theta_{60},
\end{aligned}
\tag{18}
$$

where

ψ_{60}, φ_{60}, θ_{60} are the Euler angles fixing the position of the $X_6Y_6Z_6$ system relative to the $X_0Y_0Z_0$ system.

Matrix (17) also can be derived by the method that transforms the vector given in the $X_6Y_6Z_6$ system into the $X_0Y_0Z_0$ system.

The matrix equation for the transformation has the form

$$
M_{01}M_{12}M_{23}M_{34}M_{45}M_{56}X_6 = M_{06}\cdot X_6 = X_0, \tag{19}
$$

where

X_0 and X_6 are, respectively, the columns of the coordinates of the vector in the $X_0Y_0Z_0$ and $X_6Y_6Z_6$ systems;

M_{06} is the matrix for the transition from the $X_6Y_6Z_6$ system to the $X_0Y_0Z_0$ system. /34

Eq. (19) yields

$$
M_{06} = M_{01}\cdot M_{12}\cdot M_{23}\cdot M_{34}\cdot M_{45}\cdot M_{56}. \tag{20}
$$

M_{60} and M_{06} are transposed matrices with respect to each other, so once M_{06} is determined, M_{60} is readily found.

Performing the multiplication of the matrices in the right-hand side of Eq. (20), and equating the elements of matrix (17) to transposed matrix M_{06}, we derive nine equations, from which it is easy to determine the Euler angles fixing the position of the tongs link in terms of the mechanism's generalized coordinates.

Of the nine equations, we shall use only the three needed to determine the Euler angles:

$$\cos\theta_{60} = \sin\alpha_{12}\, n_{23} + \cos\alpha_{12}\, n_{33};$$
$$-\cos\psi_{60}\sin\theta_{60} = \sin\gamma_{01}\, n_{13} + \cos\gamma_{01}(\cos\alpha_{12} n_{23} + \sin\alpha_{12}\, n_{33}); \qquad (21)$$
$$\cos\varphi_{60}\sin\theta_{60} = \sin\alpha_{12}\, n_{22} + \cos\alpha_{12}\, n_{32}.$$

$$u_{13} = \cos\gamma_{23}\sin\gamma_{45}\sin\alpha_{56} + \sin\gamma_{23}(\cos\alpha_{34}\cos\gamma_{45}\sin\alpha_{56} + \cos\alpha_{56} + \sin\alpha_{34});$$
$$u_{23} = \sin\gamma_{23}\sin\gamma_{45}\sin\alpha_{56} - \cos\gamma_{23}(\cos\alpha_{34}\cos\gamma_{45}\sin\alpha_{56} + \cos\alpha_{56}\sin\alpha_{34}); \qquad (22)$$
$$u_{33} = -\sin\alpha_{34}\cos\gamma_{45}\sin\alpha_{56} + \cos\alpha_{56}\cos\alpha_{34};$$
$$u_{22} = -\sin\gamma_{23}\sin\gamma_{45}\cos\alpha_{56} = \cos\gamma_{23}(\cos\alpha_{34}\cos\gamma_{45}\cos\alpha_{56} - \sin\alpha_{34}\sin\alpha_{56});$$
$$u_{32} = \sin\alpha_{34}\cos\gamma_{45}\cos\alpha_{56} + \sin\alpha_{56}\cos\alpha_{34}.$$

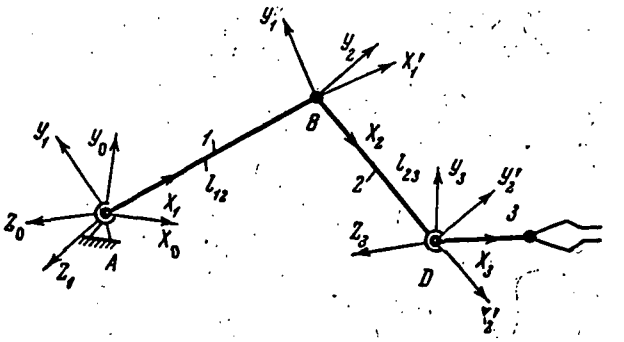

Figure 2.

Eqs. (21) and (22) provide the Euler angles and their derivatives with respect to time. Knowing the Euler angles and their derivatives, it is easy to use known formulas to find the projections of the angular velocity and the angular acceleration of link 6 on the fixed, $X_0Y_0Z_0$, and movable $X_6Y_6Z_6$, axes.

Let us next consider the kinematics of the spatial slave with spherical pairs shown in Figure 2 (a manipulator of the "Ruka" type [1]). This mechanism has seven degrees of freedom. Link 1 forms a 3d class spherical pair with the support, link 1 forms a 5th class turning pair with link 2, and link 2 forms a 3d class spherical pair with link 3.

Let us associate a coordinate system with the links in the mechanism as follows. Let us associate the $X_0Y_0Z_0$ system with the support, placing the origin at A. Let us associate the $X_1Y_1Z_1$ system with link 1, directing the X_1 axis along the axis of link 1, and the Z_2 axis parallel to the axis of turning pair B. The origin of the $X_1Y_1Z_1$ system too is at A. Let us associate the

$X_2Y_2Z_2$ system with link 2, placing the origin at B, and let us direct the X_2 axis along axis 2, and we direct the Z_2 axis along the axis of turning pair B. Let us associate the $X_3Y_3Z_3$ system with link 3, placing the origin at hinge D. Let us direct the X_3 axis along the axis of link 3, and the Z_3 axis parallel to the axis of rotation of the jaws of the tongs link. 35

Let arbitrary point O have coordinates $X_3Y_3Z_3$ in the $X_3Y_3Z_3$ system. Let us find the coordinates of this same point in the $X_0Y_0Z_0$ system.

The $X_2Y_2Z_2$ system can be combined with the $X_3Y_3Z_3$ system by transfer along the X_2 axis by the magnitude l_{23} and three successive turns through three Euler angles, ψ_{32}, θ_{32}, and φ_{32}.

The transfer matrix has the form

$$L_{23} = \begin{Vmatrix} l_{23} \\ 0 \\ 0 \end{Vmatrix}. \tag{23}$$

The rotation matrix for the transition from the $X_3Y_3Z_3$ system to the $X_2Y_2Z_2$ system can be derived by the transposition of the resultant matrix for the three turns through angles ψ_{32}, θ_{32}, and φ_{32}, which determine the position of the $X_3Y_3Z_3$ system relative to the $X_2Y_2Z_2$ system.

$$M_{23} = \begin{Vmatrix} n_{11} & n_{12} & n_{13} \\ n_{21} & n_{22} & n_{23} \\ n_{31} & n_{32} & n_{33} \end{Vmatrix}, \tag{24}$$

where

$$n_{11} = \cos\psi_{32}\cos\varphi_{32} - \sin\psi_{32}\cos\theta_{32}\sin\varphi_{32};$$
$$n_{12} = -\cos\psi_{32}\sin\varphi_{32} - \sin\psi_{32}\cos\theta_{32}\cos\psi_{32}; \quad n_{13} = \sin\psi_{32}\cdot\sin\theta_{32};$$
$$n_{21} = \sin\psi_{32}\cos\varphi + \cos\psi_{32}\cos\theta_{32}\sin\varphi_{32};$$
$$n_{22} = -\sin\psi_{32}\sin\varphi_{32} + \cos\psi_{32}\cos\theta_{32}\cos\varphi_{32};$$
$$n_{23} = -\cos\psi_{32}\sin\theta_{32}; \quad n_{31} = \sin\theta_{32}\sin\varphi_{32};$$
$$n_{33} = \sin\theta_{32}\cos\varphi_{32}; \quad n_{33} = \cos\theta_{33}.$$

The $X_1Y_1Z_1$ system can be combined with the $X_2Y_2Z_2$ system by parallel transfer along the X_1 axis by the magnitude l_{12} and rotation about the Z_1 axis through angle γ_{12}. The transfer matrix for the transfer from the $X_2Y_2Z_2$ system to the

$X_1Y_1Z_1$ system has the form

$$L_{12} = \begin{Vmatrix} l_{12} \\ 0 \\ 0 \end{Vmatrix}. \tag{25}$$

The rotation matrix for the transition from the $X_2Y_2Z_2$ system to the $X_1Y_1Z_1$ system has the form

$$M_{12} = \begin{Vmatrix} \cos\gamma_{12} & -\sin\gamma_{12} & 0 \\ \sin\gamma_{12} & \cos\gamma_{12} & 0 \\ 0 & 0 & 1 \end{Vmatrix}. \tag{26}$$

The $X_0Y_0Z_0$ system can be combined with the $X_1Y_1Z_1$ system by three successive turns through Euler angles $\psi_{10}\theta_{10}\varphi_{10}$. The matrix for the transition from the $X_1Y_1Z_1$ system to the $X_0Y_0Z_0$ system has the form

$$M_{01} = \begin{Vmatrix} b_{11} & b_{12} & b_{13} \\ b_{21} & b_{22} & b_{23} \\ b_{31} & b_{32} & b_{33} \end{Vmatrix}, \tag{27}$$

where the matrix elements b_{ij} (i, j = 1,2,3) have a form similar to that of the matrix elements n_{ij} (i, j = 1,2,3) in Eq. (24), with the only difference being that the subscript "32" for angles ψ, θ, φ is replaced by the subscript "10". /36

The matrix equation for the transformation of the coordinates of the point given in the $X_3Y_3Z_3$ system to the $X_0Y_0Z_0$ system can be written in the form

$$X_0 = M_{01} M_{12} (M_{23} \cdot X_3 + L_2) + L_1, \tag{28}$$

where

X_0 and X_3 are, respectively, the columns of coordinates of an arbitrary point in the systems.

Operating on the matrices included in Eq. (28), we obtain

$$X_0 = b_{11}[\cos\gamma_{12}(X_3 n_{11} + Y_3 n_{12} + Z_3 n_{13} + l_{23}) = \sin\gamma_{12}(X_3 n_{21} + Y_3 n_{22} + Z_3 n_{33}) + l_{12}] + b_{12}[\sin\gamma_{12}(X_3 n_{11} + Y_3 n_{12} + Z_3 n_{13} + l_{23}) + \cos\gamma_{12}(X_3 n_{21} + Y_3 n_{22} + Z_3 n_{33})] + b_{13}(X_3 n_{31} + Y_3 n_{32} + Z_3 n_{33});$$

$$Y_0 = b_{21}[\cos\gamma_{12}(X_3 n_{11} + Y_3 n_{12} + Z_3 n_{13} + l_{23}) = \sin\gamma_{12}(X_3 n_{21} + Y_3 n_{22} + Z_3 n_{23}) + l_{12}] + b_{22}[\sin\gamma_{12}(X_3 n_{11} + Y_3 n_{12} + Z_3 n_{13} + l_{23}) + \cos\gamma_{12}(X_3 n_{21} + Y_3 n_{22} + Z_3 n_{23})] + b_{13}(X_3 n_{31} + Y_3 n_{32} + Z_3 n_{33}); \quad (29)$$

$$Z_0 = b_{31}[\cos\gamma_{12}(X_3 n_{11} + Y_3 n_{12} + Z_3 n_{13} + l_{23}) - \sin\gamma_{12}(X_3 n_{21} + Y_3 n_{22} + Z_3 n_{23}) + l_{12}] + b_{32}[\sin\gamma_{12}(X_3 n_{11} + Y_3 n_{12} + Z_3 n_{13} + l_{23}) + \cos\gamma_{12}(X_3 n_{21} + Y_3 n_{22} + Z_3 n_{23})] + b_{33}(X_3 n_{31} + Y_3 n_{32} + Z_3 n_{33}).$$

The velocities and accelerations of an arbitrary point in link 3 can be determined by the differentiation of Eq. (29) with respect to time.

Let us find the Euler angles ψ_{30}, φ_{30}, and θ_{30}, that fix the position of tongs link 3 relative to the $X_0Y_0Z_0$ system.

The matrix equation for the transformation of the coordinates of the vector from the $X_3Y_3Z_3$ system to the $X_0Y_0Z_0$ system has the form

$$X_0 = M_{03} \cdot X_3. \quad (30)$$

The equation for the transformation of the coordinates of the vector for the transition from the $X_3Y_3Z_3$ system to the $X_0Y_0Z_0$ system can be written in the following form by using the transition matrices M_{32}, M_{21}, and M_{01}

$$X_0 = M_{01} M_{12} M_{23} X_3 \cdot X_3. \quad (31)$$

Comparing Eqs. (30) and (31)

$$M_{03} = M_{01}M_{12}M_{23}. \quad (32)$$

Multiplying the matrices in the right-hand side, we derive the expressions for the elements in terms of known generalized coordinates.

The matrix of direction cosines, M_{30}, fixing the position of the $X_3Y_3Z_3$ system relative to the $X_0Y_0Z_0$ system is similar in form to Eq. (17), except that the subscript "60" for angles ψ, θ, and φ is replaced by "30".

Equating the elements of the M_{30} matrix and the transposed matrix, M_{03}, from Eq. (32), we derive nine equations for finding the Euler angles.

The three equations needed to solve the problem are /37

$$\cos\theta_{30} = b_{31}(\cos\gamma_{12}n_{13} - \sin\gamma_{12}n_{23}) + b_{32}(\sin\gamma_{12}n_{13} + \cos\gamma_{12}n_{23}) + b_{33}n_{33};$$

$$\sin\psi_{30}\sin\theta_{30} = b_{11}(\cos\gamma_{12}n_{13} - \sin\gamma_{12}n_{23}) + b_{12}(\sin\gamma_{12}n_{13} + \cos\gamma_{12}\cdot n_{23}) + b_{13}n_{33}; \quad (33)$$

$$\sin\varphi_{30}\sin\theta_{30} = b_{31}(\cos\gamma_{12}n_{11} - \sin\gamma_{12}n_{21}) + b_{32}(\sin\gamma_{12}\cdot n_{11} + \cos\gamma_{12}\cdot n_{21}) + b_{33}n_{31}.$$

The derivatives of the Euler angles with respect to time can be found by differentiating Eq. (33).

The angular velocities and accelerations of link 3 now can be found quite readily from known formulas.

REFERENCES

1. Kobrinskiy, A. Ye., Stepanenko, Yu. A., "Some Problems of the Theory of Manipulators," V sb: Mekhanika mashin [In collection: Mechanics of Machines], Issue 7-8, Nauka Press, 1967.

2. Moroshkin, Yu. F., "Determination of the Configuration of Mechanisms," Doklady AN SSSR , 82, No. 4, 1952, pp. 533-536.

3. Moroshkin, Yu. F., "Principles of the Analytical Theory of Mechanisms," Trudy seminara po TMM, Issue 54, 1954.

4. Kislitsin, S. G., "The Tensor Method in the Theory of Spatial Mechanisms," Trudy seminara po TMM, Issue 54, 1954.

5. Litvin, F. L., "The Use of Helical Calculations and Matrices to Study Spatial Gearing," Trudy Leningr. politekhn. in-ta im. M. I. Kalinina No. 182, 1955.

6. Chan Chi-hsian, "A Kinematic Analysis of Mechanisms with Lower Pairs by the Square Matrix of 4th Order Method," Teoriya mashin i mekhanizmov, Issue 92-93, 1962.

7. Lebedev, P. A., Kinematika prostranstvennykh mekhanizmov [Kinematics of Spatial Mechanisms], "Mashinostroyeniye" Press, 1966.

8. Gantmakher, F. G., Teoriya matrits [Matrix Theory], Fizmatgiz, 1953.

N73-26028

SOME QUESTIONS OF THE DISCRETE CONTROL OF DEEP-WATER MANIPULATORS

E. L. Onishchenko

ABSTRACT. The use of manipulators to take geological samples and install measuring instruments on the ocean floor is discussed. Methods of performing complex operations using a manipulator connected by cable to the command element are presented.

The work involved in obtaining geological samples and in installing measuring instruments on the bottom in deep ocean waters requires the use of manipulators. Manipulators can be installed in special research submarines and bathyscaphes. In these cases, the operator sees the object in his immediate vicinity and the set of operations he performs can be quite complicated. /38

Attempts are presently being made to build an autonomous manipulator to do a predetermined volume of work in accordance with a special program. However, programmed control presumes, for the present, the performance of only the simplest operations, and proves to be unsuitable when the need arises to perform more complex, deep-water operations.

An unmanned vehicle with manipulators, lowered from the research vessel, can be used for investigations at depths of from 4 to 6 km. Control of the manipulators is by cable connecting them with the master element and control panel. Here the operator, who is aboard the research vessel can use deep-water television to observe the bottom on the television screen and use the manipulator to perform quite complex operations. The cable, in addition to its main purpose, which is the transmission of electrical control signals, also acts as the mechanical connection with the vehicle so, in addition to good electrical characteristics, must have high mechanical strength. The greater the depth of submersion of the vehicle, the more important the weight of the cable. The following formula can be used to approximate the maximum permissible length of the cable [1]

$$l_{\text{lim}} = \frac{F_t - (P_a - P_v)}{P - V},$$

where

F_t is the permissible cable tension;

P_a is the weight of the vehicle in air;

$P_a - P_v$ is the weight of the vehicle at the given depth;

P is the weight of one meter of cable;

v is the volume of one meter of cable.

Calculations show that the maximum permissible length of type TKPG-31 cable, which is a multicore cable, the strength element of which is steel braid, for example, is 1590 meters even when the vehicle has zero buoyancy and that of type TKPU-33 cable is 960 m [1].

Accordingly, a change must be made from multicore cables to rope-cable, /39 which has high mechanical strength, to control manipulators at great depths. An example of rope-cable for this purpose is the KTBF-6 logging cable with a break strength of 6 tons and the KTBF-8 with a break strength of 8 tons. These cables have three copper current-carrying conductors.

Manipulators with an open loop control system can be used when the work to be done with a manipulator is simple. Here the control system for manipulators with three current-carrying conductors in the cable can be successfully designed by using comparatively simple control system circuits. For example, let us assume communication channel multiplexing such that the working conductors in the cable can be used as desired by the operator to control one or the other of the manipulator drives. The simultaneous transmission of control signals to several drives is precluded in this case.

A manipulator must be controlled by a follow-up system when the type of work is rather complicated. This means that the simultaneous operation of several drives must be provided for. Delivery of a power supply to the vehicle from the surface for purposes of controlling two manipulators with seven degrees of freedom each calls for a cable with at least 16 current-carrying conductors. The simultaneous control of several manipulator drives working in the follow-up mode by a cable with three working conductors is possible only if the communication channel (CC) multiplexing system is more complicated than the open loop control system. Multiplexing can be code-, frequency-, and time-division.

Two CC multiplexing methods are used in practice: frequency-division, and time-division [2].

Each of n_0 transmitted signals is assigned its own carrier frequency for frequency-division channeling. Signals are separated by bandpass filters on the receiving side and, after passing through a demodulator, are fed into the amplifier input.

However, frequency-division channeling gets complicated and, consequently, is not very dependable, when a great many commands are transmitted. Then too, it is desirable to use the frequency-division channeling to transmit information with a broad frequency spectrum, and a maximum rational frequency of manipulator control signals not in excess of 1 Hz.

The requirements for simplicity, dependability, and small overall size of CC multiplexing force us to turn to the time-division channeling. Here commands are fed into the CC in a strictly determined sequence over a predetermined time interval. Switches are required to switch the cable at the command and reception points in turn to the corresponding command element potentiometers and control units. Dependable circuit operation requires that the distributors operate synchronously and in phase. Figure 1 is a block diagram of a discrete (pulsed) system such as this.

The circuit contains command element (CP) and feedback (FBP) potentiometer pickups. The error signal, ΔU, is picked off the CP and FBP cursors, fed into the amplifier, A, and then into the servo unit, SU, causing the working element, WE, to move according to this signal.

Time-division channeling thus results in the control signal being fed to the follow-up system discretely in the form of individual pulses, the amplitudes of which are equal to the input signal amplitude, and the duty ratio is determined by the number of commands transmitted over the CC. Figure 2 shows the time distribution of commands in the CC from n command element potentiometers.

The switch in Figure 1 henceforth will be called the pulse element (PE) of the automatic regulating system (ARS). /40

The output function of the PE is a sequence of pulses of width t_c and interval T, the envelope of which corresponds to continuous signal x(t) at the

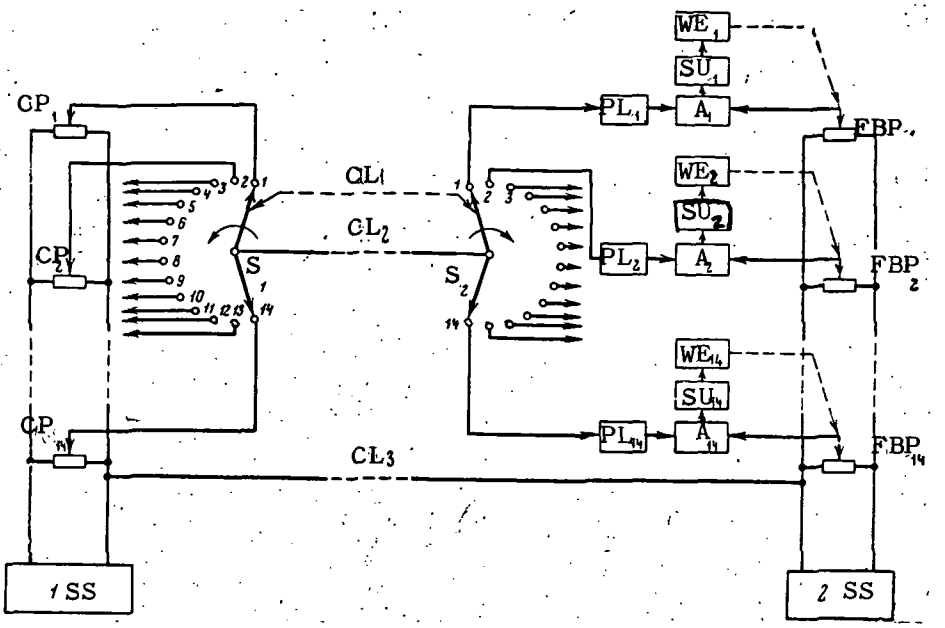

Figure 1. Block diagram of a manipulator control system using a time system for multiplexing a communication channel. 1 - 1st supply source; 2 - 2nd supply source.

PE input. The PE threfore can be considered to be an amplitude modulator with a carrier in the form of a sequence of single pulses [3]. The output function of the PE thus can be written as the product of the input function X(t), times the function of unit pulses $U(t_c, t)$ of width t_c and repetition interval T

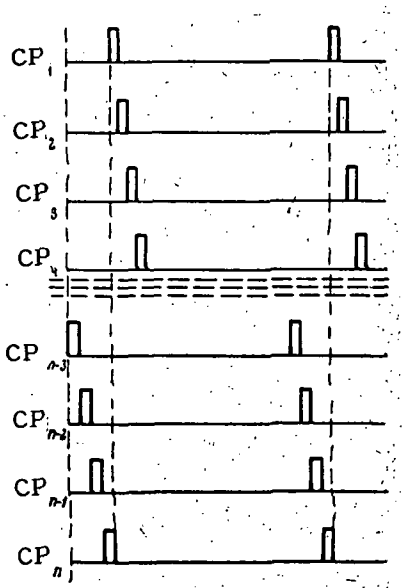

Figure 2. Time distribution of commands in the CC from n command element potentiometers.

$$A(t) = U(t_c, t) \cdot x(t). \qquad (1)$$

The function $U(t_c, t)$ is even and periodic, so it can be presented in the form of a Fourier series

(2)

where

$\omega_s = 2\pi/T$ is the chopping frequency

$$C_n = \frac{1}{T}\int_0^{t_c} e^{-jn\omega_s t}\,dt = \frac{1 - e^{-jn\omega_s t_c}}{jn\omega_s T};$$

C_n is the Fourier coefficients.

Substitution of C_n values into Eq. (2) yields the analytical notation for the function $U(t_c, t)$ 41

(3)

Eq. (3) makes it apparent that the function of unit pulses, apart from the constant component, contains an infinite set of harmonics, each of which is characterized by amplitude U_{ch}, angular frequency ω_{ch}, and initial phase ψ_{ch}

$$U_{ch} = \frac{2\sin\frac{k\pi t_c}{T}}{k\pi};$$

$$\omega_{ch} = k\omega_s;$$

$$\psi_{ch} = k\omega_s \frac{t_c}{2};$$

Substituting Eq. (3) into (1), we obtain the relation between the pulse signal at the output of the PE and the continuous signal at the input

$$A(t) = \frac{t_c}{T} x(t) + \frac{2t_c}{T} \sum_{n=1}^{\infty} \frac{\sin\frac{n\pi t_c}{T}}{\frac{n\pi t_c}{T}} x(t) \cdot \cos n\omega_s \left(t - \frac{t_c}{2}\right).$$

If a continuous input siganl, x(t), is a complex periodic function that can be presented as the sum, l, of the harmonic functions with frequencies in the band from 0 to f_0, then the frequency spectrum, x(t), is a line spectrum consisting of l lines. In this case, the line frequency spectrum of the pulse signal from the PE output will, in addition to the fundamental frequency spectrum for signal x(t), contain side frequencies differing from the fundamental frequencies by the magntiude $n\omega_s$ [3].

The side frequencies appearing as a result of the chopping can cause pulsations at the ARS output. A positioning link, connected to the PE output, is used to eliminate these undesirable pulsations, as well as to assist the manipulator slave in holding the position corresponding to the amplitude of signal A(t) for

time aT, where a ≤ 1. Each pulse from the PE is stored by the positioning link for time aT. In the majority of cases, the operation of the positioning link (PL), is based on a rapid accumulation of a charge by the capacitor during t_c, the time the control pulse is acting on the PL and subsequent retention of this charge for $t_c < t \leq aT$.

The PL thus converts the discrete signal from the PE output into a step-function signal (when a = 1), thereby approximating continuous input signal x(t). We have a zero-order PL when the indicated approximation occurs using current discrete values of the corresponding continuous signal.

Figure 3 is the block diagram of one manipulator drive. The following notations apply: k_1, k_2 are the "contacts" of the pulse element (switch); PL is the positioning link; W_s is the manipulator control system from the electronic amplifier to the piston of the working element. Figure 4 shows the time diagrams explaining the operation.

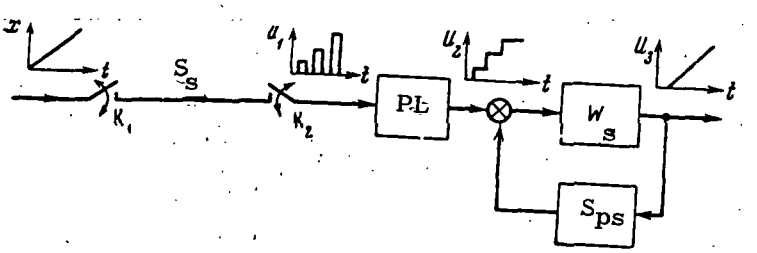

Figure 3. Block diagram of the discrete control of one manipulator drive.

The pulse transient function of a zero-order PL is a unit rectangular pulse of width aT [4]: Q(t) = 1(T) - 1(t - aT).

The PL transfer function will equal the Laplace transform of the pulse transient function [5]

$$K(p) = \int_0^\infty Q(t)\, e^{-pt} dt = \int_0^\infty 1e^{-pt} dt - \int_{aT}^\infty 1e^{-pt} dt = \frac{1}{p}(1 - e^{-paT}). \qquad (4)$$

The PL spectrum function, S_ω, can be obtained from the K(p) transform by replacing the operator p by jω, that is,

$$S_\omega = \frac{1 - e^{-j\omega aT}}{j\omega} = \frac{2\sin\frac{aT\omega}{2}}{\omega} e^{-j\omega aT/2}.$$

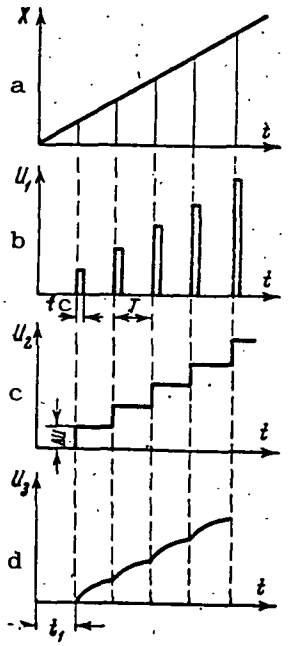

Figure 4. Time diagrams explaining the operation of the arrangement in Figure 3. a - x(t); b - $u_1(t)$; c - $u_2(t)$; d - $u_3(t)$.

The PL phase characteristic then will be $\Phi(\omega) = -aT \cdot \omega/2$.

What follows from consideration of the PL spectral function is that the introduction of the PL delays the signal at its output with respect to the input signal for a time equal to half the delay period aT. The amplitudes of the side frequencies different from the fundamental frequencies by $n\omega_s$ are reduced by the use of a PL. Eq. (4) shows that the positioning link functions as an integrator at high PE chopping frequencies.

The lower limit of the chopping frequency, ω_{smin}, thus can be determined from the Kotel'nikov theorem, from which it follows that if a continuous function, x(t), has a finite frequency spectrum from 0 to f_0 Hz, it can be completely determined (that is, the whole frequency spectrum, x(t), is transmitted) by the sequence of its discrete values following with period $T = 1/2f_0$ [6].

Thus, time T must be based on the condition that

(5)

to completely determine the continuous function x(t) with finite frequency spectrum 0 - 1 Hz, its discrete values after period T.

Period T should be selected as small as possible from the point of view of a reduction in the dealy caused by the PL and the bringing of its transfer function close to the integrator's function. On the other hand, the transient time, t_t, for the system, W_s, also imposes its requirements on T. When $T < t_t$ there is a transient dynamic error that will increase with time as x(t) changes (in Figure 4, the function x(t) is conditionally shown as changing linearly). /43

Time T is selected for the condition

$$t \geq t_t, \tag{6}$$

or for the condition $T > t_r$, where t_r is the transient rise time, depending on the nature of the transient (in the final analysis on system Q in terms of speed, K_Q).

It can be approximated that t_r is inversely dependent on system Q in terms of speed: $t_r = \pi/K_Q$.

Thus, increase in K_Q makes it possible to reduce delay time because of the reduction in T. In a real system, K_Q is selected on the basis of necessary operating speed, as well as to provide system invariance to disturbances caused by the load. Thus, the PE and PL parameters (in the final analysis, time T) are determined individually for each concrete system, depending on its K_Q.

Let us use Eq. (6) to find T for a real system with t_t = 360 msec

$$T \geqslant 360 \text{ msec}. \tag{7}$$

Thus, the PE in a real system must supply the PL input with discrete values of the continuous function x(t) with period

$$360 \text{msec} \leqslant T < 500 \text{ msec} \tag{8}$$

Taking T = 450 msec, we obtain

$$\omega_s = \frac{2\pi}{T} = \frac{2}{0{,}45} = 14 \text{ rad}$$

where n_0 is the number of commands transmitted over the communication channel.

Thus, the switch should switch channels with frequency $f_{ch} = 1/t_c$ = 36 Hz.

Figure 5 shows oscillograms of one slave drive with discrete control. The magnitude of the voltage of the "step" fed into the system input is 2.5 V.

The oscillogram shows that the time delay in the initiation of the movement of the working element, t_1, depends on the time of supply of the "step" relative to the time of supply of pulses from the PE output. The maximum t_1 can take is

$t_{lmax} = T$.

The oscillograms illustrate the possibility of the appearance of a transient dynamic error when the Eq. (7) condition is not satisfied. This is why K_Q was reduced in a real system (by reducing the amplifier gain and the capacity of the oil pump supplying the hydraulic system) which, in the finaly analysis, results in a $t_t > 360$ msec. Channel switching frequency simultaneously was increased to 83 Hz (t_c 12 msec, T = 168 msec). The oscillogram shows that the working element cannot "follow" the signal delivered in the form of a "step" in time T (the PE output pulse repetition period). The result will be an accumulation of the transient dynamic error when a "step" again is supplied in time T.

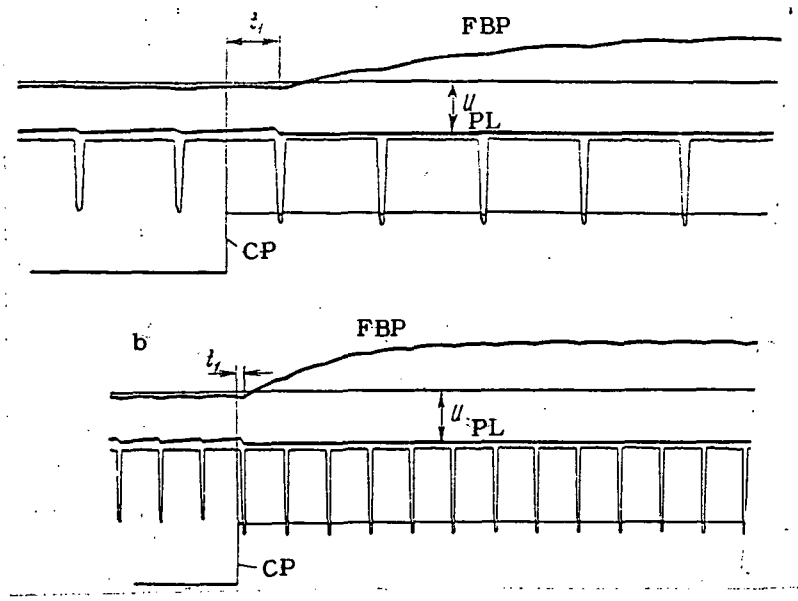

Figure 5. Oscillogram of the processes in a follow-up system with discrete control (the case of $T > t_t$). CP is the voltage across the cursor of the command potentiometer; U_{PL} is the voltage across the output of the positioning link; FBP - is the voltage across the cursor of the feedback potentiometer; a - when $I \geq 360$ msec; b - when $T \geq 360$ msec is not satisfied.

The following conclusion can be drawn from the foregoing.

1. Control of deep-water manipulators operating on the follow-up system principle with transmission of control signals over cables is possible only when a multiplex communication channel is used.

2. Most acceptable from the point of view of simplicity of design, dependability, and small size is time-division multiplexing.

3. The parameters of the pulse element for the time system for CC multiplexing are selected so as to provide the required manipulator dynamics for each concrete case.

References

1. Marakuyev, V. I., "Cables for Underwater Television Sets," Trudy IOAN SSSR, 74, 1965.

2. Tumevin, V. N., Osnovy telemekhaniki [Fundamentals of Telemechanics], "Energiya" Press, 1966.

3. Yulius, T. T., Tsifrovyyl i impul'snyye sistemy avtomaticheskogo upravleniya [Digital and Pulsed Automatic Control Systems], "Mashinostroyeniye" Press, 1964.

4. Itskhoki, Ya. S., Impul'snyye ustroystva [Pulse Devices], Sov. Radio Press, 1959.

5. Kuzin, L. T., Raschet i proyektirovaniye diskretnykh sistem upravleniya [The Calculation and Design of Discrete Control Systems] "Mashgiz," 1962.

6. Markov, V. V., Malokanal'nyye raznorelevnyye linii [Lines With Few Channels and Different Relays] Sov. Radio Press, 1963.

N73-26079

PROSPECTS FOR THE BUILDING AND USE OF COMPUTER CONTROLLED MANIPULATORS

M. B. Ignat'yev, F. M. Kulakov, A. M. Pokrovskiy

ABSTRACT. The economic advantages of computer-controlled manipulators are discussed. The basic stages of the work required to build automatic manipulators, as well as a linguistic approach to the synthesis of control programs for manipulator movement, are also presented.

The development of science and technology is giving rise to an ever-increasing requirement for manipulators under human control. Yet the necessity is felt more and more acutely for the use of manipulators requiring much less human participation, manipulators capable of automatically performing a predetermined set of operations and of moving and orienting themselves independently in an unfamiliar situation. This is primarily the result of a sharp increase in the number of operations under conditions that threaten human health, the need to perform operations under conditions which practically completely preclude human presence. This pertains to a number of branches of the heavy, metal-working, and chemical industries, as well as to oceanology. Particularly pertinent is the question of the need to replace man when working in the ocean depths where the danger to man is extreme and work often is simply impossible. Man in the ocean needs an automatic manipulator-helper, unsusceptible to various dangers, able to conduct rescue, assembly-construction, repair, and scientific-research operations, not in need of constant feeding, and which can be sacrificed if necessary. /45

The building of automatic manipulators with predetermined autonomy involves the realization of extremely complex control algorithms, something that is possible, naturally, only when computers are used.

The Economic Advantages of the Use of Electronic Computer Controlled Manipulators

Let us consider the basic factors involved in the cost and engineering desirability of using an electronic computer controlled manipulator and those of using a manipulator under human control.

Let us assume the manipulator must function in some environment. The variability of the environment, that is, the different types of situations

encountered in it, can be characterized by the magnitude n. The manipulator's variability, that is, its ability to function normally in these situations, obviously should be equal to, or greater than, the environmental variability. Let us assume that man functions as well as the computer in a given environment. /46 We will not consider the psychophysiological factors, his capacity to tire, to make mistakes, or the limited precision of the work.

The total cost to build and use a computer controlled manipulator is determined by the one-time cost to manufacture the manipulator, P_1, the computer P_2, and the cost to operate them, respectively $S_1\tau$ and $S_2\tau$, where τ is time. In turn, the components of costs P_2 and $S_2\tau$ will be greater the greater the variability of the environment, since the complexity of the computer controlling the manipulator will increase with increase in variability. In the general case, these components will be positive increasing functions of n, which can be, approximately, considered as linear

$$P_2 = p_2 n, \tag{1}$$

$$S_2 = s_2 n\tau, \tag{2}$$

where p_2, s_2 are specific costs per unit of variability. Total costs will equal

$$P = P_1 + p_2 n + (S_1 + s_2 n)\tau. \tag{3}$$

The cost to build and operate a manipulator under human control is made up of the one-time costs to manufacture the mechanical part of the manipulator P_1^*, the devices for protecting and supporting the operator P_3 (special mobile shielded cabin, deep-water bathyscaphe, seat, etc.), and the operating costs, which include the cost of employing the man, $S_3\tau$, of the protective devices $S_4\tau$, and of the manipulator $S_1\tau$.

Total costs in this case will be determined by the formula

(4)

Assuming that $P_1 = P_1^*$ and $S_1 = S_1^*$, the condition of equality of P and P* provides us with the expression for the maximum variability of the environment

in which it is economically advantageous to use a computer controlled manipulator

$$n_{\max} = \frac{P_3 + (S_3 + S_4)\tau}{p_2 + s_2\tau}. \qquad (5)$$

This relationship shows that it is economically advantageous to use only manipulators with little variability, in other words, narrowly-specialized manipulators, under conditions in which complex operator protection and support are not required (P_3 and S_3 are small). Automatically-controlled manipulators become economically advantageous under more difficult conditions.

Finally, only the computer controlled manipulator is economically advantageous under conditions in which the presence of a man is practically impossible, that is, when P_3, $S_3 \to \infty$. The economic advantage of the use of a computer controlled manipulator will increase with increase in operating time when the condition

is satisfied.

This condition will always be satisfied when computer dependability is high, that is when s_2 is small. The process of further increase in the economic effectiveness of an automatic manipulator will occur with increase in computer economy and dependability, that is, with decrease in p_2 and s_2, and possible spheres for its use will expand.

Apropos the cost of the mechanical part of manipulators (P_1 and P_1^*), it should be noted that the mechanical part of the manipulator can be simplified in the case of computer control by making the control program more complicated and thus solve problems of dynamic correction, corrections for mechanical deformations and wear, algorithms for the control of a mechanical system with great redundancy in the number of mechanical degrees of freedom can be realized, etc. The requirement imposed on the mechanical part is substantially higher, when human control of a manipulator is involved despite the fact that man has strong self-learning algorithms. Fatigability and convenience requirements result in substantially complicating the mechanical part of the manipulator and in making it more expensive. Thus, realization of the mechanical part of a manipulator under human control is much more costly than the corresponding part of

a computer controlled manipulator. This creates an additional reserve, increasing the economic effectiveness of the use of computer controlled manipulators. Moreover, lengthly training of each operator is required before operators can learn how to control a manipulator. The experience they gain is an individual thing and cannot be generalized and passed along to another operator. Control learning algorithms can be transferred from one machine memory to another when computers are used, they can be generalized, and can be stored indefinitely, thus providing additional advantages in the use of computers to control manipulators.

A whole series of papers, primarily foreign [1-11], deal with major investigations in progress on building computer controlled manipulators, and with their increased use. These questions are the concern of such American firms as "Unimation," "ATF," "Space ships," and others, as well as of the laboratories of the Massachusetts Institute of Technology and the Stanford Research Institute. A great deal of work is being done under contract to the National Aeronautics and Space Administration (USA). Available publications are basically informational in nature and cannot serve as the basis for the development of computer controlled manipulators.

Basic Stages in the Development of Automatic Manipulators

The building and further improvement of computer controlled manipulators is a lengthy, multistage process. It is desirable, in the initial stages of this process, to pay attention to the development of very simple manipulators with very low variability, similar to the commercial manipulators of the "Unimate" and "Versatran" types [2-5]. The use of such manipulators is already economically justified, even at the contemporary state of computer technology.

Manipulators such as these have storage for a program to move the robot's multilink actuators ("arms") to perform certain motor acts. Figure 1 is the block diagram of such a manipulator. It consists of a slave section (SS), which is a system of servodrives, a link position sensor system (PS), and a computer (C), which includes the storage (S), the control unit (CU), and the computer itself (CD), as well as the analog-code (A-C) and code-analog (C-A) converters. The manipulator control system has two basic operating modes: the learning mode and the working mode. The operator, in the learning mode, ordinarily takes the manipulator actuator through the required sequence of working positions with the

help of a supplementary learning system. The program for the motor act is stored (in the block diagram of Figure 1, key 1 is closed, keys 2 and 3 are open). /48
The manipulator is program controlled in the working mode (keys 2 and 3 closed, key 1 open). The control unit regulates the rate at which the manipulator works. The very simple computer provides for making a correction to the rate at which the manipulator is working in order to attain some minimum error in carrying out the program. There are no difficulties in building today's commerical manipulators, in principle.

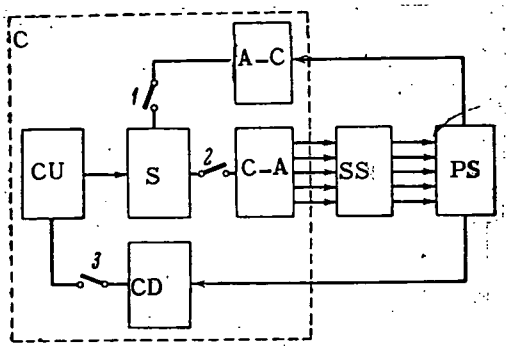

Figure 1. Block diagram of a program controlled manipulator.

A general shortcoming of program controlled manipulators, and one restricting their sphere of activity, is that, in essence, they stop performing even when changes in the external environment are insignificant (unforeseen). Therefore, the natural way to further improve computer controlled manipulators is to increase their variability and give them the capacity to interact with the outside world; that is, to collect and process data on the outside world and develop their own behavior program accordingly.

Present work in this field still is scientific-research in nature and pursues the goal of connecting the main trends in the investigation of artifical thinking; recognition of images, proof of geometric theorems, making decisions, and language problems, into one composite physical system.

The generalized block diagram of a manipulator with automatic control can be presented in the form of the block diagram shown in Figure 2. The essential difference between it and that in Figure 1 is primarily one of a great many feedback sensors. This system, in addition to the link position sensors similar to the proprioceptors of living organisms, has groups of tactile (TS), auditory (AS), and video (VS) sensors which perceive the effects of the external environment and which are similar to the exteroceptors, of living organisms. The signals from these sensors are fed into a special computer unit called a situation analyzer (SA). This unit generates information on the particular class to which an object belongs (object identification), on its dimensions and

coordinates, and on the location of object and manipulator tongs with respect to each other. This information is fed into the control system (S) where it is used in the process of forming and realizing the program of motor acts by the manipulator. Associated with the S are the arithmetic unit (AU) and control unit (CU) which help realize the manipulator control program. The (CU) ensures interaction between the arithmetic unit and the storage, as well as the situation analyzer. The block diagram also includes a special recoding unit (RU) for communication between man and manipulator. /49

The manipulator control program should be organized on the hierarchical principle and should have several levels. The lowest level is programs similar to the stable stereotypes of human or animal movements. They envision the sequence and magnitude of movement of each manipulator link and describe the state of all sensitive elements in the process of implementing the program. The highest program levels build the motor acts from the programs for the lowest levels according to the command signals, including the constant flow of data from the feedback sensors concerning the location of the object and of the manipulator tongs with respect to each other, the dimensions of the object, and the like.

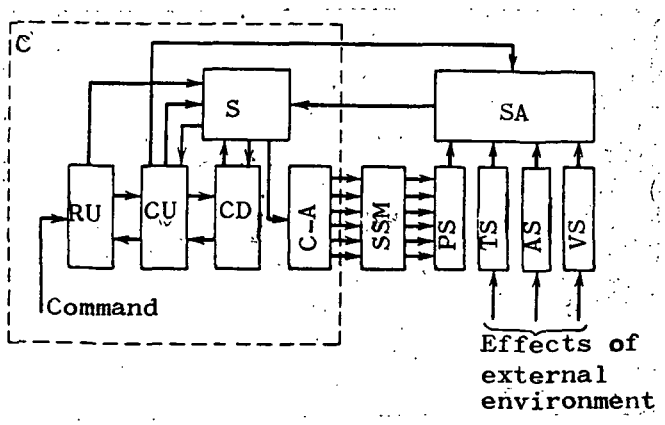

Figure 2. Block diagram of a computer controlled manipulator.

The entire control program should be organized to include such criteria, for example, as the energy (movement should be accomplished with a minimum expenditure of energy), time (movement should be accomplished in minimum time), and others.

The highest control system levels should also provide for the formation of the manipulator's "internal world." At the same time, the computer controlled manipulator should acquire the capacity to select from the tremendous flow of data to its sensitive elements only useful information with direct significance for reaching the assigned goal. Thus, the manipulator's capacity for self-learning is increased

substantially. A manipulator with a certain minimum of initial concepts will, in operation, continuously expand and more thoroughly examine them, and this will help it look for and find ways to reach the goal, to optimize these ways, to find ways to bypass obstacles, and the like.

The Linguistic Approach to the Synthesis of Programs for Controlling the Movements of Manipulators

The problem of building computer controlled manipulators involves finding solutions to a number of complex scientific and technical problems. One of the main problems is that of the development of the principles underlying the synthesis of the special programs in accordance with which the automatic manipulator should operate. These programs should, to some degree, simulate the functioning of the central nervous system (CNS), and be performed by the computer in real time. Flowing from this problem is another, equally complex one, that of building small, dependable, economical, high capacity computers capable of realizing these complex, multilevel programs. Only the first will be considered in what follows. The actual prospects of solving the second stem from the great successes achieved in the field of microelectronics, as well as from the appearance of new computer building ideas and principles [12], and in essence reduce to building computers from homogeneous, general-purpose computing media. /50

The use of the linguistic approach is proposed to solve the first problem. This is explained by the considerable successes attained in explaining the logical structure of language, and in developing a quite orderly, and practically completed, structural linguistics apparatus. Moreover, inasmuch as the subject of linguistic investigation is language, in whose structure there is reflected the structure of the brain and of the CNS, the methods used in linguistics also prove useful when considering other complex systems. An example of this is the work done by Narasimhan [13, 14], who has pushed the linguistic approach to the problem of image recognition.

The main features of the linguistic approach, as applicable to a broad class of complex systems, are the following. First, the individual levels in the structure of the system, each described by its own language, its own dictionary and grammatical rules, are isolated. Second, the process by which the system reaches the goal is considered as a process of converting from one language level to another. Third, the quantitative characteristics of this process are

$A_1 = B_2 B_8 B_7 \cdot$

obtained by introducing the concepts of isomorphic and homomorphic conversions, idiomatically different language levels, measures of assignment ambiguity, measures of the complexity of converting from one level to another, and the like. For example, the complexity of automation of planning or production, of objects of some sort is determined by the cost to converting from the corresponding levels. Conversion costs are largely determined by the translation volume. Attempts are made to develop languages which are close as possible to each other in order to reduce the complexity of the translation.

Given this approach, the manipulator control program has a multilevel, hierarchical structure. Each level in the system can be characterized by its own dictionary and grammar.

Let us consider the k^{th} level of a hierarchical control system. Let the dictionary for this level consist of n_1 symbols $\{A_1, A_2, \ldots, A_{n_1}\}$ and the grammar of r_1 rules $F_1, F_2, \ldots, F_{r_1}$. These rules permit combining the symbols of the k^{th} level language into certain words, such as

$$F_1: A_1 \rightarrow A_1 A_3, \qquad (6)$$
$$F_2: A_4 A_1 A_2 \rightarrow A_4 A_5 A_2.$$

A tremendous number of grammatically correct words in the language of the particular level that are certain control commands that must be transmitted to lower levels can be built by using some sequence of rules. Thus, a limited alphabet of symbols and number of rules provides the means for building a tremendous number of words representing diverse commands. The problem of transmitting commands from one level to another will involve translating a word recorded in the language of one level into a word belonging to the language of another level. Thus, in addition to the alphabets and rules of both languages, it is also necessary to have a translator, that is, rules for translating from one language to another.

$A_3 =$

$B_3 B_8 B_7 \cdot$

A_1

A hierarchical program consisting of k levels will have k alphabets, k groups of rules, and k-1 translators. investigation of the rules for translating from one language into another should keep in mind the following relationships between the symbols (words) in both languages.

1. The unambiguous correspondence between a symbol (word) in one language and a symbol, or word, in another language /51

(7)

2. The ambiguous correspondence

(8)

3. A symbol (word) in one language corresponds to several symbols (words) in another languague, synonyms

(9)

4. A symbol (word) found in a definite context can be translated unambiguously

(10)

5. When a specific set of symbols (words) is found the set is always translated in the same way, regardless of how the symbols (words) are translated individually, an idiomatic expression

(11)

Figure 3 shows in the form of a tree, how a signal can be transmitted from higher to lower levels. If A_1 is a generalized command for the accomplishment of some motor act, f_i is the specific signals controlling the slave organs.

Several signal paths can come together at some level in a more complex case, higher level signals, local feedback signal, and signals from receptors (sensors), for example. Converting these signals into the language of the particular level, we obtain some phrase of the type

$$D_3D_8D_4D_5D_7D_3D_8D_4D_5 \qquad (12)$$

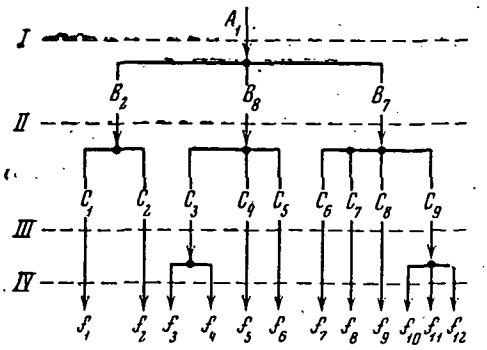

Figure 3. Tree of transmission of a signal from higher (I-IV) to lower levels.

where D_3D_8 are signals from the sensors; $D_4D_5D_7$ are the signals from local feedbacks, and $D_3D_8D_4D_5$ are signals from higher levels.

In this case, the command transmission problem becomes more complex because now it is impossible to translate each word separately, and instead the whole phrase must be translated as an entity.

The first of the levels it is necessary to consider is that linking the outside world with the control unit. /52 Obviously, orders must be issued to the automatic manipulator at the topological level; that is, in the following form: "Take the spanner wrench, find the nuts, screw the nuts on the bolts." But regardless of the form in which the commands may be given (by voice, using punch cards, etc.) there always is a limited set of words and grammar to use to build quite a variety of sentences.

The organization of the levels within the control unit s internal structure is particularly complex. The processing of data obtained from the outside world, the clarification of goals, the definition of subgoals, the organization of the collection of missing data and the structure of elementary, and more complex, movements all occur at these levels. Some results of investigating the structure of these levels, as applicable to the task of building motor acts are reviewed in references [15-17].

Simulation of a Programm Controlled Manipulator

We investigated a model of programm controlled manipulator to see if it was feasible to develop programs that would provide known autonomy of manipulator behavior.

The slave element of the model, whose kinematic diagram is portrayed in Figure 4, has four degrees of freedom (β, γ, ψ, φ), not counting the tongs, and is fitted with four electrohydraulic servodrives with potentiometric link position sensors. The manipulator tongs (Figure 5) have four tactile contact-type sensors which, together with the position sensors, form the manipulator's primitive "sensing organs." Sensor 1 records the fact that the object is positioned between /53

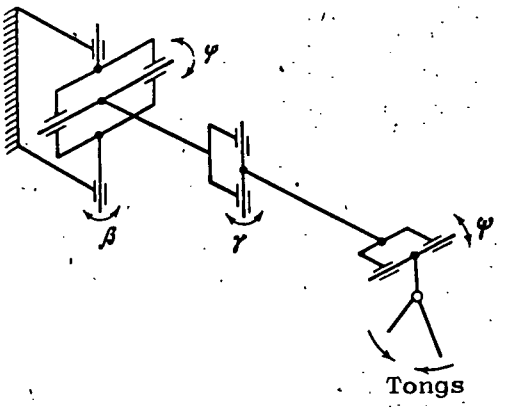

Figure 4. Kinematic diagram of the working element of a manipulator model.

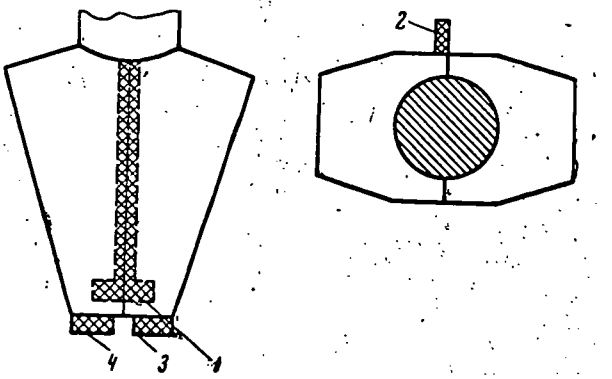

Figure 5. Tongs of the manipulator working element.

the jaws of the tongs, and sensors 2, 3, and 4 register contact between the object and the external surface of the tongs. In addition, sensors 3 and 4 can record contact between the tongs and the surface on which the objects may be when the tongs are in the vertical position. A standard UM1-NKh controller is used to control the manipulator [18].

The controller's six output channels, equipped with code-analog converters, form the servo controls for the manipulator. Eight input channels are used to feed data from the feedback sensors to the computer.

A program that searches for and collects objects from a surface of arbitrary shape was developed and realized for the model under consideration. The program envisages the following operations: (1) search for objects on the surface; (2) determination of the positions of the objects relative to the manipulator; (3) ascertainment of the possibility of seizing the object; (4) selection of the position of the tongs convenient for seizing the object; (5) seizing the object; (6) moving the seized object to a specified area; (7) return of the tongs to where the object had been discovered and continuation of the search.

The storage volume occupied by the program is 42015-digit words.

The tongs searching movement (scanning mode) is as follows. When β = constant, angle γ changes discretely by step $\Delta\gamma$ from one extreme position to the other. Upon arrival at one of the extreme positions, increment $\Delta\beta$ is added to angle β, and scanning with respect to γ continues. The tongs thus follow the trajectory shown by the arrows in Figure 6, and explore the region marked by the dot-dash line within specified coordinate limitations. The axis of the

tongs is kept vertical during the search process, by adjusting angle ψ. Angle φ can change such that the end of the tongs will follow the surface outline, and to this end the tongs periodically touch the surface with sensors 3 and 4.

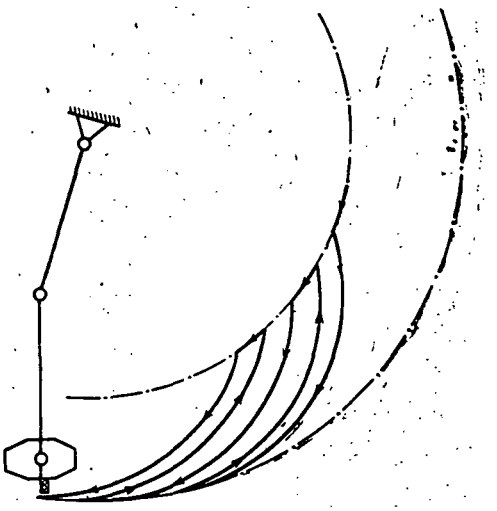

Figure 6. Movement of tongs in the scanning mode.

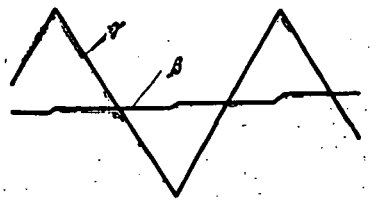

Figure 7. Change in the β and γ coordinates of the working element in the scanning mode.

The oscillograms in Figure 7 show the temporal changes in the controlling voltages supplied by the computer to the servodrives for angular coordinates β, γ in the scanning mode. It is obvious that when the search selected method is used and when the step with respect to angle β is small enough, sensor 2 is the first to touch the surface of the object being sought. Search stops in this case, and the coordinates of the tongs are stored. This is followed by a test shift of the object because of change in angle γ by $\Delta\gamma$. 54

Figure 8. Change in the φ and γ coordinates of the working element and in the mode for selecting the position of the tongs. a - sensor 3 operated; b - sensors 3 and 4 operated.

If the object shifts, it can be seized; if not, an obstacle has been encountered, and must be bypassed.

The oscillograms in Figures 8a and b show the test shift in terms of γ (section a), and the time delay sufficient to detect this shift (section b).

The first thing to happen in the mode for selecting the position of the tongs convenient for seizing the object, is the raising of the tongs over the object by changing angle φ (section c, Figures 8a and b). This is followed by the tongs opening and moving over a trajectory normal to the scanning line by an amount approximately equal to three-fourths the width of the tongs and, finally, by the lowering of the tongs until they contact the object (section d). The following cases are possible:

1. Operation of sensor 1, which serves as the signal to seize the object. Seizure is accomplished by lowering the tongs to the limit, and closing them.

2. Operation of sensor 3, which serves as the signal to move the tongs so as to reduce angle γ until sensor 1 operates. The object now is seized. If sensor 4 operates instead of sensor 1, the object has not been discovered, and scanning must continue.

3. Operation of sensor 4. Here we have the same operation as in the second case, but angle γ is increased.

4. Simultaneous operation of sensors 3 and 4. This means that seizure of the object is impossible, and scanning must continue.

The oscillograms (see Figures 8a and b) show the changes in the controlling voltages corresponding to angles γ and φ when sensor 3 operates (section e). It may be seen that after contact with the object, coordinate φ increases to the maximum, and γ increases by $\Delta\gamma$. After this, angle φ decreases until contact with the object when γ = constant. Figure 8b (section k) shows that sensor 4 operates after sensor 3 action (the object has not been discovered, and the manipulator shifts to the scanning mode).

The investigation of the manipulator model described confirmed the fact that writing programs providing sufficient autonomy of manipulator behavior when performing individual tasks, and which are of practical interest, is possible even when medium-capacity computers are used.

REFERENCES

1. Ernst, H. A., MH - 1.A. "Computer - Operated Mechanical Hand," Proceedings 1962 Spring Joint Computer Conference, 21, 1962, p. 39.

2. Engelberger S. F., "Role of Industrial Robots in Improving Production Operations," Automation, 11, No. 6, 1964, p. 62.

3. Barnes, S., "The Coming Age of Robots," Machine Design, 36, No. 27, 1964, p. 150.

4. Mosher, R. S., "Industrial Manipulators," Scientific American, 211, No. 4, 1964, p. 88.

5. Rozenblat., "Automatic Devices and Robots for Doing Dirty Jobs in Factories," Elektronika, 40, No. 6, 1967, p. 63.

6. McGuire, A., "Thinking Automatic Devices," Elektronika, 40, No. 9, 1967, p. 51.

7. Rosen, C. A., Nilsson, N., "An Intelligent Automation," IEEE Internat. Conv. Rec., 15, No. 9, 1967, p. 50.

8. Balmer, T. R., "Manipulator Arm Has Five Programs," Design News, 22, No. 14, 1967, p. 36.

9. Fishlock, D., "Four Finger Exercise," New Science, 34, No. 543, 1967, p. 282.

10. Kobrinskiy, A. Ye., Chisla upravlyayut stankami [Numbers Control Machine Tools], "Nauka" Press, 1967.

11. Kobrinskiy, A. Ye., Stepanenko, Yu. A., "Some Problems in the Theory of Manipulators," V sb. Mekhanika mashin [In collection: Mechanics of Machines], No. 7-8, "Nauka" Press, 1967.

12. Yevreinov, E. V., Kosarev, Yu. G., Odnorodnyye universal'nyye vychislitel'nyye sistemy vysokoy proizvoditel'nosti [Homogeneous High-Capacity General Purpose Computer Systems] "Nauka" Press, Novosibirsk, 1966.

13. Narasimhan, R., "Labelling Schemata and Syntactic Descriptions of Pictures," Information and Control, 7, 1964, June; 151.

14. Narasimhan, R., "Syntax-Directed Interpretation of Classes Events Comm. of ACM, 1965, March: 166.

15. Ignat'yev, M. B., Golonomnyye avtomaticheskiye sistemy [Holonomic Automatic Systems] AN SSSR Press, Moscow-Leningrad, 1963.

16. Ignat'yev, M. B., "The Question of the Use of Models of Structural Linguistics to Analyze and Synthesize Complex Systems," V kn. Tezisy dokladov k XX nauchno-tekhnicheskoy konferentisii LIAP [In book: Abstracts of Reports to the XX Scientific and Technical Conference of the Leningrad Institute of Aviation Instruments], 1967.

17. Ignat'yev, M. B., Kan, G. S., Pokorovskiy, A. M., "On the Use of Mathematical Linguistics Methods to Describe the Structures of Biological Systems for the Control of Movement," V kn: Tezisy dokladov i soobshcheniy na Vsesoyuznom mezhvuzovskom simpoziume po prikladnoy matematike i kibernetike [In book: Abstracts of Reports and Communications to the All-Union Inter-Higher Educational Institution Symposium on Applied Mathematics and Cybernetics], Gor'kiy, 1967.

18. Kulik, V. T., Printsipy algoritmizatsii i postroyeniya uptravlyayushchikh mashin [*Principles of Presenting Controllers in Algorithmic Form and* of Controller Construction], Gos. izd. tekh. lit., Kiev, 1963.

N73-26080

SOME PRINCIPLES INVOLVED IN THE CONSTRUCTION OF UNAMPLIFIED CONTROL SYSTEMS FOR ELECTROMECHANICAL MANIPULATORS

Ya. I. Aronov

ABSTRACT. The requirements for manipulator control systems are listed. General principles involved in the construction of unamplified reversible follow-up systems using selsyns are discussed.

The efficiency of the operator-manipulator system is determined by the manipulator's control system. Manipulator control systems should satisfy the following requirements in order to perform a wide range of operations for minimum expenditure of the operator's strength: /56

1. Ensure that the slave "arms" copy the movements of the master "arms" with the necessary speeds and accelerations.

2. Create conditions for the operator to control the forces applied to the manipulator slave elements completely, or partially, to scale, for medium and large load-carrying capacity manipulators.

3. Ensure a minimum expenditure of the operator's muscular energy when working with the manipulator.

These requirements are satisfied by control systems with active force reflection, otherwise known as reversible follow-up systems (RFS). A number of schemes for reversible follow-up systems have been developed in the Soviet Union and abroad [1, 2] which, as a rule, are rather complex automatic control systems using a combination of two transformer follow-up systems. One is for position following, the other for force following. Complicated correction mechanisms are required for quality operation of a reversible follow-up system such as this. Thus, a control system with one degree of manipulator mobility includes quite complicated amplifier-converter electronic equipment. A manipulator set (two master and two slave arms) with seven degrees of mobility is controlled by 14 RFS.

The use of complicated equipment, made up of many elements, creates difficulties in providing failure-free operation of a manipulator, especially in those branches of industry where a breakdown, or failure, in manipulator control can be disastrous. Manipulators with the simplest possible control

systems must be built for these branches.

Such systems, obviously, must be built of elements that will work when signals are strong enough and thus will not require amplifiers. Such reversible follow-up systems as unamplified manipulator control systems can be characterized in accordance with this criterion. The best example of an unamplified reversible follow-up system is a selsyn-type synchronous indicator follow-up system [3]. /57

This system has position reversibility. The selsyn rotors will match regardless of the shaft to which the controlling action is applied; to the shaft of the selsyn transmitter, or to the shaft of the selsyn receiver. The indicator system also has the property of moment reversibility: a moment applied to the shaft of the selsyn transmitter is reproduced at the shaft of the selsyn receiver, and vice versa. The error in the position of receiver and transmitter shafts is determined by the magnitude of the synchronizing moment, equal to the difference in the moments applied to these shafts.

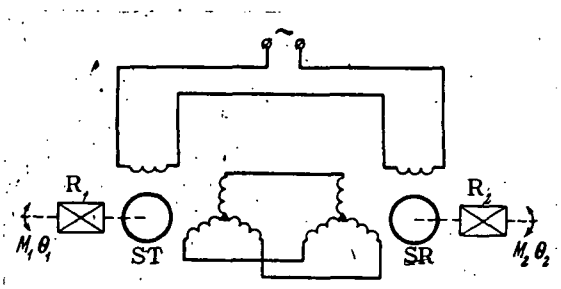

Figure 1. A reversible follow-up system using power selsysn in the indicator mode.

The magnitude of a system's maximum synchronizing moment when the most powerful indicator selsyns (for example, the ND-521 transmitter NS-501 receiver) are used is 2.6 kgf-cm, which is clearly inadequate if these systems are to be used as manipulator control systems.

Our industry has produced SS-195 type power selsyns with a specific synchronizing moment of 1.5 cm/deg for power synchronous follow-up systems. However, they cannot be used in a manipulator because each such selsyn weighs more than 60 kg. Thus, lack of power selsyns with the necessary power ratings and, at the same time, acceptable size substantially limits the possibility of using selsyn synchronous follow-up systems for manipulator control.

Of the indicator seslyns produced by our industry, the ND-521 is the most suitable for operation in the power mode. A follow-up system made up of a pair of these selsyns (the ND-521 is also used as the receiver) is stable and has completely satisfactory static and dynamic characteristics. The system's

maximum synchronizing moment is 12 kgf-cm when the shafts of the transmitter and receiver are mismatched by 70 degrees. Reduction gears R_1 and R_2 (Figure 1), must be installed between the shaft of the selsyn transmitter and the master element, and, correspondingly, between the shaft of the selsyn receiver and the slave element in order to use this particular system, even with a light-duty manipulator. This increases the synchronizing moment and the accuracy with which the system settles out by a factor of i (where i is the reduction gear ratio), while at the same time raising the possibility that the shafts in the system will make a false match in 360: i positions, and that there will be considerable distortion in the transmission of moments from the slave to the master because of friction and inertia in the reduction gears and selsyns. The position of the slave "arms" is monitored visually by the operator, so the possibility of a false match between the manipulator's master and slave "arms" presents no danger. The operator can always match their positions before beginning work, as well as while the work is going on.

To clarify the properties of the system as it transmits force, let us consider the equation of moments when the motion of the input shaft with constant acceleration is given: 58

$$M_1 = M_2 + M_{Fr1} + M_{Fr2} + (I_1 + I_2)\frac{d^2\Theta_1}{dt^2},$$

where

M_1 and M_2 are the moments on the master and slave shafts, respectively;

M_{Fr1} and M_{Fr2} are the selsyn and reduction gear moments of friction normalized to the input shaft;

I_1 and I_2 are the selsyn rotor and gear link moments of inertia normalized from the selsyn shafts to the system's input and output shafts;

Θ_1 is the angle imparted by the shaft of the master mechanism.

The equation shows that the operator, in addition to becoming aware of the useful signal, equal to the applied load moment, M_2, also will become aware of the slave and master mechanism gearing moments of friction, M_{Fr2} and M_{Fr1}, normalized to the master shaft, and the normalized dynamic moments attributable to the inertia in the selsyn rotors and in the gearing associated with them $(I_1 + I_2)\, d^2\Theta_1/dt_2$.

The magnitudes of the normalized friction moments are directly dependent on the reduction gear ratio, i, and the normalized dynamic moments will be directly proportional to the square of the gear ratio. Harmful moments attributable to the forces of friction and inertia can be several times the load moment, M_2, applied to the slave element when reduction is great.

The operator then will find it difficult to monitor the forces applied to the slave element and will in addition, have to exert a great deal of force even to control an unloaded manipulator. The effect of the harmful moments on the operator's arm can be reduced, and control of the manipulator can be facilitated, by the introduction of proportionality in the transmission of the moment from the slave to the master element.

Now the equation of moments will be

$$M_1 = M_{Fr1} + m(M_2 + M_{Fr2}) + (I_1 + mI_2)\frac{d^2\Theta_1}{dt^2},$$

where m is the proportionality factor.

Let us, in order to explain how porportional transmission of moment in a synchronous indicator follow-up system is possible, consider the equation of moments for a selsyn transmitter and receiver [3].

The moment of the shaft of the selsyn transmitter (ST) is

$$M_T = \frac{3}{2} \cdot \frac{1{,}02 \cdot 10^4}{\omega} \cdot \frac{E_{sT}E_{sR}}{2Z} \cdot \frac{W_T W_R}{W_{sT} W_{sR}} \sin(\alpha - \beta) \times \left[\cos(\varphi_R - \varphi_T)\frac{X}{Z} - \sin(\varphi_R - \varphi_T)\frac{R}{Z}\right]. \quad (1)$$

The moment on the shaft of the selsyn receiver (SR) is

$$M_T = \frac{3}{2} \cdot \frac{1{,}02 \cdot 10^4}{\omega} \cdot \frac{E_{sT}E_{sR}}{2Z} \cdot \frac{W_T W_r}{W_{sT} W_{sR}} \sin(\beta - \alpha) \times \left[\cos(\varphi_R - \varphi_T)\frac{X}{Z} + \sin(\varphi_R - \varphi_T)\frac{R}{Z}\right], \quad (2)$$

where

E_{sT} is the actual value, for the angle, of the maximum emf induced in the transmitter synchronization phase;

E_{sR} is the same for the receiver;

Z is the modulus of complex circuit resistance for each pair of series-connected transmitter and receiver phases;

W_{sT} is the effective number of turns in the transmitter excitation winding;

W_{sR} is the same for the receiver;

α is the transmitter angle of rotation;

β is the receiver angle of rotation;

ω is the angular frequency;

φ_R is the receiver supply voltage time phase;

φ_T is the transmitter supply voltage time phase.

As may be seen from Eqs. (1) and (2), the moments on transmitter and receiver are equal in absolute magnitude when the supply is in-phase.

If the receiver and transmitter are supplied with voltages shifted in phase, the moment on the receiver will be greater than that on the transmitter, that is, the moment transmitted from receiver to transmitter will be in proportion.

The following condition should be satisfied in order to provide specified proportionality when X = R:

Figure 2. Reversible follow-up system using power selsyns with proportional moment.

The shift in the phase of the voltage supplied to the field winding of one selsyn relative to another is achieved by connecting capitance, C, in series with one of the field windings.

The synchronous follow-up system using ND-521 power selsyns with proportional moment described above (Figure 2) was used to control the links of a manipulator with a 5 kg load capacity. The system provided manipulator efficiency with the following technical data (motion, rocking of the hand): (1) load capacity

5 kgf; (2) proportionality in the transmission of moment from slave to control element 1:1; (3) maximum speed of end of working tool 685 mm/sec; (4) maximum acceleration 2690 mm/sec^2; (5) touching force 600 gf.

However, this scheme cannot be used for high capacity manipulators (severe distortions in the forces being monitored because of harmful moments of inertia and friction, etc).

A scheme has been developed for medium capacity manipulators (up to 10 kg), in which the harmful moments from forces of friction and inertia, are largely balanced at the shaft of the controlling mechanism by a special follow-up system using a motosyn (a combined selsyn-motor) [5].

The combined selsyn-motor was invented by D. V. Svecharnik [4]. The SDS-3M, an industrial type combined selsyn-motor, was developed by the "Teplopribor" Scientific Research Institute (Moscow) and put into production [4]. Figure 3 is a longitudinal cross section of the motor. The principal components are the stator 1, internal rotor 2, and hollow rotor 3. The stator of the SDS-3M motor is similar to the stator of the ND-521 selsyn. The hollow aluminum rotor can turn in bearings with respect to the internal rotor shaft. The internal rotor winding is single-phase, that of the stator three-phase. All three phases of the motor can be sued when the motor is used in a follow-up system as a combined selsyn-motor, in which case the stator winding is the synchronization winding. Figure 4 shows how the SDS-3M motor is connected to drive an electromechanical manipulator. Only two phases of the stator winding, connected in series with a condenser, are used. The hollow rotor motor depends /60 on the angle of rotation of the internal rotor relative to the stator when the power supply to the motor is as shown in Figure 4. When the winding axes coincide there is no rotating magnetic field in the gap, and the hollow rotor is stationary. A rotating magnetic field is created in the gap with rotation of the internal rotor and the hollow rotor begins to rotate. The hollow rotor moment and speed depend on the absolute magnitude of the angle of rotation and reach maxima at rotation of approximately 80-100°. The direction of rotation, and the sign of the moment, depend on the sign of the angle of rotation.

The SDS-3M motosyn has the following technical characteristics: maximum SDS-3M motor starting torque exceeds 4000 g-cm; idling speed is approximately

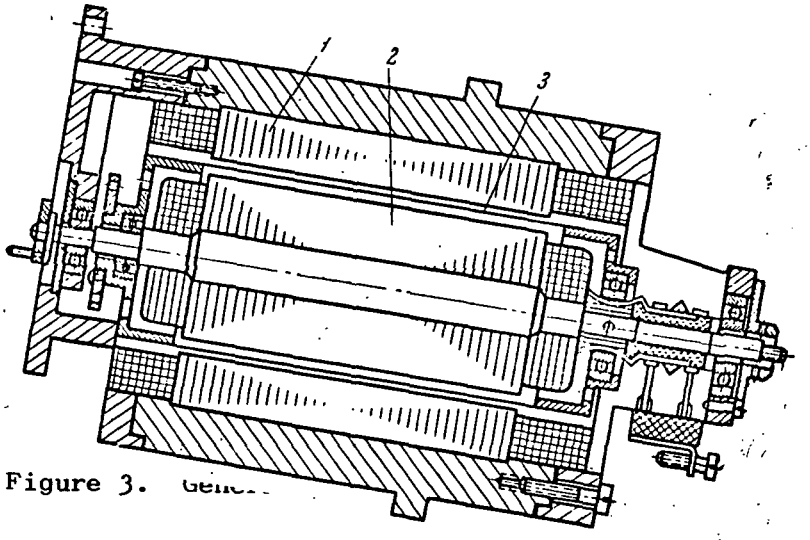

Figure 3. Gene...

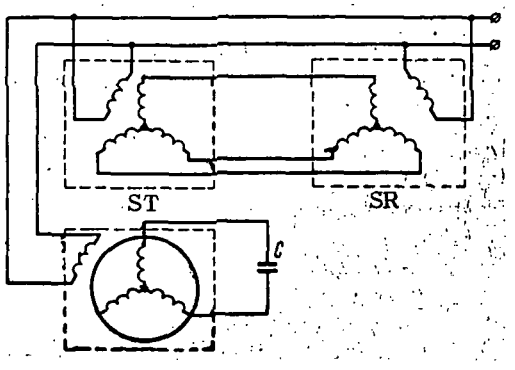

Figure 4. Electric circuit of an unamplified reversible follow-up system with a motosyn.

2700 rpm. The ...cal characteristic (moment in terms of speed) decreases monotonously with a nonlinearity of 25% when the angle of rotation of the internal rotor is $\Theta = 90°$. The motor has satisfactory regulation characteristics. The machine's utilization factor (the ratio of power realized in the form of starting torque to the active power required by the machine when starting) is 77.8% equal to that of conventional motors of corresponding size with a hollow rotor operating "all out." The SDS-3M can operate "all out" with a moment of 400 gf-cm ($\Theta = 70°$) with a 30% connection time. Intensive air-cooling of the motor is necessary for normal operation /61 because continuous connection in the start mode for 30 minutes will cause the internal rotor winding to heat to 130°C.

The stator and rotor winding supply is 45 V 50 Hz, and the capacitance of the condensor in the stator winding is 300 μf.

Figures 4 and 5 show the electrical and kinematic diagrams of a control system with one degree of meanipulator mobility using motosyns. The slave mechanism, I (see Figure 5), includes selsyn receiver 1, reduction gear 2, and output shaft 3. The control mechanism, II, consists of selsyn-transmitter 4, reduction gear 5, and flexible coupling 6, connected through geared transmission 7 to solid rotor 9 of SDS-3M motor 10. The solid rotor shaft is coupled to system input shaft 14. The coupling is connected to motor housing 10 on the other side

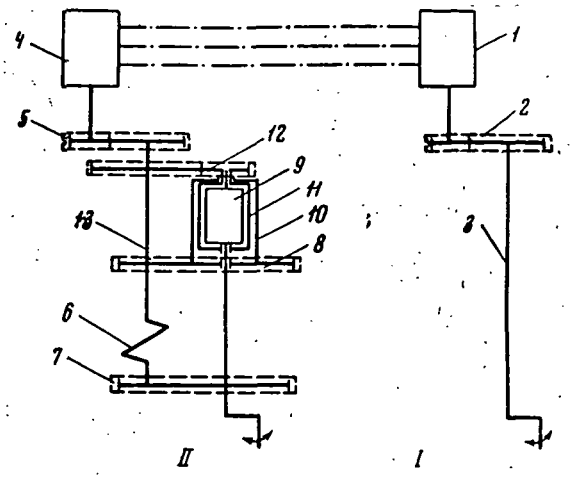

Figure 5. Kinematic diagram of an unamplified RFS with a motosyn.

through geared transmission 8. The hollow rotor of the SDS-3M is connected through geared transmission 12 to drive output shaft 13. Electrically (see Figure 4) the selsyns (transmitter ST and receiver SR) are connected in what is the conventional arrangement for selsyns operating in the indicator mode. The SDS-3M motor rotor winding is connected to the net, and the stator winding is connected to the net in series with condenser C, selected to create a time shift of 90° in the rotor and stator winding phases. A closed proportional follow-up in which the solid rotor follows the SDS-3M stator results when there is closure of the stator of the SDS-3M and its hollow rotor by a mechanical transmission.

The system operates as follows. Flexible coupling 6 is deformed when drive input shaft 14 turns (see Figure 5) and solid rotor 9 of the SDS-3M motor is mismatched relative to its stator 10. Hollow rotor 11 now turns, turning reduction gear 5 and selsyn transmitter 4 through geared transmission 12. Friction and inertia in this part of the kinematic chain are balanced simultaneously matching the SDS-3M motor stator and its solid rotor 9 through transmission 8. Selsyn receiver 1 matches the slave mechanism output shaft with control mechanism input shaft 14. This is how the slave element tracks the position of the master.

Moment M_2, applied to the slave mechanism shaft, is transmitted by selsyn transmitter 4 through reduction gear 5, flexible coupling 6, and geared transmission 7 to input shaft 14. Simultaneously, the SDS-3M motor stator is mismatched with its solid rotor 9 through geared transmission 8 because of deformation of flexible coupling 6. The result is to set up a counteracting moment, M_k, on shaft 13. Chaning the SDS-3M supply voltage, the gear ratio of transmission 12, and the stiffness of flexible coupling 6, we can make this counteracting moment, M_k, equal to the friction moment of the kinematic chain from the hollow rotor of the SDS-3M motor to selsyn transmitter 4 and to the friction moment of the kinematic chain of the slave mechanism normalized to shaft 13. 62

The proportion in which the moment is transmitted then will be close to unity, $M_1 = M_2$, or, in order for moment M_k to exceed the magnitudes of the harmful moments, $M_1 < M_2$, that is, the moment applied to shaft 3 of the slave mechanism will be transmitted to shaft 14 of the control mechanism in a definite proportion.

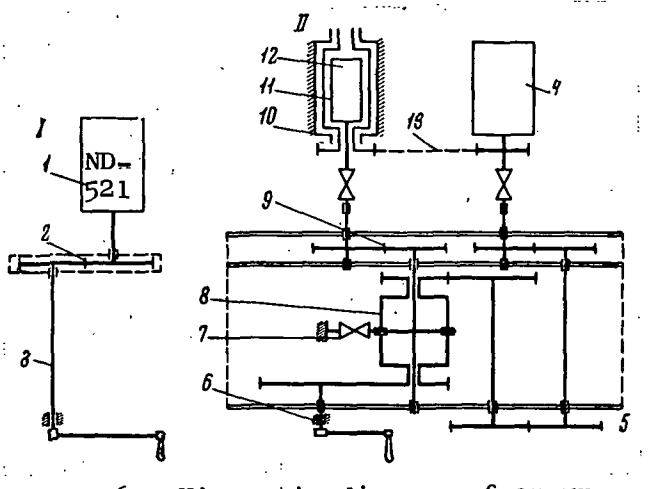

Figure 6. Kinematic diagram of an unamplified RFS with a motosyn. Static variant. 1 - selsyn transmitter; 2 - slave mechanism reduction gear; 3 - system input shaft; 4 - selsyn receiver; 5 - master mechanism reduction gear; 6 - system output shaft; 7 - flexible coupling; 8 - differential; 9 - geared transmission; 10 - SDS motorsyn stator; 11 - motosyn hollow rotor; 12 - motosyn solid rotor; 13 - geared transmission.

There are design problems involved in the realization of the kinematic scheme discusssed when applied to manipulators. Then too, slip rings and brushes must be installed to bring the power supply to the rotating stator of the motosyn, reducing control system reliability. The control system shown in Figure 6 is devoid of the shortcomings noted above. Here the SDS stator is fixed and matching of the balancing follow-up system is accomplished through a differential, which facilitates the structural configuration of the manipulator gear box and reduces electrical contacts in the circuit to a minimum.

This control system has been built for a 10 kgf capacity manipulator. The manipulator is highly dependable in operation, is simple in design and operation, yet has such completely satisfactory technical characteristics as swinging motion of the "hand" for example. The mean linear speed of the tip of the operating tool is 370 mm/sec. Maximum acceleration of the tip of the operating tool is 1540 mm/sec^2. The touching force of the unloaded manipulator is 700 fg. The proportionality in the transmission of force is 1:1.7.

REFERENCES

1. Sirazitdinov, B. G., Zubkov, D. I., "A Reversible Follow-up System for Transmission of Forces and Movements Over a Distance," Izv. VUZov Priborostroyeniye, No. 3, 1961.

2. Masakudu, E., Akira, K., "Servomanipulators," Keysoku-to seyge, No. 7, 1963.

3. Svecharnik, D. V., Sel'siny i ikh primeneniye v sistemakh avtomatizatsii proizvodstvennykh protsessov [Selsyns and Their Use in Systems for the Automation of Production Processes], Gosenergoizdat, 1962.

4. Aronov, Ya. I., Isayev, V. L., Patent No. 1899907, Byulleten' izobreteniy, No. 1, 1967.

5. Svecharnik, D. V., Patent No. 107434, Byulleten' izobreteniy, No. 8, 1958.

N73-26081

PRINCIPAL PARAMETERS AND OPERATING INDICES FOR REVERSIBLE FOLLOW-UP SYSTEMS

V. S. Kuleshov, I. N. Yegorov

ABSTRACT. An engineering approach to the analysis of the principal parameters and operating indices for reversible follow-up systems is presented. Structurally symmetrical and structurally asymmetrical systems are discussed.

Many remote-controlled master-slave manipulators have been designed to include the property of active reflection of the forces developed by the slave member on the operator's shaft. These systems received the designation reversible follow-up systems (RFS) because they follow from the master side, as well as from the slave side [1]. 63

Reversible follow-up systems are a special class of two-dimensional automatic regulating systems, the control coordinates of which are the external moments generated by the operator and by the load. The control coordinates are considered to be the positions of the operator and load shafts.

The use of reversible follow-up systems to control master-slave manipulators fixes a number of particularly specific indices of their quality of performance. It is obvious that inherent in reversible follow-up systems as in any other automatic regulating system, are specific dynamic indices such as frequency properties and stability indices. Indices of quality of performance in transient modes are highly important in the designing of RFS.

However, at the basis of any method used to design RFS is the need to ensure first of all specific indices of quality of performance under steady-state conditions. This is so because the basic conditions under which master-slave manipulators perform, and in which the property of force reflection should be most completely manifested are just such steady-state conditions. These conditions refer to motion of master and slave shafts at constant speed under the influence of external moments generated by the operator and by the load. Moreover, the smaller the error in the measurement of the loading moments generated by the operator when the shafts move at a predetermined speed, the greater the sensitivity of the reversible system.

Moreover, when shafts are stationary, when the error in the operator's

perception of the loading moments is infinitesimally small, it is important to estimate the proportionality of the force reflection as well as the precision in matching the angular coordinates of the operator's shaft and the load shaft when external moments are acting. All these performance indices depend on definite reversible system parameters [2].

The literature does not, at this time, contain a general procedure for evaluating the principal reversible performance indices, and the relationship between system parameters and their performance indices under steady-state conditions is not always established. So it is difficult to make a comparative analysis of the different reversible system variants when designing master-slave manipulators and to make a valid selection of RFS parameters and elements for specified performance quality indices. This article attempts to fill this gap and suggests an engineering approach to analysis of RFS principal parameters and operating indices. As a practical matter, all types of reversible follow-up systems can be broken down into two basic types, which we shall arbitrarily call structurally symmetrical and structurally asymmetrical. /64

Let us understand a structurally symmetrical RFS to be one in which the main circuit consists of two symmetrical systems, closed with respect to position. The structurally symmetrical arrangement usually includes elements and couplings needed to compensate for the "internal" moments, and this causes asymmetry. However, this does not change the original structural symmetry of the system.

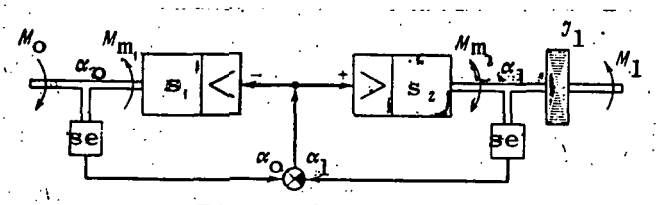

Figure 1.

A structurally asymmetrical RFS includes a slave system closed with respect to position, and a manipulator master element system closed with respect to moment. This enables the operator to control the position of the slave elements with the former and to perceive the force developed by the slave at the master. Let us move on to a consideration of these two basic types of RFS.

Let us examine the principal parameters and operating indices for a reversible follow-up system by using the example of the structurally-symmetrical system in Figure 1.

The dynamics of the operation of this system can be described by the following system of differential equations written in Laplace transforms for zero initial conditions

$$\begin{aligned} M_{m_1}(P) &= I_1 P^2 \alpha_o(P) - M_o(P); \\ M_{m_2}(P) &= (I_2 + I_1) P^2 \alpha_1(P) + M_1(P); \\ M_{m_1}(P) &= C_1(P)[\alpha_1(P) - \alpha_o(P)] - b_1(P) P\alpha_o(P); \\ M_{m_2}(P) &= C_2(P)[\alpha_o(P) - \alpha_1(P)] - b_2(P) P\alpha_1(P), \end{aligned} \tag{1}$$

where

$M_{m_1}(P)$, $M_{m_2}(P)$ are the moments developed by the slaves attributable to the operator, and load, respectively;

$M_o(P)$, $M_1(P)$ are the moments applied to the shafts of the slave elements by the operator and by the load;

$$I_1 = I_{m_1} + I_{k_1}; \quad I_2 = I_{m_2} + I_{k_2}, \tag{2}$$

where

I_m is the motor rotor moment of inertia;

I_k is the moment of inertia of the links in the kinematic chain for the corresponding degree of freedom;

I_1 is the moment of inertia of the load at the slave;

$\alpha_o(P)$, $\alpha_1(P)$ are the coordinates of operator and load shafts, respectively;

$C_1(P)$, $C_2(P)$ are the transfer functions of the elements in the system between the coordinates of the input and moment developed by the motors;

$b_1(P)$, $b_2(P)$ are the transfer functions of the internal negative feedbacks in terms of operator and load shaft speeds. /65

Thus, if nonself-excited direct current motors and armature circuit control are used as the slave elements in the system, and if the internal feedbacks used to correct system properties are lacking, we will have

(3)

where

k_m is the slave motor moment transmission coefficient;

R_a is the resistance of the motor armature circuit;

τ_e is the electrical time constant for the motor armature circuit;

k_ω is the motor's counter-emf coefficient;

$W_{am}(P)$ is the amplifier transfer function, including the series correction circuit.

Transforming the system of equations at (1), we obtain

$$\begin{aligned} M_o(P) &= M_1(P) + I_1 P^2 \alpha_o(P) + b_1(P) P \alpha_o(P); \\ M_2(P) &= M_1(P) + (I_2 + I_1) P^2 \alpha_1(P) + b_2(P) P \alpha_1(P); \\ M_1(P) &= C_1(P)[\alpha_o(P) - \alpha_1(P)]; \\ M_2(P) &= C_2(P)[\alpha_o(P) - \alpha_1(P)]. \end{aligned} \tag{4}$$

Figure 2 is a structural diagram corresponding to the systems of differential equations at (1) and (4).

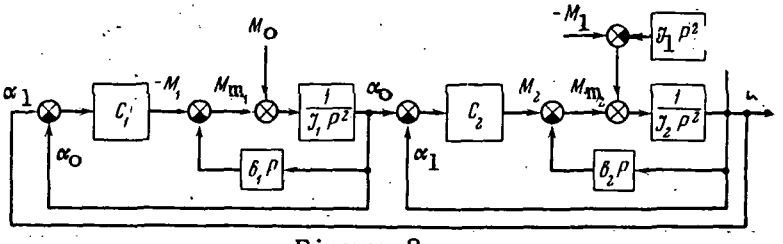

Figure 2.

As may be seen from the system of differential equations at (4), the precision with which position is followed by a reversible follow-up system is determined by the magnitude of the external moments, M_o and M_1, as well as by the parameters $C_1(P)$ and $C_2(P)$

(5)

$C_1(P)$ and $C_2(P)$ will be understood to be the magnitudes of the dynamic rigidity of the reversible follow-up system with respect to M_o and M_1.

In steady-state conditions, when M_o, M_1 = const; α_o, α_1 = const

$$\alpha_o - \alpha_1 = M_o / C_1 = M_1 / C_2, \tag{6}$$

where

C_1 and C_2 are the coefficients of the transfer functions $C_1(P)$, $C_2(P)$.

The error in the angular coordinates of the operator's shaft and of the load shaft is determined by the coefficients of the transfer functions for the elements in the circuit between the input to each drive, and the moments developed by the motors.

The experimental determination of these coefficients under steady-state conditions can be made by applying a moment that is constant in magnitude to the operator's shaft, or to the load shaft, with the position of one of the shafts locked. /66

(7)

The principle operating indices of reversible follow-up systems can be analyzed by using the general dynamics equation, derived from the original system of differential equations at (1).

The general dynamics equation for the operation of an RFS for the system studied has the form

(8)

Under steady-state operating conditions, when $P\alpha_o(P) = P\alpha_1(P)$ = constant

$$M_{\alpha_1}(P) = \frac{C_1(P)}{C_2(P)} [M_1(P) + b_2(P) P\alpha_1(P)] + b_1(P) P\alpha_o(P). \tag{9}$$

Solving this equation with respect to $P\alpha_o(P) = P\alpha_1(P) = P\alpha(P)$ we obtain

(10)

Eq. (10) establishes one of the basic operating indices for a reversible system, that of the sensitivity of the RFS to the action of external moments.

It is obvious that $P\alpha_o = P\alpha_1 = \text{const}$ is possible when one of the following conditions is satisfied

$$\begin{aligned} &M_o(P)\,C_2(P) - M_1(P)\,C_1(P) = \text{const};\\ &M_o(P) = \text{const}; \quad M_1(P) = \text{const}. \end{aligned} \tag{11}$$

The sensitivity of operation of a reversible follow-up system with respect to externally acting moments can be established for steady-state conditions from the following relationships.

When $M_o = \text{const}$; $M_1 = 0$; $P\alpha_o = P\alpha_1 = P\alpha = \text{const}$

$$\frac{P\alpha}{M_o} = \frac{C}{b_2C_1 + b_1C_2} = D_1. \tag{12}$$

When $M_1 = \text{const}$; $M_o = 0$; $P\alpha_o = P\alpha_1 = \text{const}$

$$\begin{aligned} &= 0;\ P\alpha_{on} = P\alpha_{H} = \text{const}\\ &\frac{P\alpha}{M_1} = \frac{C_1}{b_2C_1 + b_1C_2} = D_2, \end{aligned} \tag{13}$$

where b_1 and b_2 are the coefficients of the transfer functions $b_1(P)$; $b_2(P)$.

The coefficients D_1 and D_2 can be called the coefficients of the quality factor for the system with respect to the external moments, and they establish the sensitivity of operation of the RFS under steady-state conditions.

One of the basic features of reversible follow-up systems distinguishing them from conventional automatic regulating systems is the property of active reflection at the operator s shaft of load moments applied to the manipulation element. This property of RFS can be analyzed using Eq. (8), the general work dynamics equation. What follows from this equation is that the operator perceives the external load moments $[M_1(P) + I_1P^2\alpha_1(P)]$ with a definite reflection proportionality factor.

The magnitude of the force (moment) reflection proportionality factor is the most important parameter of a reversible follow-up system. The proportionality factor for a structurally-symmetrical RFS arrangement is

(14)

From the general dynamics equation it also follows that the operator, in addition to the external load moments, also perceives the so-called internal moments inherent in the reversible follow-up system proper

$$M_{in_1}(P) = I_1 P^2 \alpha_{o_1}(P) + b_1(P) P \alpha_{o_1}(P);$$
$$M_{in_2}(P) = I_2 P^2 \alpha_1(P) + b_2(P) P \alpha_1(P). \qquad (15)$$

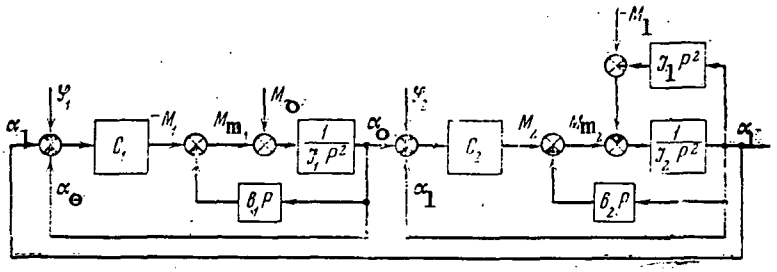

Figure 3.

The presence of "internal" moments causes an error in the operator's perception of the external load moments:

$$M_{o_1}(P) = n(P)\,[M_1(P) + I_1 P^2 \alpha_1(P)] + \Theta_M(P), \qquad (16)$$

where

$$\Theta_M(P) = M_{in_1}(P) + n(P)\,M_{in_2}(P) \qquad (17)$$

is the error in the operator's perception of the load moments.

It is obvious that precision in the operator's perception $[M_1(P) + I_1 P^2 \alpha_1(P)]$ is determined by system parameters, as well as by its mode of operation. Thus, if the friction moments in the system are negligibly small, $\Theta_M(P) = 0$, when the positions of the operator and load shafts are locked. Let us consider methods for compensating for internal moments in structurally symmetrical RFS arrangements.

The dynamics of the operation of an RFS with compensating signals $\varphi_1(P)$, and $\varphi_2(P)$, the block diagram of which is presented in Figure 3, can be described by the following system of differential equations written in Laplace transforms for zero initial conditions

$$
\begin{aligned}
M_{o_1}(P) &= M_1(P) + M_{in_1}(P);\\
M_2(P) &= M_1(P) + I_1 P^2 \alpha_1(P) + M_{in_2}(P);\\
M_1(P) &= C_1(P)[\alpha_{o_1}(P) - \alpha_1(P) - \varphi_1(P)];\\
M_2(P) &= C_2(P)[\alpha_{o_2}(P) - \alpha_1(P) - \varphi_2(P)].
\end{aligned}
\tag{18}
$$

The fundamental work dynamics equation for the structurally symmetrical RFS with compensating signals has the following form

(19)

Eq. (19) shows that two fundamentally different methods of compensating for "internal" moments are possible

I
$$
\varphi_1(P) - \varphi_2(P) = \frac{M_{in_1}(P)}{C_1(P)} + \frac{M_{in_2}(P)}{C_2(P)}; \tag{20}
$$

II
$$
\varphi_1(P) - \varphi_2(P) = m\left[\frac{M_{o_1}(P)}{C_1(P)} - \frac{M_1(P) + I_1 P^2 \alpha_1(P)}{C_2(P)}\right]. \tag{21}
$$

Here m is external moment signal transmission factor. /68

The first compensation method is based on feeding signals to the RFS that are proportional to the "internal" moments, and measured by indirect methods. Indirect methods of measuring M_{in} are extremely complex and imprecise, so the second method of compensating for M_{in} is most often used.

It should be noted that compensating signals proportional to the external influences on the operator, as well as on the load, shaft should be fed into the structurally symmetrical RFS.

If

$$
\varphi_1(P) - \varphi_2(P) = m\frac{M_{o_1}(P)}{C_1(P)},
$$

then

(22)

$$
M_{o_1}(P) = \frac{C_1(P)}{(m+1)C_2(P)}[M_{1_1}(P) + I_{1_1} P^2 \alpha_1(P) + M_{in_2}(P)] + \frac{M_{in_1}(P)}{m+1}.
$$

If

$$\varphi_1(P) - \varphi_2(P) = m \frac{M_1(P) + I_1 P^2 \alpha_1(P)}{C_2(P)},$$

then

$$M_{o1}(P) = \frac{C_1(P)(m+1)}{C_2(P)} [M_1(P) + I_1 P^2 \alpha_1(P)] + \frac{C_1(P)}{C_2(P)} M_{in_2}(P) + M_{in_1}(P). \quad (23)$$

As may be seen from Eqs. (22) and (23), signals proportional to the external influence of just one side change the proportionality factor for the operator's perception of load moments.

The simultaneous supply of signals proportional to the external influences attributable to operator and load, that is, the Eq. (21) condition is satisfied makes the general working dynamics equation for the RFS into

$$M_o(P) = \frac{C_1(P)}{C_2(P)} [M_1(P) + I_1 P^2 \alpha_1(P)] + \frac{[I_1 P^2 + b_1(P) P] \alpha_{o1}}{m+1} \quad (24)$$

As may be seen from Eq. (24), the influence of the "internal" moments on the precision of the operator's perception of load moments has been reduced by a factor of (m + 1).

Let us examine the operation of an RFS with couplings compensating for the "internal" moments under basic steady-state conditions.

When $P\alpha_o(P) = P\alpha_1(P) = P\alpha(P) = \text{const}$, the fundamental work dynamics equation for the RFS of Eq. (24) becomes

$$M_{o1}(P) = \frac{C_1(P)}{C_2(P)} M_1(P) + \frac{1}{m+1} \left[b_1(P) P\alpha_o(P) + \frac{C_1(P)}{C_2(P)} b_2(P) P\alpha_1(P) \right]. \quad (25)$$

Solving this equation for $P\alpha(P)$, we derive an expression which determines the sensitivity of operation of the RFS when compensating couplings are added

$$P\alpha(P) = (m+1) \frac{M_{o1}(P) C_2(P) - M_1(P) C_1(P)}{b_2(P) C_1(P) b_1(P) C_2(P)}. \quad (26)$$

The quality factors for the system in terms of external moments have the following form.

When M_o = const, M_1 = 0 /69

$$D_1 = \frac{P\alpha}{M_{op}} = (m+1)\frac{C_2}{b_2C_1 + b_1C_2}. \tag{27}$$

When M_1 = const: M_o = 0

$$D_2 = \frac{P\alpha}{M_1} = (m+1)\frac{C_1}{b_2C_1 + b_1C_2}. \tag{28}$$

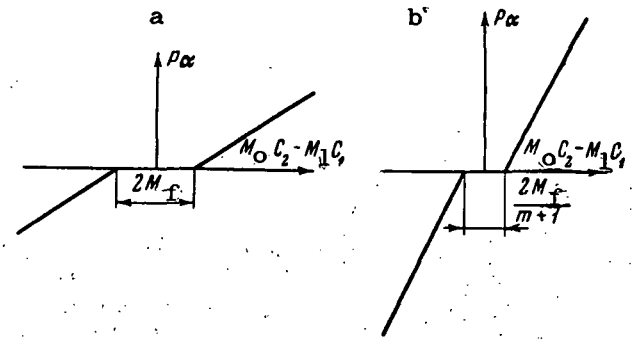

Figure 4. Graphs of the Pd(P) relationships. a - without compensating couplings b - with compensating couplings.

The system quality factor, that is, sensitivity to the action of external moments, increases by a factor of (m + 1).

Friction moments in the kinematic chains are included in the internal moments inherent in the reversible follow-up system. Dry friction moments, which considerably distort the functioning of the reversible system, can have very definite influence.

Let us consider the operation of an RFS with dry friction moments in the kinematic chains on the operator, as well as on the load side. The work dynamics equation for this system has the form

$$\begin{aligned} M_o(P) = \frac{C_1(P)}{C_2(P)}[M_1(P) + (I_1 + I_2)P^2\alpha_1(P) + b_2(P)P\alpha_1(P) + \\ + |M_{f_2}|\operatorname{sign} P\alpha_1(P)] + |M_{f_1}|\operatorname{sign} P\alpha_o(P) + \\ + [I_1P^2 + b_1(P)P]\alpha_o(P). \end{aligned} \tag{29}$$

It is obvious that the precision of the operator's perception of the load moments will be determined to a large extent by the magnitude of the dry friction moments.

The sensitivity of RFS operation is determined by the expression

$$P\alpha(P) = \frac{M_{o_2}(P)\,C_2(P) - M_{1_2}(P)\,C_1(P) - \{|M_{f_{1_2}}|\,C_2(P) + |M_{f_{2_2}}|\,C_1(P)\}}{b_2(P)\,C_1(P) + b_1(P)\,C_2(P)} \qquad (30)$$

when $$M_{o_2}(P)\,C_2(P) - M_{1_2}(P)\,C_1(P) > |M_{f_{1_2}}|\,C_2(P) + |M_{f_{2_2}}|\,C_1(P)$$

and $$P\alpha(P) = 0$$

when $$M_{o_2}(P)\,C_2(P) - M_{1_2}(P)\,C_1(P) < |M_{f_{1_2}}|\,C_2(P) + |M_{f_{2_2}}|\,C_1(P). \qquad (31)$$

Consequently, the graph of $P\alpha(P) = f[M_o C_2 - M_1 C_1]$ has a dead zone (Figure 4a).

With the supply to the structurally symmetrical arrangement of a compensating signal of the type

$$\varphi_1(P) - \varphi_2(P) = m\left[\cdot^{M}\right.$$

the work dynamics equation for the RFS can be written

70

$$\begin{aligned} M_{o_2}(P) = {} & \frac{C_1(P)}{C_2(P)}[M_1(P) + I_1 P^2 \alpha_{1_2}(P) + \\ & + \frac{C_1(P)}{C_2(P)(m+1)}\{[I_2 P^2 + b_2(P)\,P]\,\alpha_{1_2}(P) + |M_{f_{2_2}}|\,\mathrm{sign}\,P\alpha_{1_2}(P)\} + \\ & + \frac{1}{m+1}\{[I_1 P^2 + b_1(P)\,P]\,\alpha_{o_2}(P) + |M_{f_{1_2}}|\,\mathrm{sign}\,P\alpha_{o_2}(P)\}. \end{aligned} \qquad (32)$$

The sensitivity of the operation of an RFS with compensating couplings, signals for which are proportional to the external moments, is determined by the following expression when friction is present in the kinematic chains

$$P\alpha(P) = (m+1)\frac{M_{o_2}(P)\,C_2(P) - M_{1_2}(P)\,C_1(P)}{b_2(P)\,C_1(P) + b_1(P)\,C_2(P)} \qquad (33)$$

when

If this condition is not satisfied, $P\alpha(P) = 0$. Figure 4 shows the relationship

when compensating couplings proportional to the external influences are added.

Thus, the presence of friction moments in the kinematic chains of an RFS reduces its sensitivity to the action of external moments and reduces the precision with which the operator perceives load moments. The insertion of compensating couplings in the structurally symmetrical RFS very nearly balances this negative influence.

Let us consider the principal parameters and operating indices for reversible follow-up systems of the structurally asymmetrical type. Figure 5 is a block diagram of such a system, and the dynamics of its operation can be described by the following system of differential equations written in Laplace transforms for zero initial conditions

$$\begin{aligned}
&M_{m_1}(P) = I_1 P^2 \alpha_0(P) - M_0(P);\\
&M_{m_2}(P) = (I_2 + I_1) P^2 \alpha_1(P) + M_1(P);\\
&M_{m_1}(P) = C_1(P)\{M_0(P) - I_{K_1} P^2 \alpha_{0p} - B_1(P) P\alpha_0(P) -\\
&\qquad - n[M_1(P) + (I_1 + I_{K_2}) P^2 \alpha_1(P)]\};\\
&M_{m_2}(P) = C_2(P)[\alpha_0(P) - \alpha_1(P)] - b_2(P) P\alpha_1(P),
\end{aligned} \tag{34}$$

where

$$I_1 = I_{m_1} + I_{K_1}; \qquad I_2 = I_{m_2} + I_{K_2}.$$

Note that in this arrangement the moment sensors measure the external moments on the master or slave side, as well as the dynamic moments attributable to the inertia in the links in the kinematic chain. This is explained by the fact that in practice it is extremely difficult to install the moment sensors in the output of the kinematic chain of the control or manipulation elements, so they are installed in the slave units after the motors.

We also noted that the magnitude of the moment of inertia of the kinematic chain is variable, and depends on its position.

This system of equations can be transformed into one more convenient for subsequent analysis 71

(35)

C2

$$W_{1m}(p) = \frac{n_1}{M_1} = \frac{k_{1m}}{(T_m p + 1)};$$

$$\Theta_M(P) = M_{in_1}(P) = n(P) M_{in_2}(P) = (I_{K_1} + I_{m_1}) P^2 \alpha_0(P) +$$
$$+ b_1(P) P \alpha_0(P) + n(P) [(I_{K_2} + I_{m_2}) P^2 \alpha_1(P) + b_2(P) P \alpha_1(P).$$

Figure 5.

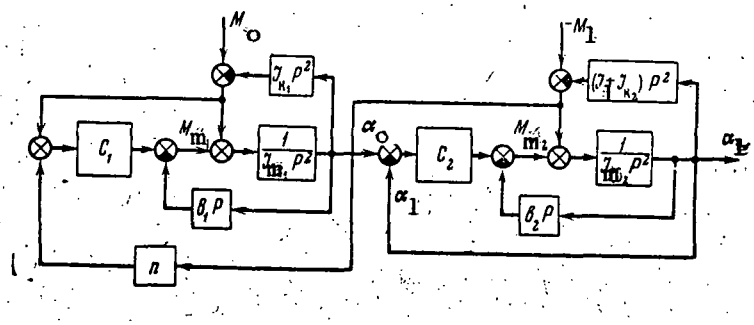

Figure 6.

Figure 6 is the structural diagram of a structurally asymmetrical reversible follow-up system. The general work dynamics equation for this system can be found by solving (35), and has the form

(36)

Since $C_1(P)$ is a transfer function with an extremely large amplification factor, we can consider that

$$M_0(P) \approx n[M_1(P) + (I_1 + I_{K_2}) P^2 \alpha_1(P)] +$$
$$+ I_{K_1} P^2 \alpha_0(P) + \frac{I_{m_1} P^2 \alpha_0(P) + b_1(P) P \alpha_0(P)}{C_1(P)} \qquad (37)$$

or

(38)

where

n is moment proportionality factor;

$\Theta_M(P)$ is the error in the operator's perception of the load moments

(39)

At the same time, we have the following for a structurally symmetrical scheme without compensation for "internal" moments /72

Consequently, the structurally asymmetrical RFS scheme considered provides sufficiently complete compensation for that part of the "internal" moments inside the circuit of the arrangement used for moment measurers.

The general work dynamics equation for a structurally asymmetrical reversible follow-up system under steady-state conditions when $P\alpha_o(P) = P\alpha_1 = (P)\alpha(P) =$ = const has the form

$$M_{o\gamma}(P) \tag{40}$$

In accordance with this equation, the sensitivity of operation of a structurally asymmetrical RFS can be expressed by the following relationship

(41)

The RFS quality factors in terms of the external moments can be determined under steady-state operating conditions.

When

$$M_{o} = \text{const} \qquad M_1 = 0$$

When

$$M_1 = \text{const} \qquad M_{o} = 0 \qquad \frac{P}{M}$$

The conclusion is that under steady-state operating conditions the precision of the operator's perception of the load moments, as well as the sensitivity of the structurally asymmetrical RFS, is determined only by the loader parameters, that is, by the parameters for the active force reflection channel. It is

obvious that the accuracy of position tracking by such a system is determined only by the parameters of a slave drive closed with respect to position.

The structurally asymmetrical RFS scheme does not require the use of additional couplings to compensate for internal moments. All this means that in designing master-slave manipulator control systems we should use structurally asymmetrical schemes which permit delimiting the functions of the direct and return channels while ensuring specified quality indices.

REFERENCES

1. Kuleshov, V. S., Lakota, N. A., "A Structural and Analytical Presentation of Reversible Follow-Up Systems," V sb. Mekhanika mashin [In collection: Mechanics of Machines], Issue 7-8, "Nauka" Press, 1967.

2. Petrov, B. A., Batyukov, A. I., "Some Special Featues in the Calculation of Reversible Follow-Up Systems," V sb. Mekhanika mashin [In collection: Mechanics of Machines], Issue 7-8, "Nauka" Press, 1967.

3. Edziri, M., Kamoi, A., "Servomanipulators," Keysoku to seyge, 2, No. 2, 1963.

N73-26082

SOME QUESTIONS FROM THE USE OF REVERSIBLE FOLLOW-UP SYSTEMS WITH INDEPENDENT FOLLOW-UP AND FORCE REPRODUCTION CHANNELS

B. A. Petrov, V. Ye. Paramonov

ABSTRACT. Questions concerned with the use of independent follow-up and force reproduction channels in manipulators are discussed. The question of selecting the site of operator influence, as well as of the use of the slave mechanism as the reproduction channel output, are considered.

Let us take up a question of substantial practical significance, one that 73
arises with the realization, in a manipulator, of a system with independent follow-up and force reproduction channels [1], namely that of selecting the site of operator influence.

As we know [2, 3] there is no specific concept of system "input" and "output" for reversible follow-up systems. These definitions are purely arbitrary and any of the channels of a reversible drive can be taken as the master, and the other as the slave, as desired by the designer. Let us note that for symmetrical systems, which systems with combined [4] and intersecting channels may be, "input" and "output" are equivalent and, consequently, this question does not arise in their design.

Here we should refine the concept of system "symmetry." The technical literature on control systems for remote-controlled master-slave manipulators often gives different meanings for the concept of "symmetry." Some authors take drive symmetry to mean the symmetry of the drive structure [5], while others, in addition to symmetry of structure, also mean symmetry of drive parameters. According to the second definition, a symmetrical drive should provide equal "input" or "output" reactions to equal disturbing influences at the "output" or "input." In other words, the "output-input" and "input-output" transfer functions are identical for a symmetrical reversible follow-up system. This definition of symmetry, in our opinion, is more precise, and we shall adhere to it.

On the strength of the second definition of symmetry for a symmetrical reversible drive, the dynamics of drive operation do not depend on the site of operator and load action. Asymmetrical RFS (reversible follow-up systems), which include system with independent channels differ. Let us consider the

dynamics of its operation to include the effects of operator and load in order to determine the site of operator action in a system with independent channels. For simplicity in consideration of the question, let us take it that the moment sensors generating signals proportional to the moments acting at the outputs of the reproduction, M_1, and follow-up, M_2, channels have negligibly small deformations, and that they are installed directly on the manipulator's slave and master elements.

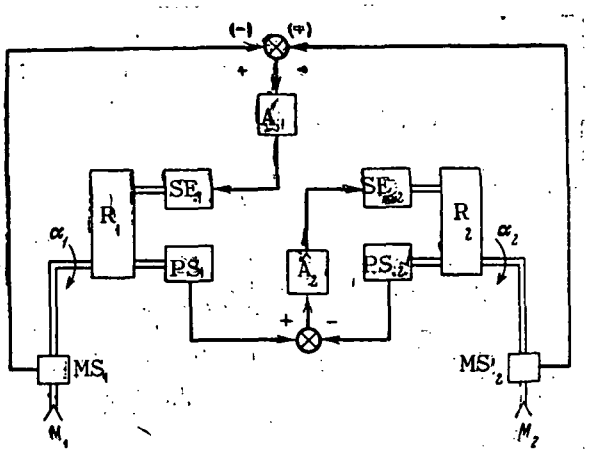

Figure 1.

Figure 1 is a block diagram of an RFS with independent follow-up and force reproduction channels, in which the following designations have been adopted: R_1, R_2 are reduction gears; SE_1, SE_2 are the slave elements in the reproduction and follow-up channels, respectively; PS_1, PS_2 are position sensors; MS_1 MS_2 are moment sensors; A_1, A_2 are amplifiers in the reproduction and follow-up channels, respectively; M_1, M_2 are the moments acting at the outputs of the reproduction and follow-up channels; α_1, α_2 are the generated angles for these channels. /74

System operation is as follows. The follow-up channel, PS_1, PS_2, A_2, SE_2, and R_2 generates position α_1. The reproduction channel, MS_1, MS_2, A_1, SE_1, and R_1 generates moment M_2. These two channels are connected such that the output of one is the input of the other, and vice versa.

Thus, when the operator, for example, acts from the reproduction channel side, M_1, the follow-up channel, controlled by position error $\delta_\alpha = (\alpha_1 - \alpha_2)$, will match the position of the shaft of the reproduction channel, α_1, and the reproduction channel, controlled by moment error $\delta_m = M_1 - M_2$, will help the operatior impart motion, generating at his output a moment coinciding in direction (sign) with the operator's moment.

Appearance of load moment M_2 at the follow-up channel will cause MS_2 to generate a signal which, depending on the direction of the sign of this moment,

will either help the operator impart motion or retard this motion, damping the effect on the channel for reproducing the signal M_1, from the moment sensor. The retarding action of moment M_2 will continue until operator moment M_1 becomes equal, or proportional, to load moment M_2; that is, until moment error δ_m disappears. System operation will be analogous when action by the operator is at the output of the follow-up channel.

The reproduction channel, generating a moment which coincides in direction (when there is no load moment) with the operator's moment at its output will impart motion in both cases. The signs of the signals in the comparison element in the reproduction channel indicated in Figure 1, generally speaking, are purely arbitrary and depend on the relationship and signs of the effective moments M_1 and M_2. The signs without parentheses are for the case when the operator acts at the reproduction channel output and the load has a retarding influence. The signs in parentheses are to indicate when the operator's influence at the follow-up channel output is the same as that of the load. It should be kept in mind that if the position sensors are installed ahead of the flexible couplings of the moment sensors, and if their deformations are taken into accoutn, the signs of the signals in the comparison element in the follow-up channel will also depend on the site of operator influence. /75

Based on the assumptions made above, the dynamics of the operation of RFS with independent channels, a block diagram of which is shown in Figure 1, can be described by the following system of differential equations

$$\left.\begin{aligned} n_1 &= W_1(p)\,\delta_m + W_{1m}(p)\,M_1; \\ n_2 &= W_2(p)\,\delta_n - W_{2m}(p)\,M_2; \\ \delta_m &= \tau_1 M_1 - \tau_2 M_2; \\ \delta_n &= n_1 - n_2. \end{aligned}\right\} \qquad (1)$$

Let us, for reasons of simplicity in considering the question, assume that

$$W_1(p) = \frac{n_1}{\delta_m} = \frac{k_1}{(T_{1m}p + 1)(T_{1a}p + 1)}; \qquad (2)$$

(3)

$$W_2(p) = \frac{n_2}{\delta_n} = \frac{k_2}{p\,(T_{2m}p + 1)(T_{2a}p + 1)}; \qquad (4)$$

$$W_{2m}(p) = \frac{n_2}{M_2} = \frac{k_{2m}}{(T_{2m}p + 1)}, \qquad (5)$$

where

n_1 is the speed at the output of the force reproduction channel;

n_2 is the speed at the output of the follow-up channel;

M_1 is the moment acting at the output of the reproduction channel;

M_2 is the moment acting at the output of the follow-up channel;

δ_m is the moment error acting at the input to the reproduction channel;

δ_n is the speed error acting at the input to the follow-up channel;

τ_1, τ_2 are the sensor conversion factors;

α_1 is the generated angle for the reproduction channel;

α_2 is the generated angle for the follow-up channel;

k_1 is the amplification factor for the reproduction channel circuit;

k_2 is the amplification factor for the follow-up channel circuit;

k_{1m}, k_{2m} are the coefficients of disturbing moments M_1 and M_2;

T_{1m}, T_{2m} are the time constants for the slave elements in the reproduction and follow-up channels including the moving parts in the mechanisms;

T_{1a}, T_{2a} are the electrical time constants for the amplifiers in the reproduction and follow channels;

$p = d/dt$ is the differential operator.

The solution of the system of equat $|Y| = -\frac{1 + W_2(p)}{W_{2m}(p)[W_1(p)\tau_1 + W_{1m}(p)]}$.

$$\left.\begin{aligned} M_1 &= \frac{\tau_2 W_1(p) W_2(p) + W_{2m}(p)}{W_{2m}(p)[W_1(p)\tau_1 + W_{1m}(p)]} n_1 - \frac{\tau_2 W_1(p)[1 + W_2(p)]}{W_{2m}(p)[W_1(p)\tau_1 + W_{1m}(p)]} n_2; \\ M_2 &= \frac{W_2(p)}{W_{2m}(p)} n_1 - \frac{1 + W_2(p)}{W_{2m}(p)} n_2. \end{aligned}\right\} \qquad (6)$$

The system of equations at (6) in matrix form is

(7)

By the analogy of the operation of an RFS to an electric four-terminal

network [8], [4], matrix [7] is the matrix of the conductivity of a reversible drive.

The solution of matrix equation (7) will be

$$[n] = [Y]^{-1}[M]. \tag{8}$$

The reciprocal matrix $[Y]^{-1}$ can be found from Cramer's rule

/76

$$[Y]^{-1} = \frac{1}{\Delta}\begin{bmatrix}\Delta_{11}\Delta_{21}\\ \Delta_{12}\Delta_{22}\end{bmatrix}; \qquad \Delta_{ik} = (-1)^{i+k} A_{ki}, \tag{9}$$

where $\Delta = |Y|$ is the determinant of matrix [Y]; A_{ki} is the minors of matrix [Y].

As Mason has shown [6, 7], when the determinant is a function of the minimum phase type (that is, has neither zeroes nor poles in the right half-plane) the system is stable, and the system is unstable when the case is reversed.

The determinant of a system with stable circuits is a stable function, so all that need be considered to have stability is the distribution of the zeroes of the determinant.

Proceeding from system of equations at (6), the determinant will be

$$|Y| = -\frac{1 + W_2(p)}{W_{2m}(p)[W_1(p)\tau_1 + W_{1m}(p)]}. \tag{10}$$

Or, when Eqs. (2), (3), (4), and (5) are considered Eq. (10) takes the form

$$|Y| = -\frac{(T_{1m}p + 1)[p(T_{2m}p + 1)(T_{2d}p + 1) + k_2]}{k_{2m}p[k_1\tau_1 + k_{1m}(T_{1d}p + 1)]}. \tag{11}$$

Hence, the characteristics equation of a reversible drive will be

$$F(p) = (T_{1m}p + 1)[k_2 + p(T_{2m}p + 1)(T_{2d}p + 1)] = 0. \tag{12}$$

This equation can be broken down into two parts, one of which depends on the parameters of the reproduction channel, the other on the parameters of the follow-up channel.

It is not difficult to see that system stability depends only on the parameters of the follow-up channel equation, the roots of which can be found by solving

$$F_1(p) = k_2 + p(T_{2m}p + 1)(T_{2a}p + 1) = 0. \quad (13)$$

The parameters of the force reproduction channel equation

$$F_2(p) = T_{1m}p + 1 = 0, \quad (14)$$

have no influence on system stability.

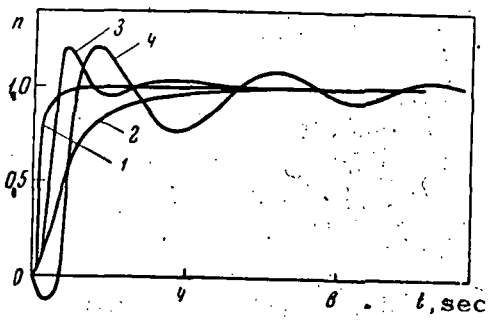

Figure 2.

The parameters of the characteristic equation, $F_1(p)$ and $F_2(p)$, for the system channel that will operate on the load, become variables that depend on the nature and magnitude of the load. If, for example, the load is purely inertial in nature, the magnitude of time constant, T_m, in Eqs. (13) or (14) will be a variable.

If the inertial load acts on the reproduction channel, stability of the system as a whole will not change, but its dynamic properties will deteriorate, with increase in load.

And if the inertial load acts on the follow-up channel, the dynamic properties of the system will change slightly, but the stability margin will be reduced and the system will become unstable when magnitude T_{2m} is equal to, or greater than, T_{mc}.

The value of T_{mc} for selected k_2 is determined by the expression /77

$$T_{mc} = (a + 1)/k_2, \quad (15)$$

where $a = T_m/T_a$.

Figure 2 illustrates the above hypothesis and shows the transient processes at the system output when there is a stepwise change in the disturbance at its input for the following values of the parameters: k_2 = 6.5 1/sec; k_1 = 10 rad/ /kgf-m·sec; $T_{1a}T_{2a}$ = 0.02 sec; $T_{1m} = T_{2m}$ = 0.1 to 0.8 sec; $k_{1m} = k_{2m}$ =

= 0.66 rad/kgf-m·sec; $\tau_1 = \tau_2 = 1$.

Curves 1 and 2 follow system reaction when the load acts on the reproduction channel; curves 3 and 4 follow system reaction when the load acts on the follow-up channel.

The transient processes are constructed from the expressions for the disturbance transfer functions, found using Eq. (3), and have the form

$$\Phi_{ik}(p) = n_i(p)/M_k(p) = \Delta_{ik}/\Delta. \tag{16}$$

Based on Eq. (16), and considering Eqs. (2-6), when the load is acting on the follow-up channel we will have

$$\Phi_{21}(p) = \frac{n_2}{M_1} = \frac{W_2(p)[W_1(p)\tau_1 + W_{1m}(p)]}{1 + W_2(p)} = \frac{k_2[k_1\tau_1 + k_{1m}(T_{1m}p + 1)]}{[p(T_{2m}p + 1)(T_{2a}p + 1) + k_2](T_{1m}p + 1)(T_{1a}p + 1)}. \tag{17}$$

When the load is acting on the reproduction channel, the expression for the transfer function will be

$$\Phi_{12}(p) = n_1/M_2 = \tau_2 W_1(p) = \tau_2 k_1/(T_{1a}p + 1)(T_{1m}p + 1). \tag{18}$$

Eqs. (17) and (18) will yield system sensitivity for the first and second cases, and is defined as the ratio of the steady-state speed to the steady-state moment.

$$S_2 = n_{2ss}/M_{1ss} = \tau_1 k_1 + k_{1m}; \tag{19}$$

$$S_{12} = n_{1ss}/M_{2ss} = \tau_2 k_1. \tag{20}$$

Since, in most cases, k_m is less than, or near, unity, as a practical matter it can be considered that when $\tau_1 = \tau_2$, system sensitivity will be the same when the effect is at the output of the follow-up channel, and at the output of the reproduction channel.

The moment transmission factor (scale factor) is determined from the moment transfer functions, which, using Eq. (8), will be

$$\Phi_{m1}(p) = \frac{M_1}{M_2} = \frac{\Delta_{12}}{\Delta_{11}} = \frac{Y_{12}(p)}{Y_{22}(p)} = \frac{\tau_2 W_1(p)}{\tau_1 W_1(p) + W_{1m}(p)}; \tag{21}$$

$|M'| =$
$|M''| =$
$|M'''| =$

$$\Phi_{m2}(p) = \frac{M_2}{M_1} = \frac{\Delta_{21}}{\Delta_{22}} = \frac{Y_{21}(p)}{Y_{11}(p)} = \frac{W_2(p)\,[W_1(p)\,\tau_1 + W_{1m}(p)]}{\tau_2 W_1(p)\,W_2(p) + W_{2m}(p)}. \qquad (22)$$

Substituting the values of the polynomials $W_1(p)$, $W_2(p)$, $W_{1m}(p)$, and $W_{2m}(p)$ from Eqs. (2-5) into Eqs. (22) and (23), we obtain

$$\Phi_{1m}(p) = \frac{k_1\tau_2}{\tau_1 k_1 + k_{1m}(T_{1a}p + 1)}; \qquad (23)$$

$$\Phi_{m1}(0) = \frac{M_{1ss}}{M_{2ss}} = m_1 = \frac{\tau_2 k_1}{\tau_1 k_1 + k_{1m}}; \qquad (24)$$

$$\Phi_{m2}(p) = \frac{k_2\,[k_1\tau_1 + k_{1m}(T_{1a}p + 1)]}{\tau_2 k_1 k_2 + p\,(T_{\mu m}p + 1)\,(T_{1a}p + 1)\,(T_{2a}p + 1)\,k_{2m}}; \qquad (25)$$

78

$$\Phi_{m2}(0) = \frac{\tau_1 k_1 + k_{1m}}{\tau_2 k_1} = m_2 = \frac{M_{2ss}}{M_{1ss}}. \qquad (26)$$

Thus, what follows from Eqs. (24) and (26) is that the moment perceived by the operator as attributable to the reproduction channel will be somewhat less (when $\tau_1 = \tau_2$) than the load moment ($m_1 < 1$), but if the operator is acting at the input to the follow-up channel, the moment he perceives will be somewhat greater than the actual magnitude (when $\tau_1 = \tau_2$ $m_2 > 1$).

The scale factors for the values of the parameters assumed above, will be, respectively

$$\tau_1 = \tau_2; \quad m_1 = \frac{10}{10 + 0{,}66} = 0{,}94; \quad m_2 = \frac{10 + 0{,}66}{10} = 1{,}066.$$

The influence of the magnitude of factor k_m will be negligible as the reproduction channel transmission factor, k_1, increases. Here the transmission scale factor will depend completely on the ratio of the moment sensor conversion factors

$$m_1 = \tau_2/\tau_1 = 1/m_2. \qquad (27)$$

An analysis of the influence of the load on system operation in terms of where it is acting and including the elasticity of the kinematic transmissions in the slave mechanisms in the follow-up and reproduction channels is quite difficult to make because of the increase in the degree of the characteristic

$$\left.\begin{aligned} |M'| &= |Y'|\,|n'|; \\ |M''| &= |Y''|\,|n''|; \\ |M'''| &= |Y'''|\,|n'''|. \end{aligned}\right\}$$

equation. However, we shall try to establish certain theses for this case.

If, for example, the elasticity of the kinematic transmission in the reproduction channel is considered, the following system of differential equations will apply in this case

$$\left.\begin{aligned} M_0 &= \left[A_0(p) + \frac{c_1}{p}\right] n_0 - \frac{c_1}{p} n_1; \\ M_1 &= \frac{c_1}{p} n_0 - \frac{c_1}{p} n_1; \\ M_1 &= \frac{\tau_2 W_1(p) W_2(p) + W_{2m}(p)}{W_{2m}(p)[\tau_1 W_1(p) + W_{1m}(p)]} n_1 - \frac{\tau_2 W_1(p)[1 + W_2(p)]}{W_{2m}(p)[\tau_1 W_1(p) + W_{1m}(p)]} n_2, \\ M_2 &= \frac{W_2(p)}{W_{2m}(p)} n_1 - \frac{1 + W_2(p)}{W_{2m}(p)} n_2; \\ A_0 &= J_0 p + b_0, \end{aligned}\right\} \quad (28)$$

where

c_1 is the stiffness factor for the kinematic transmission in the slave mechanism of the reproduction channel;

J_0 is the moment of inertia of the moving parts ahead of the flexible link;

b_0 is the coefficient of velocity in the flexible link.

The system of equations at (28) is in matrix form

$$\left.\begin{aligned} |M'| &= |Y'||n'|; \\ |M''| &= |Y''||n''|, \end{aligned}\right\} \quad (29)$$

where

$$|M'| = \left|\frac{M_0}{M_1}\right|; \quad |M''| = \left|\frac{M_1}{M_2}\right| -$$

are the matrices of the moments of the first and second systems,

$$|n'| = \left|\frac{n_0}{n_1}\right|; \quad |n''| = \left|\frac{n_1}{n_2}\right| -$$

are the velocities matrices, and

$$|Y'| = \begin{vmatrix} Y'_{11}(p) & Y'_{12}(p) \\ Y'_{21}(p) & Y'_{22}(p) \end{vmatrix}; \quad |Y''| = \begin{vmatrix} Y''_{11}(p) & Y''_{12}(p) \\ Y''_{21}(p) & Y_{22}(p) \end{vmatrix} -$$

are the conductivity matrices.

The parameters of a generalized system made up of a chain coupling of two

$$\left.\begin{aligned} |M'| &= |Y'||n'|; \\ |M''| &= |Y''||n''|; \\ |M'''| &= |Y'''||n'''|. \end{aligned}\right\}$$

reversible systems (by analogy with four-terminal networks) are determined by the following relationships:

$$Y_{11}(p) = \frac{-|y'| + Y'_{11}Y''_{11}}{-Y'_{22} + Y''_{11}} = \Delta_{22}; \tag{30}$$

$$Y_{12}(p) = -\frac{Y'_{12}Y''_{12}}{-Y'_{22} + Y''_{11}} = -\Delta_{12}; \tag{31}$$

$$Y_{21}(p) = \frac{Y''_{21}Y'_{21}}{-Y'_{22} + Y''_{11}} = -\Delta_{21}; \tag{32}$$

$$Y_{22}(p) = \frac{Y'_{22}Y''_{22} - |y''|}{-Y'_{22} + Y''_{11}} = \Delta_{11}; \tag{33}$$

$$|y| = \Delta = -\frac{Y''_{22}|y'| - Y'_{11}|y''|}{-Y'_{22} + Y''_{11}}, \tag{34}$$

where

$|y'|$; $|y''|$ are the determinants of the composite systems;

$\Delta = (y)$ is the determinant of the generalized system;

Δ_{ik} is the minors of the generalized system.

As before, the characteristic equation will be

$$F(p) = \Delta = |y| = 0.$$

Using Eq. (34), and considering the system of equations at (28), we have, for the characteristic equation,

$$F(p) = -\frac{[1 + W_2(p)]\{A_0(p)[c_1\tau_1 W_1(p) -$$
$$W_{2m}(p)[p + c_1\tau_1 W_1 (p)$$

(35)

As may be seen from Eq. (35), the numerator can have two factors, so system stability is determined by the roots of each, and when Eqs. (2-5) are included, we have

$$F_1(p) = [p(T_{2m}p + 1)(T_{2a}p + 1) + k_2] = 0; \tag{36}$$

$$F_2(p) = (T_{1m}p + 1)(T_{1a}p + 1)(J_0p^2 + b_0p + c_1) +$$
$$+ c_1(J_0p + b_0)[\tau_1 k_1 + k_{1m}(T_{1a}p + 1)] = 0. \tag{37}$$

$$\left.\begin{aligned} |M'| &= |Y'||n'|; \\ |M''| &= |Y''||n''|; \\ |M'''| &= |Y'''||n'''|. \end{aligned}\right\}$$

If we disregard T_{1a}, we can, by opening the brackets and grouping the terms in Eq. (37), obtain

$$F_2(p) = T_{1m}J_0p^3 + (J_0 + b_0T_{1m})\,p^2 + [b_0 + c_1T_{1m} + c_1(\tau_1k_1 + k_{1m})\,J_0]\,p + \\ + c_1[1 + b_0(\tau_1k_1 + k_{1m})] = 0. \tag{38}$$

Proceeding from Eq. (38), the condition for stability will be

$$c_1(k_1\tau_1 + k_{1m})\,J_0^2 + b_0T_{1m}(b_0 + c_1T_{1m}) > 0, \tag{39}$$

which always is feasible for any parameter values.

Thus, a changing inertial load on the follow-up channel will change T_{2m}, and, as shown above, system stability will deteriorate. Loading the reproduction channel will change J_0, but this will not cause a deterioration in stability conditions. /80

If we consider the elasticity of the kinematic transfers of the reproduction channel as well as of the follow-up channel, then equations of the elastic transfer of the follow-up channel will also be added to system of equations (29)

$$\left.\begin{aligned} M_2 &= \frac{c}{p}(n_2 - n_{fu}); \\ M_1 &= \frac{c_2}{p}n_2 - \left[A_s(p) + \frac{c_2}{p}\right]n_{fu} \\ A_s(p) &= J_sp + b_s \end{aligned}\right\} \tag{40}$$

where

n_{fu} is the speed at the output of the follow-up channel, including the flexible transmission;

M_1 is the moment at the output;

J_s is the moment of inertia of the moving parts in front of the flexible element (read from the output);

b_s is the speed losses in the flexible link.

A reversible system as a whole can be represented in the form of a chain connection of three composite reversible systems with matrix equations

(41)

$n'/;$
$n''/;$
$n'''/.$ } 108

Here the following equations can be used to find the system's generalized parameters

$$Y_{11}(p)=\frac{Y'_{11}Y''_{11}Y'''_{11}+|y'|(Y''_{22}-Y'''_{11})-Y'_{11}|y''|}{Y'_{22}Y''_{22}-|y''|+Y'''_{11}(Y''_{11}-Y'_{22})}=\Delta_{22}; \tag{42}$$

$$Y_{12}(p)=\frac{Y'_{12}Y''_{12}Y'''_{12}}{Y'_{22}Y''_{22}-|y''|+Y'''_{11}(Y''_{11}-Y'_{22})}=-\Delta_{12}; \tag{43}$$

$$Y_{22}(p)=\frac{-Y'_{22}Y''_{22}Y'''_{22}+Y'''_{22}|y''|-|Y'''|(y'_{11}-Y'_{22})}{Y'_{22}Y''_{22}-|y''|+Y'''_{11}(Y''_{11}-Y'_{22})}=\Delta_{11}; \tag{44}$$

$$Y_{21}(p)=\frac{Y'_{21}Y''_{21}Y'''_{21}}{Y'_{22}Y''_{22}-|y'''|+Y'''_{11}(Y''_{11}-Y'_{22})}=-\Delta_{21}; \tag{45}$$

$$|y|=-\frac{-Y''_{22}Y'''_{22}|Y'|+Y'_{11}y'''_{22}|y''|+|y'||y'''|-Y'_{11}Y''_{11}|y'''|}{Y'_{22}Y''_{22}-|y''|+Y'''_{11}(Y''_{11}-Y'_{22})}=\Delta; \tag{46}$$

where

$\left|y'\right|$; $\left|y''\right|$; $\left|y'''\right|$ are the determinants of the composite systems;

$\Delta = \left|y\right|$ is the determinant of the generalized system;

Δ_{ik} is the minors of the generalized system.

Substituting the conductivity values from Eq. (28) and Eq. (40) into Eqs. (42) - (46) for the system determinant, we obtain

$$|y|=-\frac{\{A_S(p)[p(1+W_2(p))+c_2W_{2m}(p)]+c_2(1+W_2(p))\}\{A_0(p)[p+c_1(\tau_1W_1(p)+W_{1m}(p)]+c_1\}+c_2A_S(p)\tau_2W_1(p)W_2(p)[pA_0(p)+c_1]}{\{p+c_1[\tau_1W_1(p)+W_{1m}(p)]\}\{c_2W_{2m}(p)+p[1+W_2(p)]\}+pc_2\tau_2W_1(p)W_2(p)} \tag{47}$$

For disturbance transfer functions

$$\Phi_{21}(p)=\frac{n_S}{M_0}=\frac{\Delta_{21}}{\Delta}=\frac{c_1c_2W_2(p)[\tau_1W_1(p)+W_{1m}(p)]}{(A_S(p)\{p[1+W_2(p)]+c_2W_{2m}(p)\}+c_2[1+W_2(p)])A_0(p)\times \{p+c_1[\tau_1W_1(p)+W_{1m}(p)]+c_1\}+c_2A_S(p)\tau_2W_1(p)W_2(p)\times [pA_0(p)+c_1];} \tag{48}$$

$$\Phi_{12}(p)=\frac{n_0}{M_1}=\frac{\Delta_{12}}{\Delta}=\frac{c_1c_2\tau_2W_1(p)[1+W_2(p)]}{(A_S(p)\{p(1+W_2(p)]+c_2W_{2m}(p)\}+c_2[1+W_2(p)])(A_0(p)\times \{p+c_1[\tau_1W_1(p)+W_{1m}(p)]+c_1\}+c_2A_S(p)\tau_2W_1(p)W_2(p)\times [pA_0(p)+c_1].} \tag{49}$$

/81

For moment transfer functions

$$\Phi_{m1}(p) = \frac{M_0}{M} = \frac{\Delta_{12}}{\Delta_{11}} = \frac{c_1 c_2 \tau_2 W_1(p)[1 + W_2(p)]}{\{A_s(p)[p(1 + W_2(p)) + c_2 W_{2m}(p)] + c_2(1 + W_2(p)\} \times} \times \\ \times [p + c_1(\tau_1 W_1(p) + W_{1m}(p)] + c_2 p A_s \tau_2 W_1 W_2 ; \quad (50)$$

(51)

For the sensitivity and scale factor for transmission of moments, determined for steady-state conditions from Eqs. (48) - (51) and including Eqs. (2) - (5), we will have

$$S_{21} = \frac{n_{s\,ss}}{M_{0\,ss}} = \frac{k_1\tau_1 + k_{1m}}{b_0(\tau_1 k_1 + k_{1m}) + b_c \tau_2 k_1 + 1} ; \quad (52)$$

(53)

$$m_1 = \frac{M_{0\,ss}}{M_{1\,ss}} = \frac{\tau_2 k_1 k_2}{(\tau_1 k_1 + k_{1m})(b_c k_{2m} + k_2)} ; \quad (54)$$

$$m_2 = \frac{M_{1\,ss}}{M_{0\,ss}} = \frac{k_2(\tau_1 k_1 + k_{1m})}{k_{2m}[b_0(\tau_1 k_1 + k_{1m}) + 1]\tau_2 k_1 k_2} . \quad (55)$$

If we ignore the terms containing the parameters $b_o \ll 1$ and $b_s \ll 1$ in Eqs. (52) - (55), the relationships obtained will be identical with Eqs. (19), (20), (24), and (26) established for a reversible system without consideration for flexible links.

The characteristic equation for the generalized system will be

$$F(p) = |y| = \{A_s(p)[p(1 + W_2(p)) c_2 W_{2m}(p)] + \\ + c_2(1 + W_2(p)\}\{A_0(p)[p + c_1(\tau_1 W_1(p) + W_{1m}(p))] + c_1\} + \\ + c_2 A_s(p)\tau_2 W_1(p) W_2(p)[pA_0(p) + c_1] = 0. \quad (56)$$

The parameters of the characteristic equation depend on the load. If the load is at the output of the follow-up channel, the variables will be the parameters of the polynomial $A_s(p) = J_s p + b_s$. If the load is inertial, the moment of inertia, J_s, will change from $J'_s \ll J_s \ll J'_s + J_1$ where J'_s is the

value of the moment of inertia for system idling speed and J_1 is the load's moment of inertia. The variables will be the parameters of the polynomial $A_0(p) = J_0 p + b_0$ if the inertial load is at the output of the reproduction channel. The moment of inertia, J_0, as in the preceding case, will vary in limits $J_0' \ll J_0 \ll J_0' + J_1$.

Characteristic Eq. (56) will not factor in two, so analysis of the influence of the load on system operation in terms of where applied requires cumbersome mathematical computations, and is not presented here.

We note that in a system with flexible kinematic links, the influence of a load at the output of the reproduction channel, as in the preceding case, has much less effect on operational stability than when the influence is at the output of the follow-up channel. /82

System sensitivity does not, practically speaking, depend on where load and operator act, and deterioration in the dynamic properties of the system with increase in load is fully permissible for manipulators (because of limited operator capabilities and safe working conditions), so the use of the manipulator slave mechanism as the output of the force reproduction channel, and of the master mechanism as the output of the follow-up channel, can be considered more rational.

Figure 3 is the block diagram of a reversible follow-up system with independent follow-up and force reproduction channels. This scheme derives from Eqs. (2) - (5), (29), and (41) and includes a load acting the reproduction channel output.

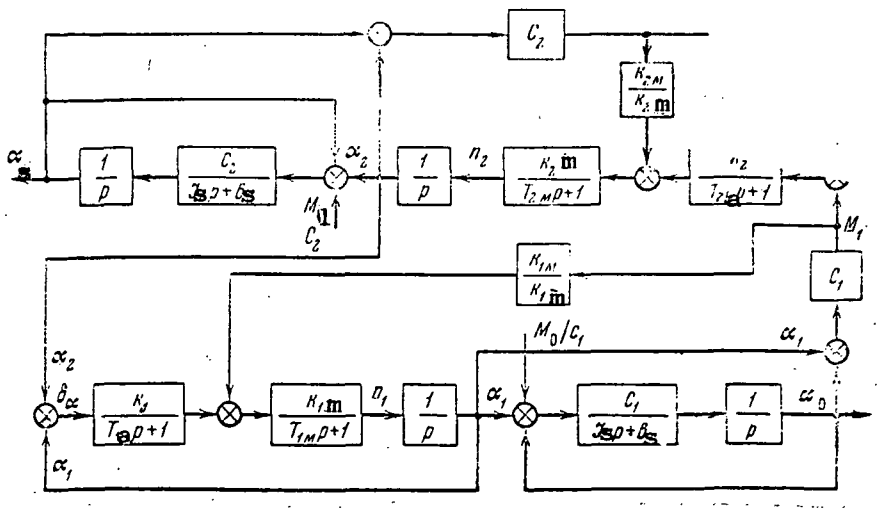

Figure 3.

Thus, in remotely-controlled master-slave manipulators based on reversible follow-up systems with independent follow-up and force reproduction channels, it is desirable to use the manipulator's slave mechanism as the outputs of the reproduction channels of reversible systems.

REFERENCES

1. Goertz, R. C., et al., "Electronically Controlled Manipulator," Nucleonics, 12, No. 11, 1954, pp. 46-47.

2. Goertz, R. C., et al., "A Force-Reflecting Positional Servomechanism," Nucleonics, 10, No. 11, 1952, pp. 43-46.

3. Edziri, M., Kamoi, A., "Servomanipulators," Keysoku to seyge, 2, No. 2, 1963, pp. 483-490.

4. Petrov, B. A., "A Reversible Follow-Up System Using DC Motors," Patent No. 167230, Byull. izobreteniy, No. 1, 1965.

5. Kuleshov, V. S., Lakota, N. A., "Structural and Analytical Presentation of Reversible Follow-Up Systems," V sb. Mekhanika mashin [In collection: Mechanics of Machines], No. 7-8, "Nauka" Press, 1967.

6. Mason, S. J., "Feedback Theory - Further Properties of Signal Flow Graphs," Proceedings of the I.R.E., 44, 1956, pp. 920-926.

7. Prisposablivayushchiyesya avtomaticheskiye sistemy [Adapting Automatic Systems], Translation from the English, under the editorship of Ya. Z. Tsypkin, IL, 1963.

8. Petrov, B. A., "Some Special Features in the Design of Reversible Follow-Up Systems," V sb. Mekhanika mashin [In collection: Mechanics of Machines], "Nauka" Press, No. 7-8, pp. 53-62.

N73-26083

AN ANALYTICAL METHOD FOR THE SYNTHESIS OF REVERSIBLE FOLLOW-UP SYSTEMS

M. S. Voroshilov

ABSTRACT. The technical and design requirements of reversible follow-up systems are presented. A synthesis scheme is proposed for the realization of these requirements.

Reversible follow-up systems for manipulators can, in the majority of cases, /83 be considered as a set of two interconnected systems, the first of which ensures copying the movements of the master arm by the slave arm, while the second reproduces the forces perceived by the slave arm at the master arm.

Designing reversible follow-up systems reduces to finding a reasonable compromise between attempts to obtain higher qualitative system indices and attempts to obtain these indices with simpler equipment. Extremely diverse synthesis methods are used to solve this problem. Synthesis can be treated as a problem of building a reversible follow-up system meeting a set of specifications, or as one of building an optimum system for specified limitations.

Given the state of the art, it is advisable to impose the following requirements on synthesis methods used to build reversible follow-up systems.

1. The synthesis methods should ensure the building of reversible follow-up systems with optimum dynamic characteristics for existing limitations on the power of slave drives and meeting specifications for all other indices. Moreover, planned systems should be simple in design, dependable in operation, and built of physically practicable elements.

2. Selection of main system elements should include their structural and energy characteristics. The energy characteristics of the main elements should provide specified limiting dynamic characteristics for the system as a whole.

3. Synthesis methods should derive from a specific, theoretically substantiated criterion of optimality, expressed perferably in unambiguous analytical form.

4. Synthesis methods should be as general-purpose as possible; that is, suitable for the design of single-circuit and multicircuit systems, autonomous and interconnected systems, linear systems and systems with a limited zone of

linearity, and the like.

5. The synthesis method should provide an opportunity for the optimization of follow-up system regulation laws, and an opportunity to optimize control.

As a rule, reversible follow-up systems should meet the following specifications. /84

1. The follow-up systems should provide smooth movements of the manipulator slave arm for specified speeds and accelerations.

2. The systems should accurately reproduce at the master arm force perceived by the slave arm. For ease of control, the friction forces generated in the kinematic chain of manipulator master and slave arms should be reduced to the minimum, or should be adequately compensated for by using the corresponding reactions on the slave drives.

3. The systems should ensure specified follow-up precision.

4. The systems should have optimum dynamic characteristics under conditions of limiting the power of the slave drives and power sources.

5. The systems should have design characteristics corresponding to specified manipulator operating conditions.

The following synthesis scheme is proposed for the realization of the above requirements.

The type and parameters of the slave drives are determined in the first stage of the design of a reversible follow-up system. The properties of the drives usually limit the opportunities for improving the quality of adjustment by specific limits. The design and power characteristics of the drives should correspond to specifications. The dynamic characteristics of follow-up systems with the above-indicated drives should be optimum. The limiting dynamic characteristics of the follow-up system must be evaluated when selecting slave drives to compare different possible variants. The selection of the slave drives predetermines the remaining functionally necessary elements in the system and permits compiling a preliminary block diagram and determining the order of the differential equation which characterizes the motion of the system under transient and steady-state operating conditions.

Optimization criteria are selected, and the parameters of the desired transfer function, or desired equation of motion, providing the required indices of the optimization criteria are developed in the second stage of design.

Correction devices providing the specified parameters for the optimum system are developed in the third stage.

The scope of this article does not permit examining all stages of the designing of a reversible follow-up system, so we shall limit ourselves to some of the problems of the synthesis of follow-up systems operating under definite, concrete, conditions.

Let us assume it to be necessary to create a system which is optimum in speed of operation in the limit mode for reproduction of a suddenly applied, abrupt input. The possibilities of increasing operating speed in real systems are limited by the magnitude of the maximum moment developed by the slave motor during the reproduction of a given trajectory of motion. The optimum system operating speed is reached when its slave motor, under the most difficult follow-up mode develops the maximum rotary moment in the required direction for the whole of the transient. Observance of this condition ensures maximum operating speed and minimum power consumption to reproduce a given trajectory. The curve computation is not particularly difficult if the input controlling influence is given. The specified transient curve for the most characteristic controlling influence and which considers all limitations introduced by the power section of the follow-up system can be taken as the basis for the synthesis of the optimum follow-up system. The criterion of optimality in this case is the degree of approximation of the transient curve reproduced by the system to the optimum curve calculated for the same controlling influence. /85

The optimum transient curve for an abrupt input can be calculated using the formulas in Table 1.

TABLE 1

t	$\Omega_{opt}(t)$	$S_{\varphi opt}(t)$
$0 < t < \xi_2 t_r$	$a_1 t$	$\frac{1}{2} a_1 t^2$
$\xi_2 t_r < t < t_r$	$a_2 (t_r - t)$	$a_2 t_r t - \frac{1}{2} a_2 t^2 - - \frac{1}{2} a_2 \xi_2 t^2 r$

where

a_1 is the maximum acceleration during motor speedup;

a_2 is the maximum acceleration when the motor is braked;

t_r is the regulating time (transient time);

Ω is the angular velocity;

$\xi_1 = a_1/(a_1 + a_2)$;
$\xi_2 = a_2/(a_1 + a_2)$.

The optimum trajectory also can be presented in the form of a trigonometric sum:

$$S_{\varphi_{opt}}(t) = A_{0_{opt}} + \sum_{k=1}^{\nu} (A_{k_{opt}} \cos k\omega t + B_{k_{opt}} \sin k\omega t), \quad (1)$$

where k = 1, 3, 5, 7...

$$A_{k_{opt}} = \frac{16}{(\pi k)^2}$$
$$B_{k_{opt}} = \frac{16}{(\pi k)^3} \varphi_{ss}, \quad (2)$$

$A_{o_{opt}} = \frac{1}{2} S_{\varphi_{ss}}$; $S_{\varphi_{ss}}$ is the steady-state value of $S_\varphi(t)$.

From Table 1

(3)

Maximum accelerations a_1 and a_2 are calculated from the formulas

(4)

where

M_{max} is the motor's maximum torque;

M_r is the normalized moment of resistance;

J'_Σ is the summed normalized moment of inertia of the drive.

The M(t), a(t), Ω(t), and $S_\varphi(t)$ curves for the optimum transient state are

shown in Figure 1.

Eqs. (3) and (4) characterize the interconnection between the power characteristics of the slave drive and the maximum dynamic curves for an optimum follow-up system. The preliminary selection of the motor is made from Eqs. (3) and (4) obtained from the condition of attainment of optimum operating speed. After /86
selection of the motor, a block diagram of the system is compiled from the functionally necessary elements and the order of the differential equation of its motion is determined.

The main task of the follow-up system synthesis is formulated as follows. Necessary for a stable system whose motion is described by the equation

$$D(p)\,S_{\varphi}(t) = R(p)\,S_{\varphi_g}(t) - N(p)\,M(t), \tag{5}$$

where

$D(p) = p^n + b_1 p^{n-1} + \ldots + b_{n-1} + b_n$;

$R(p) = p^m + c_1 p^{m-1} \ldots + c_m$;

$N(p) = P^v + d_1 p^{v-1} + \ldots d_v$;

$S_{\varphi_g}(t)$ is the trajectory given for reproduction;

$M(t)$ is the generalized disturbing force among all allowable parameters $b_1, b_2, \ldots, b_n$, is determination of those for which the trajectory $S_{\varphi}(t)$ would differ from some optimum trajectory $S_{\varphi opt}(t)$ by the amount of allowable error.

An analytical solution of this problem is possible by using the approximate direct method of solving differential equations proposed by the author and called the periodic solutions method. The method is based on the following assumption: The trajectory of a stable self-regulating system, $S_{\varphi}(t)$, fixed in a finite time segment $0 < t < t_r$, during the transient for a given action $S_{\varphi_g}(t)$, can be reproduced by this same system in the same time segment for the corresponding steady-state periodic motion $S_{\varphi_p}(t)$ if the following conditions are observed: (1) the controlling influences for the transient $S_{\varphi_g}(t)$ and for the steady-state periodic motion $S_{\varphi_{gp}}(t)$ coincide on time segment $0 < t < t_r$; (2) the period of

periodic influence $T \gg 4t_r$; (3) outside time segment $0 < t < t_r$ the periodic influence $S_{\varphi_{gp}}(t)$ should change in such a way as to ensure the practical identity of the initial conditions for t = 0 for transient and periodic motions (Figure 2).

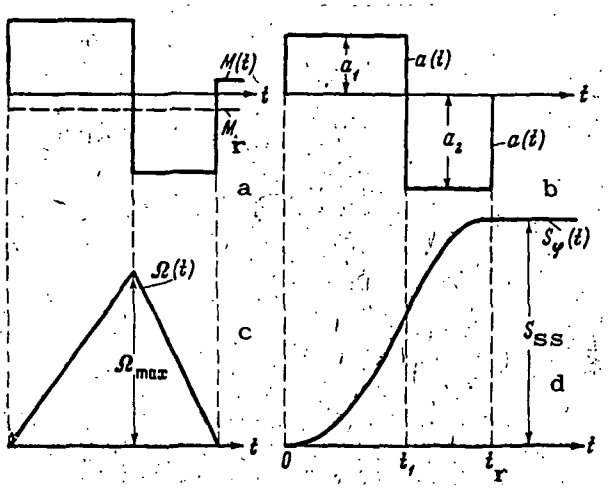

Figure 1. Curves of an optimum transient state a - M(t); b - a(t); c - $\Omega(t)$; d - $S_\varphi(t)$.

The practical coincidence of motion trajectories $S_\varphi(t)$ and $S_{\varphi p}(t)$ on segment $0 < t < t_r$ permits replacing the corresponding cumbersome and complicated method of analyzing the transients of self-regulating systems by the periodic solutions method.

As an example, let us determine the motion trajectory for a system described by Eq. (5) by the periodic solutions method, considering that the given equation is linear. Let us replace the nonperiodic actions in the right-hand side of the Eq. $R(p)S_{\varphi_g}(t) - N(p)M(t)$ with the corresponding periodic action, given in the form of the trigonometric series

/87

(6)

where

$\omega = 2\pi/T$;

T is the period of the action;

C_0, C_k, D_k are constants determined from Euler-Fourier formulas.

We will seek the solution of Eq. (5) with a changed right member as the sum of the functions

Each of these functions, taken separately, should satisfy Eq. (5). Substituting the functions $S_{\varphi_{ka}}(t)$, $S_{\varphi_{kb}}(t)$, $S_{\varphi_0}(t)$ into Eq. (5) with the right-hand side of

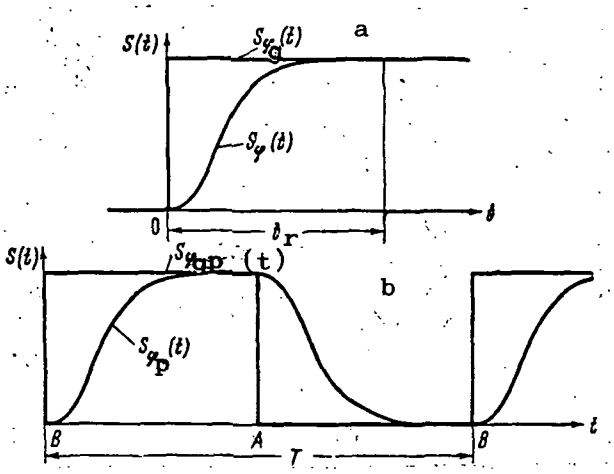

Figure 2. Trajectories of motion in the transient (a) and periodic (b) states.

Eq. (6), and comparing the coefficients when the time functions are the same, we determine the values of A_k and B_k

(7)

where

$$\lambda_{1k} = \frac{F_{1k}}{F_{1k}^2 + F_{2k}^2} \tag{8}$$

$$\lambda_{2k} = \frac{F_{2k}}{F_{1k}^2 + F_{2k}^2}. \tag{9}$$

The functions F_{1k} and F_{2k} can be determined by using the formulas in Table 2.

The trajectory reproduced by a system for the corresponding periodic motion is determined by the trigonometric sum

$$S_{\varphi p}(t) = A_0 + \sum_1^{\nu} A_k \cos k\omega t + \sum_1^{\nu} B_k \sin k\omega t; \quad S_{\varphi}(t) \approx S_{\varphi_p}(t). \tag{10}$$

Now let us move on to the solution of the main problem of synthesis. Let us assume that the optimum trajectory of system motion, Eq. (5), over a segment $0 < t < t_r$ is defined by Eq. (1) and that the actual system motion trajectory is determined by Eq. (10). Appearing with the equality $S_{\varphi_p}(t) \approx$ /88
$\approx S_{\varphi_{opt}}(t)$ is the following analytical connection between the parameters of Eq. (5) $b_1, b_2, \ldots, b_n$ and the parameters of the optimum transient curve, described by Eq. (5)

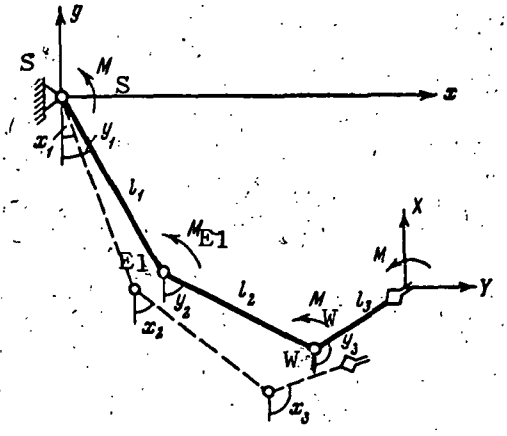

(11)

where

$$\varphi_{1k} = \left[D_k \frac{A_{k\,opt}}{A^2_{k\,opt} + B^2_{k\,opt}} - C_k \frac{B_{k\,opt}}{A^2_{k\,opt} + B^2_{k\,opt}} \right];$$
$$\varphi_{2k} = \left[D_k \frac{B_{k\,opt}}{A^2_{k\,opt} + B^2_{k\,opt}} + C_k \frac{A_{k\,opt}}{A^2_{k\,opt} + B^2_{k\,opt}} \right]. \qquad (12)$$

TABLE 2

order of equation n	F_{1k}	F_{2k}
2	$-[(k\omega)\, b_1]$	$-[(k\omega)^2 - b_2]$
3	$[(k\omega)^3 - (k\omega)\, b_2]$	$-[(k\omega)^2 b_1 - b_3]$
4	$[(k\omega)^3 b_1 - (k\omega)\, b_3]$	$[(k\omega)^4 - (k\omega)^2 b_2 + b_4]$
5	$-[(k\omega)^5 - (k\omega)^3 b_2 + (k\omega)\, b_4]$	$[(k\omega)^4 b_1 - (k\omega)^2 b_3 + b_5]$
6	$-[(k\omega)^5 b_1 - (k\omega)^3 b_3 + (k\omega)\, b_5]$	$-[(k\omega)^6 - (k\omega)^4 b_2 + (k\omega)^2 b_4 - b_6]$
7	$[(k\omega)^7 - (k\omega)^5 b_2 + (k\omega)^3 b_4 - (k\omega)\, b_6]$	$-[(k\omega)^6 b_1 - (k\omega)^4 b_5 + (k\omega)^2 b_5 - b_7]$
8	$[(k\omega)^7 b_1 - (k\omega)^5 b_3 + (k\omega)^3 b_5 - k\omega\, b_7]$	$[(k\omega)^8 - (k\omega)^6 b_2 + (k\omega)^4 b_4 - (k\omega)^2 b_6 + b_8]$

This analytical connection is presented in developed form for differential equations of various orders by the formulas in Table 3. Systems with parameters b_1, b_2 ..., b_n, calculated using the formulas in Table 3, will reproduce the given optimum motion trajectory accurately to the ν^{th} harmonic. $\nu = n/2$ for even values of n; $\nu = (n-1)/2$ for odd values of n. The derived differential equation for the system is checked for stability after the calculated determination of the coefficients of the characteristic equation b_1, b_2, ..., b_n. If the system is unstable, it cannot reproduce the designated optimum motion trajectory so this trajectory must be changed. In the case of an abrupt controlling action for example, the optimum curve, determined using the formulas in Table 1, or the Eq. 1 trigonometric sum, is reproduced by the follow-up system whose order of differential equation of motion is $n \leq 4$. For systems with an equation of motion of a higher order, an attempt to reproduce the above-indicated optimum curve upset motion stability; that is, the maximum speed of operation of the system in this case is limited by the potentials of the slave drive, as well as by the properties of other functionally necessary elements. The problem of synthesizing a system with optimum operating speed when an adequate margin of stability is available is also solved when the system's characteristic equation is presented in the form of the product of several equations whose order is $n \leq 4$. Each of these equations can be synthesized

separately by the method presented above. As an example, let us consider the characteristic seventh order equation, which can be presented in the form of the product of two third and fourth order equations

∠89

$$D_7(p) = p^7 + b_1p^6 + \ldots + b_6p + b_7 = D_3(p)\,D_4(p) = (p^3 + b_{13}p^2 + \ldots + b_{33})(p^4 + b_{14}p^3 + \ldots + b_{34}p + b_{44}).$$

TABLE 3

n	Coefficient of optimum system equation	n	Coefficient of optimum system equation
2	$b_1 = -\frac{\varphi_{11}}{1-\varphi_{21}}\omega = \frac{\varphi_{11}}{Q_2}\omega$ $b_2 = \frac{1}{Q_2}\omega^2$	4	$b_1 = 3\frac{\varphi_{13}-3\varphi_{11}}{Q_4}\omega;\ Q_4 = 8+\varphi_{23}-9\varphi_{21}$ $b_2 = \frac{80+\varphi_{23}-81\varphi_{21}}{Q_4}\omega^2$
3	$b_1 = 24\frac{1-\varphi_{21}}{Q_3}\omega;\ Q_3 = \varphi_{13}-3\varphi_{11}$ $b_2 = \frac{\varphi_{13}-27\varphi_{11}}{Q_3}\omega^2$		$b_3 = 3\frac{\varphi_{13}-27\varphi_{11}}{Q_4}\omega^2$ $b_4 = \frac{72}{Q_4}\omega^4$
	$b_3 = 24\frac{1}{Q_3}\omega^3$	6	$b_1 = \frac{-2\varphi_{11}+\varphi_{13}-\frac{1}{5}\varphi_{15}}{Q_6}\omega$
5	$b_1 = 16\frac{3(1-\varphi_{21})-\frac{1}{3}(1-\varphi_{23})}{Q_5}\omega$ $b_2 = \frac{26\varphi_{13}-68\varphi_{11}-2\varphi_{15}}{Q_5}\omega^2$ $b_3 = \frac{81(1-\varphi_{21})-(1-\varphi_{23})}{Q_5}16\omega^3$ $b_4 = \frac{25\varphi_{13}-450\varphi_{11}-\frac{9}{5}\varphi_{15}}{Q_5}\omega^4$ $b_5 = \frac{384}{Q_5}\omega_5$ $b_5 = \varphi_{13}-2\varphi_{11}-\frac{1}{5}\varphi_{15}$		$b_2 = \frac{68(1-\varphi_{21})-\frac{26}{3}(1-\varphi_{23})+\frac{2}{15}(1-\varphi_{25})}{Q_6}\omega^2$ $b_3 = \frac{-68\varphi_{11}+26\varphi_{13}-2\varphi_{15}}{Q_6}\omega^3$ $b_4 = \frac{450(1-\varphi_{21})-\frac{25}{3}(1-\varphi_{23})+\frac{9}{25}(1-\varphi_{25})}{Q_6}\omega^4$ $b_5 = \frac{-450\varphi_{11}+25\varphi_{13}-\frac{9}{5}\varphi_{15}}{Q_6}\omega^5$ $b_6 = \frac{384}{Q_6}\varphi^6$ $Q_6 = 2(1-\varphi_{21})-\frac{1}{3}(1-\varphi_{23})+\frac{1}{25}(1-\varphi_{25})$

We will consider the fourth order equation to be the basic one. The

parameters of this equation can be determined using the formulas in Table 3 to include the specified regulation time t_r. A third order equation takes into account the additional influence on the transient of the links of a system with smaller time constants. The parameters of this equation too are determined using the formulas in Table 3, but include regulation time $t_{r1} < t_r$. The smaller t_{r1} as compared to t_r, the closer the system transient curve will be to the specified optimum curve. Stability of motion will be preserved for any values of t_{r1} and t_r. Knowing the coefficients of the third and fourth order /90
equations, it is easy to determine the coefficients of a seventh order equation. The proposed method of synthesis is applicable in all cases when the input actions causing the system transient are predetermined. The synthesis therefore should be preceded by investigations to determine the most characteristic standard, or maximum, operating conditions for the follow-up system for the existing working conditions.

The proposed synthesis method also is applicable to some degree to nonlinear follow-up systems if all the nonlinear links can be combined into a common nonlinear link, structurally linked to the linear part of the system.

Let us examine Eq. (13)

(13)

where

F(S, pS, t) is a nonlinear function of the variable $S_\varphi(t)$ and of its derivative.

We will say that the function $S_{\varphi_g}(t)$, M(t), $S_\varphi(t) \approx S_{\varphi_{opt}}(t)$ is given. In this case the function F(S, p, S, t) can be determined without particular difficulty.

Let us present the variables $S_{\varphi_g}(t)$, M(t), $S_{\varphi_{opt}}(t)$, and F(S, p, S, t) in the form of a finite sum of sinusoidal functions

$$S_{\varphi_{opt}}(t) \approx \left[A_{0_{opt}} + \sum_1^{\nu} (A_{k_{opt}} \cos k\omega t + B_{k_{opt}} \sin k\omega t)\right];$$

$$R(p) S\varphi_g(t) - N(p) M(t) \approx \left[C_0 + \sum_1^{\nu} (C_k \cos k\omega t + D_k \sin k\omega t)\right] b_n S_{\varphi_{ss}}; \quad (14)$$

$$F(S, pS, t) = F_1(t) \approx \left[f_0 + \sum_1^{\nu} (f_k \cos k\omega t + h_k \sin k\omega t)\right] b_n S\varphi_{ss}.$$

Substituting each of the sinusoidal functions into Eq. (13) with the changed right-hand side and comparing the coefficients when the time functions are the same, we determine the auxiliary functions φ_{1k} and φ_{2k}

$$\varphi_{1k} = D_{k\Sigma}\frac{A_{k\,opt}}{A^2_{k\,opt}+B^2_{k\,opt}} - C_{k\Sigma}\frac{B_{k\,opt}}{A^2_{k\,opt}+B^2_{k\,opt}};$$
$$\varphi_{2k} = D_{k\Sigma}\frac{B_{k\,opt}}{A^2_{k\,opt}+B^2_{k\,opt}} + C_{k\Sigma}\frac{A_{k\,opt}}{A^2_{k\,opt}+B^2_{k\,opt}}, \qquad (15)$$

where

$$D_{k_\Sigma} = D_k + h_k;$$

$$C_{k_\Sigma} = C_k + f_k.$$

The parameters of the linear part of the system, b_1, b_2, ..., b_k, are determined using the formulas in Table 3.

The point of the proposed nonlinear equation synthesis method is that in essence a linear equation is synthesized, but the influence of the nonlinearity of the curves for some links can be included by the introduction of the corresponding additional disturbing actions.

Another formulation of the basic synthesis task is possible.

What must be found for a stable automatic regulation system such as Eq. (5) for specified parameter values and specified disturbing actions is that control, $S_{\varphi_g}(t)$, for which the motion trajectory, $S_\varphi(t)$, would differ from the given /91 optimum motion trajectory, $S_{\varphi_{opt}}(t)$, by no more than the value of the permissible error.

Using the method of periodic solutions for this case, we can obtain the following analytical relationships

$$C_{0_{opt}} = \frac{1}{S\varphi_{ss}}(A_{0_{opt}} + m_0 M);$$
$$C_{k_{opt}} = \frac{1}{b_n S\varphi_{ss}}[(A_{k_{opt}}F_{2k} - B_{k_{opt}}F_{1k}) + m_k M]; \qquad (16)$$
$$D_{k_{opt}} = \frac{1}{b_n S\varphi_{ss}}[(A_{k_{opt}}F_{1k} + B_{k_{opt}}F_{2k}) + n_k M].$$

The functions F_{1k} and F_{2k} are deciphered in Table 2. The non-periodic disturbing action in Eq. (5) is replaced by a periodic disturbing action and is expanded in a trigonmetric function series

$$N(p)M(t) = \left[m_0 + \sum_1^{\nu}(m_k \cos k\omega t + n_k \sin k\omega t)\right] M \cdot b_n. \qquad (17)$$

Finally

$$S\varphi_{opt}(t) = \left[C_{0\,opt} + \sum_1^{\nu}(C_{k\,opt}\cos k\omega t + D_{k\,opt}\sin k\omega t)\right] S_{\varphi g}. \qquad (18)$$

Along with optimum dynamic characteristics, reversible follow-up systems should have the required precision of follow-up and the required precision of force reflection. There are different ways to increase the regulation precision. In some cases, the system gain is increased, but its dynamic characteristics change significantly as a result. The most effective method of increasing regulation precision without significant change in dynamic characteristics is the method that uses an additional isodromic element to increase regulation precision and to compensate for unneeded friction forces.

The concluding stage of the automatic regulation system synthesis is the selection of the correctors and the determination of their parameters. The correctors should ensure optimum values of system parameters [(the coefficients b_1, b_2, ..., b_n in Eq. (5)] or optimum values of control paramters [(the coefficients $C_{k_{opt}}$, $D_{k_{opt}}$ in Eq. (18)]. Preference in the selection of correctors should be given to direct regulating feedbacks because they do not raise the order of the differential equation of system motion, reduce the influence of nonlinearities, ensure stability of characteristics, or increase operating speed, nor do they require complex additional elements for practical realization.

In the motion of a follow-up system can be characterized by a n^{th} order differential equation, then the number of independently acting correctors necessary for complete optimization of characteristics is equal to n. The number of independent correctors necessary to obtain a specified form of transient curve can be one or two less.

Some correctors are already installed in the initial block diagram of the

system made up of functionally necessary elements. We can, in systems with an isodromic element ensuring given regulation precision under steady-state operating conditions, use a common system amplification factor and isodromic element time constant as the correctors. Both values submit to change readily. Correctors /92 that raise the order of the system differential equation are unsuitable in this case because they do not close the gap between the number of correctors necessary to attain the optimum transient and the number of correctors actually installed in the system. The parameters of the correctors selected are calculated as follows. The coefficients of differential Eq. (5), b_{10}, b_{20}, ..., b_{n0}, corresponding to the optimum transient are determined using the formulas in Table 3. The equations for coefficients b_1, b_2, ..., b_n are determined as a function of the variable and invariable system parameters and links from the block diagram of the system including the selected correctors. Corrector parameters are calculated using equations which derived as a result of comparing coefficients b_{10}, b_{20}, ..., b_{n0} with coefficients b_1, b_2, ..., b_n. These equations, as a rule, are solvable relative to the magnitudes of interest to us.

Let us dwell on the specifics of the synthesis of interconnected systems.

Let us consider the reversible follow-up system with independent control channels, the block diagram of which is shown in Figure 3a. In this case, we have a set of two regulating systems.

The first regulating system, consisting of amplifier 1, the drive (blocks 2, 3, 4, 5, 6), and position sensors 7, 15, is the follow-up system.

The second regulating system, consisting of amplifier 9, the drive (blocks 10, 11, 12, 13, 14), and force sensor 8 is intended for transmitting forces from the slave arm to the master arm.

Let us consider the equations of motion of this reversible system. The master arm drive is

$$pS_{m_m}\left(p+\frac{1}{T_m}\right)=\frac{k_{am}}{c_{emf_m}T_m}u_{\delta m}+k_{F_m}F_m-k_{m_m}M'_{\dot{u}_m}. \qquad (19)$$

The slave arm drive is

(20)

$$[(J_2+J_0)p+(c_2+c_0)]\,p\bar{y}=\bar{M}_2+\bar{M}_0.$$

$$\left.\begin{aligned} X\xi_1 + Y\eta_1 &= M_S - M_{E2}; \\ X\xi_2 + Y\eta_2 &= M_{E1} - M_W; \\ X\xi_3 + Y\eta_3 &= M_W - M_T; \end{aligned}\right\}$$

where

S_{mm} and S_{ms} are the angles of rotation of the output shafts of the motors of the master and slave arms;

T_m and T_s are the electromechanical time constants of the drives;

K_{am} and K_{as} are the amplification factors of the respective amplifiers;

$C_{emf\ m}$ and $C_{emf\ s}$ are the coefficients of the emf of the motors;

K_{Fm} and K_{Fs} are the coefficients of the forces;

K_{mm} and K_{ms} are the coefficients of the moments;

M'_{ism} and M'_{iss} are the summed idling moments attributable to friction forces.

The position sensors are

$$u_{\delta s} = k_{\delta S}(S_{mm} - S_{ms}). \tag{21}$$

The force sensors are

$$u_{\delta m} = k_{\delta F}(F_m - F_s), \tag{22}$$

where

F_s and F_m are the forces acting on the slave and master arm;

$K_{\delta S}$ is the position coefficient;

$K_{\delta F}$ is the force coefficient.

Solving Eqs. (19) - (22) simultaneously, we obtain Eqs. (23) and (24)

$$\left(p^2 + \frac{1}{T_s}p + \frac{k_{as}k_{\delta S}}{c_{emfs}T_s}\right)S_{ms} = \frac{c_{emfs}T_m k_{Fs}}{k_{am}k_{\delta F}}\left[p^2 + \frac{1}{T_m}p + \frac{k_{am}k_{\delta F}k_{as}k_{\delta s}}{c_{emfs}T_m k_{Fs}c_{emfs}T_{emfs}}\right]S_{mm} - \\ - k_{Fs}(1 + \psi_{Fm})F_m - k_{ms}M'_{iss} + k_{mm}M'_{ism}; \tag{23}$$

$$pS_{ms}\left[p^3 + \left(\frac{1}{T_m} + \frac{1}{T_s}\right)p^2 + \left(\frac{1}{T_m T_s} + \frac{k_{as}k_{\delta S}}{c_{emfs}T_s}\right)p + \frac{k_{as}k_{\delta s}}{c_{emfs}T_s T_m}\right] = \\ = \frac{k_{as}k_{am}k_{\delta S}k_{\delta F}}{c_{emfs}c_{emfm}T_s T_m}[(1 + \psi_{Fm})F_m - F_s] - \frac{k_{as}k_{\delta S}}{c_{emfs}T_s}k_{mm}M'_{ism} \tag{24}$$

/94

where

$$\psi_{Fs} = \frac{k_{Fs}c_{emf\ m}T_s}{k_{am}k_{\delta_F}}$$

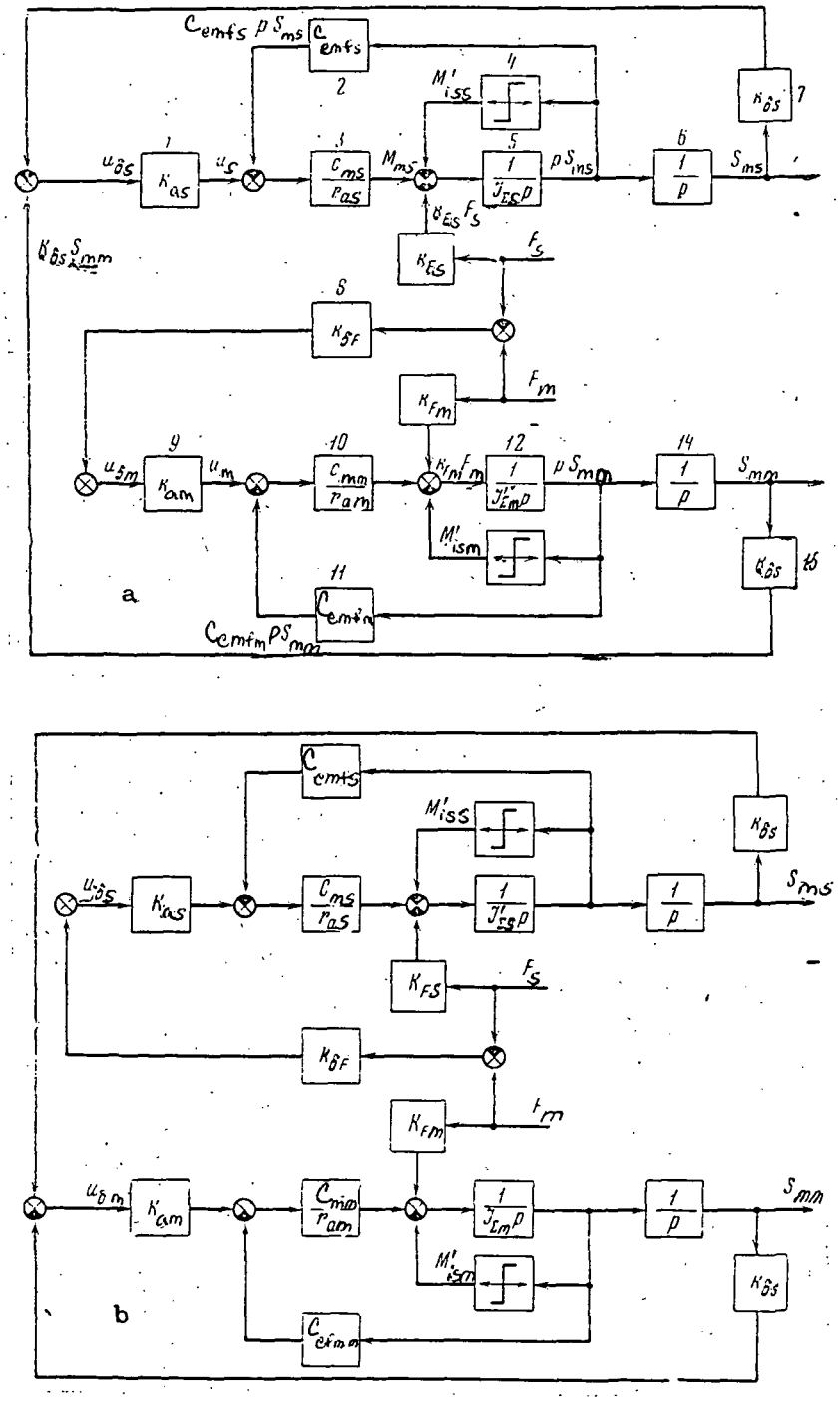

Figure 3. Reversible follow-up systems with independent control channels. a - first variant; b - second variant.

Another coupling arrangement also is possible (Figure 3b). In this case

(25)

Solving Eqs. (19), (20), and (25) simultaneously, we obtain

$$S_{mm}\left(p^2+\frac{1}{T_m}p+\frac{k_{am}k_{\delta S}}{c_{emfm}T_m}\right)=\frac{k_{am}k_{\delta S}}{c_{emfm}T_m}S_{ms}+k_{Fm}F_m-k_{mm}M'_{iSm} \tag{26}$$

$$pS_{ms}\left(p+\frac{1}{T_S}\right)=\frac{k_{as}k_{\delta F}}{c_{emfs}T_S}[F_m-(1+\psi_{FS})]-k_{ms}M'_{iss}, \tag{27}$$

where

$$\psi_{FS}=\frac{k_{FS}c_{emfs}T_S}{K_{as}k_{\delta F}}.$$

A detailed consideration of Eqs. (23), (24), and (26), (27) leads to the following conclusions.

1. The drives for follow-up and force reflection are interconnected in the reversible follow-up system (see Figure 3a), but in the reversible follow-up system (see Figure 3b) they are autonomous.

2. A variable load, and a variable slave arm moment of inertia, have a significant influence on the operation of the follow-up drive in a reversible follow-up system (see Figure 3a), and follow-up precision and the dynamic characteristics of the follow-up drive in the system (see Figure 3b) are determined uniquely by the parameters of the master arm.

Thus, the second variant of the block diagram (see Figure 3b) is the more advantageous.

Eqs. (23), (24) and (26), (27) can be synthesized in accordance with the method presented above to obtain a reversible system optimum in speed of operation and built according to the diagram (see Figure 3).

If an isodromic element is added to the force reflection system (see Figure 3b) the influence of the idling moments is additionally compensated for and Eq. (27) will have the following form

$$p^2S_{ms}\left(p+\frac{1}{T_S}\right)=\frac{k_{as}k_{\delta F}}{c_{emfs}T_S}[(F_m-F_S)_p+k_{ie}(F_m-F_S)] \tag{28}$$

when $M'_{is\ s}$ = const, where K_{ie} is the coefficient of the isodromic element. In the steady-state operating mode

$$F_m = F_s. \tag{29}$$

The advantages noted here of a system built in accordance with the block diagram (see Figure 3b), as compared to the system in Figure 3a, also are retained in more complex reversible systems with independent control channels. Conditions for the independence of regulating systems are ensured when the position sensors are connected directly to the shafts of the slave motors and when the dynamic forces acting on the force sensor of the master arm can be ignored in practice.

Conclusions /95

The investigations have established that:

1. The maximum operating speed of follow-up systems is limited by the properties of the power elements, which usually are electric or hydraulic drives.

2. Follow-up system drives optimum in operating speed should develop maximum accelerations in the required direction throughout the transient in limit modes.

3. Optimum dynamic characteristics of systems operating in limit modes are determined from sufficiently simple calculation equations and known power curves of preselected slave drives.

Thus, criteria exist which permit the comprehensive evaluation of each selected drive even prior to designing the follow-up system as a whole.

4. The use of the proposed periodic solutions method can establish a simple, unambiguous analytical connection between the optimum transient curve fixed in the limit mode with a given input action, and with the parameters of the follow-up system reproducing the optimum curve. This relationship permits determining the parameters of an optimum system, or its optimum control.

The proposed method of follow-up systems synthesis based on the above-indicated analytical relationships is sufficiently universal; that is, equally suitable for designing linear and some types of nonlinear systems, single-circuit and multi-circuit systems, etc.

The method provides for the building of optimum systems when there are limitations on the capacity of power elements and power supply sources.

The use of isodromic elements, and of other known equipment, makes it

possible to increase significantly follow-up precision and accuracy in the reflection of forces.

N73-26084

THE QUESTION OF MANIPULATOR ACTIVATION BY REVERSIBLE FOLLOW-UP SYSTEMS

Yu. A. Stepanenko

ABSTRACT. The problems of manipulator activation by reversible follow-up systems in each of the drives are discussed. These include the mismatches between input and output coordinates, and the manipulator tongs and their corresponding master arm element, as well as the problems of precision and activation in one drive and the simultaneous operation of all drives.

Most modern master-slave manipulators are activated by reversible follow-up /96 systems (RFS) in each of the drives. This activation method causes the load (forces and moments) acting on the manipulator tongs to be reproduced at the master arm and perceived by the operator with certain distortions. Some of these errors are fundamental in nature and can be attributed to the particularities of the RFS and the kinematics of the manipulator.

The operation of the RFS is accompanied by a definite mismatch between input and output coordinates, and the moment reproduced by it at the input depends on the load, as well as friction and the time lag in the drive units and links in the master and slave mechanical arms. These questions are examined in reference [1].

On the other hand, the manipulator tongs, and the element corresponding to it on the master arm, are mismatched because of the open kinematic circuit in the manipulator arms and the finite stiffness of the drives. The operator must apply forces and moment different from those acting on the tongs in order to balance the mismatched arms. The errors occurring in each RFS, as well as those resulting from the interacting of the RFS when working in open kinematic circuits in the manipulator arms, adversely affect the final activation.

Precision and Activation In One Drive

Figure 1 is a generalized block diagram of the RFS. The input, 2, and output, 4, devices are understood to mean links in the master and slave mechanical arms imparting moments of inertia, J_1 and J_2, respectively, and coefficients of viscous friction c_1 and c_2. Let us designate the moment of inertia of the object of manipulation, 5, imparted to the output link of the drive, 3, as J_0. M_0 is the moment of the external forces acting on the object.

c_0 is the imparted coefficient of viscous friction of the object. Operator 1 creates M_1. Activator 6 measures moment M_2 at the drive output and acts on the input device with moment M'_1. The activator transfer function is $W_2(p)$. The slave arm acts on the object with moment M_2'. The input, x, and output, y, coordinates are linked by

/97

(1)

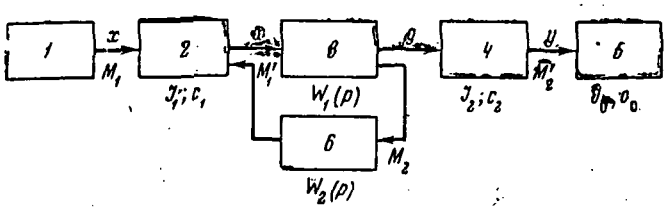

Figure 1.

where the Laplace transforms are designated by vinculums. $W_1(p)$ and $W_3(p)$ are the drive transfer functions with respect to the input coordinate x, and to the drive moment at the output, M_2.

The equation of motion for the output device and the object is

(2)

Substituting into Eq. (1), we obtain

$$x = W_4(p)\,\bar{y} + W_5(p)\,\overline{M}_0, \tag{3}$$

where

$$W_4(p) = \frac{1 - k_2 p W_3(p)(T_2 p + 1)}{W_1(p)};\quad W_5(p) = \frac{W_3(p)}{W_1(p)};$$

$$T_2 = \frac{J_2 + J_0}{c_2 + c_0};\quad k_2 = c_2 + c_0.$$

Eq. (3) gives the possibility of determining the mismatch between the input and output devices for a given law of motion for the object.

Let us now move on to determination of the activation error, which, obviously, is equal to (see Figure 1)

(4)

where K_2 is the scaling factor.

The equation of motion of the input device is

$$(J_1 p + c_1)\, p\bar{x} = \overline{M}_1 + \overline{M}_1; \tag{5}$$

and is, for the object,

(6)

Moments M'_1 and M_2 are linked by

$$\overline{M}'_1 = -W_2(p)\,\overline{M}_2. \tag{7}$$

Substituting Eqs. (5), (6), and (7) into Eq. (4) and using Eq. (2), we obtain

$$\delta\overline{M} = k_1 (T_1 p + 1)\, p\bar{x} + [W_2(p)\, k_2 (T_2 p + 1) - k_0 k_2 (T_0 p + 1)]\, p\bar{y} - [W_2(p) - k_2]\overline{M}_0,$$

where $k_1 = c_1$; $k_0 = c_0$; $T_1 = J_1/c_1$; $T_0 = J_0/c_0$.

Having used Eq. (3), linking x and y, we obtain finally

$$\delta\overline{M} = [k_2 W_3(p)(T_2 p + 1) + k_1 W_4(p)(T_1 p + 1) - k_0 K_2 (T_0 p + 1)]\, p\bar{y} + [k_1 W_5(p)(T_1 p + 1)\, p - W_2(p) + K_2]\,\overline{M}_0. \tag{8}$$

for the activation error in one drive.

We can obtain the mismatch and the activation error for steady-state conditions from general Eqs. (3) and (8).

In the case of a fixed object, for example, and constant moment M_0, /98

where K_1 and K_3 are the amplification factors for transfer functions $W_1(p)$ and $W_2(p)$.

Since most manipulators use a transmission displacement scale of 1:1, $k_1 = 1$, and the mismatch will be determined only by the stiffness of the drive

(9)

The activation error for a fixed object is zero. The activation error when the object is in uniform motion will be $\delta M = (K_2 c_2 + c_1/K_1)\dot{y}$.

The mismatch will depend on the rate of motion and, in the simplest case, ($W_1 = 1$; $W_2 = 1$; $W_3 = -K_3$) will be defined as $\delta y = K_3 (c_2 + c_0)\dot{y} - K_3 M_0$.

Similarly, we can derive expressions for acceleration, for deceleration with

constant acceleration, and the like.

Simultaneous Operation of Drives

Errors in the operator's perception of the load acting on the tongs of the manipulator are caused not only by the imprecise transfer of moment by each of the drives. Another reason for errors is connected with the special features of manipulator kinematics. The mechanical arms have an open kinematic circuit, in which the drives of all the links are interconnected. If in an individual drive the error in moment δM does not directly depend on the mismatch of input and output links δy [see Eq. (8)], then under conditions of simultaneous operation of the drives in a open kinematic circuit the summed effects of these mismatches will directly and adversely affect the activation precision. Indeed, in this case the position of the tongs will differ from the position of the corresponding element of the master arm, and consequently, even in ideal RFS's, which transfer all moments with perfect precision, in order to balance the master arm the operator must apply forces and moments different from those which act on the tongs. As will be shown below, there are some specific positions of the manipulator in which the activation error increases sharply. The fact that the operation of every real RFS is accompanied by its own errors in the transfer of moment only aggravates the situation.

Before moving to an analysis of activation errors, it is necessary to refine certain details. In order to simplify the calculations the present article will examine only the movements of a manipulator in the base plane, that is, in the plane passing through the shoulder S, the elbow El, and the wrist, W (Figure 2). The preceding section examined a linear model of an RFS with constant moments of inertia for the input and output devices. It is impossible to disregard changes in the moments of inertia when operating a manipulator making substantial movements, so the results of the preceding section can be used only when examining manipulator activation in a local area, where it is permissible to consider the moments of inertia constant and it is possible to linearize the dynamics equations. Thus, the results of the following analysis, strictly speaking, are correct near some given position of the manipulator, taken as the initial position. Of course, by considering different initial positions it is possible to cover the entire work space and obtain an idea of the precision of activation in different working operations. The apparatus of the linear theory

of accuracy was used in the analysis [2].

Let the load X, Y, and M act on the object in the manipulator tongs (see Figure 2). Let us designate the moments of the load relative to the corresponding joints as M_S, M_{E1}, and M_W. Then

/99

(10)

where the designations $l_i \sin y_i = \xi_i$; $l_1 \cos y_i = \eta_i$ $(i = 1, 2, 3)$ are introduced is correct for the slave arm.

All the magnitudes in system (10) will receive certain increments when the transition is made to the master arm of the manipulator. Thus, moments M_S, M_{E1}, and M_W are transferred to the RFS with certain errors δM_S, δM_{E1}, and δM_W. Eq. 8 must be used to find them. Moments M_S, M_{E1}, and M_W are substituted for M_O.

Figure 2.

Mismatch δy_i in the coordinates of the slave arm (y_i) and the master arm (x_i) is found by using Eq. (3). Linearizing ξ_i and η_i with respect to these variables, we find that these parameters for the master arm will take the form $(\xi_1 + \eta_1 \delta y_i)1/k_s$; $(\eta_1 - \xi_i \delta y_i)1/k_s$, respectively, where k_s is the scale factor that includes the different length of the links of the slave and master arms.

And, finally, in order to balance the master arm the operator must apply forces $X + \delta X$, $Y + \delta Y$ and moment $M + \delta M$. Then, for the master arm we derive the equations in increments

(11)

These expression are used to find the operator's error in perceiving the load $(\delta X, \delta Y, \delta M)$ for some initial position of the manipulator, determined by the values of ξ_i and η_i.

The determinant of system (11) equals

$$\Delta = \xi_1\eta_2 - \xi_2\eta_1 = l_1 l_2 \sin(y_1 - y_2). \qquad (12)$$

Since the load on slave arms X, Y, and M is arbitrary, system (11) has no solution in straight elbow positions of the manipulator ($y_1 = y_2$), and near these positions activation errors vanish. This result can be explained by the fact that when the elbow is straight, moment M_{E1} carries no information about the load, a significant part of which is preceived directly by support S, and consequently, distorted information about the load is transmitted by the master arm. /100

Let us illustrate these results by a simple example. Let the manipulator lift a load along a straight line inclined at an angle of 45° to the base plane (see Figure 3, a). The motion mode is quasi-static, that is, static equilibrium conditions are satisfied at any moment. The manipulator is ideal, without limitations in the joints [2]. The initial data: $l_1 = 0.5$ m; $l_2 = 0.3$ m; $l_3 = 0.2$ m; $K_1 = 1$; $K_3 = 0.02$ rad/kgfm; $k_m = 1$; $X = Y = -5$ kgf; $M = -5$ kgfm. Since the mode is quasi-static; $\delta M_S = \delta M_{E1} = \delta M_W = 0$, and the mismatch of the arms, in accordance with Eq. (9), will be $\delta y = -K_3 M_0$.

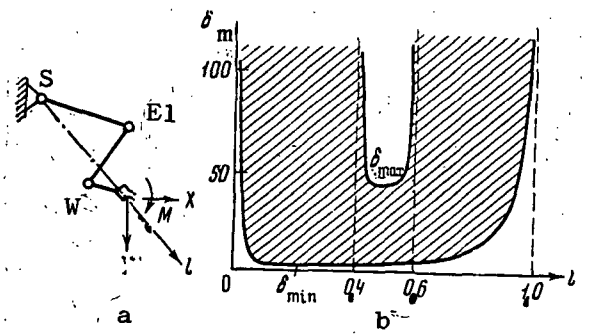

Figure 3. Example of the determination of activation errors. a - diagram of the loading of the manipulator; b - insensitivity zone.

The mean error for this manipulator was determined as $\delta_m = \frac{1}{3}(|\delta X| + |\delta Y| + |\delta M|)$. Maximum and a minimum magnitudes of the mean error when the position of the manipulator is changed within the limits of the service angle [3] were calculated for different points on the straight line examined and over which the load was lifted.

The results of the calculation are presented in Figure 3b. As may be seen, even in the highly favorable case examined, the magnitude of the mean error is great over a substantial section. It is interesting to note the connection of these results with reference [4], where the growth in the errors for mechanisms near the extreme positions was investigated. The straight elbow position in a certain sense may be considered as "extreme", although as applied to manipulators this term demands a more precise definition, since the manipulator, possessing a specific service [3], can occupy

such a position for operations in a larger part of the working volume (see Figure 3).

The analysis made showed that in those cases when an extremely precise activation is required, it is necessary to delineate the working zone which will comprise only a part of the total working space precisely and also to choose the stiffnesses and transfer functions of the RFS on the basis of the condition of ensuring the required activation precision.

REFERENCES

1. Kuleshov, V. S., Lakota, N. A., "Structural and Analytic Presentation of Reversible Follow-Up Systems," V sb: Mekhanika mashin [In collection: Mechanics of Machines], No. 7-8, "Nauka" Press, 1967.

2. Bruyevich, N. G., Tochnost' mekhanizmov [Precision of Mechanisms], OGIZ, 1946.

3. Vinogradov, I. B., Kobrinskiy, A. Ye., Stepanenko, Yu. A., Tyves, L. I., "Features of the Kinematics of Manipulators and Volumes Methods," This collection.

4. Kobrinksiy, A. Ye., "Kinematic Errors of Mechanisms in Near Limit Positions," Trudy seminara po teorii mashin i mekhanizmov [Proceedings of the Seminar on the Theory of Machines and Mechanisms], No. 33, 1950.

N73-26085

AN INVESTIGATION OF ENGINEERING METHODS OF DESIGNING ELECTROHYDRAULIC FOLLOW-UP DRIVES FOR UNDERWATER MANIPULATORS

V. S. Yastrebov

ABSTRACT. Questions of engineering methods of analysis and synthesis of electrohydraulic control systems for underwater manipulators with position feedbacks are discussed. An approximation of a control system by an aperiodic unit is presented.

The practical use of manipulatory devices is a comparatively recent event. /101
The idea of using manipulators became reality in different fields of engineering. However the theoretical principles of manipulator analysis and synthesis are still insufficiently developed. The existing literature devoted to the theory of manipulators (in particular, underwater ones), does not formulate the requirements for control systems, or for the kinematic characteristics of the working elements, with finality. Nor is there a unified method of engineering analysis and synthesis of these devices.

The published papers are basically devoted to reversible manipulator control systems [1, 2] with a number of essential features which limit the use of developed procedures for analysis and synthesis of manipulator control systems with position feedbacks only.

The process of building underwater master-slave manipulators involves very complex questions connected with the theory of these devices, as well as a need to solve problems dictated by the particularities of the environment.

It is quite natural that only theoretical principles of reversible systems can be developed for underwater manipulators at the present time. Their technical realization is hindered for the time being by a number of purely engineering questions (information on forces, acceptable and dependable structural design of the working element and feedbacks, and so forth). At the same time, building efficient operating models of underwater master-slave manipulators without force reflection, which are finding more and more application in ocean research, is definitely impeded by the lack of engineering calculation methods.

This paper is devoted to questions of the engineering procedure for the

analysis and synthesis of an electrohydraulic control system for an underwater master-slave manipulator with position feedbacks.

Manipulators are extremely unusual devices, differing significantly from the systems and mechanisms in practical use. This is primarily a system with many degrees of freedom, as many as eight and more. The operation of each slave drive depends on the state of all the other drives. It is evident that the variability of parameters, and of the loads (static and inertial) acting on the drives in /102
particular, is determined by the structural features of the manipulator. The variability of the loads also is the result of the functioning of the manipulator. The static and inertial loads change in steps.

Parameters also can vary when all control systems are supplied from a common source. This relationship can exist in the control circuits as well as in the power circuits supplying the slave motors.

Finally, parameter variability, of loads in particular, occurs due to the environment. The hydrostatic pressure and the decreasing water temperature with depth increase the static and dry friction forces as well as system delay.

The difference in design from the majority of existing systems should be taken into consideration if the analysis of the manipulator is based on the theory of control systems. The control system of a manipulator is a complex of interconnected control circuits. Such systems are known as multidimensional. An analysis of a manipulator control system as a complex requires knowledge of many load to drive relationships as a function of the output parameters of the other follow-up systems. This is a separate question and requires special research.

The subject of investigation in this paper is one control circuit with one degree of freedom. The influence of the other of the manipulator's follow-up systems is taken into consideration by the corresponding disturbances. The following basic requirements, based on the theoretical and experimental investigations conducted, and which the control system for a master-slave manipulator should satisfy, can be formulated: (a) constancy of transient characteristics over the entire range of operating loads and disturbances; (b) absence of over-regulation over the entire range of operating loads and control signals; (c) the value of the nonresponse zone should be minimum; (d) smoothness of motion of the slave drives in the initial and final stages of motion over the entire

range of operating loads and control signals; (e) the supply parameters should ensure minimum interference between manipulator control circuits; (f) the transient parameters should be chosen on the basis of the operations to be performed by the manipulator; (g) correspondence between the characteristics of a high-speed master-slave manipulator and the human arm should be provided for all degrees of freedom.

Manipulator control systems invariance with respect to load disturbances, as is known, can be provided by the corresponding choice of system gain, or by adding feedback providing information on load changes. The former provides partial invariance, so-called invariance to ε. The second method, in principle, provides absolute invariance. But it is very difficult to build load feedbacks into electrohydraulic systems. In other words, the method that merely achieves partial invariance by the corresponding choice of system gain may be the most acceptable.

This then raises the question of how to satisfy two conflicting factors: on one hand, a comparatively high gain; on the other, a transient of sufficiently high quality.

A two-mode control system can meet this requirement [3].

Saturation often becomes the standard operating mode in two-mode control /103
systems because it occurs with comparatively feeble control signals. But if the change in the control signal is slow enough, saturation cannot occur, and the system functions as a linear system.

There are adequate grounds for considering a two-mode control system as the optimum because it best satisfies the conflicting requirements of speed and transient quality. A similar control system can be designed by, using a semiconductor triode amplifier operating in a pulse-width modulation mode, for example. This makes for a highly responsive system and virtually eliminates the nonresponsive zone.

The advisability of a pulse mode of operation for the amplifier, and for the entire system, can arise when the influence of the many nonlinearities inherent in a slide valve mechanism and slave motor on the operation of the follow-up drive is substantial.

The pulse mode of operation can be limited, in practice, to any point in the control system by the corresponding choice of the value for the linearized oscillations frequency.

Slave motor speed control is ensured when the pulse mode is taken to the slave motor. However, this system operation mode is accompanied by an unproductive flow of the working fluid through the slide valve, reducing drive efficiency.

This fact often makes it advisable to limit the pulse mode in a manipulator control system to the output of the semiconductor amplifier (linearized oscillations frequency 200 Hz). The control element in the hydraulic amplifier then will respond only to the mean control current value for the period.

Linearized oscillations take place as far as the slave drive at lower frequencies to 100-125 Hz.

Hydraulic amplifiers with a nozzle-slide valve control element are in use today in electrohydraulic control systems. They are highly responsive, quick-acting, and have stable characteristics during changes in temperature. Movements of the slide valve, which is located in the space between two calibrated nozzles, changes the pressure drop at the ends of the slide-valve, causing a corresponding movement regulating the supply of high-pressure liquid to the slave motor expanse.

Let us make our further analysis of an electrohydraulic follow-up drive for a master-slave manipulator on the basis of the following assumptions:

the processes occurring in the hydraulic drive will be looked at in terms of changes in the controlled parameter;

there is no non-response zone or overlap in the slide-valve mechanism;

dry friction and obliteration of the slide-valve are negligibly small;

the temperature and viscosity of the working fluid are constant during the entire operating time;

the pressure at the slide-valve mechanism input is constant;

the fluid flow in the hydraulic lines is laminar;

the resistance of the hydraulic lines is negligibly small.

A semiconductor amplifier operating in the pulse-width modulation (PWM) mode is, strictly speaking, nonlinear link. Considering, however, that the highest frequency of the control signal is very much lower than the linearized oscillations frequency, the relationship between the amplifier output and the input may be considered linear. At the same time, the frequency of the input signal for which this assumption is correct can be found by using the following inequality

/104

$$|\omega_{in}| < \left|\frac{1}{10} \div \frac{1}{6}\right| \frac{\pi}{T_e}, \quad (1)$$

where

T_e is the relay amplifier time constant.

The operating time of semiconductor triodes is measured in microseconds, so it can be taken that the assumption made is valid for all operating frequencies of the manipulator control system input signal.

Without dwelling on the derivation of the relationship between amplifier transmission factor and circuit parameters (Figure 1), we can write:

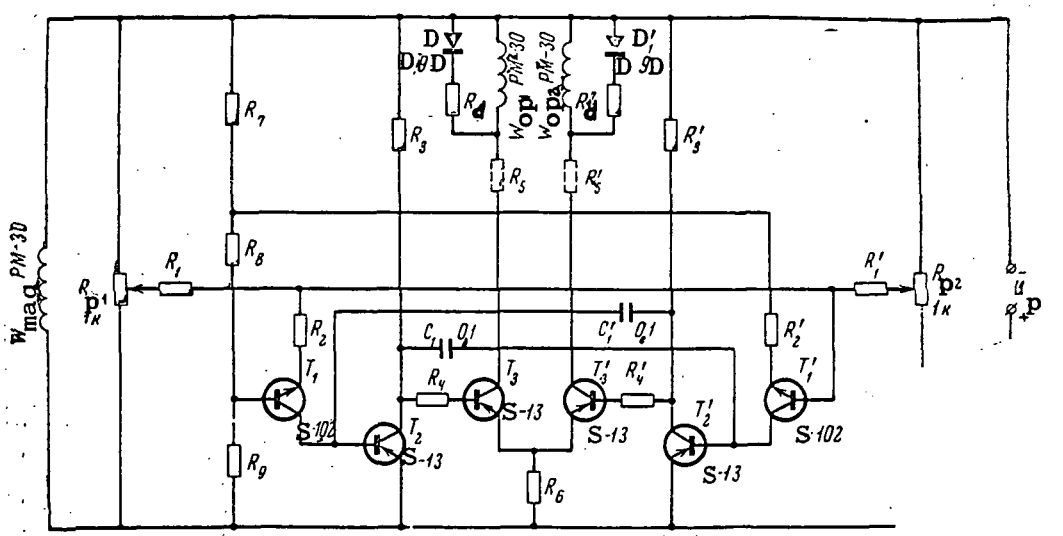

Figure 1. Schematic diagram of a pulse-width modulator.

We see that the magnitude of the amplifier transmission factor for a given supply voltage is inversely proportional to the magnitude of resistor R_5, R_5^1 in the collector circuit of triodes T_3 (T_3^1).

The equation characterizing the dynamics of the electromechanical transmission relay (ETR) when it is not loaded by the reactions of the fluid jets will, in operator form, be

$$\alpha(p)\cdot(T_2^2p^2+2\xi_1\cdot T_2\cdot p+1)=K_{ETR}^0\cdot J_0(p);$$
$$T_2=\sqrt{J\left|\frac{\partial\alpha}{\partial M}\right|};$$
$$\xi_1=\frac{f}{2\sqrt{J\left|\frac{\partial M}{\partial\alpha}\right|}}. \qquad (2)$$

where

J is the moment of inertia of the slide-valve, kgf/sec^2;

f is the coefficient of viscous friction, kgf·sec/cm.

The ETR movement gain, K_{ETR}^O, disregarding the action of the fluid jet reaction on the slide-valve is determined experimentally. This magnitude depends on the value of the ETR magnitizing voltage. As will be seen from the graph (Figure 2), K_{ETR}^O increases with decrease in the maguitizing voltage.

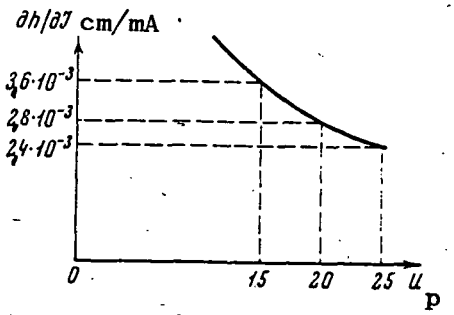

Figure 2. Nature of the change in the ETR gain in terms of the supply voltage.

The ETR transfer function for a hydraulic amplifier, including the action of the hydrodynamic forces on the slide-valve, will be

(3)

where

$$T_3=\frac{T_2}{\sqrt{1+K_{MJ}(K_{ph}\cdot K_{Mp}+K_{Mh})}};$$
$$\xi_2=\frac{\xi_1}{\sqrt{1+K_{MJ}(K_{ph}\cdot K_{Mp}+K_{Mh})}};$$
$$K_{ETR}^h=\frac{K_{ETR}^0}{1+K_{MJ}(K_{ph}\cdot K_{Mp}+K_{Mh})}.$$

The equation of the fluid flow through the nozzle after its linearization by expansion into a Taylor series can be written /105

(4)

where

K_{Qh} is the hydraulic amplifier (HA) gain in terms of the flow in cm^2/sec;

K_{Qp} is the HA static characteristic elasticity factor in $cm^5/sec/kgf$.

If we take the relative conductivity of the constant and variable chokes when $h_0 = 0$ as equal to unity, then the fluid flow through the nozzle will equal the fluid flow through the constant choke. Then the factors of the generalized static characteristic can be approximately determined by the following expresssions: $K_{Qh} = Q_h/h_0$; $K_{Qp} = Q_h/p_f$.

The general form of the equation of pressure drop at the ends of the distribution slide-valve is $Q_h = K_{Qh}h - K_{Qp} \cdot P_f$,

$$\Delta p_f = \frac{1}{F_{sv}}\left[m\frac{d^2x}{dt^2} + f\frac{dx}{dt} + (C_{sp} + C_h)\cdot X + |R_{fr}|\operatorname{sign}\frac{dx}{dt} + R_0\right],$$

where

F_{sv} is the area of the end of the slide-valve, cm^2;

m is the mass of the slide-valve and movable parts, $kgf/sec^2/cm$;

X is slide-valve displacement, cm;

f is the viscous friction factor, kgf/sec/cm;

C_{sp} is the stiffness of the centering springs, kgf/cm;

C_h is the unbalanced hydraulic force factor, kgf/cm;

R_{fr} is the dry friction force, kgf;

R_0 is the force of obliteration sealing, kgf.

The equation of the pressure drop at the ends of the slide-valve can be greatly simplified if we disregard the influence of the slide-valve mass transient, the viscous and dry frictions, and the forces of obliteration sealing of the slide-valve at the time of touching. The values of these component forces are much less than the transposed forces. Let us just consider the effect of the centering spring forces and of the unbalanced hydrodynamic force /106

in the equation.

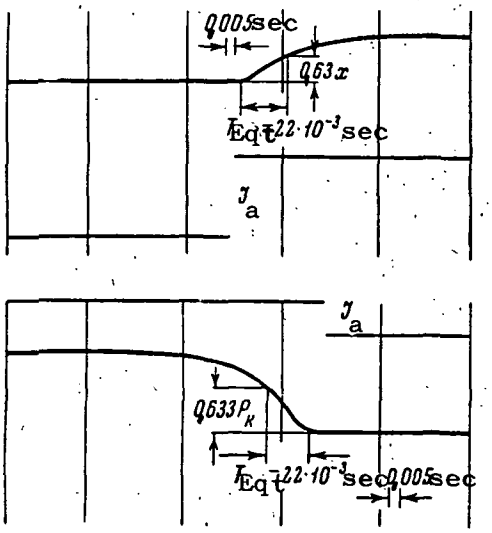

Figure 3. Oscillograms of transients in a hydraulic amplifier.

Solving the derived equations simultaneously, we obtain, finally, the transfer function of this link

$$W_{ha}(p) = K_{ph}/(T_{ha}p + 1). \quad (5)$$

The time constant for the hydraulic amplifier for the parameters chosen for the control system is $25 \cdot 10^{-3}$ sec.

The time constant for the oscillating link and characterizing the operation of an ETR unloaded by the reactions of the jets is much smaller than that for a hydraulic amplifier. Consequently, its influence on the nature of the course of the transient will be slight, so the oscillating link can be closely approximated by an amplifying link with a gain of K^{O}_{ETR}.

In this case the dynamic block diagram, representing an electromechanical converter and a hydraulic amplifier, can be converted into an equivalent, aperiodic link with gain K_{eha} and equivalent time constant T_{eha}.

$$T_{eha} = T_{ha}/(1 + K_{ETR}K_{ph} \cdot K_{YP}); \quad (6)$$
$$K_{eha} = K_{ha}/(1 + K_{ETR}K_{ph} \cdot K_{YP}).$$

The error caused by the approximation was evaluated by an experimental check. This was done by connecting the working chambers of the slide-valve to DDM-60 type pressure sensors. The control current and pressure sensor signals were recorded by loops on an oscillogram (Figure 3).

In addition, the transient characteristics of slide-valve movement were taken experimentally.

The experimentally derived transient curves (Figure 3) confirm that an electromechanical converter and a hydraulic amplifier with a nozzle-valve type sensitive element can be approximated by an aperiodic link with an equivalent time constant of the order of $20 \cdot 10^{-3}$ sec, with sufficient precision for

/107

engineering calculations.

The fluid flow through the slide-valve can be determined by

$$Q_{sv} = G_x \cdot U_x \sqrt{P_1 - P_R} \cdot \operatorname{sign} X, \tag{7}$$

where

G_x is the hydraulic conductivity of the slide-valve slot;

U_x is the dimensionless coefficient of the relative opening of the slide-valve slot;

P_R is the pressure of the liquid at the slide-valve input, kgf/cm^2;

P_1 is the pressure, determined by the load on the motor piston, kgf/cm^2.

The fluid flow through the slide-valve depends on the load applied to the drive piston. The load on the manipulator drive is a variable, depending on change in the generalized coordinates, as well as on the magnitude of the working force applied to the tongs.

Since the slave drives of the manipulator operating element are influenced by the variable static and inertial loads [4], the equation of the load characteristic of the slide-valve is nonsteady-state.

Precise methods for studying systems described by nonsteady-state nonlinear equations are extremely complex. Approximate research methods that are sufficiently accurate for practical work are used for engineering calculations. One of them is the coefficient freezing method.

This method assumes that system stability depends only on the instantaneous values of the variable coefficients in the equation. The system therefore is considered to be steady-state at successive moments in time. It is completely natural that the results of such research are more accurate the smaller the rate of change for equation coefficients during the transient. Nonlinear equation (7) can be approximated by a linear dependency only when a great many limitations are imposed. As V. A. Khokhlov [6] has shown, its linearization by the method of expansion into a Taylor series in the neighborhood of point $X = X_0$ and $P = P_{xx}$

$$Q_{sv} = K_x \cdot X - K_{\Delta p} \cdot P, \tag{8}$$

where

$$K_x = Q_{sv}/X;$$

$$K_{\Delta p} \simeq K_x \cdot X_0/2P_1$$

does not yield a linear dependency because the function is discontinuous, nonconstant, and dependent on movement of the slide-valve. V. A. Khokhlov's paper suggests investigating the stability and the transient characteristics of a slave drive using the following simplified equation

$$M\frac{d^3q}{dt^3} + f\frac{d^2q}{dt^2} + |R_{fr}|\frac{d}{dt}\left[1(t)\cdot\operatorname{sign}\frac{dx}{dt}\right] + K_n\frac{dq}{dt} = K_v X. \qquad (9)$$

The admissability of this substitution was checked by the mathematical simulation method and showed that the nonlinear term under the radical in Eq. (7) had little influence on the stability margin. And it is suggested that a rough analytic estimate of stability be made using Eq. (8), assuming that the slide-valve moves from its neutral position to one side only. A more accurate investigation of the follow-up drive should be made using Eq. (7) and the mathematical simulation method.

The compressibility of the fluid trapped in the motor chambers and lines must be taken into consideration when investigating the dynamics of pressure-loaded drive piston movements proper.

Fluid compressibility depends to a considerable degree on the quantity of dissolved air contained. According to T. M. Bashta [7], the air content in the fluid varies from 5 to 15 percent, depending on hydraulic system design. But at pressures above 90-100 kgf/cm^2 the volume of air inclusions becomes so insignificant, that the bulk modulus for the medium is determined basically by the fluid's bulk modulus. System modulus of elasticity is chosen in the following way, when the drive is connected to the distributor by a rigid pipeline. The bulk modulus for oil can be taken as equal to $2\cdot10^4$ kgf/cm^2, and as $1.2\cdot10^6$ kgf/cm^2 for brass pipelines. The calculated normalized modulus of elasticity for a hydraulic circuit is $1.8\cdot10^4$ kgf/cm^2. The use of a somewhat lesser modulus of elasticity for a hydraulic circuit, something of the order of $1.4\cdot10^4$ kgf/cm^2, is recommended in practice. /108

The normalized modulus of elasticity for the system will be substantially lower when flexible hoses are installed between the drive and the hydraulic distributor. The data in [8] suggest that the normalized modulus of elasticity for the system with flexible hoses should be taken as equal to no more than $0.9 \cdot 10^3$ kgf/cm^2.

Considering the full fluid flows in delivery and drain mains, and the middle position of the hydraulic cylinder piston, we can write [9]

$$Q_c = \frac{V}{2E} \cdot \frac{dp}{dt} = \frac{K_c V}{2} \cdot \frac{dp}{dt}. \tag{10}$$

The presence of hydraulic mains between the distributor and the drive moreover increases the inertial load on the drive piston. The magnitude of this mass load can be taken into consideration by

$$M_f = m_f \left(\frac{F_p}{f_{fr}}\right)^2, \tag{11}$$

where

m_f is the mass of the fluid trapped between the piston and the distributor, kgf·sec^2/cm;

F_p is the area of the piston, cm^2;

f_{fr} is the sectional area of the hydraulic mains, cm^2.

Based on the equations of working fluid flow through the slide-valve, we can write

$$(T_w p + 1)\,\Delta p(p) = K_w X(p) - K_v p q(p), \tag{12}$$

where

$T_w = K_{df} V_0 / 2(K_{\Delta p} + K_l)$;

$K_w = K_x / (K_{\Delta p} + K_l)$: $K_v = F_p / (K_{\Delta p} + K_l)$.

The time constant T_w characterizes the exponential process of the increase in the pressure drop Δp at the working piston for stepwise movement of the slide-valve and a locked working piston (when $q = 0$).

The pressure drop in the equation of the load characteristic for the

slide-valve is entirely determined by the load applied to the drive piston. This equation can be written

$$\Delta p = \frac{1}{F_p}\left(M\frac{d^2q}{dt^2} f \frac{dq}{dt} + K_p q + |R_{df}| \operatorname{sign}\frac{dq}{dt} + R_{h.d}\right), \qquad (13)$$

where

f is the coefficient of viscous friction, kgf·sec/cm;

K_p is the transmission factor for the positioned load, kgf/cm;

R_{df} is the dry friction force, kgf;

M is the summed normalized mass, kgf·sec^2/cm.

The viscous friction force is determined primarily by the friction in the ring gap between the cylinder and the piston, and by the friction in the lines. The hydrodynamic resistance force occurs when the working element moves in water. The calculation shows that the magnitude of these forces in the total force balance for the drive is very minor however.

The dry friction forces developing in the slave motor packings are very substantial. This type of load is one of the primary loads for underwater manipulator control systems. As is known, the dry friction force curve is nonlinear, and is determined by the law for the speed of the drive's output shaft. /109

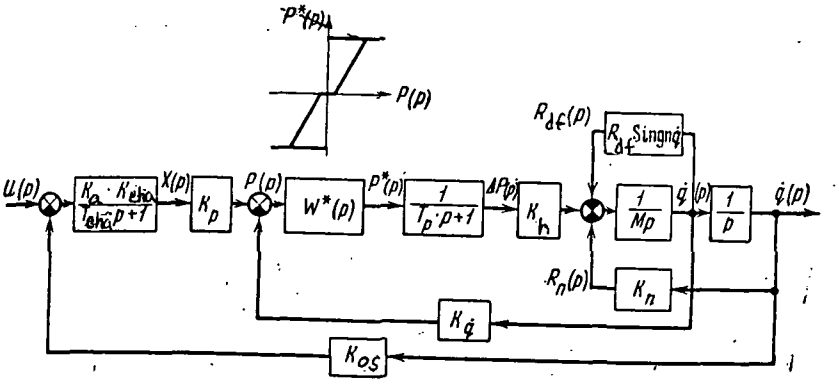

Figure 4. Dynamic block diagram of a control system.

The derived equations, including the comments made, can be represented by a dynamic block diagram (Figure 4).

It is most desirable to use the logarithmic frequency method to analyze the stability and the parameters of the transient in general form, as well as to synthesize the system according to the given characteristics. Such quality indices as overregulation when the stepwise action at the input is isolated, and the transient time, determined by the required manipulator speed of response, should be taken as the basis for solving problems of manipulator control synthesis.

As has been noted, the influence of a disturbance created by the load can be reduced to a minimum by increasing system gain. However, this increase should be reasonable, conforming to the basic quality indices, as well as to the possibility of arriving at a sufficiently simple technical realization of the correctors. The question of choosing the necessary speed of response by the manipulator control circuits is perhaps more difficult. There is no question that it must be solved on the basis of operations which must be performed. The fastest responding drives for general-purpose manipulators usually have a transient time of the order of 0.08 to 0.1 second, and the slowest of 0.3 to 0.5 second.

Let us, by way of an example, consider the circuit controlling the drive for withdrawing the manipulator "shoulder." The logarithmic amplitude-phase curve (Figure 5) shows that the uncorrected control system does not provide the required transient quality for the gain selected. The correction in this case can be made by a passive series network with transfer function

$$W_g(p) = (T_{2g}p + 1)(T_{3g}p + 1)/(T_{1g}p + 1)(T_{4g}p + 1). \qquad (14)$$

The time constants for this link correspond to the coupling frequencies ω_{1g}, ω_{2g}, ω_{3g}, ω_{4g}. Note that the region of the amplitude curve intersecting the frequency axis at a slope of 20 db per decade should be selected such that the ratio ω_{3g}/ω_c is at least 4, and the ratio ω_{3g}/ω_{2g} is at least 10.

A preliminary estimate of the effect of the fundamental nonlinearities on the stability of the follow-up drive can be made by using the harmonic balance method. The structural conversions of the system into a single-circuit one are shown in Figure 6 for purposes of investigating drive stability including but one nonlinearity. /110

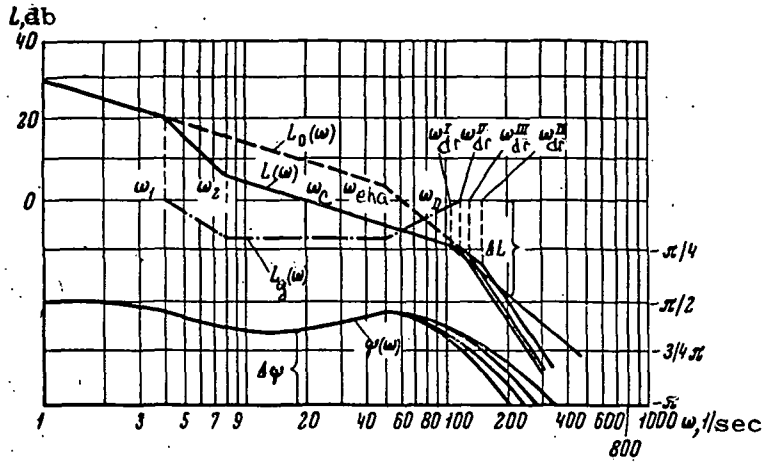

Figure 5. Logarithmic amplitude-phase characteristic curves of a control system.

The limit of system stability will be determined by the general frequency criterion

$$W_1(j\omega)F(a_1\omega) = -1.$$

The system contains two fundamental nonlinearities: dry friction and saturation. The investigation of their effect on stability can be made consecutively, assuming that there is no saturation when the amplitudes of natural oscillations of the system are small. Dry friction is what exerts a substantial damping effect. On the other hand, the damping effect of dry friction becomes immaterial when the amplitudes of the natural oscillations are large and now there is a significant increase in the influence of saturation.

Let us use the following equation

$$p\left[\frac{K_{co}VM}{K_{co}K_pV+2F_p^2}p^2+\frac{fK_{co}V}{K_{co}K_pV+2F_p^2}p+1\right]+$$
$$+\left|\frac{R_{df}}{K_{co}K_pV+2F_p^2}\right|p[1(\bar{t})\operatorname{sign} pq]=\frac{K_v}{K_{co}K_pV+2F_p^2}X(p).$$

to make an accurate investigation of stability and of the transient characteristics, including the existing nonlinearities.

Figure 7 shows the results of mathematical modeling based on equations obtained. The oscillograms show the system to be stable when the speed quality factor for the drive is K = 80. Overregulation in the transient curve decreases, but the static error increases, with increase in dry friction forces.

Overregulation in the transient curve increases with increase in the normalized mass, and the magnitude of the overregulation in the transient curve

decreases with decrease in the normalized mass and dry friction forces.

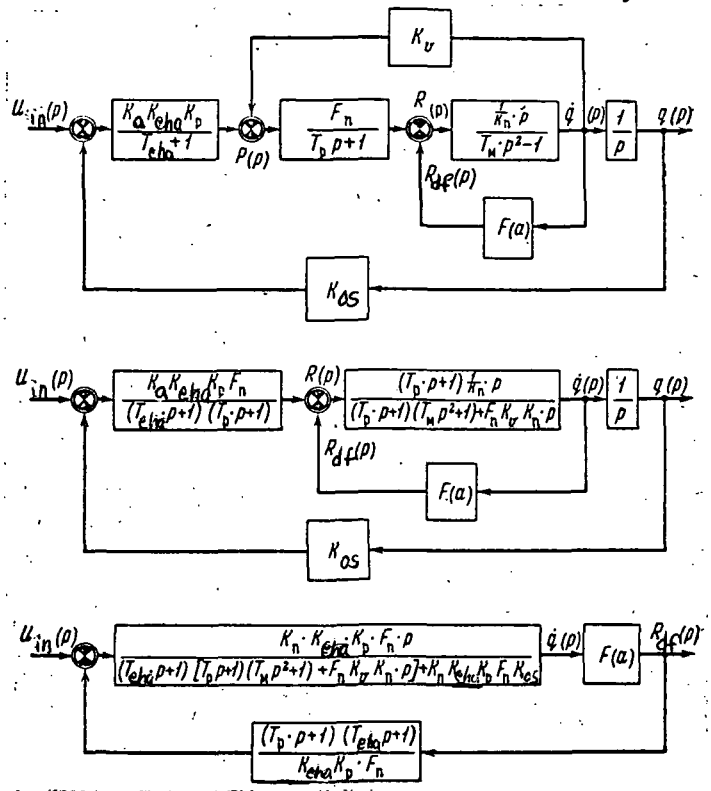

Figure 6. Diagram of structural conversions.

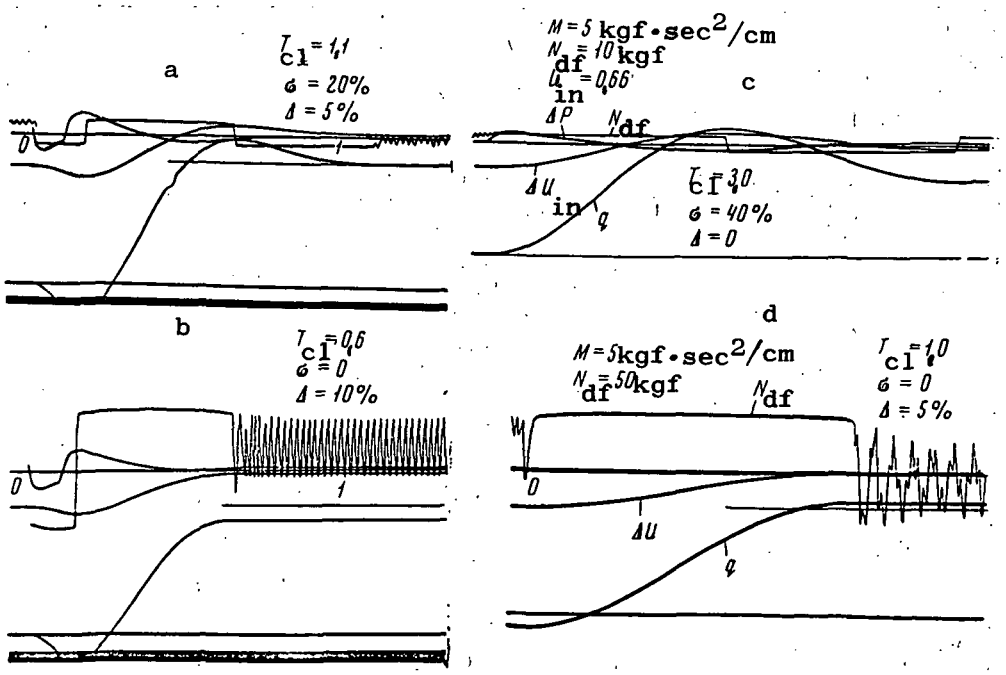

Figure 7. Oscillograms of control system transients. a - when M = = 1 $\frac{\text{kgf}\cdot\text{sec}^2}{\text{cm}}$, N_{df} = 10 kgf; b - M = 1 $\frac{\text{kgf}\cdot\text{sec}^2}{\text{cm}}$, N_{df} = 50 kgf.

The analysis leads to the following conclusions. /112

1. An electrohydraulic manipulator control system can be approximated right down to the slide-valve mechanism by an aperiodic link with sufficient accuracy for practical work.

2. The use of simplified Eq. (12) is acceptable, given the limitations imposed, for making a preliminary investigation of an electrohydraulic manipulator follow-up drive.

3. A detailed investigation of an electrohydraulic manipulator follow-up drive based on Eq. (15) must be made.

REFERENCES

1. Kuleshov, V. S., Lakota, N. A., "A Structural and Analytical Presentation of Reversible Follow-Up Systems," V sb. Mekhanika mashin [In collection: Mechanics of Machines], No. 7-8, "Nauka" Press, 1967.

2. Petrov, B. A., Batyushkov, A. I., "Some Peculiarities in the Calculation for Reversible Follow-Up Systems," V sb. Mekhanika mashin [In collection: Mechanics of Machines], No. 7-8, "Nauka" Press, 1967.

3. Teler, D., Pestel', M., Analiz i raschet nelineynykh sistem avtomaticheskogo upravleniya [Analysis and Calculation of Nonlinear Automatic Control Systems], "Energiya" Press, 1965.

4. Yastrebov, V. S., "An Investigation of the Dynamics of a Manipulator Operating Organ," V sb. Mekhanika mashin [In collection: Mechanics of Machines], No. 7-8, "Nauka" Press, 1967.

5. Kuzovkov, N. T., Teoriya avtomaticheskogo regulirovaniya, osnovannaya na chastotnykh metodakh [The Theory of Automatic Control Based on Frequency-Response Methods], Oborongiz [State Scientific and Technical Publishing House of Literature on Defense], 1960.

6. Khokhlov, V. A., Elektrogidravlicheskiy sledyashchiy privod [The Electro-Hydraulic Follow-Up Drive], "Nauka" Press, 1967.

7. Bashta, T. M., Mashinostroitel'naya gidravlika [Machine-building Hydraulics], Gostekhizdat [State Publishing House of Technical and Theoretical Literature], 1963.

8. Leshchenko, V. A., Gidravlicheskiye sledyashchiye privody dlya avtomatizatsii stankov [Hydraulic Follow-Up Drives for the Automation of Machines], Mashgiz [State Scientific and Technical Publishing House of Literature on Machinery Manufacture), 1962.

9. Yastrebov, V. S., "An Electro-Hydraulic Follow-Up Drive for Sea Operations," in Trudy IOAN SSSR [Transactions of the Institute of Oceanology of the Academy of Sciences of the U.S.S.R.), 74, 1965.

N73-26086

THE FIRST EXPERIMENT IN BUILDING AN AIRTIGHT MAGNETOMECHANICAL MASTER-SLAVE MANIPULATOR

V. A. Ovsyannikov

ABSTRACT. The use of magnetic couplings to make manipulators airtight is discussed. The special properties of magnetic couplings and magnetomechanical transmissions making their use in manipulators advantageous are presented.

The requirements for manipulator airtightness have grown in recent years in connection with the development of a number of new fields of engineering. Work with highly toxic materials, or maintenance of a special atmosphere inside a volume being serviced (inert gas, lack of oxygen, moisture, etc.) required a new approach to the problem of making manipulators airtight. The use of stuffing boxes failed to ensure airtightness, and, in addition, heavy friction losses significantly reduced manipulator response. Let us consider making manipulators airtight by using magnetic couplings. /113

Magnetic couplings have many special properties that make them advantageous to use in a manipulator:

(1) the capability of transmitting forces through a solid nonmagnetic partition without contact with the half-couplings;

(2) the capability of operating as a safety coupling, slipping of the coupling occurs when the maximum moment is exceeded;

(3) the capability of transmission, in addition to rotary and forward motion, along a nonmagnetic partition;

(4) the capability of transmission of shaft rotation at constant angular speed when shafts are out of alignment.

The magnetic field for the coupling can be easily created by an electromagnet. But the use of an electromagnet for couplings is limited because of bulkiness, heavy weight, energy consumption, and cooling of water or compressed air consumption.

Permanent magnet couplings lack these drawbacks and are featured by being highly dependable, always ready to work, durable, and easy to maintain. This is why shielded synchronous permanent magnet couplings are used in a manipulator.

Direct magnetic coupling of the control and slave units provides airtightness, maneuverability in operation, simplicity, and economy. Figure 1 shows a magnetomechanical manipulator with a load-rating of 3 kg.

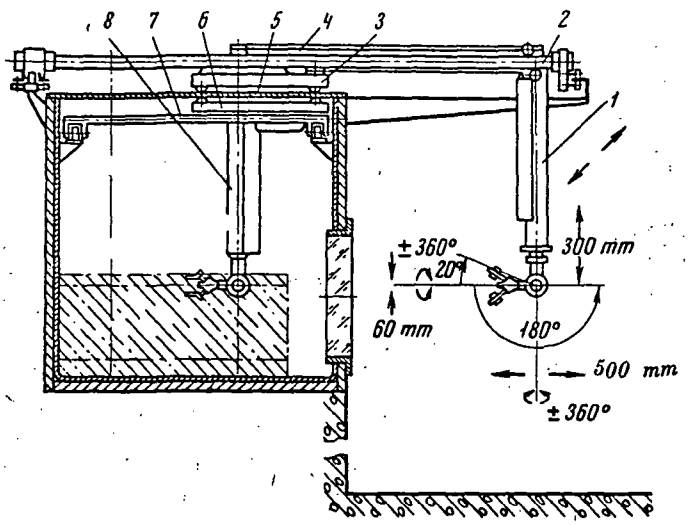

Figure 1.

The manipulator consists of control unit 1, which is an open, multilink, three-dimensional mechanism, upper bridge 2, driving half-coupling 3, connecting bands and rods 4, airtight nonmagnetic partition 5, driven half-coupling 6, lower bridge 7, and slave unit 8, which is a mechanism similar to the control unit. This drawing shows the maximum movements of which the manipulator is capable for each degree of mobility, as well as the manipulator working volume (shaded section). /114

The manipulator has (Figure 2a) the following degrees of mobility: movement of tong jaws (coordinate α), rotation of the hand (β), flexing - unflexing of the hand (γ), rotation of the vertical tube (δ), raising - lowering of the hand (ε), "forward - back" motion (η), and "left - right" motion (λ).

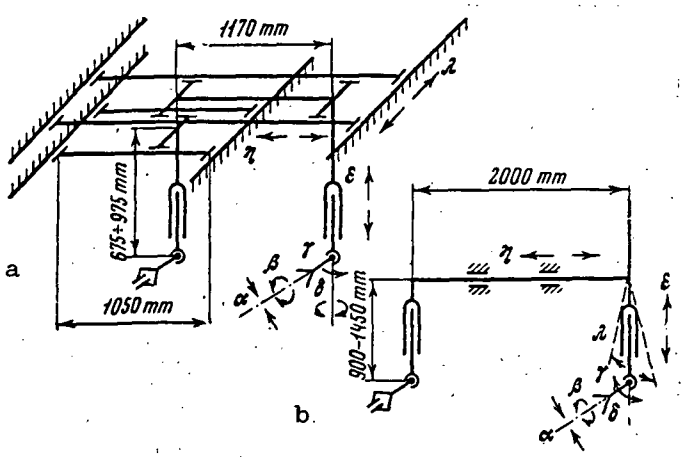

Figure 2. Kinematic diagrams
a - magnetomechanical manipulator; b - mechanical manipulator.

Figure 2b shows the dimensions and degrees of mobility of a mechanical manipulator for purposes of comparison. In contrast to the magnetomechanical manipulator, the "left - right" motion (λ) is achieved by swinging the arm relative to the axis of the horizontal tube.

The gripping motion of the magnetomechanical manipulator is transmitted from the operator's arm

to the jaws of the detachable tool through the control levers, the bevel gearing, the telescopic tubes, the bands, the magnetic coupling, and the telescopic tubes and bevel gearing of the slave unit.

The rotation and flexing motion of the hand is transmitted to the tool through the bevel differential, the telescopic tubes, the bands, two magnetic couplings, and the telescopic tubes and bevel differential of the slave unit. The rotation of the hand causes rotation of the couplings to one side, and the flexing of the hand causes rotation of the couplings to different sides.

The rotation of the tube around the vertical axis is transmitted through the bands to the couplings, and from them to the vertical tube of the slave unit. The "up - down" motion is transmitted by the band to the magnetic coupling, and from it through the bevel gearing and band to the slave arm. The movable tubes are counterbalanced.

The "forward - back" motion is transmitted from the control unit, which moves along the upper bridge, through the rods to the magnetic couplings, which attract the slave arm, which is held beneath the overhead of the service volume by the attractive force of the magnetic half-couplings. The lower bridge supports the slave unit when the magnetic couplings are overloaded. The "left-right" motion is transmitted by the movement of the upper bridge along the service volume.

The design of the manipulator is such that it can be disassembled without loss of airtightness of the volume on the operator's side. The control unit can be disassembled in the operator's zone, and the slave unit in the repair zone. The manipulator is fitted with motion stops installed on the control unit (except for the two horizontal motions). /115

The material of the control unit is aluminum alloys and carbon steels, and the material of the slave unit is acid-resisting steels and titanium alloys. It is desirable to make the partition - ceiling of a single sheet of mark Kh18N10T stainless steel, but the manipulator worked well with a butt-welded partition. The thickness of the partition is three millimeters.

The design of the magnetomechanical manipulator is such that it can be moved horizontally to any point in the service area. This quality significantly

decreases the number of manipulators needed to service a long volume, because the magnitude of the "left-right" travel is limited by the length of the volume. For example, four to five nonairtight mechanical manipulator arms are required to service a volume four meters long, but one or two arms are sufficient when magnetomechanical manipulators are used.

Manipulators tests showed the design to be efficient enough to be used in an airtight insulated volume.

The results of the measurements made of the forces during motion in all degrees of mobility are tabulated below. The table also lists, for comparison, the forces on the control handle of the mechanical manipulator shown structurally in Figure 2b. A comparison may be very relative because the mechanical manipulator has a higher load rating, and a somewhat different motion arrangement and design. Cable (light and low-inertia) transmissions are used for transmission for the most part.

An examination of the results of the measurements shows that the forces on the control handle of the magnetomechanical manipulator are of the same order of magnitude as forces of the mechanical one. The exception is the "up-down" force, which is greater in the magnetomechanical manipulator. This is explained by the fact that sliding friction couples (bushing - shaft and key - keyway) are used to transmit vertical motion. Apparently, it is desirable to install /116 rolling couples instead of sliding couples, something that will increase the diameter of the vertical tubes somewhat. Greater gripping force to full compression in the mechanical manipulator is caused by the action of the return spring.

Magnetomechanical Transmissions

A physical representation of a synchronous magnetomechanical transmission used for all types of manipulator motion except hand flexing and rotation can be made in the form of an elastic transmission with inertial masses as shown in Figure 3. The synchronous transmission can transmit rotation in any direction, and the moments the shafts apply to each other can be perceived at each. The synchronous transmission here examined operates on the basis of a zero-order synchronizing moment, that is, when the half-couplings match the moment is zero. Mismatch of the shafts by angle φ occurs when the moment applied by the

TABLE

Motion	Unit of measurement	Magnetomechanical manipulator		Mechanical manipulator		
		idle	load 3 kgf	idle	load 8 kgf	load 15 kgf
Gripping to full compression	kgf	0.3	-	3	-	-
Rotation of hand	kgf·cm	3.6	30	7.5	225	-
Flexing of hand	kgf.cm	14	140	15	225	-
Rotation of vertical tube	kgf.cm	5	6	7.5	82.5	-
"Up-down"	kgf	5	12	3	-	25
"Forward-back"	kgf	1.5	1.5	2.5	-	5
"Left-right" (swing through 45° angle)	kgf	1.5	1.5	0.5	2	-

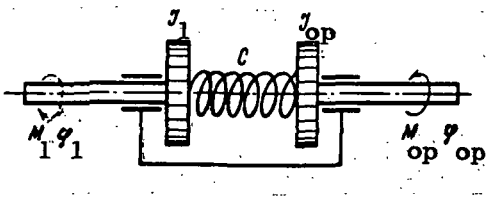

Figure 3.

operator, M_{op}, is equal to the load moment, M_l. Disregarding friction, moment $M_m = |M_{op}| = |M_l|$ acts on the coupling, and the system is in equilibrium. The magnitude of the mismatch determines the precision with which a given load moment is transmitted. Figure 4 shows the angle of the mismatch between the magnetic half-couplings as a function of the moment generated by the magnetomechanical manipulator coupling in the static state. The gap between the half-couplings is six millimeters. The lower part of the curve may be replaced by a straight line with insignificant error. This curve can be used to calculate the magnitude of normalized coupling stiffness, C_n, otherwise called the specific synchronizing moment, $C_n = M_{mw}/\varphi_{mw}$, where $M_{mw} \approx 0.75\ M_{ms}$ • M_{mw} is the maximum working moment acting at the coupling. M_{ms} is the maximum static moment transmitted by the coupling; φ_{mw} is the angle of mismatch, corresponding to the maximum working moment. /117

The couplings of a magnetomechanical manipulator have a quite high value of normalized stiffness for a 6 mm gap between half-couplings. It is equal to 370 kgf·cm/rad.

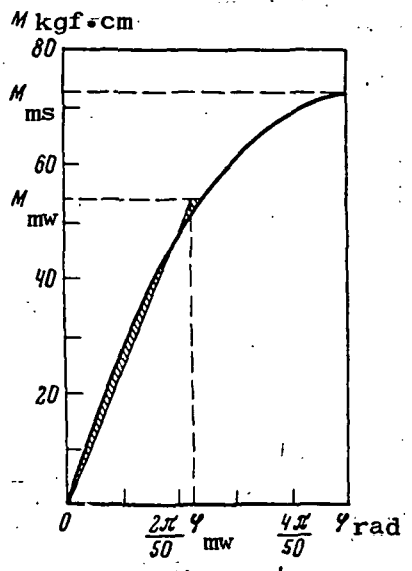

Figure 4.

The time lag in transmission was perceived in this manipulator design only when motions of tong jaws were abrupt. The angle of the mismatch was so small that it was practically imperceptible in operation.

A more complex magnetomechanical transmission was used in the drive for the other motions, hand rotations and flexing. Used here is a dual magnetomechanical differential, representation of which is in the form of an elastic transmission with inertial masses, as shown in Figure 5. The differential transmits two independent motions.

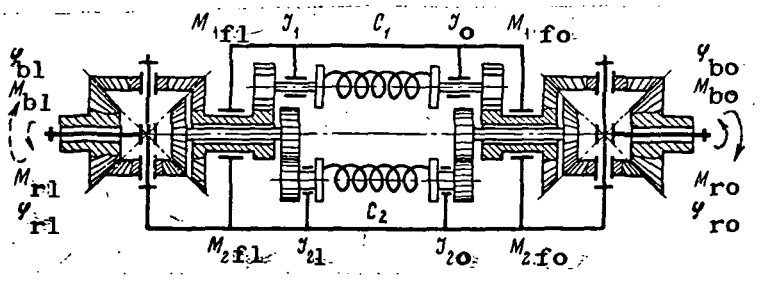

Figure 5.

The conditions for the differential for copying the motions are: (1) equality of stiffness of magnetic couplings $C_1 = C_2$; (2) equality of moments of friction at the shafts of the first and second branches of the transmission at the operator and load: $M_{1fo} = M_{2fo}$ and $M_{1fl} = M_{2fl}$; (3) equality of moments of inertia, normalized to the shafts of the half-couplings, for the first and second branches of the transmission at the operator and load: $I_{1op} = I_{2op}$ and $I_{11} = I_{21}$.

Violation of the first and second conditions causes dissociation of motion, that is, the tool experiences load rotational moment M_{rl}, which differs from the operator rotational moment, M_{ro}, when the hand is rotated by the operator

rotational moment, M_{ro}, and there is no flexing of the hand. In other words, the operator flexing moment, M_{fo}, equals zero, and the angular operator flexing rate, φ_{fo}, equals zero. Nor are the angular rotation rates φ_{rl} and the φ_{ro} equal. The tool receives an additional load flexing moment, M_{fl}, which differs from the operator flexing moment, and an angular load rate that differs from the angular operator rate. Violation of the third condition causes, dissociation of motion, but only for dynamic loads.

The transmission friction moments are determined by the general laws of machine mechanics. The bearing friction moments for the bearings supporting the end half-couplings are increased by the additional axial force of attraction of the magnetic half-couplings. Figure 6 is the attractive force curve for the half-couplings, F, in terms of different gaps, l_r, between them. /118

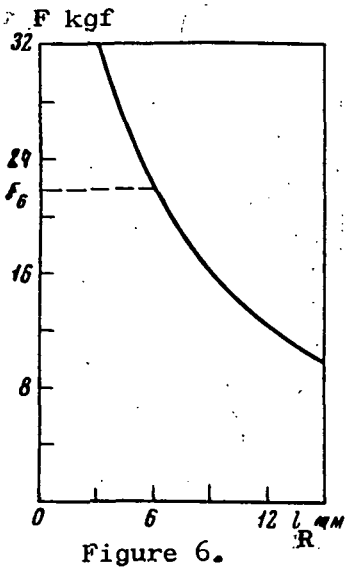

Figure 6.

The precision of magnetomechanical transmissions increases with increase in stiffness and a decrease in friction losses. Magnetomechanical transmissions of both types may begin to oscillate under periodic loads, or as a result of random dynamic action on the manipulator handle, or tool. High stiffness values for the couplings, and for the damping properties of the transmissions for the manipulator and the operator's arm, reduce the oscillation potential. System oscillations were not observed during tests of the magnetomechanical manipulator.

The maximum coupling working moments were chosen correctly. "Stripping" of the magnetic couplings did not occur under a 3 kgf load regardless of direction of movement.

REFERENCES

1. Artobolevskiy, I. I., Teoriya mekhanizmov [Theory of Mechanisms], "Nauka" Press, 1967.

2. Kobrinskiy, A. Ye., Stepanenko, Yu. A., "Some Problems of Manipulator Theory," V sb. Mekhanika mashin [In collection: Mechanics of Machines], No. 7-8, "Nauka" Press, 1967.

3. Kostin, N. F., "Manipulators with Permanent Magnet Couplings," V sb. Mekhanika mashin [In collection: Mechanics of Machines], No. 7-8, "Nauka" Press, 1967.

4. Belov, A. P., Vasin, G. P., Ovsyannikov, V. A., "An Airtight Manipulator," Patent No. 167124, Byulleten'izobreteniy, No. 24, 1964.

N73-26087

THE INFLUENCE OF MANIPULATOR KINEMATICS ON THE SELECTION OF THE GEOMETRIC PARAMETERS OF BOXES AND CHAMBERS

G. I. Lukishov, Yu. V. Miloserdin

ABSTRACT. The role working condition kinematics play in selecting the geometric parameters of boxes and chambers is discussed. Efficiency and cost factors are evaluated.

Boxes and chambers [1] used to work with radioactive materials are more massive objects which utilize manipulators for performing various technological processes from a distance. The most widely used types of manipulators at the present time are master-slave manipulators that use a mechanical coupling for the sword ("through-the-wall") and telescopic types, because they are cheaper, simpler, and more reliable in operation. /119

One of the important cost and engineering specifications is the capacity to perform technological operations in a minimum working volume while making maximum use of the capabilities of the installed manipulators when used with all-purpose boxes and chambers. This leads to the conclusion that decisive in the selection of the geometric parameters of boxes and chambers are the structural features and kinematic characteristics of manipulators.

Let us introduce the following criteria in order to make a comparative evaluation of the effectiveness with which manipulators and boxes (chambers) can be used: K_{mu} - the coefficient of manipulator use; K_s - the coefficient of service of the working volume of the box (chamber).

Let us examine the geometry of boxes and chambers under conditions when working with different types of manipulators by using the volume method of analysis in order to determine the magnitudes of K_{mu} and K_s.

There is a completely definable service zone for each type of manipulator consisting of a volume, each point in which can be reached by the tongs installed on the manipulator's slave part. However, when the manipulator is placed in a box (chamber) not all of the manipulator service zone (MSZ) can be used because basically the work is done in the horizontal plane of the table top and maximum service of the table top is a primary requirement. Let us, therefore, call that part of the MSZ which can be used for work the active part, and the

remainder the passive part of the MSZ.

Let us call the ratio of the volume of the MSZ active part, V_{am}, to the volume of the entire service zone, V_{sm}, the coefficient of manipulator use, K_{mu}.

Then

/120

$$K_{mu} = \frac{V_{am}}{V_{sm}}. \quad (1)$$

Two manipulators work in conjunction with each other at each operator position in the majority of cases, and if there are several such positions at the object being worked on there will be the corresponding number of pairs of manipulators. When two manipulators work together both MSZ intersect and there is an area in which it is possible for two manipulators to work. Let us call this area the joint service area, and let us call the ratio of the volume of the joint service area, V_{amj}, to the volume of the MSZ active zone, V_{am}, the coefficient of joint service, m; that is

$$m = V_{amj}/V_{am}. \quad (2)$$

It is, moreover, desirable to distinguish the areas of reduced load capacity and of limited viewability. Separation of these areas is what makes it possible to correctly position the equipment and attachments when organizing production work. The joint service area should be clear of fixed equipment, and the more complicated jobs, those requiring the use of the tongs of both slave parts of the manipulators, should be done here. But it must be remembered that when working with several manipulators the summed active part of the service zone will be reduced with increase in the joint service area, that is

$$V_{am} = \sum_{i=1}^{n} v_{iam} - \sum_{i=1}^{n-1} v_{iamj}, \quad (3)$$

where

n is the number of manipulators installed;

v_{am} and v_{amj} are the active part of the MSZ and the joint service area for one manipulator.

This expression takes the form

(4)

when manipulators of the same type are used in the same installation at the object being worked on.

Manipulators with manual control can be used only if visual observation is possible. This is why the design and quality of the observation system installed at the object being worked on has a definite influence on the efficiency with which manipulators are used.

Windows made of a set of lead glasses [2] are used as observation systems in boxes and chambers. There are two indices that can be used to evaluate the utility of window design; the coefficient of scannability of the work volume, P_v, and the coefficient of scannability of the table, P_t. These coefficients can be found from the following relationship;

$$P_v = V_s/V; \tag{5}$$

$$P_t = F_s/F, \tag{6}$$

where

V and V_s are the volume of the work space of the object being worked on, and the volume of that part of it scanned;

F and F_s are the area of the table top and the area of that part of it scanned.

Two types of scannability coefficients must be distinguished, however; the static, P_v^s and P_t^s, and dynamic, P_v^d and P_t^d. /121

The static scannability coefficients characterize the maximum viewability for the most advantageous placement of the operator's eye with respect to the window not associated with the process of working with the manipulator.

The dynamic coefficients characterize the viewability when the operator is working with the manipulators in all zones of their active use. If the static coefficients for each type of window and type of box (chamber) are constants, the dynamic coefficients will depend on the type of manipulator and their values will change with the position of the operator relative to the observation system when working with the manipulators. Hence the selection of the geometric dimensions of the window, and its installation at the operator's position for the object being worked on should be based on a study of the nature of the change in

the scannability of the work volume and the plane of the table top for different positions of the operator relative to the window. At the same time, the principal requirement should be assurance of scannability of the active part of the MSZ, particularly in the zone of the plane of the table top. But when one considers the limitation of observation window size, determined by the production capabilities of the manufacturer, as well as by the high cost, scannability of the whole of the active part of the MSZ becomes impossible when working in deep boxes and chambers. The result is to cause certain areas of the active part of the MSZ to become passive. Figure 1 shows diagrams of scanning the work volume of a chamber in the vertical plane.

Rays $O_1'O_1'$ - $O_2'O_2'$ determine the maximum viewability (nonsimultaneous) of the observation system, and rays $1_1'1_1'$ - $1_u'1_u'$ and $2_1'2_1'$ - $2_u'2_u'$ determine the viewability from operator positions 1 and 2 when working with the manipulator. Section aa of the table top becomes a passive part when working in position 2. /122

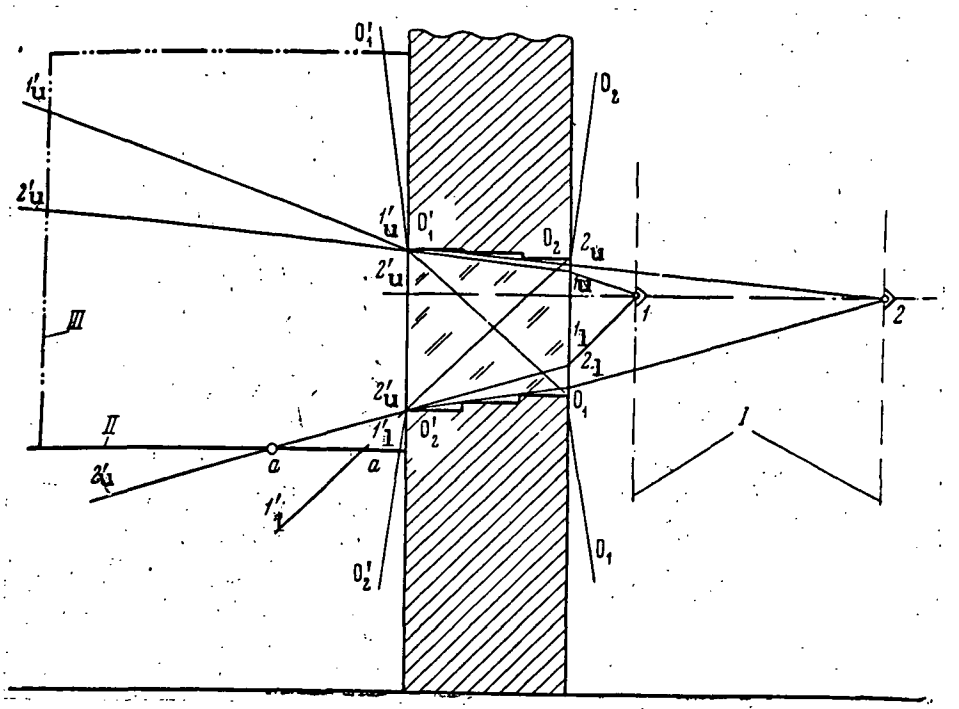

Figure 1. Diagrams of the view of the work volume of a chamber in the vertical plane. 1 - extreme operator working positions; II - table; III - limit of work volume.

Let us, in order to evaluate the scannability of the active part of the MSZ, introduce the criterion P_{am}, the coefficient of scannability of the active part of the MSZ, and which we can determine by using the following expression

(7)

where

V^{s}_{am} is the volume of the scanned active part of the MSZ when the manipulator is in use (can be determined by the boundary surface constructed for all parts of the work).

One can, upon taking the factor of scannability into consideration, establish what the scanned volume of the active part of the MSZ will be in the event of joint operation of several manipulators. The following expression can be used

$$V^{s}_{am} = \sum_{i=1}^{n} v_{iam} - \sum_{i=1}^{n-1} v_{iamj} - \sum_{i=1}^{n} (1 - P_{am})\, v_{iam} = \\ = \sum_{i=1}^{n} v_{iam} - \sum_{i=1}^{n-1} v_{iam} m_i - \sum_{i=1}^{n} v_{iam}(1 - P_{am}). \tag{8}$$

This expression takes the form

$$V^{s}_{am} = nv_{am} - (n-1)\, mv_{am} - n\,(1 - P_{am})v_{am} = \\ = (nP_{am} - nm + m)\, v_{am} = \left(P_{am} - m + \frac{m}{n}\right) v_{am} \tag{9}$$

when manipulators and observation systems of the same type are used in the same installation at the object being worked on. Thus, if the factor of scannability of the active part of the MSZ is taken into consideration, the coefficient of use of the manipulator at the object being worked on (in a box or chamber) will equal

$$K_{mu} = \frac{V^{s}_{am}}{V_{sm}}, \tag{10}$$

where

$$V_{sm} = \sum_{i=1}^{n} v_{ism}.$$

This expression takes the form

$$K_{mu} = \left(P_{am} - m + \frac{m}{n}\right) \cdot \frac{v_{am}}{v_{sm}}. \tag{11}$$

for the special case when manipulators and observation systems of the same type are used in the same installation at the object being worked on. The m/n ratio can be ignored when n > 4. This will yield an error of less than 10 percent. Then

$$K_{mu} \approx (P_{am} - m) \frac{v_{am}}{v_{sm}}. \quad (12)$$

The coefficient of service of the work volume should be maximum for each type of manipulator if efficient use is to be made of the work volume of the box or chamber. This is attempted when the geometric parameters of the box, or chamber, are selected. The coefficient of service of the work volume of the box (chamber), K_s, will be understood to mean the ratio of the scanned volume of the active part of the MSZ to the total volume of the work zone, V; that is

$$K_s = \frac{V_{am}^{s}}{V}. \quad (13)$$

Let us see how manipulator kinematics affect the magnitude of the coefficients /123 K_{mu} and K_s.

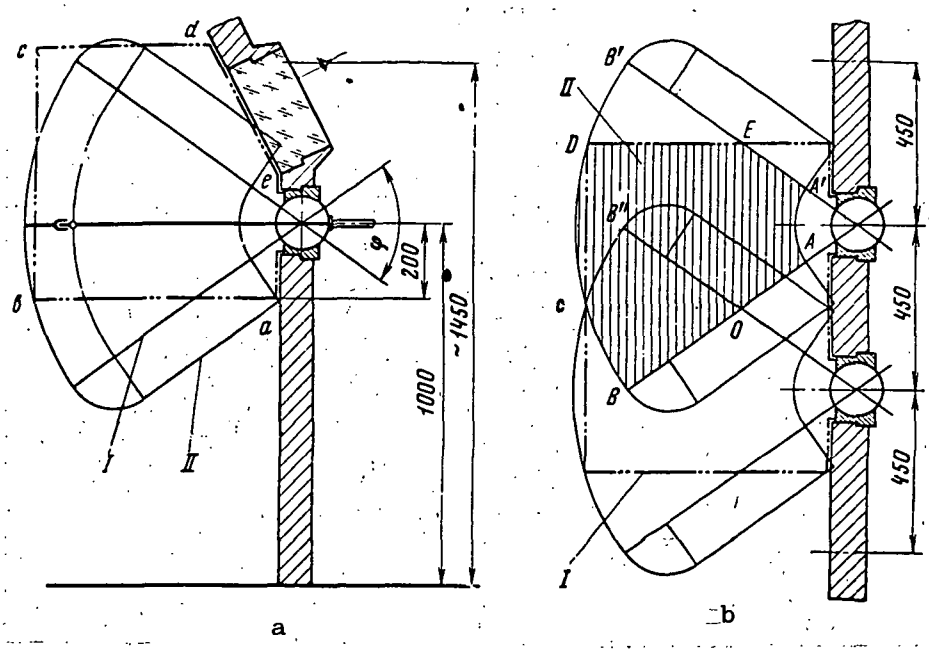

Figure 2. Diagram of an installation of sword manipulators. a - cross section: I - sword manipulator (SM) MSZ without hand link; II - with hand link; b - plan view: I - limit of optimum work zone for one work site; II - 30 mm active part (for one SM without hand link).

Figure 2 is a diagram of an installation of sword manipulators (SM) in a protective wall. SM are used only in boxes [3, 4] because of limited dimensions. Figure 2a gives the optimum dimensions for the height of the center of support for the SM, and for the table top, based on human anthropometric data. The observation window should be made using the principle of maximum closeness of the lower edge of the glass (particularly on the work zone side) to the table top level. Remember, however, that the best position of the eye when at work in the "standing" position is at a height of 1300-1450 mm. Figure 2b shows the mutual positioning of two manipulators in plan when working jointly.

The total service zone (v_{sm}) for an SM without a hand link is determined by the volume of the truncated spherical sector with solid angle φ, the bases of which are the spherical surfaces with center at the apex of the sector (in the center of the spherical support). See the axial section ABB'A'. The angle in the majority of SM designs is $\varphi = 70°$. The active part of the MSZ (v_{am}) and the area of joint service (v_{amj}) are determined by the volumes of the figures with sections ABCDEA' and OBCB" in plan. The MSZ is expanded substantially when SM with the same sword lengths are fitted with hand links.

Analysis of the kinematics of the SM reveals that the ratio of the length of the master part, l_m to that of the slave l_s changes constantly, and this results in a reduction in the forces and movements transmitted. The maximum value of the reduction factor should be $i = l_m/l_s \leq 4$. This is based on practical considerations (the limit of the force the operator exerts on the control lever should not exceed 5 kgf). The maximum service depth will equal 700 mm (sword travel = 500 mm) when the SM is installed in a protective wall with a maximum thickness of 200 mm. This corresponds, approximately, to the service depth with gloves in thin-walled boxes (Figure 3). /124

A comparison of SM and glove service areas leads to the conclusion that the geometric parameters of work volumes of glove boxes and boxes equipped with SM can be standardized and based on the above diagrams. The volume of the work area of a box with an SM is that of the volume of a figure with cross section abcde. But it should be noted that SM have good potentials ($K_{mu} \cong 0.8$) and a high service factor ($K_s \cong 0.9$), even when their design is comparatively simple. The joint service area is relatively small ($m \cong 0.25$), however.

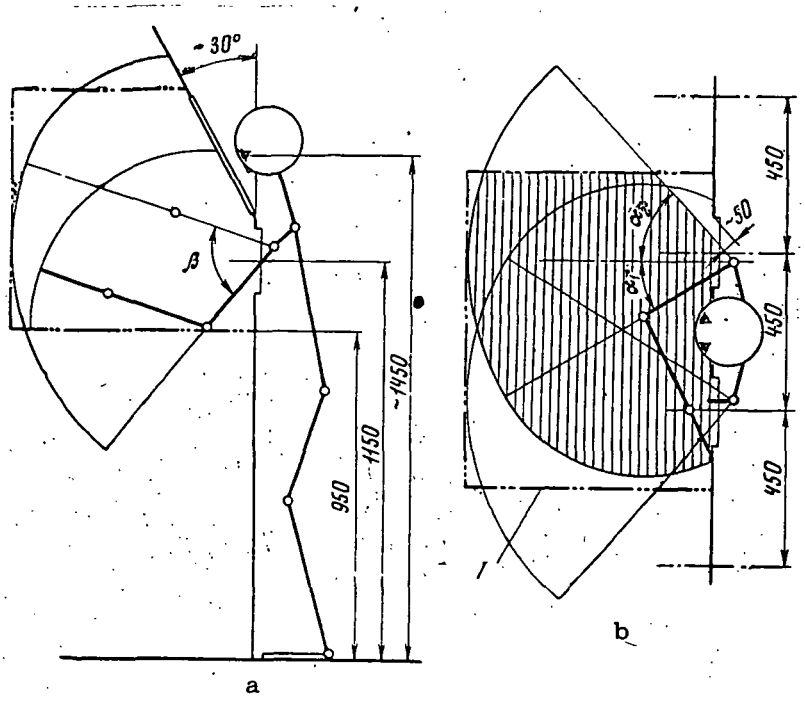

Figure 3. Service areas in a glove box. a - cross section; b - plan view; I - limit of optimum work area for one operator's position.

The work volume of the box must be studied from all operator positions in order to select the geometric dimensions of the observation window. The operator can, when the maximum travel of the sword in the support is 600 mm, work without leaving the front wall of the box, so the angle of view in the vertical plane remains virtually constant. But the angle of view in plan changes constantly. However, because of the reverse copying of movements when the sword is moved in the horizontal plane, the operator automatically assumes the most satisfactory position at the observation window in order to see the extremes of the area. It is therefore sufficient to provide scannability of the work volume under static conditions in order to provide normal scannability of that volume. Mandatory requirements for the installation of the observation system should be scannability of the box's table top and of the manipulator's active service zone.

The use of thick flint glass with a high index of refraction (n_D = 1.75) in observations windows makes it possible to scan almost the entire work volume of the box through windows with comparatively small inside dimensions. The optimum /125 window dimensions are readily determined by using graphic and analytical methods.

Figure 4 is the schematic diagram of an installation with a telescopic type mechanical master-slave manipulator (TM). Manipulators such as these [5] usually

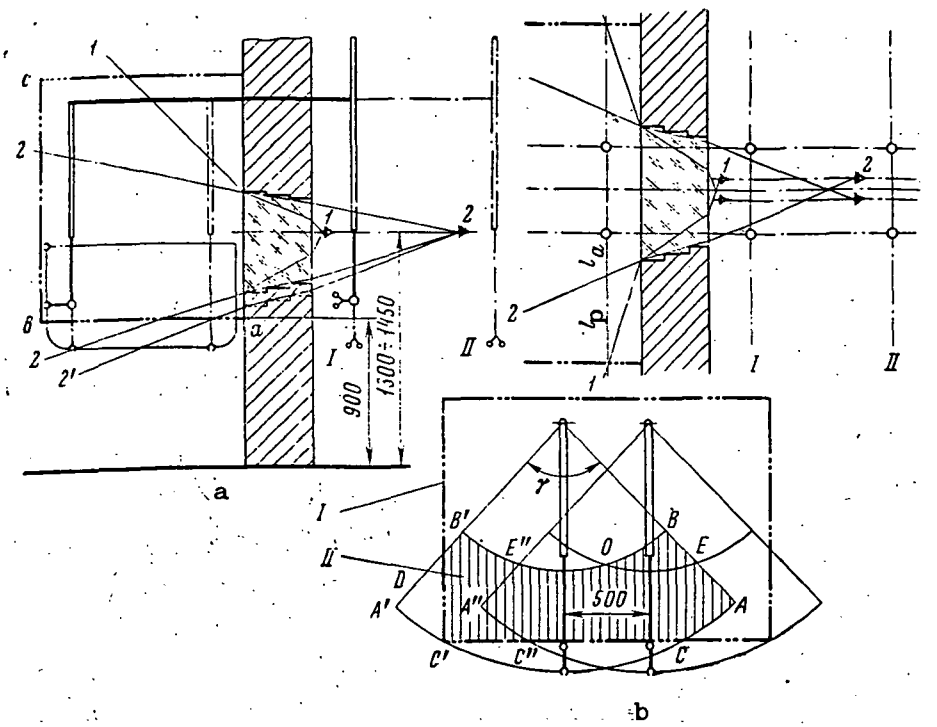

Figure 4. Schematic of the installation of telescopic type mechanical master-slave manipulators. a - cross section; b - plane view; I - limit of optimum chamber work zone; II - active part 30 M (for one manipulator).

are installed in chambers and in large boxes. The numerical values of the dimensions shown are determined from human anthropometric data. As may be seen, the TM service zone is determined by the vertical travel of the telescopic rod, and of the slave mechanism, by movement along the axis of the horizontal rod and its swinging angle. See section AA'B'B. The active part of the MSZ (v_{am}) and the area of joint service (v_{amj}) are determined by the volumes of figures with cross sections ACC'DB'B' and ACC"A"E"OE, respectively. The height at which the axis of the horizontal rod is placed must be chosen correctly in order to provide the most rational service for the chamber's work volume, while at the same time meeting the specification for maximum convenience in servicing the table top.

Each chamber operator's position usually is serviced by two manipulators. We obtain the work volume for the chamber (box) for one operator's position by tracing the boundaries of the manipulators along vertical planes to their intersection with the table top and introducing a ceiling plane near the horizontal rods. See the cross section abcd. Let us consider the viewing angle for different operator positions to determine the geometric dimensions of the

observation window, and the height at which it should be installed.

Figure 4 shows the viewing angle for two extreme operator positions, from which it will be seen that when the selection of the geometric dimensions of the window are incorrectly selected, and when its installation makes no sense, most of the volume of the active part of the MSZ will be passive (see sections l_a and l_p). This is why it is important that the active zone of the MSZ always be found in the scanned area. The optimum dimensions of the window can be determined here as well by the graphical-analytical method. /126

We can conclude as follows by evaluating the geometry of the work volume of the chamber (box) with a TM.

1. The work volume ($K_s \cong 0.25$) is used poorly when the MSZ ($K_{mu} \cong 0.9$) is used well. This latter can be explained by the high value of the unserviced part of the TM base plane (of the plane passing through the axes of the horizontal and vertical rods).

2. The absolute value of the volume of the active part of the MSZ is several times that for the SM.

3. The volume of the area of joint servicing is adequate ($m \cong 0.6$).

What follows from the foregoing is that determination of geometric parameters and chambers (including their observation systems) must be based on investigation of the kinematics of the manipulator under working conditions, attempting in the process to obtain the most advantageous values for the coefficients K_{mu} and K_s.

The evaluation of the efficiency with which the work volume of the box (chamber) is used still must take into consideration the area (beyond the limits V^s_{am}) used to install the technological and auxiliary equipment (V_{te}) and the location of the transportation facilities (V_{tf}). And the coefficient of utilization of the work volume of the box, or chamber, K_u, will be characterized by the ratio of the sum of all of the usefully used volumes, V_u, to the total work volume, V

$$K_u = \frac{V_u}{V} = \frac{V^s_{am}}{V} + \frac{V_{te}}{V} + \frac{V_{tf}}{V}. \qquad (14)$$

The cost estimate of the quality of design of the box (chamber) can be made by using the index of the cost per unit of used work volume

$$C = \frac{G}{V_u} = \frac{G_b + G_{te} + G_{tf}}{V_u}. \tag{15}$$

where

G_b is the cost of the box with standard equipment (manipulator, observation system, filters);

G_{te} and G_{tf} are the costs of the special technological equipment and transportation facilities.

The cost factor will be found from the following expression

$$C = \frac{G_b}{V_u} = \frac{G_{bh} + G_m + G_{oc} + G_f}{V_u} = C_{bh} + C_m + C_{oc} + C_f, \tag{16}$$

where

G_{bh}, G_m, G_{os}, G_f are the costs of the box housing, manipulators, observation system, and filters;

C_{bh}, C_m, C_{os}, C_f are the cost factors for the above indicated components of the box,

for all-purpose boxes and chambers in which special technological equipment and transportation facilities are not preinstalled, and where only standby volumes are envisaged (just in case of need).

A comparative estimate of the value of the cost factor for the different types of boxes should be made with respect to the glove box. The ratio of the cost factor for any box, C, to the cost factor for the glove box, C_0, and taken as the standard for comparison purpose, is called the relative cost factor q /127

$$q = \frac{C}{C_0}. \tag{17}$$

REFERENCES

1. Khimicheskiye protsessy i oborudovaniye [Chemical Processes and Equipment], IL, 1956.

2. Lukishov, G. I., Chelyuk, O. K., "A New Design for Heavy Series Radiation Windows," Atomnaya energiya, 20, No. 1, 1966.

3. Lukishov, G. I., Smirnov, V. P., Rodionov, K. D., "The MSh-P-5 Stepping Manipulator," Atomnaya energiya, 21, No. 2, 1966.

4. Lukishov, G. I., Rodionov, K. D., Shcherbenok, G. U., "A Chain of Radiation Boxes for Working With γ-Active Materials," Atomnaya energiya, 22, No. 2, 1967.

5. Logunov, M. M., "Principles of an Installation of General-Purpose Mechanical Master-Slave Manipulators," V sb. Mekhanika mashin [In collection: Mechanics of Machines], No. 7-8, "Nauka" Press, 1967.

N73-26088

PRINCIPLES OF THE CURTAILMENT OF SOURCES OF COMMAND SIGNALS IN MULTIFUNCTIONAL BIOELECTRIC CONTROL SYSTEMS

Ye. P. Polyan, A. Yu. Shneyder, E. I. Plamm

ABSTRACT. Bioelectric control systems for several slave mechansims using a single muscle are discussed.

Motor, as well as bioelectric, components are of practical interest for use /128 as control signals in the man-machine system, because they reflect the degree of muscular tension and, in the final analysis, characterize the motor components of motion. Bioelectric control systems (BECS) can be used for this purpose, and in fact are used today in different branches of medicine and engineering [1-3].

The simplest form of a BECS can be realized when the signal source is just one muscle (a single-channel control system).

In fact, however, a greater number of control muscles is required to control devices that functionally resemble the motions of the individual parts, or the entire extremity, of man. A two-channel control system, in which each muscle would control the corresponding direction of motion of a reversible slave mechanism (SM), is needed, for example, to control the closing and opening of the fingers of an artificial hand, the pronation and supination of the hand, the flexion and extension of the forearm in the elbow joint, and other movements of the prosthetic device. This is where proportional and relay control principles have found application [4, 5].

But one degree of freedom is not enough to carry out the most widely used functions. The system must be given greater functionality by introducing additional pairs of controlled movements. And this gives rise to the task of making a rational selection of the control system design, the timeliness of which will constantly improve by virtue of the increase in functionality. This is where the different principles involved in the building of bioelectric control systems can find their application.

The principle most widely used in the building of a BECS is that in which each pair of muscles controls its own SM, regardless of the condition of the other muscles, and yet has no influence of the operation of the other SM. Systems

such as these provide control of all movements simultaneously, in sequence, or in any combinations. Systems such as these can be called independently (simultaneously) controlled bioelectric systems. But the number of channels will increase in proportion to the increase in the number of movements controlled, and the control system will become unwieldy. /129

Information can be transmitted from several sources over one channel by using a variety of coding methods; frequency, or time, for example. Coding in terms of the level, or shape, of the control signals is virtually impossible without the use of special, complicated converters, so amplitude and frequency curves for the biopotentials of the different muscles are commensurate [6-9].

The use of systems with independent control creates additional problems with respect to the selection and training of several independently contracting muscles, the number of which in a healthy extremity, to say nothing of an amputated, or paralyzed one, is limited. And if, in addition, one takes into consideration the technical difficulties associated with system unwieldiness, as well as some of the biomechanical peculiarities of motor acts, a whole series of which are performed in a time sequence, rather than simultaneously, one can conclude that the use of systems with independent control is not always desirable.

We can, by using a variety of coding methods, reduce the number of channels, as well as the number of control signal sources (muscles), without reducing the number of SM. Systems such as these, which provide what is basically sequential control of SM, can be called dependent sequential control systems. Here the required movement cannot be controlled until the corresponding SM is connected into the system. This requires the insertion of logic switches (LS) controlled by special commands. These are switching commands, as distinguished from SM control signals, but they can be transmitted over the same channels that carry the SM control signals, or over special channels.

The fact that the operator has broad scope in changing amplitude, time, and speed parameters of the biopotentials as he desires make it possible to use a wide variety of coding methods. A switching code in terms of one of the biopotential parameters noted is a parametric code (amplitude, speed, for example). An amplitude code can be discrete, and continuous, with switching in the former

the result of discrete contraction of the muscle, and in the latter the result of a continuous signal supply. A discrete code controls an LS with two and more stable states, or an LS with one stable state and a time relay. The control and switching signals will differ on the time line. This requires additional switching time.

A continuous code controls an LS with one, and more stable states. Here the switching of the corresponding SM takes place only while the continuous signal is being supplied. Consequently, there will be no difference on the time line if the switching and control signals are transmitted over a common channel.

Combination codes, which are a temporal combination of parametric codes for the signals from one muscle (a Morse-type code), or a combination of parametric codes for signals from different muscles, are possible and differ from the parametric code that uses single signals.

It is desirable to try to use a universal control system, one like the central nervous system, to control rather complicated technical devices and, in particular, to use the program developed by the central nervous system for controlling motor actions. These programs can be selected with the help of the biopotentials occurring in the muscles. This principle can be characterized by selecting a "bioelectric image" the use of which will result in the control signals determining the instantaneous conditions of a series of muscles taking part in natural movements (see the classification diagram). /130

Let us consider the very simple method for controlling a reversible SM by signals from but one muscle. Muscles perform two functions in this case, control and switching.

A system with relay control and amplitude selection of the command signal is an example of a system with a parametric switching code without time separation of the control and switching signals, and is one in widespread use today. Figure 1 is the block diagram. Signal voltage is amplified by amplifier 1 and fed into integrator 2, then to the level decoder 3. The signal then is fed into the corresponding power amplifier, 4 or 4', depending on signal amplitude. The loads are electromagnet relays. Relay operation (R_1 or R_2) connects the electric motor

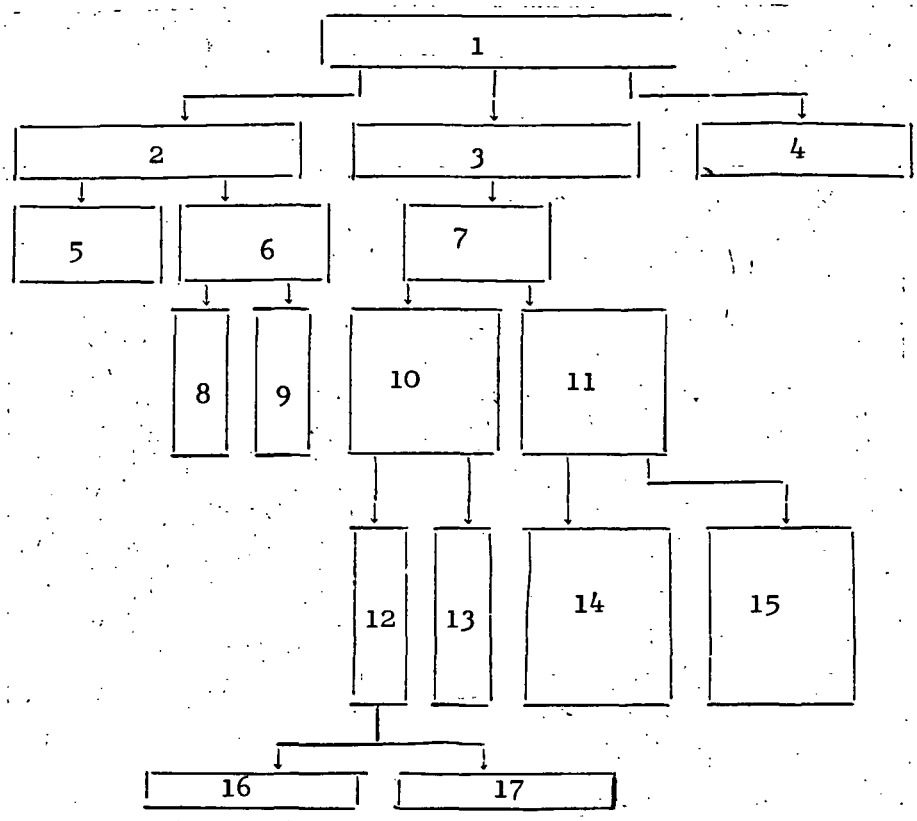

Key: 1 - Bioelectric control system (BECS); 2 - independent (simultaneous) control; 3 - dependent (sequential) control; 4 - bioelectric image; 5 - without communication channel consolidation; 6 - with communication channel consolidation; 7 - switching codes; 8 - frequency; 9 - time; 10 - parametric; 11 - combination; 12 - amplitude; 13 - speed; 14 - combination of parametric codes for 1st muscle; 15 - combination of parametric codes for different muscles; 16 - discrete; 17 - continuous.

to the supply with the required polarity. Other countries are developing similar control systems, Scott in Canada [13], and Trombly et al. in the USA [14].

The command signal amplitude selection principle has spread to proportional continuous and pulse systems [10-12].

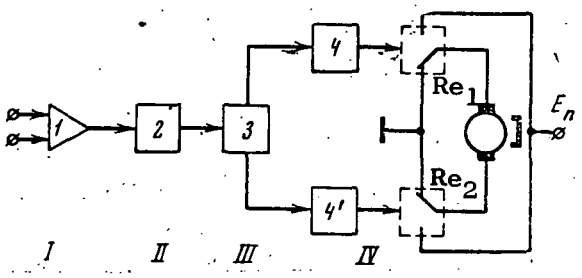

Figure 1. Block diagram of a relay control system with command signal amplitude selection. I - biopotential amplifier; II - integrator; III - level decoder; IV - power amplifier.

The amplitude code system without control and switching signal separation requires no additional switching time, but the dynamic regulation range (in the case of the proportional system) is much contracted.

The control system using signals from one muscle can use an amplitude,

as well as a speed, code without time separation of control and switching signals. This will be a proportional-relay system. The system will regulate the /131 speed so it is proportional to the input signal for one direction of rotation of the SM, but only relay control will be exercised for rotation in the other direction.

The use of a parametric code (amplitude or speed) with time separation of the control and switching signals sometimes is desirable. Time separation in this system permits the use of the full dynamic range of the input signal to regulate speed in each of the directions of SM movement.

Figure 2 is the schematic diagram of a proportional system using a speed code with time separation of control and switching signals.

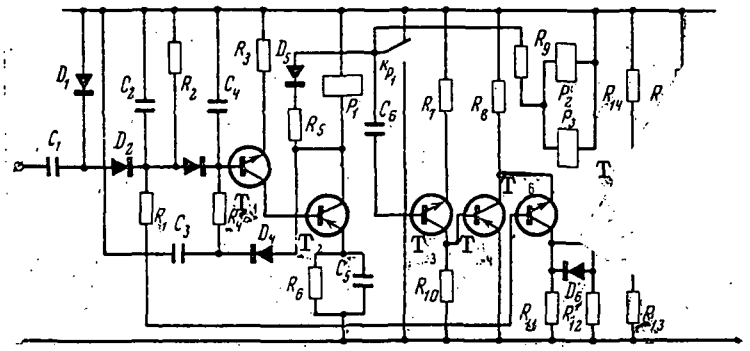

Figure 2. Schematic diagram of a proportional system with a speed switching code.

The biosignal for controlling an SM in one direction is amplitude amplified by a preamplifier, and then fed into an integrator (C_1, C_2, D_1, D_2, R_2), controlling a multivibrator (transistors T5, T6, T7). The pulses, now amplified in power (T8), are supplied to the SM motor.

The operator, in order to switch motor windings, sharply contracts his muscle and thus supplies a single signal which is amplified by a current amplifier (transistors T1, T2), connected in turn to a speed decoder (resistor R_6, capacitor C_5) and causes relay Re_1 to function. Switching of the movable contact of relay Re_1 from the supply minus to plus has the following result.

1. Relay Re_1 must be blocked (by diode D_5 and resistor R_5) in order to hold /132 the relay in the working condition while the control signal changes from the response threshold to the maximum (that is, to the level providing maximum slave

mechanism speed of movement).

2. Relays Re_2 and Re_3 operate. Their movable contacts change the polarity with which the electric motor is connected to the control channel output.

3. The sharp voltage drop across resistor R_8 delays the multivibrator for from 0.5 to 1 second (by the time required for capacitor C_6 to discharge through the circuit of transistors T3 and T4). This is done to avoid any sudden, involuntary movement of the slave mechanism.

4. Relay Re_1 becomes operative through D_5, R_5, and D_4 of the time delay network (C_3, R_4) when there is no control signal. This network is required because of the delay in operator reaction.

Change in control signal amplitude in the range of say 20 to 100 μV thus will result in a proportional change in the speed at which the slave mechanism will move in a straight line. A single sharp contraction of the muscle will cause the electric motor to switch. The switching cell delay time is 0.5 to 1 second. The operator should begin to exercise control in this period of time. He can exercise control upon entering the zone equal to, or exceeding the multivibrator response threshold (20 μV). Should the operator fail to begin control in this period of time the system will automatically return to its original state; that is, to the state of readiness to control movement in a straight line. The operator, upon finding it necessary to reverse the movement at once and at high speed, keeps the muscle in the tensed state for from 0.5 go 1 second after sending a switching signal and then begins to exercise control once again.

If the switching systems just described use a single parametric code, one based on either amplitude or speed, the combination of parametric codes is a combination code that can be used to control a great many SM by using the signals from one muscle. An amplitude code can be used, for example, to control the reverse operation of the SM, while the speed code can be used to connect one of two SM to the system. At the same time (a) the control and switching signals can be separated on the time line, in which case the control system can be of the relay type, or of the proportional type, with a full dynamic range, (b) some of the control and switching commands can be separated, a speed code, and some not separated on the time line, an amplitude code, in which case the control system can be of the relay type, or of the proportional type,

with a reduced dynamic range, or (c) if all control and switching commands are not separated on the time line we can have a relay type, or a proportional-relay type control system for three movements: two proportional with a narrowed dynamic range, amplitude code, and one relay using a speed code.

Signals generated by one muscle can be used to control a great many SM when amplitude and speed codes are used. Here the switching signal for selecting and connecting the needed SM is supplied by the corresponding number of brief pulse trains, a speed code. An amplitude code is used to reverse the SM.

A speed code, or an amplitude code, may be used to connect the needed SM to the control system.

A nonresponse zone must be built into the system when switching is done by the same code used for control purposes. In this case the system is converted /133
to the mode for selecting the needed SM, to the nonresponsive zone, by supplying a signal, say a high-amplitude one. Once this is done the SM can be selected by a train of discrete signals of the same or different widths and amplitudes, or combinations of them. There are two ways the system can be converted to the control mode. One is automatic, upon lapse of a predetermined period of time, the other is to use a second train of high-amplitude signals. The switch should have one stable state for the former, two and more for the latter.

The bioelectric control systems discussed above for controlling several SM from one muscle use different types of switches, controlled from the same muscle, or by the same channel, than those used to control the SM. There are many cases, however, when the switches can be controlled from another muscle over an autonomous channel.

The switch can, for example, connect one of four SM by making amplitude selection of the command signal. The switch will have, for this purpose, a level damper and two electronic switches, one for the high, the other for the low, level. The switching cell will connect the corresponding SM depending on the combination of conditions of the latter.

System operation is as follows (wiring diagram Figure 3a). An electromiographic signal is supplied from the preamplifier to the envelope separation unit (diodes D_1, D_2, capacitors C_2, C_3, resistors, R_1, R_3), then to the level

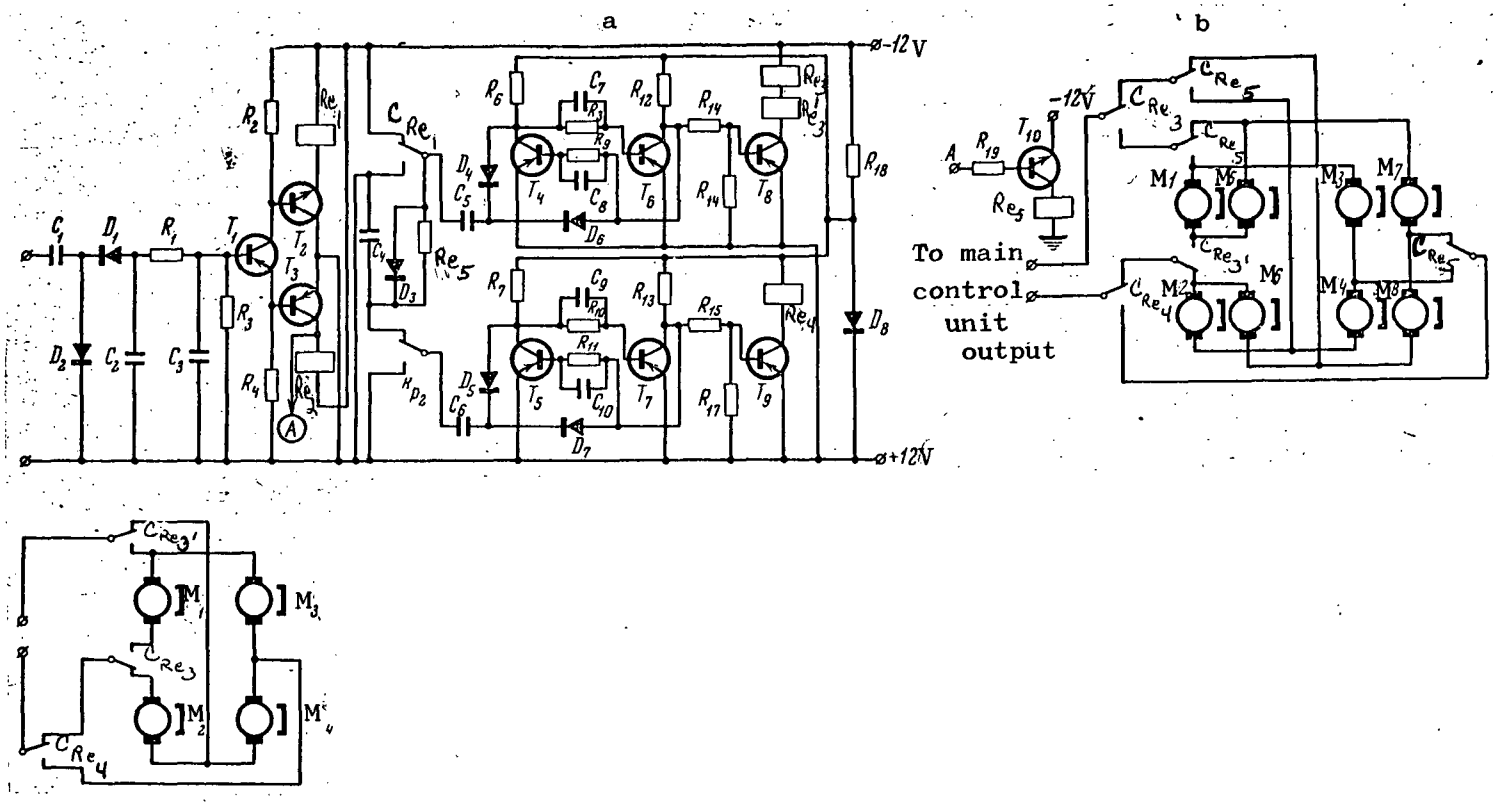

Figure 3. Switch wiring diagrams. a - four outputs; b - wiring diagram of a switch with eight outputs.

damper input (transistors T1-T3), the output stages of which are loaded respectively by two relays, Re_1 and Re_2.

A 0.5 V signal at the input causes relay Re_2 to operate, and both relays will operate when signal strength is 1 V. Operation of one, or both relays converts one, or both electron switches (symmetrical triggers with collector trigger) to the other stable state accordingly. The trigger controlled by the high level of the signal consists of transistors T4 and T6, that controlled by the low level of the signal of transistors T5 and T7. Relays Re_3, Re_3', and Re_4 are connected to the control channels of one of four SM, depending on the combination of trigger states. An interlock (C_4, D_3 and R_5) prevents the low level switch from operating when a high-amplitude signal is supplied.

A comparatively simple device, added to the above-described system, increases its functional potentials. Added to the system for this purpose is a switch with one unstable state (Figure 3b). This switch uses the same control channel (one muscle) but provides selective switching of twice as many reversible SM, as many as eight.

One of four SM (M_1 - M_4) in the first group can be connected to the control channels in a manner similar to that described. One of the four mechanisms in the second group (M_5 - M_8) can be switched, depending on the combination of stable states of the switches, when there is a control signal below the level of the first threshold (the operating threshold for relay Re_2) because this causes relay Re_5, with three groups of switching contacts, to operate. Relay Re_5 is connected to the collector circuit of transistor T10, supplied with a positive potential from the collector of transistor T3 (point A in Figure 3a).

Adding one unstable state to the switch permits the operator to obtain information on whether or not a slave mechanism in the first, or second, group /135 is connected to the output of the main control channels at a particular moment, regardless of whether or not a control signal is present.

The switch can be a device with two unstable states, in which case the amplitude selection principle can be used to control the switch. One SM can be connected to the system when there is no control signal, a second when the magnitude of the control signal is small, and a third when the magnitude is great. This system also provides the operator with information on which SM is connected to the control system.

We have, here, reviewed certain realization of a BECS with signals from one muscle. Even this quick review shows the variety of possible approaches to building systems for sequential control of several SM. The introduction into the system of even one source of biosignals can change SM control significantly, and what is even more important, qualitatively. Increasing the number of sequentially connected SM results in simultaneous control. So if there are two sources of control signals, the functions of SM control (C) and of switches (S) can be distributed between them in different ways:

TABLE

Variant	1	2	3	4	5	6
First muscle	C	C	C	S	S,S	S
Second muscle	C	S	C,S	C,S	C,S	S

Variant 1 is the simplest case: two muscles control one reversible SM. This is the most widely used practical approach to the bioelectric control method of building systems.

In variant 2 one muscle can only control the SM; the other is connected to the control system of the corresponding SM. One of the methods described above for switching with signals from one muscle can be used for this purpose. And switching can be accomplished at the same time as the SM control process is carried out.

The coding methods described above are quite varied, so the ways in which it is possible to realize them too are quite varied. It is preferable to use a conventional control system, that controlling two movements with two muscles, when but one SM is controlled. When one of the muscles has limited control capabilities (rapid fatigue, activeness low, dynamic range narrow), separation of control and switching between muscles can be desirable.

Variant 3 can be looked at in two ways:

(a) another control channel can be added to the system, one that uses control and switching by one muscle (the one reviewed above). The number of controlled movements now is increased by one, instead of two there are three, instead of four there are five, and so on. So the use of yet another source of signals is irrational. The system now has an additional channel, but system functionality has not, in essence, been increased. However, the possibility

of its use in certain cases cannot be excluded;

(b) we have a two muscle control system, and one muscle, in addition to control, performs the additional function of switching the entire system. The number of controlled movements now is twice what it was in analogous variant 2 systems. In this case the switching muscle can only use discrete codes because the continuous signal from this muscle can be used to control the SM.

Variant 4 can be used when the switching signals can be used to select a program, and then supply the command required to execute the program, for example. /136

Variant 5 is a more modern version of a two-muscle control system in which both muscles control and switch. All the virtues of any switching code, and combinations of such codes, can be utilized fully in this system. The amplitude selection principle can be used to build two-channel control systems providing independent (simultaneous) control of two pairs of movements, or the sequential control of eight movements, for example, by using different combinations of signals from the two muscles.

Finally, the switches in variant 6, as distinguished from those in variants 4 and 5, can use all switching codes (see the classification diagram), including the progressive code.

Logic switches with one and two stable states are most widely used today to control two pairs of movements with signals from two muscles [15-17].

There are different ways that control and switching functions can be distributed between several sources of control signals (three and more) when such are available and when using one of the coding methods described above. The possibilities for building control systems are tremendous in scope. Fifteen SM can be connected, for example, by combining bioelectric commands generated by four muscles [18].

If the number of possible combinations of commands exceeds the required number of slave mechanisms the "surplus" command combinations can be used for the simultaneous (parallel) control of two, or of several, SM.

The methods and principal solutions discussed above, realized and investigated in experimental bioelectric systems for controlling a considerable number

of SM with a limited number of sources of control signals, indicate the variety of possible approaches to the building of similar control systems.

REFERENCES

1. Kobrinskiy, A. Ye., Breydo, M. G., Gurfinkel', V. S., et al., "Bioelectric Control System," Dokl. AN SSSR, 117, No. 1, 1957.

2. Kobrinskiy, A. Ye., "The Use of Biocurrents for Control Purposes," Izv. AN SSSR, Energetika i avtomatika, No. 3, 1959.

3. Kobrinskiy, A. Ye., Bolkhovitin, S. V., Voskoboynikov, L. M., et al., Problemy bioelektricheskogo upravleniya [Problems of Bioelectric Control], 1960.

4. Polyan, Ye. P., Yezhov, M. D., Shneyder, A. Yu., "Electronic Units for Multi-Functional Prosthetic Devices With Bioelectric Control," Protezirovaniye i protezostroyeniye, TsNIIPP, 14, No. 10, 1964.

5. Shneyder, A. Yu., Solov'yev, L. S., Polyan, Ye. P., "A Power Amplifier With a Pulse Converter for Controlling Bioelectric Prosthetic Devices," Protezirovaniye i protezostroyeniye, TsNIIPP, No. 19, 1968.

6. Hayes, K. J., "Wave Analysis of Tissue Noise and Muscles Action Potentials," Journal of Applied Physiology, 15, No. 4, 1960.

7. Slavutskiy, Ya. L., Smayl's, S. S., "The Frequency Curve of the Human Electromyogram," Protezirovaniye i protezostroyeniye, TsNIIPP, No. 20, 1968.

8. Scott, R. N., "Myoelectrical Energy Spectra," Medical and Biological Engineering, 5, No. 3, 1967.

9. Person, R. S., Mishin, L. N., "Autocorrelation and Cross-Correlation Analyses of the Electrical Activity of Muscles," Fiziologicheskiy zhurnal SSSR, 49, No. 9, 1963.

10. Polyan, Ye. P., Slavutskiy, Ya. L., Bernshteyn, V. M., Yakobson, Ya. S., "A Bioelectric Method of Controlling Mechanisms and Devices," Patent No. 182863, Byulleten' izobreteniy, No. 12, 1966.

11. Polyan, Ye. P., "Power Amplifiers for Units for Controlling Bioelectric Prosthetic Devices Using Amplitude Selection of the Command Signal," Protezirovaniye i protezostroyeniye, TsNIIPP, No. 19, 1968.

12. Slavutskiy, Ya. L., Gol'berg, I. S., Smayl's, S. S., et al., "Investigation of Amplitude Control of Bioelectric Prosthetic Devices," Protezirovaniye i protezostroyeniye, TsNIIPP, No. 19, 1968.

13. Dorcas, D. S., Scott, R. N., "A Three - State Myoelectric Control," Medical and Biological Engineering," 4, No. 4, 1966.

14. Trombly, C. A., Prenke, E., Long, Ch., "Myoelectrically Controlled Electric Torque Motor for the Flexor Hinge Hand Splint," Orthopedic and Prosthetic Appliance J., 21, No. 1, 1967.

15. Polyan, Ye. P., "A Device for Bioelectric Control, For Example, of Prosthetic Devices," Patent No. 163326, Byulleten' izobreteniy, No. 12, 1964.

16. Polyan, Ye. P., Prekhob'ko, A. A., "A Device for Switching Control of Mechanisms for Prosthetic Devices," Patent No. 193030, Byulleten' izobreteniy, No. 6, 1967.

17. Slavutskiy, Ya. L., Shirokova, Ye. A., Gol'berg, I. S., Smayl's, S. S., "Physiological Materials On the Bioelectric Control of Two Pairs of Movements of a Prosthetic Device Using the Biocurrents from One Pair of Muscles and Switching," Protezirovaniye i protezostroyeniye, TsNIIPP, No. 17, 1966.

18. Yakobson, Ya. S., Bernshteyn, V. M., Polyan, Ye. P., "Methods for Controlling Multifunctional Bioelectric Prosthetic Devices," Protezirovaniye i protezostroyeniye, TsNIIPP, No. X(XIV), 1964.

N73-26089

SYNCHRONISM AND HETEROCHRONISM OF SYNKINESIS IN MAN

I. P. Blokhin, A. B. Gandel'sman, G. S. Kan, A. M. Pokrovskiy

ABSTRACT. The potentials of arbitrary synchronization of synkinesis in man is studied, as are elementary flexing and extension single-joint movements of the different links in the body.

Interest in the anatomical structure and peculiarities in the functioning /138 of the links of the body can, today, be common to anatomists and physiologists, as well as to engineers, mathematicians, or designers.

Wide-ranging study of the functional peculiarities of the man-operator is very necessary in order to reach a complete determination of the potentials of man-machine systems, to optimize the relationship between human capabilities and the operational properties of the machine.

The terms "simultaneous and nonsimultaneous movements" are widely used in practice. This characteristic of movements is so strongly entrenched in the vocabulary that the question is raised of whether or not simultaneous, or synchronized, movements made by man at will seem, at first glance, to be artificial.

Investigation of the synchronization of synkinesis also is of theoretical interest in connection with the evaluation of the coordination potentials of human movements, because it reveals the peculiarities of controlling the different links in the human motor apparatus.

This investigation attempted to determine the possible degree of synchronization of the elementary, symmetrical, and unilateral movements made by the links in the human lower and upper extremities.

Investigation Procedure

The task posed for investigation while different parts of the body were moving was to perform synkinesis at any convenient tempo, with particular attention given to the simultaneity of closing of contacts at the end of each movement. Once preliminary tests were out of the way, we proceeded to carry out the assignment. A K-105 oscillograph was used to make graphic recordings of the

times of beginning, duration, and of contact individually for each link in the human body involved in synkinesis. The installation shown in Figure 1a was assembled for this purpose.

A movable contact, 1, was fastened to the links of the body completing synkinesis studied (see Figure 1). The number of such links usually was 2. Flexing-extending movements in the following joints were studied: talocrural, knee, hip of right and left leg, as well as the shoulder, elbow, radiocarpal and metacarpal-phalangeal joints of the right and left arms. /139

All experiments were divided up into several series, in each of which individual, special research tasks were carried out. An example of an oscillogram recording is shown in Figure 1b.

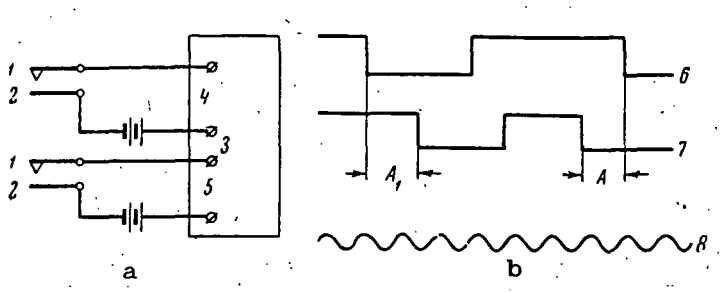

Figure 1. Diagram of an installation for recording the degrees of synchronism of synkinesis in man. a - block diagram of the installation; b - example of oscillogram recording; A and A_1 - intervals characterizing the heterochronism of synkinesis; 1 - movable contacts fastened to moving body links; 2 - fixed contacts; 3 - type K-105 oscillograph; 4 - 5 - inputs to channels I and II of the oscillograph; 6 - 7 - oscillograms from channels I and II; 8 - 0.002 second time marker.

The degree of synchronization of symmetrical synkinesis was investigated in the first series of experiments. Man, as we know, can be conditionally said to have two planes of symmetry; the vertical, or right-left side (YY_1), and the horizontal, or lower-upper (XX_1) (Figure 2). So the first series of experiments included investigation of the degree of synchronization of the right-left side movements: hand-hand (Aa), forearm-forearm (Bb), shoulder-shoulder (Cc). The mutually harmonious movements of the links of the lower extremities were studied correspondingly: foot-foot (A_1a_1), tibia-tibia (B_1b_1), and femur-femur (C_1c_1) (see Figure 2).

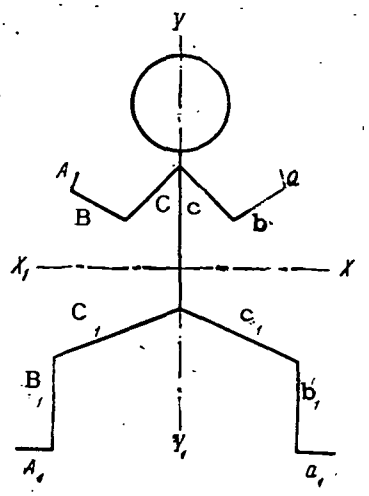

Figure 2. Diagram of the construction of the experiments to investigate the synchronism of synkinesis in man.

In this particular series, the degree of synchronization in the movements of symmetrical, that is, of the same, fingers of the right and left hands were investigated: thumb-thumb, index-index, middle-middle, ring-ring, little-little.

The second series of experiments involved the investigation of the degree of possible synchronization of movements located symmetrically with respect to XX_1; that is, of synkinesis of the lower and upper human extremities: hand-foot (AA_1), forearm-tibia (BB_1), and shoulder-femur (CC_1) (see Figure 2).

The third series studied asymmetrical synkinesis. The degree of possible synchronization of synkinesis of the fingers of one hand (the right) was studied. This series involved finger movements; thumb and index, thumb and middle, thumb and ring, thumb and little, index and middle, index and ring, index and little, middle and ring, middle and little, ring and little. /140

Used for the investigations were people leading active motor lives, many of them regular participants in sports.

The nature of the domestic, professional, and sports activities of the subjects was not associated with movements similar to those used in the experiments. The people who took part had right, as well as left, functional asymmetry.

No special attempt was made to include people with professional skills the nature of which included movements similar to those used in our experiments, machinists and pianists, for example.

Subjects ranged in age from 15 to 29, and included 27 men and women. We recorded 609 oscillograms of synkinesis. All data were processed statistically.

Results of the Investigations

First Series of Experiments

The results listed in Table 1 were obtained from the investigation of the degree of synchronism of right-left side synkinesis completed by the different

links in the upper and lower extremities.

TABLE 1. MAGNITUDE OF HETEROCHRONISM OF RIGHT-LEFT SIDE SYNKINESIS COMPLETED BY THE LINKS OF MAN'S UPPER AND LOWER EXTREMITIES (IN msec)

Body link	Right/ left	Hand-hand	Forearm-forearm	Shoulder-shoulder	Foot-foot	Tibia-tibia	Femur-femur
Statistical processing	$X \pm S_{\bar{x}}$	13.2±1.0	16.5±1.7	18.2±1.9	16.1±2.3	30.2±2.9	26.2±2.2

$\bar{X}$ - mean arithmetic; $aS_{\bar{X}}$ mean error.

The data listed in Table 1 tell us that the degree of heterochronism of movements completed by the links in the arms and legs is in the range from 13.2 to 30.2 msec. These figures characterize the magnitude of the heterochronism occurring when so-called simultaneous movements are made. Analysis of the data listed in Table 1 will show that movement made by the different links of the extremities are synchronized with different degrees of precision. In particular, the degree of synchronization of movements of the links of the arms is of higher degree than that for the movements of links of the legs. The degree of synchronization of movements of the links of the arms were recorded in the range from 13.2 to 18.2 msec, those for the movements of the links of the legs from 16.1 to 30.2 msec. These differences, expressed in mean magnitudes of heterochronism, are 15.9 msec for movements of the links of the arm, and 24.2 msec for links of the leg. This means that the precision with which links of the arm are synchronized is greater than the synchronization of movements made by the symmetrical links of the legs by a factor of more than 1.5. Further analysis of these data shows that the movements of the links of the right and left arms with respect to each other are synchronized with different degrees of precision, just as in the case of the links of the right and left legs. Greatest synchronization precision was observed during synkinesis of the right and left hands (13.2 ± 1.0 msec), and the least for movements of the right and left shoulders (18.2 ± 1.9 msec). Synchronization of the movements of the links of the right and left feet were (16.1 ± 2.3 msec). The least degree of synchronization was recorded for synkinesis of the right and left tibias (30.2 ± 2.9 msec). Differences such as these in the degree of synchronization are apparent in terms /141

of direction of shifts when evaluating the mean magnitudes, but are small in absolutes. Table 2 lists the reliability of the different mean arithmetic magnitudes of heterochronism of movements of the links of the right and left extremities.

TABLE 2. STATISTICAL RELIABILITY OF THE DIFFERENCES IN THE MAGNITUDES OF THE HETEROCHRONISM OF SYNKINESIS FOR THE LINKS OF MAN'S RIGHT AND LEFT EXTREMITIES

Hand-hand					
$p > 0,05$	Forearm-forearm				
$0,05 > p > 0,01$	$p > 0,05$	Shoulder-shoulder			
$p > 0,05$	$p > 0,05$	$p > 0,05$	Foot-foot		
$p < 0,001$	$p < 0,001$	$0,01 > p > 0,001$	$p < 0,001$	Tibia-tibia	
$p < 0,001$	$0,01 > p > 0,001$	$0,01 > p > 0,001$	$0,01 > p > 0,001$	$p > 0,05$	Femur-femur

p - level of significance of the differences in the mean arithmetic magnitudes (when $p < 0.05$, the differences are reliable).

The reliability of the quantitative differences taken from the table is determined at the point of intersection of the horizontal lines and the vertical columns, the captions for which correspond to the symmetrical body links studied.

Statistical processing resulted in determination of the reliability of the quantitative difference in a particular series of experiments and developed certain additional factors. In addition to the observed tendency to some deterioration in the indices for the synchronization of synkinesis of the distal and proximal links of the extremities, the absolute magnitudes of heterochronism of the movements of the right and left forearm and shoulder, and of the right and left femurs and tibias, are statistically unreliable ($p > 0.05$).

There is yet another fact that stands out clearly, telling us that the degree of arbitrary synchronization in the case of symmetrical movements of the right and left hands and of the right and left feet, is quite close for the two,

C3

despite the somewhat larger magnitude of heterochronism for foot movements (16.1 msec as compared to 13.1 msec), but this difference is statistically unreliable. One is led to believe that this fact is so because in real life man often runs into situations in which the need to synchronize the movements of these links of the extremities is sharply expressed. This would be the case, for example, when jumping, or kicking with the feet, or throwing with the arms. In cases such as these, just how precise will be the synchronization of the final movements of kicking with the feet, and of throwing a ball with the arms, will depend on the precision effect of the movement as a whole. Determining the links in the human body for which a greater or a lesser degree of synchronization is possible in synkinesis created the task of explaining whether or not a greater degree of synchronization would be possible for the movements of any parts of the body. This led to experiments in which synkinesis was carried out /142 for the same fingers of the right and left hands. It was assumed that the fingers of hands specialized in doing fine and coordinated complicated motor acts could be synchronized for arbitrary movements with a greater degree of precision than movements of other of the body's symmetrical links. Table 3 lists the results.

TABLE 3. MAGNITUDE OF HETEROCHRONISM OF RIGHT-LEFT SIDE SYNKINESIS PERFORMED SIMULTANEOUSLY BY FINGERS (msec)

Fingers	Right/left	Little-Little	Ring-Ring	Middle-Middle
Statistical processing	$\overline{X} \pm S_{\overline{X}}$	14,6±1,2	19,3±1,5	16,0±2,4

The data listed in this table show that the degree of arbitrary synchronization of synkinesis of the fingers is, on the whole, higher than in the case of movements made by other parts of the body. The magnitude of the heterochronism of movements of the fingers is much smaller than in the case of synkinesis of movements of the leg links. This comparison, in mean figures, is presented by the magnitudes 24.2 msec for symmetrical leg links and 14.9 msec for symmetrical fingers. A like comparison in mean magnitudes of the degree of heterochronism of the arm links and of the fingers shows 16.0 and 14.9 msec, respectively. But

of equal interest is the analyssis of the feasibility of synchronizing the movements of individual fingers. This comparison shows that the movements of the index fingers can be synchronized most precisely of all. The magnitude of the heterochronism is less in this case, 11.0 msec (see Table 3). Synchronism of the movements of the thumbs and little fingers of the right and left hands is not as good, with the heterochronism 13.8 and 14.6 msec, respectively. Most poorly synchronized in the experiments were the movements of the right and left ring fingers, where the heterochronism was 19.3 msec, that is, much higher than that observed during symmetrical movements of the links of arms and feet.

Statistical processing developed a group of fingers, the arbitrary synchronization of the movements of which is comparatively high. This group comprises the movements of the index, thumb, and little fingers. A second group includes the comparatively poorly synchronized movements of such of the fingers as the middle and ring. The difference in absolute magnitudes of the heterochronism of the movements between these groups is statistically reliable. Thus, movements of the index fingers of the right and left hands can be synchronized with even greater precision than can symmetrical movements of the hands.

Second Series of Experiments

The degree of synchronization of the synkinesis of the links of the right half of the body, symmetrical relative to the horizontal axis of symmetry (YY_1) was used. Synkinesis of the links of the upper and lower extremities, hand and foot, forearm and tibia, shoulder and femur, was performed for this purpose. Table 4 lists the results of these investigations. /143

TABLE 4. MAGNITUDE OF THE HETEROCHRONISM OF SYNKINESIS PERFORMED BY THE LINKS OF THE UPPER AND LOWER EXTREMITIES OF THE RIGHT HALF OF THE BODY (IN msec)

Body link	Arm-Leg	Hand-foot	Forearm-Tibia	Shoulder-Femur
Statistical processing	$\bar{X} \pm S_{\bar{X}}$	17,8±3,9	25,6±4,2	39,2±7,5

These data show that the degree of synchronization of the movements of the links of the upper and lower extremities is much worse than the right-left side movements. This is readily apparent from a comparison of the data in Tables 3 and 5.

The degree of synchronization of the movements in the large joints, symmetrical with respect to the vertical axis (YY_1), is in the range from 13.2 to 30.2 msec, whereas the degree of arbitrary synchronization for movements symmetrical with respect to the horizontal axis (XX_1) is in the range from 17.8 to 39.2 msec. The facts obviously are that conditions for coordination of simultaneous movements of the upper and lower extremities are more difficult. Attempts to determine if the upper or lower extremities largely lead the synkinesis of another link were futile. A link leading the synkinesis of some other part of body can be a lower, or an upper, extremity with equal probability. Analysis of the degree of synchronization of the different links of the upper and lower extremities permits the comment that movement of hand and foot can be synchronized with a higher degree of precision, and the movements of the shoulder and femur can be synchronized with least precision of all. The heterochronism is 17.8 to 39.2 msec, respectively. Statistical processing of the data confirmed this. The differences in the mean arithmetical magnitudes of heterochronism for hand-foot movements, and for shoulder-femur movements, are statistically reliable when $0.05 > p > 0.01$.

Thus synkinesis completed with respect to the horizontal axis of symmetry, that is, movements of the links of the upper and lower extremities, can be synchronized with less precision than movements symmetrical with respect to the vertical axis of symmetry.

Third Series of Experiments

Naturally, special interest is found in the possibility of synchronizing asymmetrical movements, particular the synkinesis of the fingers on one hand. This is in addition to the study of the degree to which it is possible to synchronize movements of symmetrical body links. The question was studied in a third series of experiments.

Table 5 lists the results. The data show that synkinesis of the fingers of one hand can be synchronized with greater precision that can all of the potential combinations of movements made by the other body links.

TABLE 5. MAGNITUDE OF HETEROCHRONISM OF SYNKINESIS COMPLETED BY THE DIFFERENT FINGERS (IN msec)

Little				
10,4±1,8	Ring			
19,2±1,4	6,1±0,9	Middle		
13,4±2,9	20,1±3,3	6,0±0,9	Index	
21,3±4,3	22,4±1,9	21,0±3,2	10,4±1,4	Thumb

The degree of heterochronism in the variants of finger movements studied can be as high as 6.0 and 6.1 msec (see Table 5), whereas the least magnitudes of heterochronism were 11.0 msec when the same symmetrical movements of the right and left fingers were synchronized. Analysis of the results of this series of experiments yields yet another peculiarity in the coordination of finger synkinesis. This is the best synchronization of the movements made by a series of finger positionings; movements of the little and ring, ring and middle, middle and index, and index and thumb, the degree of heterochronism of the movements of which was 10.4, 6.1, 6.0, and 10.4 msec, respectively (see Table 5). Characteristic too is the fact that the degree of possible synchronization continues to worsen with combinations of movements of fingers spaced further apart, by one, or by two fingers. The magnitudes of the heterochronism of the synkinesis of little and ring fingers, little and middle, little and index, and little and thumb were increased accordingly; 10.4, 19.2, 13.4, and 21.3 msec (see Table 5). Statistical processing of the data in this series made it possible to separate pairs of fingers, movements of which can be synchronized with maximum precision; middle-little, and middle-index. Movements of the ring-little, and index-thumb, can be synchronized with somewhat less precision. The differences in the magnitudes of the heterochronism of these pairs are statistically reliable. As a whole, the synchronization of the movements of a series of finger positions always is higher, is statistically reliable, and differs from the magnitudes of heterochronism of movements of fingers further apart.

/144

Discussion of Results

Discovering the potentials and limitations of the arbitrary coordination of movements of the links of the human body is a big problem, one that is not yet solved. Generally accepted is the fact that control functions in living organisms are performed in a manner that is very nearly perfect.

Study of the mechanisms and principles involved in the control of human motor apparatus is one of the real, promising, and practically necessary directions the research should take.

This paper has studied the potentials of arbitrary synchronization of synkinesis in man. The elementary flexing and extension single-joint movements of the different body links have been studied. Synchronism of the work of the symmetrical parts of the body had earlier drawn the attention of physiologists. L. N. Katz, in 1925 [1], noted the lack of synchronism of the /145 phase of contraction of the right and left auricles and the right and left ventricles of the heart. He established the fact that the active phase of the contraction of the muscle of the right and left heart does not begin and end at the same time. And the right half of the heart, the auricle and the ventricle, is involved by excitation 15 to 20 msec before the left. The data in [2, 4] are similar. Comparing these data with ours, it should be noted that in addition to the very close factual data on heterochronism, 6-35 msec in our experiments, and 15-20 msec in the research done by foreign authors, there is a principal difference in the facts compared. It is that the peculiarities of controlling the functioning of the right and left heart can be characterized by a unilateral upset in synchronism of function. One half of the heart always leads the other in terms of time. This phenomenon can be defined as a stable shift in phase in the functioning of these symmetrical parts of the heart. But in our investigations symmetrical synkinesis is heterchronous, with no definite temporal shift in the beginning of the contact of right or left, or lower or upper, parts of the human body. This means that upset in synchronism may occur with equal probability for the leading, or lagging, time of contact. This fact drew our attention even more because people with right-side as well as left-side functional asymmetry took part in the experiments. This means it can be thought that the anatomical factor, the different lengths of the conducting paths over which nerve impulses are propagated, is not the determinant for the exposure

of that link, right or left, lower or upper extremity, largely responsible for upsetting the synchronization of synkinesis.

The factual material in this paper allows one to talk of the impossibility of precise synchronization of arbitrary movements combined from two links. What this means is that all arbitrary synkinesis in man is heterochronous in the strict sense of the word.

This conclusion is quite apparanet from methodological positions. We can always find the magnitude of the asynchronism from the increase in the precision with which time intervals are recorded. Physiologically, this fact is of interest primarily because it permits the making of a quantitative determination of the minimum time intervals with which the arbitrary control of movements will become impossible for man. The rate of flow of the physiological processes providing for the perception and processing of current information, and the rate of flow of the control process, should be compatible. In other words, current correction of the movement is impossible.

It is natural to assume that difficulties in the synchronization of these movements will be determined by the precision of the differentiations of motor and other analyzers making corrections to the position of the body link in space, and not by the time factor, during synkinesis at very slow rates of displacement of the links. Practically speaking, the experimental materials obtained are significant in that they enabled us to determine those numerical boundaries of the magnitudes of heterochronism with respect to which arbitrary synkinesis can conditionally be broken down into simultaneous and time-different. This conditional breakdown is justified for practical purposes because the requirements with respect to the precision of synchronization of arbitrary movements can differ. But if we assume much more difficulty in carrying out the assignment when the requirements for precision in the synchronization of synkinesis are made more rigid, the goal can be reached only with some predetermined degree of probability that will be different for the different body links.

The physiological basis of heterochronism of synkinesis we observed is anatomically and functionally asymmetrical, and is shown conclusively in many papers; [5-7] and others. /146

It is desirable, in addition to this general factor, to distinguish three concrete factors which in turn can determine the greater or lesser magnitudes of the heterochronism of combined movements.

The first is the habit of the movement, that is, the frequency with which the movements of interest are repeated during work and domestic activities. The second factor is the difference in the precision of the spatial and temporal differentiations that take place in man in the course of realization of movements of the different body links. Given these positions, the fact of more precise synchronization of the movements of the arm links with each other as compared to the combination movements of the leg links, becomes clear. The upper extremities are specialized in performing finer work, from the standpoint of coordination. This principle can be explained by the high degree of precision in the synchronization of movements of the fingers as compared to movements of the arm links.

The third factor is spatial concentration; the closer the links of synkinesis are located with respect to each other, the higher the degree of synchronization. Drawing some analogy, we can say that the closer they are to the possibility of triggering and controlling these movements "from one pushbutton," the more precise the external effect of the movement. In this case the control problem is much simplified when the lengths of the paths traveled by the nerve impulses are comparatively the same. This is the case, for example, when providing a high degree of synchronization of the movements of the fingers on one hand located next to each other; middle and ring, middle and index. What this means is that a long length of the common nerve path traveled by the slave impulses provides more precise synchronization of movements. Given these positions, the fact of maximum heterochronism observed for combined movements of the leg links with those of the arms becomes more understandable. The presence of anatomically sharply differing lengths of paths carrying efferent nerve impulses determines the additional difficulties involved in controlling the synkinesis of the links in the upper and lower extremities.

Thus, these peculiarities of control of different links in the human body must be taken into consideration when organizing, and, naturally, when evaluating, the quality of the work done by the man-operator in those situations when he must control several processes taking place in parallel and

regulated by motor acts.

On the whole, this methodology for evaluating the coordination of the movements of the different body links can reveal the functionally more or less preparatory nerve connections between the centers for controlling the links of the motor acts.

Conclusions

1. Arbitrary combined movements of man are heterochronic. The degree of heterochronism differs for movements of different body links.

2. Synkinesis symmetrical relative to the vertical axis of symmetry can be synchronized more precisely than movements made with respect to the horizontal axis of symmetry.

3. Symmetrical synkinesis of the arm links can be synchronized with more precision that synkinesis of the leg links.

4. Symmetrical synkinesis of the links of man's upper and lower extremities /147 can be synchronized, but best is for the distal, worst for the proximal.

5. Synkinesis of the fingers can be synchronized more precisely than can the movements of other links of the extremities. At the same time, synchronization of synkinesis of the fingers of one hand is better than for movements of symmetrical, that is, the same, fingers of the right and left hands.

REFERENCES

1. Katz, L. N., Amer. J. Physiol., 72, No. 3, 1925, p. 655.

2. Wiggers, C., Physiology in Health and Disease, Philadelphia, 1945.

3. Braunwald, E., Fishman, A., Cournand, A., Circul. Res., 4, No. 1, 1956, p. 100.

4. Grible, P., Lind, J., Wegelius, C., Cordiologia, 33, No. 4, 1958, p. 293.

5. Starosta, V., Simmetrichnyye i asimmetrichnyye dvigatel'nyye funktsii v figurnom katanii na kon'kakh. Avtoref. diss. [Symmetrical and asymmetrical motor functions in Ice Figure Skaters. Summary of dissertion], Leningrad-Warsaw, 1963.

6. Il'in, Ye. P., "The Functional Asymmetry of the Legs," Teoriya i praktika fizicheskoy kul'tury, 1, 1963, p. 22.

7. Potseluyev, A. A., "Asymmetry in the Human Motor Function," Trudy Kazansk. ped. in-ta, No. 1, 1966, pp. 3-33.

N73-26090

THE POSSIBILITIES OF MAKING QUANTITATIVE EVALUATIONS OF THE FUNCTIONING OF CLOSED PEOPLE-OPERATOR CONTROL SYSTEMS

V. A. Taran, A. D. Korotkov, Yu. N. Kofanov,
A. A. Belov, I. G. Shramkov

ABSTRACT. The three tasks comprising the specific sections of the general methodology for evaluating ergatic systems are reviewed.

The Moscow Institute of Electronic Machinebuilding has, in recent years, been working on methods for making quantitative evaluations of the functioning of control systems in which people-operators take part. Let us conditionally call ergatic any physical system requiring the participation of man, regardless of the degree of such participation [3, 8]. Systems containing manipulators too are ergatic, the specifics of which consists of special organization of input signals to the operator. However, no particular organization of the operator's sensor field will change the principal features of the system as a whole; it has present in it a man-operator with a gamma of properties distinguishing him from the automatic device. The latter is what predetermines the research methods used. /148

Eragtic systems are more sharply defined types of adaptive systems capable of changing their structure and parameters in accordance with adaptation to operating conditions. The adaptive features of ergatic systems show up in two ways. First, the characteristics of the man-operator change during the instruction process to learn the actions to be taken to perform a specific task within the framework of a particular system. Here adaptation plays a positive role, because it takes in the system as a whole, and because the efficiency of operator performance (and hence the efficiency of the system as a whole) is increased during the instruction process. Second, the characteristics of the man-operator can change with his adaptation to the effect of external disturbances. The adaptive properties of the organism are mobilized for life-support purposes, however, and system efficiency can be reduced as a result.

The man-operator in an ergatic system often is looked upon as some sort of linearized link, as in [13], for example. But this fails to include the adaptability of the ergatic system at the same time that no proof is required of changeability of the properties of the man-operator affected by favorable, or

unfavorable factors. The need to consider the adaptive features of the operator is emphasized in papers by psychologists and researchers dealing with technical problems that include the "human" factor [4, 5].

This article will review the three tasks comprising the specific sections of the general methodology for evaluating ergatic systems. The first task is that of evaluating the degree of adaptivity of the man-operator during his instruction on how to work as part of the particular system. The second task is that of synthesizing the man-operation function described for a known level /149
of his adaption as part of the particular system. The third task involves making a quantitative evaluation of the probability of the operator performing a series of logical operations under stress.

These tasks permit building an ergatic system, the circuit of which is "operator instruction - synthesis of his model and the use in this case of a developed technique for system optimization - evaluation of stress in the system and recommendations for system modernization."

Let us represent ergatic system classification on the basis of criteria applicable when manipulators are used in these systems.

Reference [8] classifies ergatic systems in terms of number of operators, the degree to which the operator participates in system operation (in the system performing its basic task), appearance of the communication between operator and object of control and degree to which the system is hierarchical. Classification by the first three criteria is meaningful for ergatic systems with manipulators.

Ergatic systems can be broken down into monoergatic, one operator, and polyergatic, when the number of operators is more than one. However, one must distinguish monoergatic systems with back-up operators, needed to increase system dependability. Important to note here is that one operator takes part directly in performing the task assigned to the system. The organization of the sensor field for each succeeding operator in polyergatic systems depends significantly on the results of the actions taken by the preceding operator. Flow lines for assembling radio sets, and the like, are example of such systems. Systems with manipulators basically are monoergatic systems.

Ergatic systems are broken down into first and second type systems,

according to the degree of continuity of participation of the operator in causing the system to do its job. Ergatic systems of the first type can be characterized by the indirect participation of the operator in causing the system to do its job. The system (object) itself can be nonergatic and capable of independently performing its basic task. A nuclear reactor is such a system. But in the event of a failure, or for whatever reason, the object ceases to perform, the operator goes into action, the end purpose of which is to put the object back to work. In this case the operator is performing a monitoring function, looks for faults, and restores the system. But if the man-operator participates directly in causing the system to perform its basic task as its controlling link, we have an ergatic system of the second type. This is a follow-up system in most cases. According to the classification given in [13], these systems can be broken down into compensating (in which the mismatch between the required and actual positions of object coordinates is supplied to the operator's "input"), following (in which the mismatch signals and the coordinate values are supplied to the operator's "input"), and predicting (in which the operator works with a series of repeating signals and, by predicting the behavior of the object, introduces a predicting control signal). Systems with manipulators are, for the most part, ergatic systems of the second type.

Ergatic systems have two types of classification with respect to how the operator communicates with the object. The first includes so-called ergatic systems with direct communication, in which we shall conditionally include manipulators, and for which the operator is the energy source. We shall conditionally include systems with telemetry communication, and in which the manipulators have an independent power supply in the second type of ergatic systems. /150

Thus, systems with manipulators can be classified as monoergatic systems of the second type with direct, or telemetry, communications.

Some of the methods that can be used to make quantitative evaluations associated with investigation of systems with this classification characteristic are listed in what follows.

The operator, during the instruction (training) process should acquire skill in fixing the coordinates of the object he is controlling and in correctly

distributing the control actions in order to change these coordinates in accordance with instructions. This distribution of control actions is "metered" according to the information received by the operator, and is called metering. The correctness of the metering of the control actions by the operator of an ergatic system will depend on the quality with which he converts the information he has received on the behavior of the object of control. The conversion of the input information is made by the man's sensory organs, and the resulting action is a motor response, so these processes are included among the sensor-motor type of assignments. There are many cases when object control with the aid of manipulators is a process of following some random mismatch for which it is necessary to compensate. So there are many cases when these processes can be classified as compensator follow-up.

The operator, in the case of compensator follow-up, attempts to reduce the mismatch, $\varepsilon(t)$ to zero. Each realization of the follow-up process is some function of follow-up, usually continuous. The follow-up function enables us to determine the behavior of the object and, as a result, of the system as a whole. The follow-up function adequately reflects the results of the motor activity of the operator in an ergatic system in the case of continuous sensor-motor assignments.

Clearly, each special control task is limited by predetermined requirements and going beyond the limits means that the task is not carried out. And because the follow-up functions characterize the quality of operation of an ergatic system with predetermined precision, we may speak of some zone of acceptable values of realization of these functions.

All realizations of the follow-up function should be in this zone, one we shall call the acceptable control zone. If the follow-up function goes beyond the boundaries of the zone it means the man-operator in charge of the control action (motor response) had made an incorrect metering.

Research conducted in carrying out a number of engineering-psychology tasks [5, 9, 10, 13] has revealed that the man-operator reacts not only to the input signal, to the mismatch signal $\varepsilon(t)$, but also, albeit to a lesser degree to its first derivative $\dot{\varepsilon}(t)$. We can, in this case, write the canonical equation of form

The follow-up function has some scatter, limited by the zone of its acceptable values, so that the parameters of Eq. (1) can change within a predetermined range. The latter is, in turn, interrelated with the range of change in the function. Let us use the phase plane concept, that is, the plane determined by the coordinates of system error ϵ (the abscissa) and its derivative $\dot{\epsilon}$ (the ordinate). The acceptable control zone now can be expressed in terms of the phase representations in the form of an area of acceptable positions for the points represented in the phase plane. The coordinates of each of these points will be the value of the mismatch between the required and current coordinates of the object, ϵ, and its derivative, $\dot{\epsilon}$. Our phase plane then can be considered to be the plane of estimates of the follow-up lines, which are the phase analogues of the follow-up function. /151

Follow-up, as a process of establishing continuous corrections to the follow-up function mismatch, is subordinate to statistical laws because the control signal in an ergatic system depends on the degree of instruction given the operator, and the latter depends on the individual characteristics of the person being instructed. Moreover, even in a control process performed by an operator we have a gamma of random activities that are caused by external disturbances, as well as the potential of the man included in the system for controlling signals (noise) from the central nervous system. This noise is always present when man is controlling a system, and this sometimes leads to representing the operator in the form of a random signal generator. So it follows that the process reviewed can and must be investigated using probability methods [9].

Naturally, we can have only information in some degree or other associated with the functions $\dot{\epsilon}(t)$ and $\epsilon(t)$ cited above during the operating training process. It therefore is of interest to associate the components of the follow-up function with some instructional probability measure.

Let us postulate the existence of some neuropsychological apparatus for generalized evaluations, use of which compiles information on the results of the sample metering performed in the compensating follow-up process. The

operator classifies the results into two incompatible groups: successful, and unsuccessful. The quantitative measure of success then can be determined as the ratio of the measure of the subset of successful samples to the measure of the set of all samples taken at the particular moment in time. The relative share of successful samples (of controls) can be determined with sufficient accuracy for practical use by the ratio of the length of the segment of the follow-up line included in the limits of the acceptable control zone, to the total length of the follow-up line. The lengths emerge as sets, or subsets. This permits confirming that the phase plane $\{\varepsilon, \dot{\varepsilon}\}$ is the plane of evaluation.

Thus, change in the state of the learning system can be expressed by some variable which we shall call the information variable, numerically equal to the relative share of successful samples in the set of samples taken for the given time segment and for the given conditions.

Change in the information variable during the organism training process can be postulated by the following mathematical scheme

(2)

where

$y(n + 1)$ is the value of the information variable after the $(n + 1)^{\text{th}}$ sample;

$\varkappa(n + 1)$ is a random magnitude, taking the value +1 if the sample is successful, and -1 if it is not.

The recurrent Eq. (2) permits forecasting each current value of y from the preceding values and proceeding from the specified sample (the learning sequence).

Eq. (2) can be interpreted in Bush and Mosteller operators [2]

(3)

Here Q_1 and Q_2 are the known Bush and Mosteller operators; that is /152

(4)

Reference [9] points out that in this case operators for which $\alpha_1 = \alpha_2 = \alpha$; $\lambda_2 = 0$ can be taken.

The region of possible values of the parameters α and λ can be determined such that $0 \leq y(n) \leq 1$, and what follows then is that $0 \leq \alpha \leq 1$; $0 \leq \lambda \leq 1$.

Using mathematical induction we can show that the following expressions for the n-tuple application of the operators Q_1 and Q_2 to the intial value of the information variable (the apriori state of the organism) is valid

(5)

Then it can be shown, as was done in [9] for example, that in the case of the (n + 1)-tuple application of the operators Q_1 and Q_2, the following expression are valid.

$$\left.\begin{aligned} Q_1^{(n+1)}y(0) &= \alpha Q_1^{(n)}y(0) + (1-\alpha)\lambda_1; \\ Q_2^{(n+1)}y(0) &= \alpha Q_2^{(n)}y(0). \end{aligned}\right\} \tag{6}$$

As a result of the approximation of the obtained difference equations with differentials, let us write the resultant expression for the information variable in the form

(7)

when the point represented is within the limits of the region of possible controls, and in the form

(8)

when the point represented is beyond the limits of the region of possible controls.

Information as to the dynamic features of the object of control serves as the basis for constructing the region of possible controls. If, for example, it is necessary to compensate for some initial mismatch ε_0 (Figure 1), we can do so only providing that the follow-up function is contained within some acceptable region, if (and this must be particularly emphasized!) the compensation is to be made with the required precision and at the required time, T_D.

It then is possible, based on knowledge of the dynamic features of the object of control (that is, of the possible boundaries of values ε and $\dot{\varepsilon}$ which can be achieved by the given object on the basis of its physical features), to form region D, limited at the time coordinates by the boundaries of the follow-up functions 1 and 3 (Figure 1a). Boundary and acceptable follow-up functions in the time region can be given as the analogue of the corresponding functions in phase coordinates (Figure 1b). The region of acceptable controls, region D, will be the hatched field.

Figure 1. Boundary trajectories of follow-up functions. a - in coordinates ε and t; b - in coordinates $\dot{\varepsilon}$ and ε. 1 - minimum and 3 - maximum follow-up boundary functions; 2 - normal acceptable follow-up function in the time region; T_D is the finite control time (cycle); ε_0 is the initial mismatch value.

Compensating follow-up experiments have established some set of representative points $F(\varepsilon, \dot{\varepsilon})$ which, naturally, should be compared in value of coordinates with the boundary values for the D region. In sum, what is created is the possibility of activating the apparatus of linear operators Q_1 and Q_2, and as a result to obtain the information variable y(t) (Figure 2).

Because the y(t) value obtained corresponds to the finite (in the particular sample) ratio of the lengths of the corresponding trajectories, it can be shown that at the end of the sample the value of the information variable has its probability converge with that of the representative point remaining in the D region. And because the D region, by convention, is constructed to include the dynamic features of the object, no difficulties arise in limiting the set of possible values of the coordinates of the representative point, because taking

/153

the representative point beyond the limits of the D region clearly means non-fulfillment of the assignment in the particular sample. Consequently, the probability of the representative point remaining in the D region is an adequate probability that the ergatic system will carry out the assigned task.

Thus, the probability of the representative point remaining in the D region permits evaluation of the dependability of the ergatic system if the adaptation process will be carried out as a result of the specified conditions and in a specified time interval.

Eqs. (7) and (8) readily yield an automatic computer solution. The use of an automatic computer to solve the problem of quantitative evaluation of the degree of adaptation is particularly important because instructing operators in complex actions (pilots, and others, for example) takes place in trainers which are none other than analog modeling devices integrated with real equipment. If the values of the mismatch, ε, its derivative $\dot{\varepsilon}$, the boundary value for the mismatch, ε_D, and the corresponding value of the derivative $\dot{\varepsilon}_D$, are inserted in the block diagram of the modeling (Figure 3), we can obtain the value of the information variable immediately. The unit for evaluating this variable (Figure 3) also is based on an operation amplifier (integrator) 6, for solving Eqs. (7) and (8). The switches in Figure 3, K, are needed to set the sign of the input variables ε, $\dot{\varepsilon}$, ε_D, $\dot{\varepsilon}_D$; that is, to determine the quadrant in which the evaluation is being made.

The information variable values obtained can be produced in temporal coordinates, as well as in the phase plane. What are obtained in this case are individual evaluations in terms of the mismatch (Figure 4) and of its derivative.

Indications to the operator of the value of the information variable during the instruction process provide for the introduction of new feedback for use in obtaining information on the quality of control over the entire range from T_0 to T_D. Clearly, this cannot help but react favorably on accelerating instruction and increasing its quality. Savings in control cycles were 35% during the experiments in instructing operators of ergatic systems of the class reviewed. /154

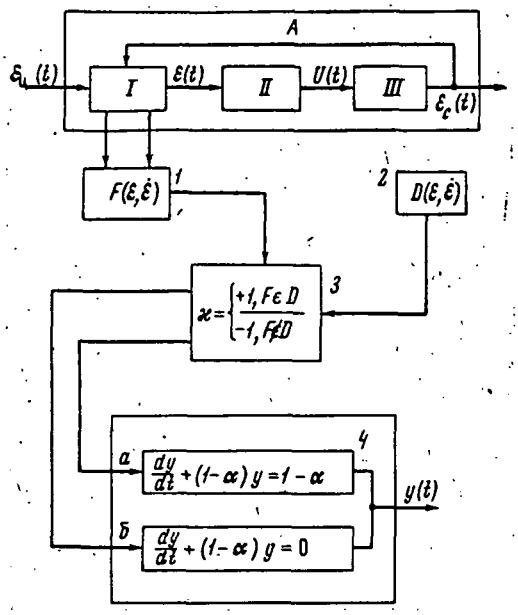

Figure 2. Block diagram for the evaluation of the information variable in the cycle of instructing the operator of an ergatic system of the second type. A - ergatic system; I - indicator; II - man-operator; III - object; 1 - formation of set of inputs; 2 - formation of set of possible controls (D region); 3 - unit for evaluating the random magnitude $\varkappa$; 4 - unit for evaluating y(t).

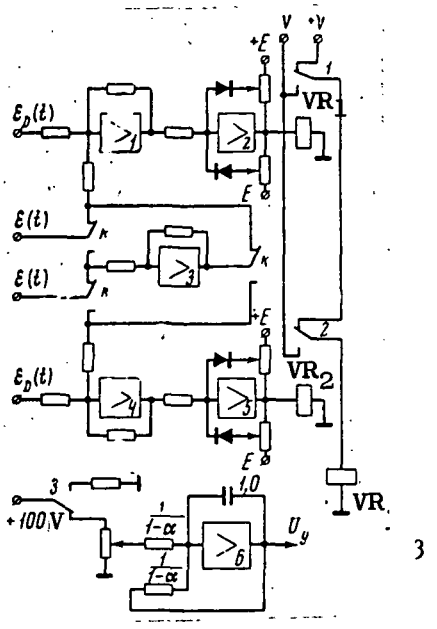

Figure 3. Block diagram of modeling of the process for evaluating control success. 1, 2, 4, 5 - operation amplifiers selecting the modulus of input magnitudes; 3 - inverter; VR_1 and VR_2 - relays in circuits of corresponding input magnitudes for specified boundary values; VR_3 - relay for putting data in the unit for evaluating the information variable of the instruction.

Figure 4. Typical recordings of the process of evaluating success of control. 1, 2, 3, - numbers of recordings as success decreases; ε_{DK} - boundary functions of the mismatch; ε_K typical acceptable mismatch function (system errors); T_D - time of cycle.

Some function $\mu(N)$, where N is the number of control cycles completed for purposes of instructing the operator, and μ is the final value of the information variable y(t) for each cycle, results from the determination of the value of the information variable in each cycle. This will provide the instruction curve, and the value of the probability of successful completion by the operator of the specified task will correspond to each cycle. This is

significantly different from the often used evaluation of instruction in terms of frequency of successful controls, determined for a group of cycles. In such case /15
the probability of a successful control is determined for a group of cycles. If, in the method proposed, the statistical collective is reduced to one control cycle, the hypothesis as to the constancy of the operator's qualities can be extended here to only the time of one control. Just how much more correct this approach is, as compared to evaluation in terms of frequency, where this hypothesis could be extended to the group of control cycles studied, is clear.

The degree to which the operator is trained can be classified as that system condition to which the stabilized level of the instruction curve corresponds.

Only after the degree of adaptation in an ergatic system has been determined can we proceed to possible approximations in the system, such as, for example, a mathematical description of the operator for a concrete time segment and for definite control conditions.

There are two ways to obtain the man-operator describing function in an ergatic system of the second type; by selecting the values of the parameters for some hypothesized structure, and by purposeful movement to the optimum relationship between the output variable models and the operator tested. The latter, naturally, is the more acceptable, because the selection of possible values for the parameters of some structure is quite lengthy.

It is proposed that the methods of the theory of sensitivity [1] be used to synthesize the parameters of the operator's describing function in an ergatic system of the second type.

References [8, 10, 12] suggest methods for evaluating the criteria of sensitivity for different types of systems, based on the fundamentals of the general theory of sensitivity developed by M. L. Bykhovskiy [1].

Let us understand system sensitivity to mean its capacity to change its quality criteria with change in parameters. The coefficient of influence is the system sensitivity criterion and is the partial derivative of some system index in terms of a given parameter, taken for the rated value of the parameter. Let us stipulate that the system index to investigate is the mismatch γ between the output function for the man-operator and his model.

Let us take some generalized scheme of an ergatic system in which all elements are replaced by some linearized structures. Let us find first of all the coefficient of influence for the parameters of these linearized structures (of the transfer functions for the units) of magnitude $\epsilon(t)$, which is a function of the error for the particular scheme.

Differentiating the transfer function for a closed system in terms of each of the parameters, and aware that each of the transfer functions is a polynomial relationship, we find the equation for the coefficient of influence in the form

(9)

where

$F_1(s)$ is the transfer function for a closed system in terms of the output magnitude $y(s)$;

$F_2(s)$ is the transfer function for a closed system in terms of the error $\epsilon(s)$;

$\partial\epsilon/\partial q_i$ is the unknown derivative (the coefficient of influence);

$[W_{in}(s)]_{g_i}$ is the influence operator, some linear structure (transfer function) formed in accordance with definite rules.

Reference [8] gives a rule for forming the influence operator when the parameter q_i is the cofficient of the polynomial in the numerator, and the denominator is the transfer function for the particular unit. So if q_i is the coefficient of a polynominal in the numerator of the transfer function for some unit $W_i(s)$ the corresponding influence operator will take the form /156

(10)

The influence operator takes the following form for q_i, which is the coefficient of the polynomial in the denominator of the transfer function $W_i(s)$

$$[W_{in}(s)]_{b\psi} = -\frac{s^{\psi}}{B_i(s)}. \tag{11}$$

The general rule for finding the reference operators can be expressed in the form

$$[W_{in}(s)]_{q_i} = \frac{\frac{\partial W_i}{\partial q_i}(s)}{W_i(s)}. \qquad (12)$$

So the method used to find the coefficients of influence is called the influence operators method.

The influence operators method provides all needed coefficients of influence simultaneously if all needed influence operators are formed and if, as has been done in Figure 5, a system for making the evaluation has been constructed in accordance with Eq. (9). Automatic computer units can be used to realize the influence operator for different cases. The signal x(t) is random, so in essence the coefficients of influence are random processes. The statistical characteristics of the coefficients of influence must be determined in this case.

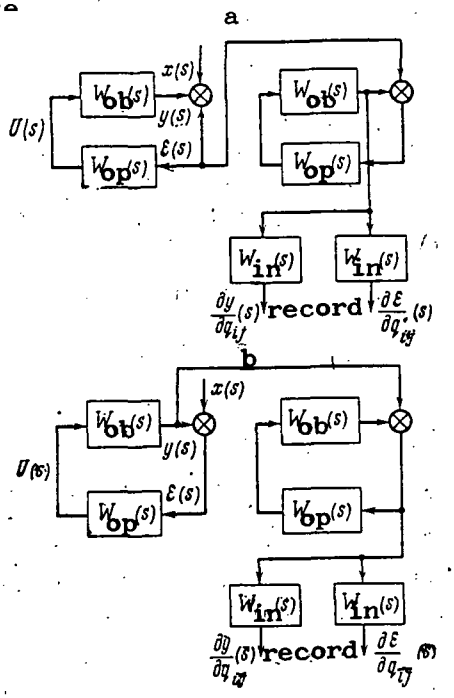

Figure 5. Generalized block diagram of the obtaining of coefficients of influence. a - variant using error signal; b - variant using output signal from controlled object.

Optimization (synthesis) of the operator function described is in terms of the criterion

(13)

where

(14)

$\varepsilon^*(t)$ is the index of the operator model.

Each new value of the criterion h is found from

$$h_i = h_{i-1} - k\frac{\partial h}{\partial q_i}, \qquad (15)$$

where

k is the step of change in h.

The coefficient of influence of form $\partial h/\partial q_i$ is associated with the coefficient of influence of form $\partial \varepsilon/\partial q_i$. As a matter of fact, if we differentiate (13) with respect to q_i we find

(16)

The influence operators method is very convenient to use to synthesize the real operator in a system. In point of fact, operators taking the course of instruction on a system of a given type to solve a given task can be used in place of $W_{op}(s)$ in order to realize the scheme shown in Figure 5. The scheme then, naturally will more precisely reflect the real status of the operator in the follow-up process. The error in evaluation; the result of scatter in operator characteristics, drift in those characteristics in terms of time, and inaccuracy in the influence operators models, is, in the final analysis reflected in the error in the coefficient of influence; that is, in errors of a second and higher order of smallness. /157

Reference [12] cites derivations of influence operators for nonsteady-state models of describing functions. The influence operator will have the following form for the parameter $q_i(t)$ contained in the polynomial in the numerator of the parametric transfer function $W_i(s, t)$ as a coefficient

$$[W_{in}(s, t)]_{a_\varphi(t)} = \frac{s^\varphi}{B_i(s, t)}; \qquad W_i(s, t) = \frac{A_i(s, t)}{B_i(s, i)}. \tag{17}$$

For the parameter $q_i(t)$, contained as a coefficient in the polynomial in the denominator of a nonsteady-state describing function (linear)

(18)

The derivations of Eqs. (17) and (18) are based on the structural conversions of the nonsteady-state models of sensitivity into linear variable systems [6, 7].

References [8, 10] have presented the bases for building an integrated sensitivity model, and it is used in [10] to synthesize a linear describing function for a man-operator in an ergatic system of the second kind. The

difference between the integrated model of sensitivity and the influence operators is that the latter need no reswitching in the system, or taps from it of any internal signals, for their realization, whereas taps are needed to build the integrated model. What are formed are two artificial auxiliary signals, making it possible to receive simultaneously all the unknown coefficients of influence using simple, universal, analog equipment. The economic effectiveness of the integrated model is much higher than it is for the influence operators method.

As experiment, making possible a comparison of the evaluation of the instruction given the operator in an ergatic system of the second type using different criteria is of interest, for it uses the criterion of success, as well as stabilization of the level of change in parameters of the describing function and the level of change in the error at the output during the training process (Figure 6).

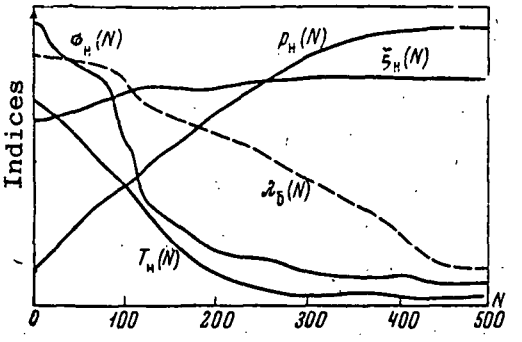

Figure 6. Comparative evaluation of stabilization of levels of parameters for instruction and model of the operator. $\sigma_H(N)$ change in system error; $P_H(N)$ - change in the probability of performing the task in the control process; $\xi_H(N)$ - change in the damping of the operator describing function during instruction; $T_H(N)$ - change during instruction of the time constant for the operator in an ergatic follow-up system; $\lambda_\sigma(N)$ - change during instruction of the intensity of the biopotentials from the flexor muscles of the hand; N - cycles of control.

The complexity in evaluating the quality of the work done by the operator when there is an increase in the percentage of logical operations in the total number of subtasks should be noted. It is of particular importance to evaluate the probability characteristics of the quality of the operator activity in an ergatic system of the second kind acting under stress conditions [11, 14].

Let us call stress the state of an ergatic system characterizing the intensification of the processes circulating in it under the influence of factors that are external with respect to the system.

Let us agree to distinguish two types of stress.

1. Q-stress - that state of the system caused by an increase in the physical load (amplitude of vibration, frequency and brightness of an input video signal on the scope, acoustic noise, weightlessness, climate, and others). It can be characterized by an increase in intensity, or by the occurrence of new input influences in the ergatic system.

Equipment and mechanism operating modes in the machine part of an ergatic /158
system are complicated by the effects of Q-stress factors, the rate of component failures increases, and so on. The levels of intensity of biopotentials in the man-operator rise, muscle cramping and tremors appear, metering of strength is upset, stiffness of posture and movements appears, pulse and respiration change, as does the electrical conductivity of the skin, and so on [5].

2. S-stress - that state of the system caused by the reactions of the man-operator to change in the psychological factors involved in the process, including change in standby time to perform certain subtasks (operations). In other words, S-stress is the consequence of the occurrence of a time deficit in the system. This type of stress is characteristic only of an ergatic system.

We noted above, in the course of determining the degree of adaptation, and the operator describing functions, that <u>conditions for cooperation</u> between man and machine were not violated in the process of the functioning of an ergatic system. Stress factors however, can violate those conditions.

Clearly, then, evaluation of stress in an ergatic system will permit designing in such a way that the conditions of cooperation will be maximized in terms of some criterion selected in advance.

Let us consider the evaluation of the efficiency of an ergatic system when S-stress is acting.

It is only in an ergatic system under stress (time deficit condition) that it is possible to accelerate the work tempo when there is an increase in labor efficiency. In point of fact, the time deficit, up to some level, is an

organizing factor for the operator. Once the threshold of stress is reached, however, the time deficiency acts negatively on the probability of performing the task, and the efficiency with which the system functions is reduced.

The magnitude

(19)

where

T is the total time assigned for the completion of all tasks;

T_i is the time already used to complete the i^{th} preceding subtasks;

i = 1, 2, ..., n;

$\bar{T}$ is the mean time needed to perform (n - i) successive subtasks, provided the operator works at average speed and without errors,

is a qualitative measure of the S-stress.

Reference [14] cites classifications of levels of urgency in completing tasks in accordance with which stress evaluations are made, and determination of the probability of the ergatic system performing its task.

1. There is no requirement for urgent performance of a subtask if the time /159 remaining is, on the average, sufficient to perform all subsequent subtasks.

But all subtaks are completed that the operator can break down into essential and nonessential. The condition for lack of urgency can be expressed in the form

$$\sum_{j=i}^{n} \bar{t}_j \leqslant T - T_i, \tag{20}$$

where

$\bar{t}_j$ is the mean time to perform the i^{th} operation (j = i, ..., n).

2. Urgent completion is necessary if there is not enough time to complete all succeeding subtasks, but completely adequate to perform essential subtasks. The urgency condition then can be expressed as

(21)

but

(22)

Here, as before, S = 1.

3. Special urgency of completion of a subtask may be required if remaining time is not sufficient to perform essential subtaks.

Then S > 1.

A series of expressions of the form [11]

(23)

where

M is the threshold of stress S;

$\bar{p}_i$ is the mean probability of completing the i^{th} subtask,

can be used to calculate the factual probability of the ergatic system completing its task.

An algorithm for calculating the time to complete each of a series of successive subtasks, as well as the probability of completing these subtasks, has been developed. Figure 7 is a typical task completion probability to stress level relationship.

Figure 7. Typical ergatic system of the second type task completion probability to stress relationship.

Evaluation of stress in an ergatic system is an important adjunct to the methodology of evaluations of the degree of adaptation and of the describing function.

REFERENCES

1. Bykhovskiy, M L., "Sensitivity and Dynamic Precision of Automatic Control Systems," Izv. AN CCCP, Tekh. Kibernetika, No. 4, 1964. /160

2. Bush, R., Mosteller, F., Stokhasticheskiye modeli obychayemosti [Stochastic Learning Models], Fizmatgiz, 1962.

3. D'Addio, E., "Automatic Regulating Systems as an Intuitive Representation and as a Formal Concept," Trudy I kongressa IFAK [Proceedings of the 1st Congress of the International Federation of Automatic Control], AN CCCP Press, 1961.

4. Druzhinin, G. V., Nadezhnost' sistem avtomatiki [Reliability of Automatic Systems], 2nd Edition, "Energiya" Press, 1967.

5. Lomov, B. F., Chelovek i tekhnika [Man and Engineering], 2nd Edition, Moscow, 1967.

6. Mikhaylov, F. A., et al., Dinamika nestatsionarnykh lineynykh sistem [Dynamics of Non-Stationary Linear Systems], "Nauka" Press, 1967.

7. Solodov, A. V., Lineynyye sistemy avtomaticheskogo upravleniya s peremennymi parametrami [Linear Automatic Control Systems With Variable Parameters], Fizmatgiz, 1962.

8. Taran, V. A., Brudnik, S. S., Kofanov, Yu. N., Matematicheskiye voprosy avtomatizatsii proizvodstvennykh protsessov [Mathematical Questions of Automating Production Processes], "Vysshaya shkola" Press, 1968.

9. Taran, V. A., Korotkov, A. D., "An Evaluation of the Pilot's State of Training on Trainers," Voprosy psikhologii, No. 5, 1967.

10. Taran, V. A., Kofanov, Yu. N., "Method of Combined Modeling for Estimating a System's Transfer Function," Materialy 5-go Vses. soveshch. po voprosam matematicheskogo modelirovaniya [Materials of the 5th All-Union Conference on Questions of Mathematical Modeling], Leningrad, 1966.

11. Taran, V. A., Belov, A. A., "Evaluation of the Reliability of Monoergatic Systems Which Operate Under Conditions of a Time Deficit," Trudy II Vses. mezhvyzovskoy konferentsii po nadezhnosti [Proceedings of the 2nd All-Union Inter-University Conference on Reliability], Leningrad, 1968.

12. Taran, V. A., Shramkov, I. G., "Determining the Permissible Deviations of the Operating Index of a System with Variable Parameters," Trudy II Vses. mezhvuzovskoy konferentsii po nadezhnosti [Proceedings of the 2nd All-Union Inter-University Conference on Reliability], Leningrad, 1968.

13. McRuer, D. T., Krendel, E. S., "The Human Operator as a Servo System Element," Franklin Inst., 267, No. 5, 1959.

C

14. Sidzhel, A., Vol'f, Dzh., "A Method of Estimating the Construction Variants of Man-Machine Systems," Zarybezhnaya radioelektronika, No. 8, 1962.

N73-26091

THE QUESTION OF MODELING CERTAIN MOTOR FUNCTIONS OF THE HUMAN ARM

A. V. Smirnov, B. S. Yastrebov

ABSTRACT. The modeling of the motor functions of the human arm by master-slave manipulators is discussed. The use of the lateral-pulse method to modulate the control signal is presented.

There are a number of different designs of manipulators in use today in a number of branches of science and engineering, but even the most modern of them lag well behind the capabilities of the human arm. /161

It is becoming evident that further improvement of manipulators can be quite successful provided careful study is made of the mechanism in the human body that controls arm movements, that the features of the control laws are exposed, and that they are modeled on the basis of the latest achievements of scientific and technical thought.

The human arm differs from a mechanism by having active, as well as kinematic, muscular ties. And the number of active muscular ties involved in some displacement usually is more than one. It should be emphasized that the muscular ties of the human arm, as distinguished from a mechanism, are active.

The bones of the skeleton of the human arm are surrounded by several layers of muscles that perform the variety of functions involved in movement. Two types of muscle interactions have come to be accepted: synergism, and antagonism. The former involves the performance of common work, the participation of the muscles in the same movement. In the case of antagonism the different groups of muscles participate in opposite movements. The central nervous system, by most precise metering of the forces of muscle-antagonists, regulates the speed of the movement, and the force, brakes the movement, and provides smoothness from the beginning to the end of the movement.

A drive using two motors can be built to serve as the analog of the muscles of the synergists and antagonists.

Control of the "antagonist" and "synergist" motors for example by changing the supply voltage will result in realization of a similar work mode.

The characteristics of the speed with which the human arm acts are distinguished by an extremely great range. Yet along with rapid movements of great power the human arm performs the most complicated and most precise operations with minimum effort. These potentials can be reached primarily because a muscle making whatever movement consists of fast and slow fibers which are grouped into different neuromotor units and are controlled by the central nervous system according to the task assigned.

The command to begin the movement, its speed, the force with which the /162
muscles are to contract, yields a train of impulses that flows along the nerve fibers from the central nervous system to the muscles. The nerve impulse repetition frequency determines the degree to which the muscle is excited.

The power of the contractile act on the part of the muscles of the human arm is determined by the nerve impulse repetition frequency, as well as by nerve impulse amplitude. The following table is from Yu. M. Uflyand [1].

TABLE

Nature of Contraction	Pulse Amplitude	Pulse Frequency
Tonic activity	50-100 μV	-
Involuntary contraction	200-400 μV	50-70 pps
Strong contraction	1500-2000 μV	200 pps

High-powered master-slave manipulators most often are built on the hydraulic drive principle. As we know, the initiation of the movement of a hydraulic drive is usually accompanied by some kicking, or jerking, the cause of which is the static friction that alwways is present with dry friction. It occurs in the packing glands of the moving part of the drive because of packing compression.

This naturally makes it difficult to use manipulators for operations requiring increased accuracy and precision.

The most rational way to eliminate the effect of static and dry friction from the control process is vibration linearization of the drive. Analogous to it, in essence, is the so-called tonic activity of man's skeletal muscles.

Muscle tonus is associated with the supply to the muscle of a train of nerve impulses with a minimum rest frequency exciting different muscle fibers alternately. Thus, the entire system is in a dynamic state with a high reaction rate to external stimulation. The inertia of the members of the body damp the rest oscillations in the rest state, thus preventing them from increasing in amplitude.

Similar control modes are widely used in modern engineering.

The essence of the operation of these systems involves setting up a vibration mode of operation of the distributors. But this mode can be limited to any element in the follow-up drive, to and including the slave motor, depending on the pulse repetition frequency.

The advantages in having the system operate in vibration modes are the high rate of speed and sensitivity of the system, the high reliability, elimination of the influence of change in temperature, cleanliness of the working fluid, reduction to a minimum of the influence of static and dry friction in system elements, and zero hysteresis and drift in amplifier circuits.

Practice in the building and operation of remotely controlled manipulators with electrohydraulic control systems has shown that high levels of static and dry friction in the slave drive will reduce sensitivity and precision and will cause kicking during starting. Contrl by lateral-pulse modulation gives the desired characteristics, thus increasing the efficiency of the manipulators.

Special selection of the frequency for vibration linearization of the control system can result in an operating mode similar to the tonic activity of the skeletal muscles of the human arm in the rest state. /163

The P. P. Shirshov Institute of Oceanology of the Academy of Sciences of the USSR has, in recent years, been engaged in research on the use and improvement of electrohydraulic control systems for underwater master-slave manipulators operating in the lateral-pulse modulation mode.

The error signal in these systems is the difference in the voltages across the position sensors for the command and slave elements. This difference voltage is converted by a transistor amplifier performing like a Class D amplifier into a pulse train changing differentially with respect to width. The converted

signal acts on the relay of a nozzle-slide type hydraulic amplifier that controls the movement of the distribution slide-valve. Displacement of the latter moves the piston in the slave cylinder.

The slide in the hydraulic amplifier oscillates at zero input signal, and the mean speed of the slide-valve for the period is zero. In the unbalanced input signal case the slide of the hydraulic amplifier spends more time at one nozzle than at the other during each switching cycle. Now the mean speed is not zero.

A symmetrical semiconductor triode multivibrator (Figure 1) is used as the source of periodic rectangular pulses that convert the continuous input signal into a train of temporarily modulated pulses.

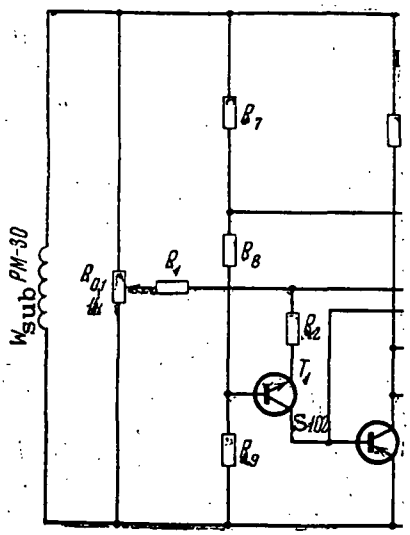

Figure 1. Principal schematic of the pulse amplifier.

The transistors have low internal resistance when conducting in the pulse mode, high efficiency, and stable temperature variation and operating voltage curves. Temperature stabilization of the working point is not required because transistor cutoff and saturation regions are easily provided by trigger pulses greater in magnitude than the current and voltage values occurring with change in temperature [2].

Transistors need not be selected in terms of parameters when semiconductor amplifiers operating in the pulse mode are used. It is sufficient to satisfy to condition $\beta \geq \beta_{min}$, where β is transistor current gain factor in a circuit

with a common emitter.

Some voltage $U_{be} \geq -0.3$ to -0.5 V must be applied between the bases and emitters of the transistors in the input stage in the balanced position in order to reduce to a minimum the zones of amplifier insensitivity. This can be done by inserting a voltage divider between bases and emitters of the transistors in the input stage. In this case the magnitude of the threshold voltage, U_{be}, is determined by the voltage drop across R_8.

The oscillograms in Figure 2 illustrate the advantages noted for a manipulator control system using lateral-pulse modulation of the control signal.

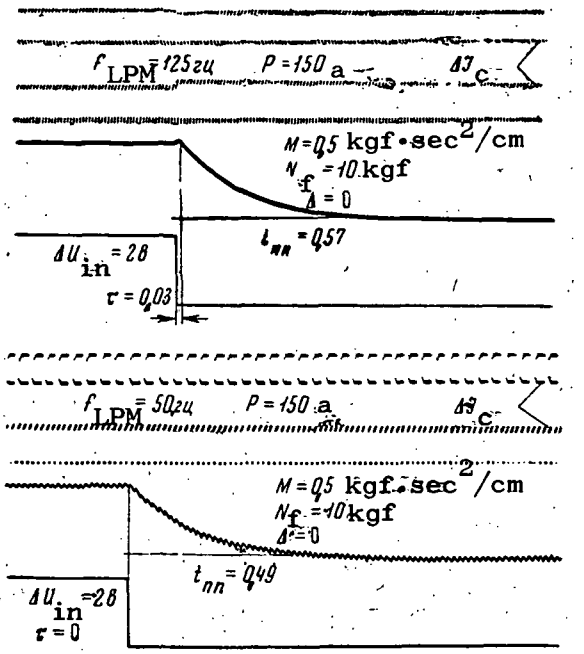

Figure 2. Oscillograms of transients in a manipulator control system using lateral-pulse modulation of the control signal.

The control signal, $U_{in} = 2$, is supplied to the input of the electro-hydraulic system for controlling the manipulator in the form of a function changing stepwise. The pressure of the working fluid at the input to the hydraulic distribution was 150 kgf/cm^2.

Oscillograms were recorded when the frequency of the linearizing oscillations was 50 and 125 Hz. In the first case oscillations of the slave motor ram with amplitudes to 0.1 mm were observed. In the second case the amplitude of the oscillation of the slave motor ram were so small (less than the turn sensitivity of the feedback potentiometer) it was barely perceptible, even to the touch. The net delay in the first case is practically zero, in the second 0.03 sec. There is no static error in the system in either case when friction is increased to 10 kgf. /165

Recapping, we can formulate the following conclusions:

1. The characteristics of master-slave manipulators can be improved by studying the mechanism that controls the human arm and by rational modeling of these functions.

2. The characteristics of master-slave manipulator control systems can be improved substantially by using the lateral-pulse method to modulate the control signal.

REFERENCES

1. Uflyand, Yu. M., Fiziologiya dvigatel'nogo apparata cheloveka [The Physiology of the Human Motor Apparatus], Izd-vo "Meditsina," 1965.

2. Kulikov, S. V., "Contactless Polarized Relay of Semiconductor Triodes," Priborostroyeniye, No. 9, 1959.

N73-2692

DETERMINATION OF THE SPATIAL POSITIONS OF THE LINKS IN A MANIPULATOR MECHANISM

A. V. Sinev, Yu. A. Stepanenko

ABSTRACT. Screw calculus methods are used in an effort to determine the position of a manipulator in space.

One of the main tasks of kinematics that comes up when investigating manipulators is to establish the working space and the work capabilities of the manipulator in different areas within that space, as well as its maneuverability and "service" [1, 2]. /166

Determination of the position of the manipulator in space is basic to these tasks. The complexity of the space mechanism and the great number of degrees of freedom make it necessary to select the most efficient and compact research method. This paper will attempt to use the methods and apparatus of screw calculus for this purpose [3, 5].

Schematic of the Mechanism in the Initial Position and Basic Notation

Let us consider a manipulator mechanism in what we shall call the initial position. The axes of all links are located along one straight line, with the axes of the three hinges parallel to each other and perpendicular to the axes of the links (Figure 1).

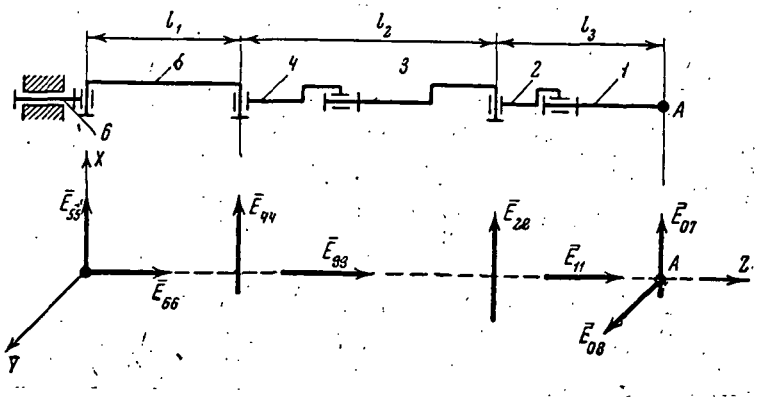

Figure 1. Initial position of mechanism.

Let us introduce the following notation. Let l_1, l_2, and l_3 be the lengths of the links, X, Y, Z the Cartesian coordinates, $\bar{u}_1$, $\bar{u}_2$, and $\bar{u}_1 \times \bar{u}_2$ a set of three unit vectors at pole O and directed along the X, Y, and Z axes. ω is the screw number. /167

Let us introduce the following screws characterizing the initial position of the mechanism: $\bar{E}_{07} = \bar{u}_1 + \omega (l_1 + l_2 + l_3)\bar{u}_2$ in the plane of the tongs, and $\bar{E}_{08} = \bar{u}_2 - \omega (l_1 + l_2 + l_3)\bar{u}_1$ perpendicular to the plane of the tongs. Thus $\bar{E}_{07}$ and $\bar{E}_{08}$ fix the spatial orientation of the tongs at point A.

Screws $\bar{E}_{11}$; $\bar{E}_{22}$; $\bar{E}_{33}$; $\bar{E}_{44}$; $\bar{E}_{55}$ and $\bar{E}_{66}$ characterize the initial position in space of the axes of the six hinges in the mechanism (Figure 1): $\bar{E}_{11} = \bar{u}_1 \times \bar{u}_2$; $\bar{E}_{22} = \bar{u}_1 + \omega (l_1 + l_2)\bar{u}_2$; $\bar{E}_{33} = \bar{u}_1 \times \bar{u}_2$; $\bar{E}_{44} = \bar{u}_1 + \omega l_1 \bar{u}_2$; $\bar{E}_{55} = \bar{u}_1$; $\bar{E}_{66} = \bar{u}_1 \times \bar{u}_2$.

Determination of the Position of the Links in the Mechanism in Space According to the Theory of Final Screw Travel

Let us make a series of successive turns from the initial position (see Figure 1): link 1 (tongs) we turn with respect to the axis $\bar{E}_{11}$ through angle φ_5 (position is counter clockwise); link 2 already turned link 1 through angle φ_4 with respect to axis $\bar{E}_{22}$; links 3, 2, and 1 through angle φ_3 with respect to axis $\bar{E}_{33}$; links 4, 3, 2, and 1 through angle φ_2 with respect to axis $\bar{E}_{44}$; links 5, 4, 3, 2, and 1 through angle φ_1 with respect to axis $\bar{E}_{55}$; and links 6, 5, 4, 3, 2, and 1 through angle φ_0 with respect to axis $\bar{E}_{66}$. Screws in new positions will be designated $\bar{E}_{ik}$, where i is number of turns, and k is the screws index.

The general formula for the final screw turn can be represented in the form [4, 5]

$$\bar{E}_{i+1,k} = \bar{E}_{ik} \cos\bar{\varphi} + (1 - \cos\bar{\varphi})(\bar{E}_{ik} \cdot \bar{E})\bar{E} + \bar{E} \cdot \bar{E}_{ik} \sin\bar{\varphi}, \tag{1}$$

where

$\bar{E}_{ik}$ is the initial position of a single screw;

$\bar{E}_{i+1,k}$ is the final position of a single screw;

E is a single screw in the axis of turn;

$\bar{\varphi}$ is a complex screw turn.

In the case considered we have pure turns because the mechanism contains only rotating couples, so all turns are active.

The position of a single screw can be represented in the form

$$\bar{E}_{ik} = C_{ik}^X \bar{u}_1 + C_{ik}^Y \bar{u}_2 + C_{ik}^Z (\bar{u}_1 \times \bar{u}_2) + \omega [C_{ik}^L \bar{u}_1 + C_{ik}^M \bar{u}_2 + C_{ik}^N (\bar{u}_1 \times \bar{u}_2)], \tag{2}$$

where

i = 0, 1, 2, 3, 4, 5 - the number of turns;

k = 1, 2, 3, 4, 5, 6, 7, 8 - the index of a single screw.

All the new positions of the screws on the horizontal lines in the table were obtained by turning the preceding screws in the kinematic chain through the same angle around a single axis, so we can derive formulas for the sequential calculation of the coefficients C_{ik}.

The screw parameters are calculated by assigning initial values to the coefficients of the reference screw, and then calculating all C_{ik} using the formulas.

Determination of the Position of the Tongs With Respect to a Fixed Coordinate System /168

The position of the tongs, as a solid body, can be assigned six coordinates in space; 3 linear, 3 angular. Let point A of the tongs move to point C with coordaintes (ρ_x, ρ_y, ρ_z). Let us take point C as the origin of the x, y, z system, the axis of which are parallel to the X, Y, Z axes. Let us plot a set of three unit vectors, $\bar{E}_{07}$, $\bar{E}_{08}$, and $\bar{E}_{09}$ from point A to point C, joined to the tongs as to a solid body. Three Euler angles (ψ - precession, θ - nutation, φ - pure rotation) characterize the rotation of a solid body about fixed point C from position with axes x, y, z to position with axes x', y', z' connected to the body. Single screws $\bar{E}_{07}$, $\bar{E}_{08}$ and $\bar{E}_{11}$ will now be directed along axes x', y', z'. Let us designate them $\bar{E}_{67}$, $\bar{E}_{68}$ and $\bar{E}_{61}$ (Figure 2).

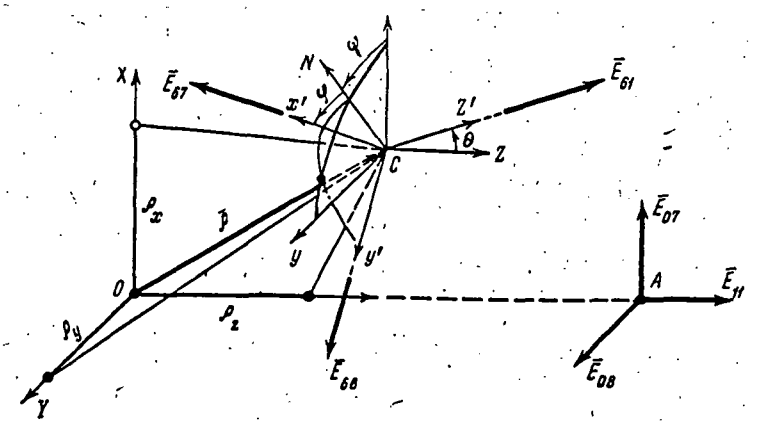

Figure 2. Coordinates of tongs as a solid body in a fixed coordinate system.

The connection between the position of a body with axes x, y, z, and the position with x', y', z' can be expressed by known formulas for nine directional cosines between axes

$$\cos(\widehat{xx'}) = \cos\psi\cos\varphi - \sin\psi\sin\varphi\cos\theta;$$
$$\cos(\widehat{yx'}) = \sin\psi\cos\varphi + \cos\psi\sin\varphi\cos\theta;$$
$$\cos(\widehat{zx'}) = \sin\varphi\sin\theta;$$
$$\cos(\widehat{xy'}) = -\cos\psi\sin\varphi - \sin\psi\cos\varphi\cos\theta;$$
$$\cos(\widehat{yy'}) = -\sin\psi\sin\varphi + \cos\psi\cos\varphi\cos\theta;$$
$$\cos(\widehat{zy'}) = \cos\varphi\sin\theta;$$
$$\cos(\widehat{xz'}) = \sin\psi\sin\theta;$$
$$\cos(\widehat{yz'}) = -\cos\psi\sin\theta;$$
$$\cos(\widehat{zz'}) = \cos\theta.$$

The position of point C relative to the coordinate origin O can be represented by the vector

$$\bar{\rho} = \rho_x\bar{u}_1 + \rho_y\bar{u}_2 + \rho_z(\bar{u}_1\times\bar{u}_2).$$

The active parts of screws E_{67}, E_{68} and E_{61} can be expressed by nine directional cosines ∠169

$$\begin{aligned}
&\mathrm{Re}(\bar{E}_{67}) = \bar{u}_1' = \bar{u}_1\cos(\widehat{xx'}) + \bar{u}_2\cos(\widehat{y}\\
&\mathrm{Re}(\bar{E}_{68}) = \bar{u}_2' = \bar{u}_1\cos(\widehat{xy'}) + \bar{u}_2\cos(\widehat{yy'}),\\
&\mathrm{Re}(\bar{E}_{61}) = \bar{u}_1' = \bar{u}_2' = \bar{u}_1\cos(xz') + \bar{u}_2\cos(\widehat{yz'}) +
\end{aligned} \tag{3}$$

Thus, the position of the screws in space can be represented in the form

$$\bar{E}_{67} = \bar{u}_1' + \omega(\bar{\rho}\times\bar{u}_1');$$
$$\bar{E}_{68} = \bar{u}_2' + \omega(\bar{\rho}\times\bar{u}_2');$$
$$\bar{E}_{61} = (\bar{u}_1'\times\bar{u}_2') + \omega[\bar{\rho}\times$$

from whence, expanding the vector products and using Eq. (3), we obtain, finally

$$\bar{E}_{67} = \bar{u}_1 \cos(\widehat{x x'}) + \bar{u}_2 \cos(\widehat{y x'}) + (\bar{u}_1 \times \bar{u}_2) \cos(\widehat{z x'}) + \\ + \omega \bar{u}_1 [\rho_y \cos(\widehat{z x'}) - \rho_z \cos(\widehat{y x'})] + \omega \bar{u}_2 [\rho_x \cos(\widehat{z x'}) - \rho_z \cos(\widehat{x x'})] + \\ + \omega (\bar{u}_1 \times \bar{u}_2) [\rho_x \cos(\widehat{y x'}) - \rho_y \cos(\widehat{x x'})]. \quad (4)$$

$$\bar{E}_{68} = \bar{u}_1 \cos(\widehat{x y'}) + \bar{u}_2 \cos(\widehat{y y'}) + (\bar{u}_1 \times \bar{u}_2) \cos(\widehat{z y'}) + \\ + \omega \bar{u}_1 [\rho_y \cos(\widehat{z y'}) - \rho_z \cos(\widehat{y y'})] + \omega \bar{u}_2 [\rho_x \cos(\widehat{z y'}) - \rho_z \cos(\widehat{x y'})] + \\ + \omega (\bar{u}_1 \times \bar{u}_2) [\rho_x \cos(\widehat{y y'}) - \rho_y \cos(\widehat{x y'})]. \quad (5)$$

$$\bar{E}_{61} = \bar{u}_1 \cos(\widehat{x z'}) + \bar{u}_2 \cos(\widehat{y z'}) + (\bar{u}_1 \times \bar{u}_2) \cos(\widehat{z z'}) + \\ + \omega \bar{u}_1 [\rho_y \cos(\widehat{z z'}) - \rho_z \cos(\widehat{y z'})] + \omega \bar{u}_2 [\rho_x \cos(\widehat{z z'}) - \rho_z \cos(\widehat{x z'})] + \\ + \omega (\bar{u}_1 \times \bar{u}_2) [\rho_x \cos(\widehat{y z'}) - \rho_y \cos(\widehat{x z'})]. \quad (6)$$

Determination of the Position of the Tongs for Known Angles of Rotation in the Hinges

Let us calculate the values of the coefficients C_{6k}^{Xk}, C_{6k}^{Yk}, C_{6k}^{Zk}, C_{6k}^{Lk}, C_{6k}^{M} and C_{6k}^{N} when k = 1, 7, 8 and let us equate the coefficients obtained to each of six components of screws $\bar{E}_{67}$, $\bar{E}_{68}$, $\bar{E}_{61}$, found using Eqs. (4) - (6) and Eq. (3) when i = 6, k = 1, 7, 8.

We have, for screw $\bar{E}_{61}$, the equality $\cos\theta = C_{61}^{Z}$; $\sin\psi \sin\theta = C_{61}^{X}$, which permit finding angles θ and ψ.

Equating the coefficients of the moment components of screw $\bar{E}_{61}$, we obtain a system of three equations for finding the coordinates of the tongs

the solution of which in matrix form is

/170

$$\begin{bmatrix} \rho_x \\ \rho_y \\ \rho_z \end{bmatrix} = \begin{bmatrix} 0 & \cos(\widehat{x z'}) & -\cos(\widehat{y z'}) \\ \cos(\widehat{z z'}) & 0 & \cos(\widehat{x z'}) \\ \cos(\widehat{y z'}) & -\cos(\widehat{x z'}) & 0 \end{bmatrix} \cdot \begin{bmatrix} C_{61}^{L} \\ C_{61}^{M} \\ C_{61}^{N} \end{bmatrix}$$

Let us find angle φ from the equality of the active components of screw $\bar{E}_{67}$: $\sin\varphi = 1/\cos\theta \cdot C^Z_{67}$. If $\theta = 0$, then $C^X_{67} = \cos(\psi + \varphi)$ and $C^Y_{67} = \sin(\psi + \varphi)$, from whence $(\psi + \varphi)$ can be determined as one angle of rotation.

It is possible to use additional relationships flowing from an identical equality for the active parts of $\bar{E}_{67}$ using Eqs. (4-6) and Eq. 3 in order to do away with ambiguity in determining ψ, θ, φ.

REFERENCES

1. Kobrinksiy, A. Ye., Stepanenko, Yu. A., "Some Problems of Manipulator Theory," V sb. Mekhanika Mashin [In collection: Mechanics of Machines], No. 7-8, "Nauka" Press, 1967.

2. Vinogradov, I. B., Kobrinskiy, A. Ye., Stepanenko, Yu. A., Tyves, L. I., "Features of Manipulator Kinematics and the Volumes Method," This collection.

3. Dimentberg, F. M., Opredeleniye polozheniy prostranstvennykh mekhanizmov [Determining the Positions of Spatial Mechanisms] AN CCCP Press, 1950.

4. Dimentberg, F. M., Vintovoye ischisleniye [Screw Calculus], "Nauka" Press, 1965.

5. Sinev, A. V., Brodotskaya, I. V., Charnaya, I. S., "A Kinematic and Power Analysis of the Spatial Mechanism of a Pneumatic Hydraulic Actuator for Stopcocks in Gas Mains," V sb. Mekhanika Mashin [In collection: Mechanics of Machines], "Nauka" Press, 1969.

Translated for National Aeronautics and Space Administration under contract number NASw-2038 by Translation Consultants, Ltd., 944 S. Wakefield Street, Arlington, Virginia 22204.